Supramolecular structures based on the intramolecular H-bonding in the 3,3'-di(acylamino)-2,2'-bipydridine unit

Please check the document version of this publication:

• A submitted manuscript is the version of the article upon submission and before peer-review. There can be important differences between the submitted version and the official published version of record. People interested in the research are advised to contact the author for the final version of the publication, or visit the DOI to the publisher's website.
• The final author version and the galley proof are versions of the publication after peer review.
• The final published version features the final layout of the paper including the volume, issue and page numbers.

Link to publication

Supramolecular Structures Based on the Intramolecular H-bonding in the 3,3'-Di(acylamino)-2,2'-Bipyridine Unit

Anja R.A. Palmans

Supramolecular Structures Based on the Intramolecular H-bonding in the 3,3'-Di(acylamino)-2,2'-Bipyridine Unit

PROEFSCHRIFT

ter verkrijging van de graad van doctor aan de Technische Universiteit Eindhoven, op gezag van de Rector Magnificus, prof.dr. M. Rem, voor een commissie aangewezen door het College voor Promoties in het openbaar te verdedigen op dinsdag 2 december om 16.00 uur

door

Ann Rita Alberta Palmans

geboren te Maaseik, België

Dit proefschrift is goedgekeurd door de promotoren:

prof.dr. E.W. Meijer
en
prof.dr. H. Ringsdorf

copromotor: dr. J.A.J.M. Vekemans

"De mensen verkeren op aarde als profetieën van de toekomst en al hun daden zijn pogingen en probeersels, want elke daad kan door de volgende worden overtroffen"

"De man zonder eigenschappen" van Robert Musil

Contents

Chapter 1

Introduction

1.1   General considerations

Supramolecular chemistry[1] —also known as the *chemistry beyond the covalent bond*— is a symbiosis of different fields of chemistry in which the unrivalled imagination of Nature often plays a prominent role. In essence, supramolecular chemistry deals with the design and synthesis of functional molecules that —by means of secondary interactions— evolve in ordered superstructures with tunable properties. Tools such as H-bonding, metal-ion complexation and hydrophobic interactions are used to achieve a spontaneous organisation of the building blocks. Many tantalising examples[2] have been presented in the last decade applying these secondary interactions [3].

*Inter*molecular H-bonding is among the secondary interactions most frequently used in the field of supramolecular chemistry. This contrasts with the assembly in natural species such as proteins in which *intra*molecular H-bonding is a preferred tool to use. Intramolecular H-bonding ensures pre-organisation of the molecules —generally of medium to high molecular weight— and leads to cooperativity in these systems[4]. In synthetic systems, however, the use of *intra*molecular H-bonds is still notably absent.

The work described in this thesis deals with intramolecular H-bonds pre-organising building blocks. More specifically, the 3,3'-di(acylamino)-2,2'-bipyridine unit is employed and the intramolecular H-bonding present will be described in detail. Furthermore, the potential of this unit will be demonstrated in a variety of synthetic systems such as rigid-rod oligomers/polymers and extended-core disc-shaped molecules. The characterisation and the properties of these systems, structured by the intramolecular H-bonds, will be discussed.

This introductory chapter will focus on *pre-organisation* of molecules prone to *self-assembly*. H-bonding as well as the use of mesogenic groups are the tools that will be applied in this thesis to achieve the organisation of matter. We will first address the topic of H-bonding — more specifically intramolecular H-bonding— and then discuss the importance of liquid crystals for supramolecular chemistry. Finally, the aim and the outline of this thesis will be presented.

1.2 The H-bond

The H-bond in supramolecular chemistry

An H-bond is in essence an electrostatic interaction between a partially positively charged hydrogen atom and a partially negatively charged atom[5]. Well-known is the remarkable behaviour of water —the high boiling point and the low density in the crystalline phase— which is a consequence of the presence of H-bonds. H-bonding is a strong and directional interaction, and therefore very effective to guarantee order *in* and *between* molecules.

A number of examples has been presented in which the building blocks are "programmed" to build up specific superstructures[6]. Ghadiri, for example, has synthesised cyclic peptide sub-units, made up of an even number of alternating *D*- and *L*-amino acids[7]. Under suitable conditions, uniformly shaped and contiguously H-bonded *β*-sheet-like cylindrical structures are formed (figure 1.1). The internal diameter of these peptide nanotubes can be controlled simply by adjusting the ring size of the sub-unit employed. As a result, nanotubes with internal pores between 7 and 13 Å have been obtained. The additional ability to tailor the outside surface properties of the tubuli by choosing an appropriate amino acid side-chain has resulted in the application of the tubuli as transmembrane ion-channels.
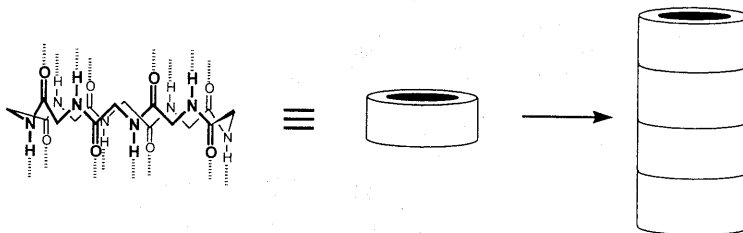
Figure 1.1: Nanotubes developed by Ghadiri et al.[7]

Lehn[8] and Kato[9] have synthesised main- and side-chain liquid crystalline polymers by linking the constituting units by intermolecular H-bonds. The molecular recognition between the complementary sub-units leads to self-association of a supramolecular liquid crystalline polymer. Lyotropic[8a] as well as thermotropic[8b] main-chain liquid crystalline polymers (LCP) were found, depending on the rigidity of the sub-units (figure 1.2). By tailoring the flexibility of the spacer in the sub-units, both lyotropic and thermotropic liquid crystalline behaviour are to be expected. In the side-chain analogues[9], liquid crystalline polymers are readily obtainable with tunable properties due to the easy coupling of various mesogenic groups via H-bonds or other non-covalent interactions to the main-chain (figure 1.3). When, for example, chiral mesogenic units are introduced, LCP's exhibiting ferroelectric properties

have been obtained[9d]. These so-called "supramolecular polymers" have attracted much attention lately because of their potential as new, highly functional materials.

thermotropic LCP   **lyotropic LCP**
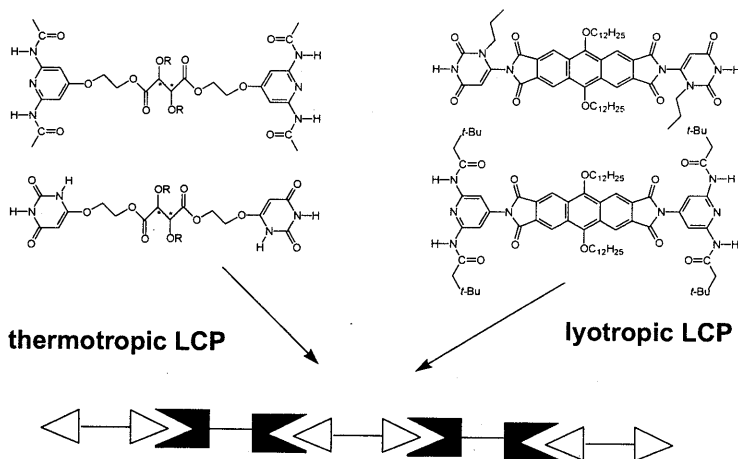
Figure 1.2: The use of H-bonds to form main-chain liquid crystalline polymers exhibiting thermotropic[8a] and lyotropic[8b] mesophases
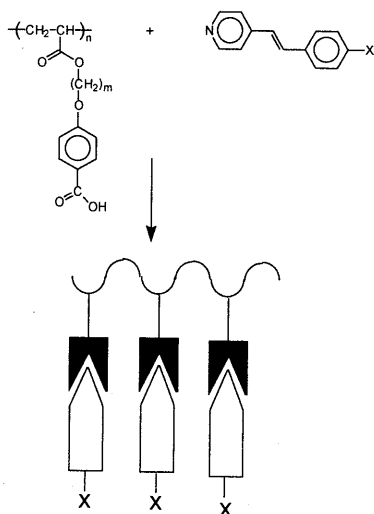
Figure 1.3: The use of H-bonds to form side-chain liquid crystalline polymers[9a]

Beijer *et al.*[10] have extended the concept of Lehn by using self-complementary pyrimidinone derivatives in which intramolecular H-bonding pre-organises this moiety for strong 4-fold intermolecular H-bonding in a *DDAA* array[10a]. The association constant between the monofunctional units is so large that in bifunctional derivatives visco-elastic behaviour[10b]

has been observed. This indicates that supramolecular polymers can exhibit properties of "normal", covalently bonded polymers.

*Intra*molecular H-bonding is also a powerful tool in the pre-organisation of molecular sub-units. The conformation in α-helical peptides is restricted so that rod-like sub-units remain. An interesting example is poly(γ-benzyl-L-glutamate). This polymer shows helical rod-like structures, stabilised by intramolecular H-bonds. A wide range of solvents can be added, leading to lyotropic liquid crystalline behaviour[11a]. Replacing the benzyl group by an *n*-alkyl group leads to thermotropic LC behaviour as the *n*-alkyl chain can act as solvent[11b].

Hamilton *et al.* have used anthranilic acid derivatives to illustrate that intramolecular interactions together with the intrinsic rigidity and a conformational preference of a secondary amide provides oligomers with a controlled and stable helical structure (figure 1.4.a)[12]. Due to the strength of the intramolecular H-bonds, this conformation is retained even in solution. Mascal *et al.* synthesised a tryptophane-derived aza-macrocycle (figure 1.4.b) which is tightly wound into the form of a double left-handed helix through transannular H-bonding interactions[13]. The kinetics of unwinding the helix was found to be beyond the range of dynamic NMR techniques. Both examples are illustrative for the strength of intramolecular H-bonds and both show how such intramolecular H-bonds can affect the secondary structure of molecules.

a)   *b)*
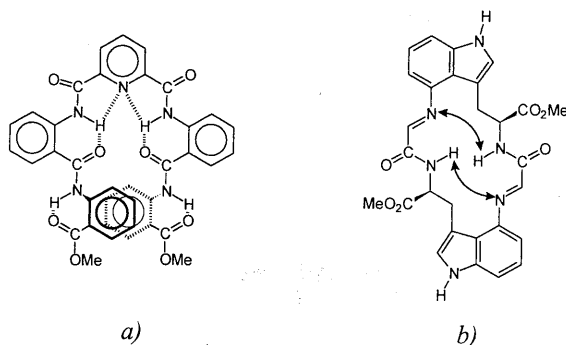
Figure 1.4: a) Anthranilic acid derivative leading to superstructures with a helical conformation by Hamilton et al.[12] b) a double helical macrocycle stabilised by intramolecular H-bonding by Mascal et al.[13], the arrows indicate where the H-bonds are formed

Due to its strength and directionality, H-bonding is a favourite interaction in supramolecular chemistry. Therefore, the characterisation and principles of H-bonding will be evaluated in more detail.

The H-bond: characterisation and strength

The most frequent H-donors and acceptors are summarised in table 1.1. The strongest H-bond is expected between H–F and F⁻ because of the high electronegativity of fluor. Despite elaborate studies, quantification of the strength of the H-bond interactions is not always obvious. For neutral molecules, the H-bond strength usually lies in the range of 20±10 kJ/mol. In ionic systems, however, the strength of H-bonds can amount to 170 kJ/mol which is comparable to the strength of weak covalent bonds. Although H-bonding often involves only one donor (D) and one acceptor (A) molecule, bifurcated (three centre) and even trifurcated (four centre) H-bonds are not uncommon.

Table 1.1   *Common H-donors and acceptors*

H-donor	H-acceptor
N–H	N
O–H	O
F–H	F
C–H	

D—H⋯A   D—H (A / A)   D—H⋯A (A / A)

simple   bifurcated   trifurcated
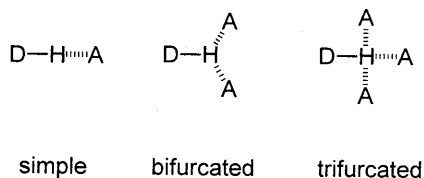
Three categories of H-bonds are discerned: weak H-bonds representing energies between 10 and 50 kJ/mol, strong H-bonds with energies between 50 and 100 kJ/mol and very strong H-bonds with energies above 100 kJ/mol[14]. Electrostatic interactions between D–H and A account for weak H-bonds. However, as D–H and A come closer, the attractive force is rapidly cancelled by repulsion. Attractive second order forces must then come along, namely polarisation (*i.e.* induced dipole in D) and delocalisation (charge transfer). This provides the energy for strong and very strong H-bonds.

A number of techniques is available to determine the strength of H-bonds of which infrared spectroscopy and NMR spectroscopy are frequently used[15]. However, these techniques are often only accurate when H-bonded and non H-bonded species are present in solution, which is the case with weak H-bonds (*i.e.* most intermolecular H-bonds). For strong and very strong H-bonds (*i.e.* many intramolecular H-bonds) ion cyclotron resonance spectroscopy has been successfully used[16]. After years of debate, this technique could finally set the H-bond strength in the [F–H–F]⁻ ion —the strongest H-bond known— at 163 kJ/mol[17]. Unfortunately, the ion cyclotron resonance technique is difficult and not commonly accessible.

Single crystal X-ray diffraction analysis is an accurate method to determine the distance and the angle, α, between donor and acceptor in the solid state. The criterion usually adopted to judge whether an H-bond is present in the solid state is:

$$d(D\text{---}A) < R_w(D) + R_w(A) + 0.50 \text{ and } \alpha(D\text{--}H\text{---}A) > 100°,$$

in which R_w is the van der Waals radius. Comparison of systems in which an H-bond strength could be measured and a D–A distance was obtained from X-ray diffraction results has led to a qualitative rule which provides an indication of the H-bond strength[14]. If the difference between the sum of the Van der Waals radii of donor and acceptor and the measured distance between donor and acceptor is larger than 0.25 Å, the H-bonds are considered to be strong and bond energies lie between 50 and 100 kJ/mol. If this difference is even larger than 0.5 Å, very strong H-bonds with bond energies exceeding 100 kJ/mol are present.

1.3   Liquid crystals

Discovered in the 19*th* century by Lehman and Reinitzer[18], liquid crystals constitute a class of molecules having the unique property of mobility while being orientationally ordered. Molecular anisotropy within a molecule or a dichotomous structure of the molecule are the simple features that account for this "self-assembly" at the molecular level. The dichotomous structure may apply to different structural properties (*e.g.* flexible and rigid) or different chemical properties (*e.g.* hydrophobic and hydrophilic) within the molecule. At the macroscopic level, the tendency to remain ordered while being mobile is used in a number of applications such as liquid crystalline displays and liquid crystalline thermometers. In view of the scope of this thesis, a more elaborate description will be limited to disc-shaped compounds exhibiting liquid crystalline behaviour

Disc-shaped molecules exhibiting liquid crystalline behaviour

Although the presence of liquid crystallinity in "leaf-shaped" molecules was already considered in 1923[19a], detailed investigations of disc-shaped molecules showing liquid crystalline behaviour are rather recent[19b]. Well-known examples include hexa-substituted benzenes and hexa-alkoxy-triphenylenes[20]. In analogy with their rod-like counterparts, a number of mesophases can be distinguished as illustrated in figure 1.5[21]. Nematic discotics (N_D) have their normal more or less pointed to the same direction. A chiral twist is induced when the different layers stack helically on top of each other, giving rise to a chiral nematic phase (N_D^*). One-dimensional order is achieved when the molecules stack into columns, in which the molecules can be arranged periodically (D_h) or aperiodically (D_o). These columns can form 2D crystal-like arrays in a hexagonal (D_h), rectangular (D_r) or oblique fashion (D_{ob}).
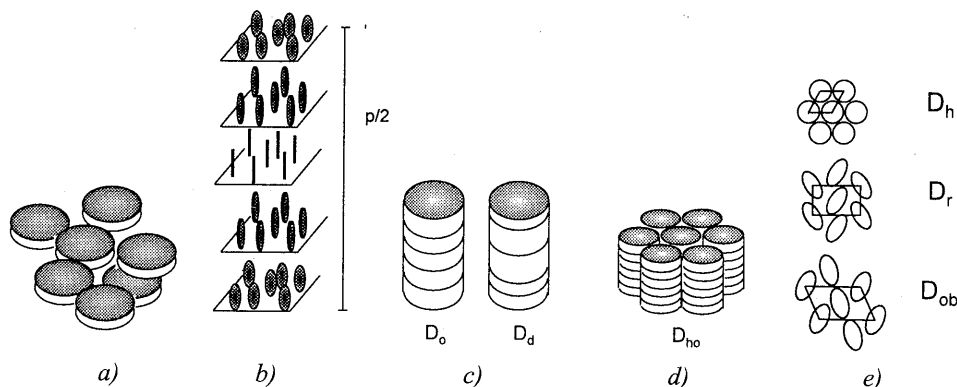
Figure 1.5: Discotic molecules in a a) nematic state N_D b) chiral nematic state $N_D{}^*$ c) columnar state, ordered D_0 and disordered D_d d) hexagonal columnar state D_{ho} ; two-dimensional packing arrays for the columnar structures in e)

A considerable amount of research has focused on the order–disorder transition in discotic liquid crystals. Selective deuteration of disc-shaped molecules has allowed for detailed ^{2}H-NMR studies to elucidate the dynamics in different parts of the molecules as a function of the phase. For hexa-alkoxytriphenylenes, it was found that a rapid rotation around the columnar axis is initiated as soon as the molecules enter the mesophase[22]. Furthermore, the degree of order present in a D_{ho} phase, expressed as the order parameter S, could be determined for various disc-shaped molecules[23]. In case of the hexa-alkoxytriphenylenes order parameters as high as 0.9 were measured in the D_{ho} phase. IR spectroscopy can also provide useful information concerning the orientation of the columns with respect to the substrate and the order parameter S[24]. Such information is crucial when applications of these systems are considered.

Columnar mesophases are currently of interest because of their potential for systems with one-dimensional charge transport. Future applications of disc-shaped liquid crystalline materials involve their use in gas sensors and as active charge transport layers in fast and high resolution xerographic and laser printing applications[25]. Recently, even the construction of molecular wires[26] and light emitting diodes (LED's) based on columnar discotics[27] have been suggested. Interesting research has focused on the mobilities of photo-induced charge carriers in columnar phases[28]. Especially hexa(hexylthio)triphenylene in the highly ordered helical phase displays very high charge-carrier mobilities that are only surpassed by those of organic single crystals[28a]. In addition, it has been shown that quasi–1D electrical conductivities as high as 0.1 S/m can be achieved by doping triphenylene derivatives with oxidants such as $AlCl_3$ and $NOBF_4$[29].

Extended-core discotic liquid crystals

To facilitate future applications, a high stability of the mesophases over a broad temperature range is desired. Early work with benzene and triphenylene derivatives pointed out that the mesomorphic temperature range becomes larger upon increasing the diameter of the aromatic core[30]. Recently, disc-shaped liquid crystals with core diameters exceeding 20 Å have been synthesised (figure 1.6). They all show mesophases from approximately room temperature to at least 300°C[31]. These results, combined with those obtained for "small" disc-shaped cores indicate that the temperature range in which liquid crystallinity occurs, is directly influenced by the diameter of the aromatic core. This may be rationalised by stronger π–stacking interactions upon enlarging the central aromatic moiety and, by consequence, a stronger tendency for phase separation between aromatic and aliphatic parts in the molecules.

K 60°C D_h 300°C I $R = n$-$C_{10}H_2$ M = Cu, Ni   -100°C $D_{tet,o}$ > 300°C

a)   b)   c)
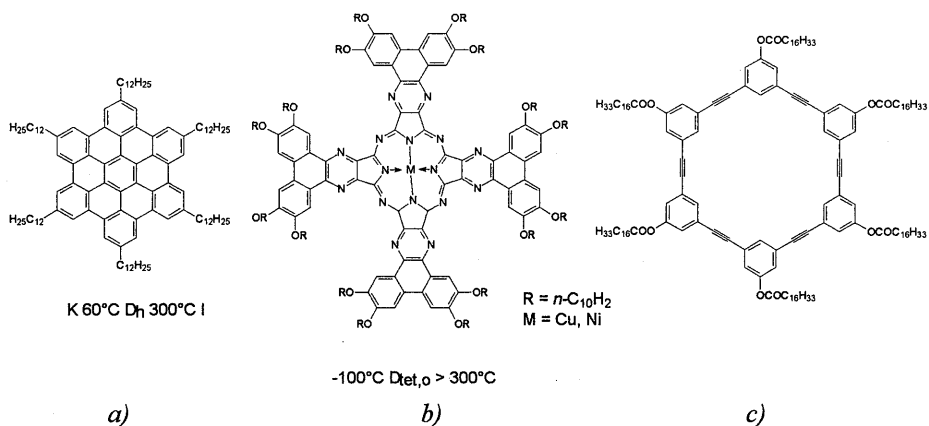
Figure 1.6: Examples of extended-core disc-shaped compounds: a) hexa-peri-hexabenzocoronene by Müllen et al.[31a] b) porphyrazinato metal(II) complexes by Ohta et al.[31b] c) macrocyclic discs by Moore et al.[31c]

The advantages of extended cores was recently shown for the benzocoronenes reported by Müllen *et al.* The latter may be considered as the large–core analogues of the well-known hexa-hexyloxy-triphenylene derivative. Comparable mobilities of photo–induced charge carriers have been measured in the D_h phase[32a] of both compounds. However, in case of the benzocoronenes a constant mobility of the charge-carriers was found from approximately room temperature up to 200°C[32b]. As a result, benzocoronenes would definitely be more effective in applications than hexa-alkoxy-triphenylene in which the D_{ho} phase —and therefore the mobilities of the charge-carriers in this phase— is limited to the temperature range of 68 to 90°C.

Supramolecular chemistry in the construction of extended-core disc-shaped compounds

Focusing on extended-core discotic liquid crystals, one can imagine to build up the rigid cores by other than covalent bonds. This might not only simplify the synthesis, but also allows the introduction of reversibility in this way. A number of disc-shaped liquid crystals based on metal–ion complexation[33] as well as intermolecular H-bonds[34] has been reported. Typical examples are shown in figure 1.7. Apart from some exceptions[35], the cores are mostly not very large and consequently the temperature range in which columnar mesophases exist is limited.

a) b) c)
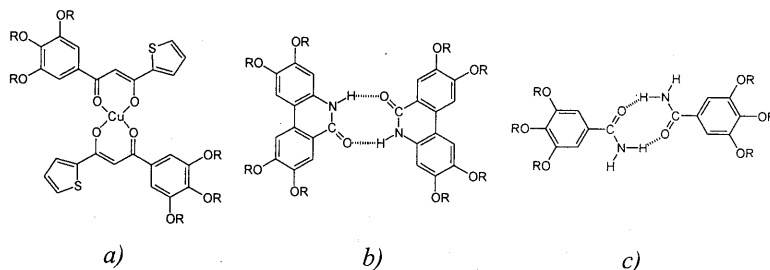
Figure 1.7: a) Disc-shaped complex based on metal complexation[33h] b) and c) self complementary amides exhibiting columnar mesophases[34a-h]

Another approach rests on the introduction of intramolecular H-bonds[36] to rigidify aromatic cores (figure 1.8). In the case of the dinitrophenylhydrazone, depicted in figure 1.8.a, intramolecular H-bonding combined with intermolecular charge transfer interactions with an alternating dipole orientation leads to columnar mesophases arranged in a hexagonal lattice[36a]. In fact, removal of the 2-nitro group results in a complete loss of the mesophase and only crystalline compounds are obtained. The azo discs, shown in figure 1.8.b, may exhibit a preferred planar conformation as a result of intramolecular H-bonding. Unfortunately, no detailed description of the liquid crystalline behaviour is available[36b].

a) b)
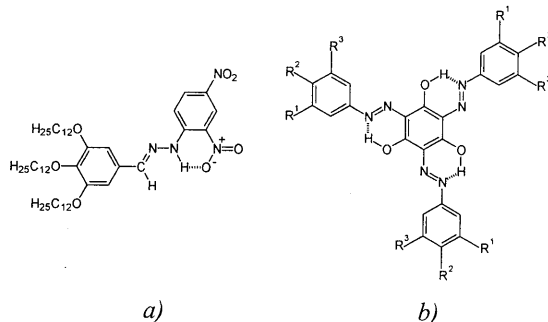
Figure 1.8: a) Dinitrophenylhydrazones[36a] and b) azo derivatives[36b] by Ringsdorf et al.

Chirality in disc-shaped liquid crystals

The first liquid crystals described were cholesterol derivatives, and therefore chiral. Chiral liquid crystals may display ferroelectric and antiferroelectric liquid crystalline phases with potential applications in liquid crystalline display devices. Chirality has also been introduced in disc-shaped liquid crystals such as the chiral pentaynes (figure 1.9.a)[37]. This has led to the observation of the chiral nematic mesophase N_D^*. Introducing chiral side-chains at the phenanthrene core[38] has afforded a switchable columnar phase (figure 1.9.b).

a)   b)
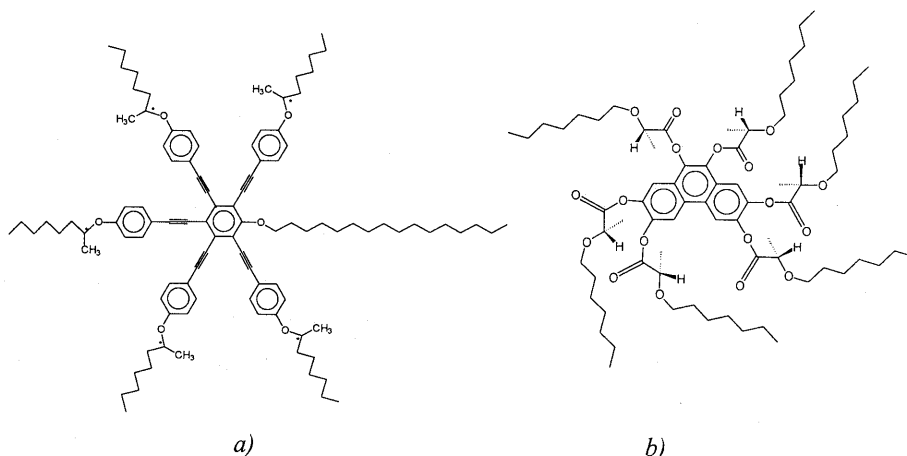
Figure 1.9: a) Chiral pentaynes showing an N_D^* phase[37] b) chiral phenanthrenes which can be switched from a tilted to a non-tilted columnar phase[38]

Until now, chirality has been introduced in discotic liquid crystals by attaching chiral side-chains to the central core. A drawback is the relatively weak chirality imparted by the introduction of chiral centres into the highly disordered chains. As a result, efforts are made to synthesise a chiral nucleus[39]. Preliminary attempts have focused on the selective α-halogenation of triphenylene derivatives. Computer simulations have shown that a chiral twist in the nucleus is to be expected.

In another approach, transfer of the chirality from the side-chain to the core may create a stable, chiral conformation of the core. No examples of such an approach have been presented up to now[40]. In contrast, the transfer of chirality of the side-chain to the main-chain in helical polymers has been studied in detail[41].

Lyotropic liquid crystals and gels based on disc-shaped molecules

The formation of a mesophase can be induced either by a change in temperature, *i.e.* thermotropic mesomorphism, or by the addition of a solvent, *i.e.* lyotropic mesomorphism. In case of disc-shaped compounds, only a few systems are known which exhibit both thermotropic and lyotropic liquid crystalline behaviour. This can be attributed to the fact that for most disc-shaped molecules forming columnar mesophases, the stability of the columnar aggregates seems to be insufficient to support the formation of lyotropic columnar mesophases. Enhanced π–stacking interactions arising from extended cores, intermolecular H-bonding[42] or metal–ligand interactions[43] might overcome this insufficient stability. Interesting systems have been acquired when phthalocyanine and triphenylene cores have been decorated with oligoethylene glycol chains[44]. The formation of columnar mesophases in water has been observed for these systems. Undoubtedly, the solubility of the ethylene glycol chains in water, together with the strong phase separation from the aromatic core to water will substantially contribute to this. The phthalocyanine derivative also shows thermotropic columnar mesophases which is of particular interest for applications in, for example, ion-conductivity.
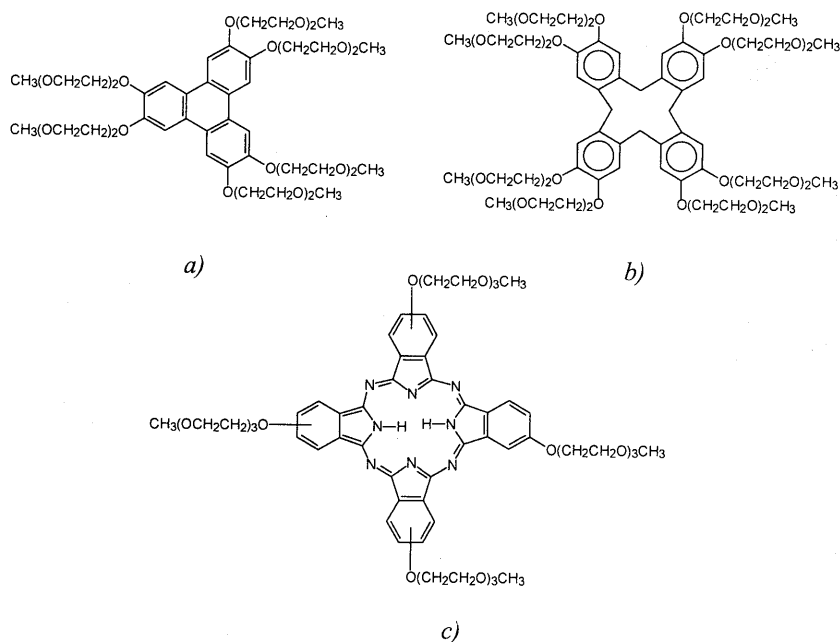
Figure 1.10: Lyotropic columnar mesophomorphism in water a) with triphenylene core by Boden et al.[44a] b) with tetrabenzocyclododecatetraene core by Zimmermann et al.[44b] c) with phthalocyanine core by Painter et al.[44c]

Molecular gels are based on low molecular-weight organic molecules that are able to solidify a liquid, and exhibit well-defined thermoreversible sol–gel transitions. In many cases, intermolecular H-bonding[45] and/or stacking of the π-systems[46] are believed to contribute to the organisation process. Typically, 3D networks are found consisting of fibrous bundles, interconnected by junction zones. The solvent is believed to be incorporated into the space between the fibers. Structural and rheological studies have been conducted and these measurements proved their strength in revealing which structural factors control the gel formation[47]. Recently, a number of "disc-shaped", C_3-symmetrical molecules have been reported to function as "molecular gels" (figure 1.11)[48]. The molecules have been found to form gels in a wide variety of solvents, both polar and apolar. Intermolecular H-bonding as well as intermolecular interactions between the long alkyl chains contribute to the formation of the network in these examples: the H-bonds organise the molecules in columnar aggregates, while van der Waals interactions between the alkyl chains interlock the different strands. The results suggest that these molecular characteristics may serve as a guiding principle for the molecular design of gel-forming materials.
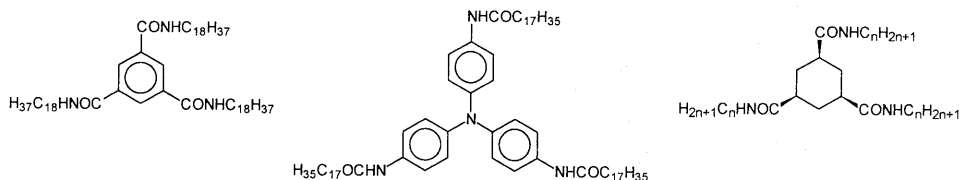
Figure 1.11: Disc-shaped molecular gelators for organic solvents[48]

1.4 Aim of the thesis

In the early eighties Kaczmarek and co-workers synthesised 2,2'-bipyridine-3,3'-diol starting from 3,3'-diamino-2,2'-bipyridine[49]. During the next decade, the intramolecular H-bonding[50] and the cooperative double proton transfer in the excited state[51] have been elaborately studied. The properties of N-acylated derivatives of 3,3'-diamino-2,2'-bipyridine were, however, never discussed although intramolecular H-bonds between the amide-NH and the pyridine-N of such molecules can also be expected. This thesis describes to which extent 3,3'-di(acylamino)-2,2'-bipyridines can be used as a new building blocks for supramolecular chemistry. The aim of this thesis is therefore twofold. Firstly, the characterisation of the intramolecular H-bonding in N-acylated 3,3'-diamino-2,2'-bipyridines and an evaluation of the overall secondary structure of this moiety will be presented. As a consequence, modifications of the bipyridine ring have been included. The reason was to introduce lipophilicity in this moiety and to enable the study of small modifications of the bipyridine moiety on the properties upon incorporation in larger structures. Secondly, a new type of disc-

shaped, C$_3$-symmetrical compounds has been designed and synthesised in which three bipyridine moieties are linked to a central benzene core *via* amide bonds. The properties of these compounds —such as thermotropic and lyotropic liquid crystalline behaviour— are investigated in detail. The expected self-assembling capacities are further evaluated by introducing chirality in the system. For this purpose, chiral peripheral side-chains derived from citronellol have been attached and a chiral alkane solvent has been used. The possibility to transfer the chirality in the side-chain to the central nucleus is addressed as well.

1.5   Outline of the thesis

A brief introduction on H-bonding and liquid crystals is presented in Chapter 1. Chapter 2 is an introductory chapter in which the synthesis and characterisation of acylated 3,3-diamino-2,2-bipyridines is presented[52, 53]. The overall secondary structure owing to the intramolecular H-bonding is used as a building block in the next chapters. In Chapter 3, the solubility problems that arise in highly symmetrical, conformationally restricted molecules are evaluated. Therefore, attempts are made to provide the bipyridine with lipophilic groups at the 5,5'-positions. Chapter 4 deals with the synthesis and characterisation of a new type of disc-shaped, C$_3$-symmetrical compounds[54]. The overall conformation and the thermotropic liquid crystalline behaviour are the main topics discussed. Also, the influence of attaching methoxy groups at the C-5 and C-5' positions of the bipyridine unit with respect to the properties is taken into consideration. In Chapter 5, the lyotropic liquid crystalline behaviour exhibited by the aforementioned compounds when dissolved in alkane solvents is studied[55]. The "molecular gel" capacities of these compounds are evaluated briefly. Chapter 6 focuses on the aggregation behaviour of C$_3$-symmetrical disc-shaped molecules in low concentrations in alkane solvents. The topic of transferring chirality from the side-chain to the central nucleus will be addressed[56]. Finally, Chapter 7 reports on the intriguing zeolite-like structure obtained for one of the model compounds[57].

1.6   References

[1]   The expression "supramolecular chemistry" was introduced in the 1980's by Lehn. *See:* Lehn, J.-M., *Supramolecular Chemistry*, VCH Publishers, Weinheim, **1995**.

[2]   Especially intriguing examples are the synthetic analogue of DNA (Koert, U.; Harding, M.M.; Lehn, J.-M. *Nature* **1990**, *346*, 339) and the synthetic analogue of the tobacco mosaic virus (Percec, V.; Heck, J.; Lee, M.; Ungar, G.J.; Alvarez-Castillo, A.J. *J. Mater. Chem.* **1992**, *2*, 1033. Percec, V.; Heck, J.; Ungar, G.J.; Batty, S.V. *J. Chem. Soc., Perkin Trans. 1* **1993**, 1411).

[3]   Some reviews concerning the use of secondary interactions in supramolecular chemistry: a) Philp, D.; Stoddart, J.F. *Angew. Chem. Int. Ed. Engl.* **1996**, *35*, 1155. b) Lawrence, D.S.; Jiang, T.; Levett, M. *Chem. Rev.* **1995**, 95, 2229. c) Hunter, C.A. *Chem. Soc. Rev.* **1994**, 101.

[4]   Well-known is the α-helix in peptides, stabilised by cooperative, intramolecular H-bonds.

[5]   Aakeröy, A.A.; Seddon, K.R. *Chem. Soc. Rev.* **1993**, 397.

[6]   Some reviews concerning this subject a) Lawrence, D.S.; Jiang, T.; Levett, M. *Chem. Rev.* **1995**, *95*, 2229. b) Fan, E.; Vicent, C.; Geib, S.J.; Hamilton, A.D. *Chem. Mater.* **1994**, *6*, 1113. c) MacDonald, J.; Whitesides, G.M. *Chem. Rev.* **1994**, *94*, 2383.

[7]   a) Khazanovich, N.; Granja, J.R.; McRee, D.E.; Milligan, R.A.; Ghadiri, M.R. *J. Am. Chem. Soc.* **1994**, *116*, 6011. b) Ghadiri, M.R. *Adv. Mater.* **1995**, *7*, 675. c) Ghadiri, M.R.; Kobayashi, K.; Granja, J.R.; Chadha, R.K.; McRee, D.E. *Angew. Chem.* **1995**, *107*, 77.

[8]   a) Fouquey, C.; Lehn, J.-M.; Levelut, A.M. *Adv. Mater.* **1990**, *2*, 225. b) Kotera, M.; Lehn, J.-M.; Vigneron, J.P. *J. Chem. Soc., Chem. Commun.* **1994**, 197. c) Lehn, J.-M. *Makromol. Chem., Macromol. Symp.* **1993**, *69*, 1.

[9]   a) Kato, T.; Kihara, H.; Ujiie, S.; Uryu, T.; Fréchet, J.M.J. *Macromolecules* **1996**, *29*, 8734. b) Kato, T. *Supramol. Sci.* **1996**, *3*, 53. c) Kato, T.; Hirota, N.; Fujishima, A.; Fréchet, J.M.J. *J. Polym. Sci., Polym. Chem.* **1996**, *34*, 57. d) Kumar, U.; Fréchet, J.M.J.; Kato, T.; Ujiie, S.; Timura, K. *Angew. Chem., Int. Ed. Engl.* **1992**, *31*, 1531.

[10]   a) Beijer, F.H.; Sijbesma, R.P.; Meijer, E.W. *to be published*. b) Hirschberg, K. *personal communication*.

[11]   a) Robinson, C. *Trans. Faraday Soc.* **1956**, *52*, 571. b) Watanabe, J. Ono, H.; Uematsu, I.; Abe, A. *Macromolecules*, **1985**, *18*, 2141.

[12]   a) Hamuro, Y.; Geib, S.J.; Hamilton, A.D. *Angew. Chem.* **1994**, *106*, 465. b) Hamuro, Y.; Geib, S.J.; Hamilton, A.D. *J. Am. Chem. Soc.* **1996**, *118*, 7529.

[13]   a) Mascal, M.; Moody, C.J.; Morrell, A.I.; Slawin, A.M.Z.; Williams, D.J. *J. Am. Chem. Soc.* **1993**, *115*, 813.

[14]   *Advances in Physical Organic Chemistry*; *Vol. 26*, (Ed. Bethell, D.), Academic Press, Ltd., London, **1990**, 225-381.

[15]   Detailed reviews are given in: a) *Hydrogen Bonding*, (Eds. Joesten, M.D.; Schaad, L.J.) Marcel Dekker, Inc., New York, **1974**. b) *Hydrogen Bonding*, (Eds. Vinogradov, S.N.; Linnell, R.H.), Van Nostrand Reinhold Compagny, **1971**.

[16]   Beauchamp, J.L. *Ann. Rev. Phys. Chem.* **1971**, *22*, 517.

[17]   Larson, J.W.; McMahon, T.B. *J. Am. Chem. Soc.* **1982**, *104*, 5848.

[18]   a) Reinitzer, F. *Monath. Chem.* **1888**, *9*, 421. b) A summary of the history of liquid crystals is described in: Collings, P.J. *Liquid Crystals*, IOP publishing Ltd, Princeton University Press, New Jersey, **1990**, 24-34

[19]   a) Vorländer, D. *Zeitschr. f. Physik. Chemie* **1923**, *105*, 211. b) Chandrasekhar, S.; Sadashiva, B.K.; Suresh, K.A. *Pramana* **1977**, *9*, 471.

[20]   Chandrasekhar, S. *Liq. Cryst.* **1993**, *14*, 3 and references cited herein.

[21]   Destrade, C.; Tinh, N.H.; Gasparoux, H. Malthête, J.; Levelut, A.-M. *Mol. Cryst. Liq. Cryst.* **1981**, 111.

[22]   Kranig, W.; Hüser, B.; Spiess, H.W.; Kreuder, W.; Ringsdorf, H.; Zimmermann, H. *Adv. Mater.* **1990**, *2*, 36.

[23]   a) Hüser, B.; Spiess, H.W. *Makromol. Chem., Rapid. Commun.* **1988**, *9*, 337. b) Möller, M.; Wendorff, J.H.; Werth, M.; Spiess, H.W.; Bengs, H.; Karthaus, O.; Ringsdorf, H. *Liq. Cryst.* **1994**, *17*, 381. c) Zamir, S.; Singer, D.; Spielberg, N.; Wachtel, E.J.; Zimmermann, H.; Poupko, R.; Luz, Z. *Liq. Cryst.* **1996**, *21*, 39.

[24]   a) Perova, T.S.; Vij, J.K. *Adv. Mater.* **1995**, *7*, 919. b) Kruk, G.; Kocot, A.; Wrzalik, R.; Vij, J.K.; Karthaus, O.; Ringsdorf, H. *Liq. Cryst.* **1993**, *14*, 807.

[25]   Boden, N.; Bissell, R.; Clements, J.; Movaghar, B. *Liq. Cryst. Today*, **1996**, *6*, 2.

[26]   van Nostrum, C.F. *Adv. Mater.* **1996**, *8*, 1027.

[27]   Christ, T.; Glüsen, B.; Greiner, A.; Kettner, A.; Sander, R.; Stümpflen, V.; Tsukruk, V.; Wendorff, J.H. *Adv. Mater.* **1997**, *9*, 49. b) Christ, T.; Stümpflen, V.; Wendorff, J.H. *Makromol. Chem., Rapid. Commun.* **1997**, *18*, 93.

[28] a) Adam, D.; Schuhmacher, P.; Simmerer, J.; Häussling, L.; Siemensmeyer, K.; Etzbach, K.H.; Ringsdorf, H.; Haarer, D. *Nature* **1994**, *371*, 141. b) van Nostrum, C.F.; Bosman, A.W.; Gelinck, G.H.; Schouten, P.G.; Warman, J.M.; Kentgens, A.P.M.; Devillers, M.A.C.; Meyerink, A.; Picken, S.J.; Sohling, U.; Schouten, A.-J.; Nolte, R.J.M. *Chem. Eur. J.* **1995**, *1*, 171. c) Adam, D.; Schuhmacher, P.; Simmerer, J.; Häussling, L.; Paulus, W.; Siemensmeyer, K.; Etzbach, K.H.; Ringsdorf, H.; Haarer, D. *Adv. Mater.* **1995**, *7*, 276. d) Adam, D.; Closs, F.; Frey, T.; Funhoff, D.; Haarer, D.; Ringsdorf, H.; Schuhmacher, P.; Siemensmeyer, K. *Phys. Rev. Lett.* **1993**, *70*, 475.

[29] a) Boden, N.; Bushby, R.J.; Clements, J.; Luo, R. *J. Mater. Chem.* **1995**, *5*, 1741. b) Arikainen, E.O.; Boden, N.; Bushby, R.J.; Clements, J.; Movaghar, B.; Wood, A. *J. Mater. Chem.* **1995**, *5*, 2161.

[30] Destrade, C.; Foucher, P.; Gasparoux, H.; Tinh, N.H.; Levelut, A.-M.; Malthête. *J. Mol. Cryst. Liq. Cryst.* **1984**, *106*, 21.

[31] a) Herwig, P.; Kayser, L.W.; Müllen, K.; Spiess, H.W. *Adv. Mater.* **1996**, *8*, 511. b) Mohr, B.; Wegner, G.; Ohta, K. *J. Chem. Soc., Chem. Commun.* **1995**, 995. c) Zhang, J.; Moore, J. *J. Am. Chem. Soc.* **1994**, *116*, 2655. d) Kretschmann, H.; Müller, K.; Kolshorn, H.; Schollmeyer, D.; Meier, H. *Chem. Ber.* **1994**, *127*, 1735. e) van Nostrum, C.F.; Picken, S.J.; Schouten, A.-J.; Nolte, R.J.M. *J. Am. Chem. Soc.* **1995**, *117*, 9957.

[32] a) These measurements were performed using the Pulse Radiolysis Time Resolved Microwave Conductivity (PR-TRCM) technique, as used at the IRI in Delft: Van der Craats, A. *personal communication.* b) Due to the experimental setup of the PR-TRCM technique, measurements can only be conducted up to 200°C.

[33] a) Barbera, J.; Cativiela, C.; Serrano, J.L.; Zurbano, M.M. *Adv. Mater.* **1991**, *3*, 602. b) Serrette, A.G.; Swager, T.M. *Angew. Chem., Int. Ed. Engl.* **1994**, *33*, 2342. c) Fischer, H.; Plesnivy, T.; Ringsdorf, H.; Seitz, M. *J. Chem. Soc., Chem. Commun.* **1995**, 1615. d) Zheng. H.; Xu, B.; Swager, T.M. *Chem. Mater.* **1996**, *8*, 907. e) Thompson, N.J.; Serrano, J.L.; Baena, M.J.; Espinet, P. *Chem. Eur. J.* **1996**, *2*, 214. f) Kroczynski, A.; Pociecha, D.; Szydlowska, J.; Przedmojski, J.; Gorecka, E. *Chem. Commun.* **1996**, 2731.

[34] a) Kleppinger, R.; Lillya, C.P.; Yang, C. *J. Am. Chem. Soc.* **1997**, *119*, 4097. b) Beginn, U.; Lattermann, G. *Mol. Cryst. Liq. Cryst.* **1994**, *241*, 215. c) Latterman, G.; Staufer, G. *Mol. Cryst. Liq. Cryst.* **1990**, *191*, 199. d) Koh, K.N.; Araki, K.; Komori, T. ; Shinkai, S. *Tetrahedron Lett.* **1995**, *36*, 5191. e) Ebert, M.; Kleppinger, R.; Soliman, M.; Wolf, M.; Wendorf, J.H.; Lattermann, G.; Staufer, G. *Liq. Cryst.* **1990**, *7*, 553. f) Serrette, A.G.; Swager, T. *Angew. Chem.*, Int. Ed. Engl. **1994**, *33*, 2342. g) Ungar G.; Abramic, D.; Percec, V.; Heck, J.A. *Liq. Cryst.* **1996**, *21*, 73.

[35] A notable exception has been presented by Usolt'tseva, N.; Praefcke, K.; Singer, D.; Gündogan, B. *Liq. Cryst.* **1994**, *16*, 601.

[36] a) Paulus, W.; Ringsdorf, H.; Diele, S.; Pelzl, G. *Liq. Cryst.* **1991**, *9*, 807. b) Van der Auweraer, M.; Catry, C.; Feng Chi, L.; Karthaus, O.; Knoll, W.; Ringsdorf, H.; Sawodny, M.; Urban, U. *Thin Solid Films* **1992**, *210/211*, 39.

[37] a) Langer, M.; Praefcke, K.; Krürke, D.; Heppke, *J. Mater. Chem.* **1995**, *5*, 693. b) G. Booth, C.J.; Krürke, D.; Heppke, G. *J. Mater. Chem.* **1996**, *6*, 927.

[38] Scherowsky, G.; Chen, X.H. *J. Mater. Chem.* **1995**, *5*, 417.

[39] a) Boden, N.; Bushby, R.J.; Cammidge, A.N.; Duckworth, S.; Headdock, G. *J. Mater. Chem.* **1997**, *7*, 601. b) Praefcke, K.; Eckert, A.; Blunk, D. *Liq. Cryst.* **1997**, *22*, 113.

[40] The observation of chiroptical switching processes when nematic liquid crystals are doped with inherently dissymetric alkenes is interesting in this perspective. The alkenes have a stable helical conformation but are, unfortunately, not liquid crystalline themselves. *See:* Feringa, B.L.; Huck, N.P.M.; van Doren, H.A. *J. Am. Chem. Soc.* **1995**, *117*, 9929.

[41]   a) Green, M.M.; Peterson, N.C.; Sato, T.; Teramoto, A.; Cook R.; Lifson S. *Science* **1995**, *268*, 1860. b) Schlitzer, D.S.; Novak, B.M. *Pol. Prep.* **1997**, *38*, 296. c) Hu, Q.-S.; Vitharana, D.; Liu, G.-Y.; Jain, V.; Wagaman, M.W.; Zhang, L.; Randall Lee, T.; Pu, L. *Macromolecules* **1996**, *29*, 1082. d) Ramos, E.; Bosch, J.; Serrano, J.L.; Sierra, T; Veciana, J. *J. Am. Chem. Soc.* **1996**, *118*, 4703 and references cited herein.

[42]   a) Kohne, B.; Praefcke, K.; Derz, T.; Hoffmann, H.; Schwander, B. *Chimia* **1986**, *40*, 171. b) Malthête, J.; Levelut, A.-M.; Liébert, L. *Adv. Mater.* **1992**, *1*, 37.

[43]   *See* reference 35.

[44]   a) Boden, N.; Bushby, R.J.; Hardy, C.; Sixl, F. *Chem. Phys. Lett.* **1986**, *123*, 359. b) Zimmermann, H.; Poupko, R.; Luz, L.; Billard, J. *Liq. Cryst.* **1989**, *6*, 151. c) McKeown, N.; Painter, J.; *J. Mater. Chem.* **1994**, *4*, 1153.

[45]   a) Hanabusa, K.; Tange, J.; Tagushi, Y.; Koyama, T.; Shirai, H. *J. Chem. Soc., Chem. Commun.* **1993**, 390. b) Keller, U.; Müllen, K.; De Feyter, S.; De Schryver, F.C. *Adv. Mater.* **1996**, *8*, 490. c) Jokic, M.; Makarevic, J.; Zinic, M. *J. Chem. Soc., Chem. Commun.* **1995**, 1723. d) Jeong, S.W.; Murata, K.; Shinkai, S. *Supramolecular Sci.* **1996**, *3*, 83. e) Hanabusa, K.; Yamada, M.; Kimura, M.; Shirai, H. *Angew. Chem.* **1996**, *108*, 2086.

[46]   a) Lin, Y.; Kachar, B.; Weiss, R.G. *J. Am. Chem. Soc.* **1989**, *111*, 5542. b) Brotin, T.; Untermöhlen, R.; Fages, F.; Bouas-Laurent, H.; Desvergne, J.-P. *J. Chem. Soc., Chem. Commun.* **1991**, 416. c) Snijder, C.S.; de Jong, J.C.; Mettsma, A.; van Bolhuis, F.; Feringa, B.L. *Chem. Eur. J.* **1995**, *1*, 594.

[47]   a) Terech, P.; Furman, I.; Weiss, R.G. *J. Phys. Chem.* **1995**, *99*, 9558. b) Terech, P. *Progr. Colloid Polym. Sci.* **1996**, *102*, 64. c) Terech, P.; Ostunai, E.; Weiss, R.G. *J. Phys. Chem.* **1996**, *100*, 3759.

[48]   a) Yasuda, Y.; Takebe, Y.; Fukumoto, M.; Inada, H.; Shirota, Y. *Adv. Mater.* **1996**, *8*, 740. b) Yasuda, Y.; Iishi, E.; Inada, H.; Shirota, Y. *Chem. Lett.* **1996**, 575. c) Zhang, S.; Zhang, D.; Liebeskind, L.S. *J. Org. Chem.* **1997**, *62*, 2312.

[49]   Kaczmarek, L.; *Polish. J. Chem.* **1985**, *59*, 1141.

[50]   a) Lipkowski, J.; Grabowska, A.; Waluk, J.; Calestani, G.; Hess Jr., B.A. *J. Cryst. and Spectr. Res.* **1992**, *22*, 563. b) Sitkowski, J.; Stefaniak, L.; Kaczmarek, L.; Webb, G.A. *J. Mol. Struct.* **1996**, *385*, 65.

[51]   a) Bulska, H. *Chem. Phys. Lett.* **1983**, *98*, 398. b) Bulska, H.; Grabowska, A.; Grabowski, Z. *J. Lumin.* **1986**, *5*, 189. c) Sepiol, J.; Bulska, H.; Grabowska, A. *Chem. Phys. Lett.* **1987**, *140*, 607. d) Bulska, H. *J. Lumin.* **1988**, *39*, 293. d) Kaczmarek, L.; Nowak, B.; Zukowski, J.; Borowicz, P.; Sepiol, J.; Grabowska, A. *J. Mol. Struct.* **1991**, *248*, 189. e) Kaczmarek, L.; Balicki, R.; Lipkowski, J.; Borowicz, P.; Grabowska, A. *J. Chem. Soc., Perkin Trans. 2* **1994**, 1603.

[52]   Palmans, A.R.A.; Vekemans, J.A.J.M.; Meijer, E.W. *Recl. Trav. Chim. Pays-Bas* **1995**, *114*, 277.

[53]   Vekemans, J.A.J.M.; Groenendaal, L.; Palmans, A.R.A.; Delnoye, D.A.P.; van Mullekom, H.A.M.; Meijer, E.W. *Bull. Soc. Chim. Belg.* **1996**, *105*, 659.

[54]   Palmans, A.R.A.; Vekemans, J.A.J.M.; Fischer, H.; Hikmet R.A.; Meijer, E.W. *Chem. Eur. J.* **1997**, *3*, 300.

[55]   Palmans, A.R.A; Hikmet, R.A.; Fischer, H.; Vekemans, J.A.J.M.; Meijer, E.W. *in preparation.*

[56]   Palmans, A.R.A.; Vekemans, J.A.J.M.; Havinga, E.E.; Meijer, E.W. *Angew. Chem.* **1997**, *in press.*

[57]   Palmans, A.R.A.; Vekemans, J.A.J.M; Kooijman, H.; Spek, A.L.; Meijer, E.W. *Chem. Commun.* **1997**, *in press.*

Chapter 2

Intramolecular H-bonding in acylated 3,3'-diamino-2,2'-bipyridines

Abstract

Various N,N'-di- and N-monoacylated 3,3'-diamino-2,2'-bipyridines have been synthesised and characterised. All molecules show strong intramolecular H-bonding between the acyl-NH of one ring and the pyridine-N of the other (and vice versa) in the solid state as well as in solution, judged from single crystal X-ray diffraction, ¹H-NMR, IR and CD spectroscopy. The intramolecular H-bonds show a remarkable stability towards polar solvents, even at high temperatures. Due to the H-bonding, this bipyridine moiety is pre-organised in a planar, transoid conformation in the solid state as well as in solution. As such, the diamino-bipyridine system can be considered as a structuring moiety, suitable to be incorporated in larger molecules. Reversible breaking and restoring of the secondary structure can be accomplished by consecutive addition of strong acid and base.

2.1 Introduction

In the late seventies, Kaczmarek and co-workers synthesised 3,3'-diamino-2,2'-bipyridine and a number of derivatives (figure 2.1) in search of new biologically active compounds[1]. It was soon found that, although the biological activities were not promising, one of the derivatives *i.e.* 2,2'-bipyridine-3,3'-diol, revealed interesting properties due to a cooperative intramolecular double proton transfer leading to strong fluorescence[2]. A characteristic feature of 2,2'-bipyridine-3,3'-diol is the presence of strong H-bonds, both in the solid state[3a] and in solution[1e, 3c]. The molecule was found to be completely planar in the solid state with a donor–acceptor distance of 2.56 Å. ¹H-, ¹⁵N-, and ¹⁷O-NMR spectra featured chemical shifts typical for species in which "fairly strong" intramolecular H-bonds are formed[3b].
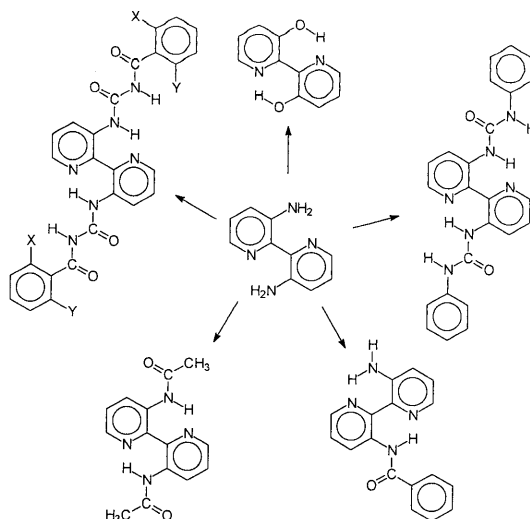
Figure 2.1: 3,3'-Diamino-2,2'-bipyridine and derivatives as synthesised by Kaczmarek and co-workers

On closer inspection, intramolecular H-bonds can also be expected to exist between the amide-NH and the pyridine-N of acylated derivatives such as 3,3'-diacetylamino-2,2'-bipyridine and 3-benzoylamino-3'-amino-2,2'-bipyridine (figure 2.1). This would result in a planar, transoid bipyridine system as represented in figure 2.2. Although intramolecular H-bonding has been elaborately investigated for various aromatic systems[4], the acylated 3,3'-diamino-2,2'-bipyridines have —to the best of our knowledge— never been included in these studies.
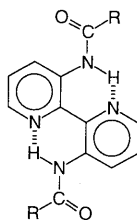
Figure 2.2: Planar conformation of acylated 3,3'-diamino-2,2'-bipyridines due to intramolecular H-bonding

Unlike in the 2,2'-bipyridine-3,3'-diol, a large variety of acylated derivatives of 3,3'-diamino-2,2'-bipyridine is conceivable. Hence, numerous possibilities for extension to or incorporation in larger structures exist. Taking advantage of the planar conformation, planar superstructures may be envisaged. Next to the field of research focusing on the use of the 2,2'-bipyridyl moiety as a ligand to build up 3D supramolecular assemblies[5], the interesting properties of a *planar* bipyridine unit may be recognised and this may evolve into a new field of research: *supramolecular chemistry in 2D*.

In this chapter, the synthesis and characterisation of 3,3'-diamino-2,2'-bipyridine and acylated derivatives thereof are described. The structures allow for the study of their intramolecular H-bonding and the overall secondary structure in the solid state and in solution. The characterisation of the structures is accomplished using NMR, IR and CD spectroscopy and single crystal X-ray diffraction analysis. A qualitative evaluation of the strength of the H-bonds in the 3,3'-di(acylamino)-2,2'-bipyridine moiety is presented. Finally, to reveal the presence/absence of cooperativity in these compounds, monoacylated compounds are compared to their diacylated analogues.

2.2 Synthesis

2.2.1 Synthesis of the precursor; 3,3'-diamino-2,2'-bipyridine

Two routes have been described leading to the key precursor molecule 3,3'-diamino-2,2'-bipyridine **2** (Scheme 2.1)[1a]. The overall yield of route 1 exceeded the yield of route 2 substantially (35% vs. 10%), making it the preferred route. Dinitrobipyridine **1** was first synthesised by Etienne and Izoret with an Ullmann coupling of 2-chloro-3-nitropyridine in a 51% yield[6]. The Ullmann coupling was carried out in dimethylformamide (DMF) with Cu as catalyst. However, optimisation of the work up procedure by soxhlet extraction with acetonitrile instead of tetrahydrofuran (THF) improved the yield (78%, lit.[6] 51%) and purity of **1** considerably (m.p. 210°C, lit.[6] 206°C). Attempts to replace DMF as the solvent in the Ullmann coupling by other solvents such as acetonitrile or N-methylpyrrolidone failed. The electron transfer reduction of the nitro groups was carried out according to the procedure described by Kaczmarek[1a] and comparable yields were obtained. The overall yield, with respect to 2-chloro-3-nitro-pyridine, was raised to 54% (lit. 35%[1a]).
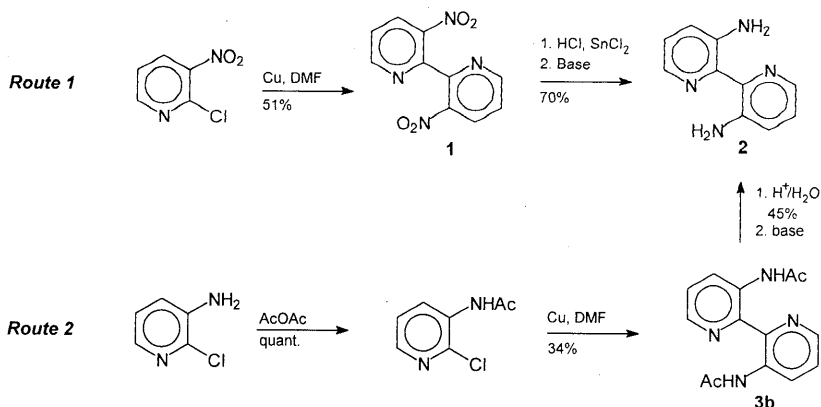
Scheme 2.1: Synthetic routes towards 3,3'-diamino-2,2'-bipyridine

2.2.2 Synthesis of N,N'-diacylated 3,3'-diamino-2,2'-bipyridines

The amine functionalities in 3,3'-diamino-2,2'-bipyridine **2** are of limited nucleophilicity: boiling in ethyl acetate or butyrolactone for several hours did not yield any acylated product. As a consequence, strong electrophiles such as anhydrides, acid chlorides, isocyanates and acylisocyanates had to be used to acylate this diamine. Four classes of diacylated 3,3'-diamino-2,2'-bipyridines were synthesised: dicarbamates, diamides, diureas and diacylureas. A survey of the compounds synthesised is given in table 2.1. The dicarbamate derivative **3a** was obtained by the reaction of **2** with di-*t*-butyldicarbonate (Boc$_2$O) in THF. This reaction proceeded slowly at reflux temperatures and a large excess of Boc$_2$O was needed for complete diacylation. The diamide and the diurea derivatives (**3b–j** and **3k,l**, respectively) were obtained by the reaction of diamine **2** with the corresponding acid chlorides or isocyanates. All isocyanates and acid chlorides were commercially available except for 8-quinolinecarbonyl chloride **4** which was obtained *via* a Skraup synthesis[7]. The diacylurea derivative **3m** was obtained from diamine **2** and benzoylisocyanate **5a**[1b] which, in turn, resulted from treatment of benzamide with oxalyl chloride[8]. Unfortunately, the diacylurea derivative **3m** proved to be insoluble in all common organic solvents thus preventing proper analysis. However, the introduction of lipophilic alkoxy chains at the phenyl ring did provide the necessary solubility and compound **3n** was obtained by reaction of 3,4,5-tridodecyloxybenzoylisocyanate **5b** with **2** and easily characterised.

Table 2.1 Diacylated 3,3'-diamino-2,2'-bipyridines: yields and relevant ^{1}H-NMR^a and IR data^b

Compound	2	3a	3b	3c	3d	3e	3f	3g	3h	3i,j	3k	3l	3m	3n
R =	–H	(structure)	(structure)	(structure)	(structure)	(structure)	(structure)	(structure)	(structure)	(structure)	(structure)	(structure)	(structure)	(structure)
Yield (%)	56	57	90	73	87	92	62	38	79	68/70	80	34	70	57
δ(NH) (ppm)	6.26	12.16	13.15	13.12	15.55	15.18	14.59	13.74	13.82	14.97	11.30; 9.65^c	12.57; 4.63	10.18^d	13.28; 8.29
δ(H4) (ppm)	7.02	8.80	9.10	9.06	9.23	9.24	9.42	9.31	9.34	9.22	8.72^c	8.86	9.23^d	8.79
δ(H6) (ppm)	7.96	8.26	8.34	8.25	8.46	8.56	8.41	8.35	8.45	8.58	8.39^c	8.10	8.96^d	8.69
ν(NH) (cm^{-1})	3352; 3221^e	2975^f	2890^f	2950^f	2745^f	2823^f	2900^f	2899^f	2921^f	2877^f	/	/	/	/

^{a} ^{1}H-NMR spectra were measured in CDCl$_3$ unless specified otherwise; ^{b}IR spectra were taken in KBr; ^{1}H-NMR spectra were measured in ^{c} DMSO-d6 and ^{d} in CDCl$_3$/ trifluoroacetic acid 3/1; ^{e} the NH stretch values in CDCl$_3$ solution were 3471 and 3261 cm^{-1}; ^{f} the absorption is broad and partially hidden under CH-stretch absorptions; as a result the indicated value represents the approximated minimum of the absorption peak.

2.2.3 Synthesis of monomeric analogues

Model compounds **6a–d** , being "monomeric" counterparts of **3d, f, i,** and **g**, respectively, (table 2.2) were synthesised to study the specific effect of intramolecular H-bonding on the bipyridine system. The amides were obtained by treating 3-aminopyridine with the appropriate acylating agent.
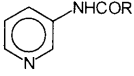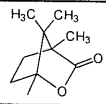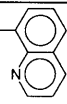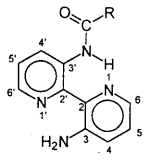
2.2.4 Synthesis of N-monoacylated 3,3'-diamino-2,2'-bipyridines

To determine whether cooperativity is operative in the diacetylated 3,3'-diamino-2,2'-bipyridines, monofunctionalised bipyridines **9a–c** were synthesised as well (table 2.2). Compound **9a** was previously described by Kaczmarek[1c] and obtained in a two step procedure *via* the symmetrical [5,4-b:6,7-b]-dipyrido-1,3-diazepinium intermediate (scheme 2.2). The benzimidate ester **7** could be obtained from benzonitrile[9]. Subsequently, the imidate ester reacted with **2** to give diazepine **8** in a yield of 88%. The hydrolysis of the diazepine ring in acetic acid proceeded much slower than described and as a result a yield of only 33% was obtained of crystalline material (lit.[1c] 75%). We found that the reaction of **2** with 2 equivalents of *(R)*-α-methylbenzylisocyanate yielded the monoacylated product **9b** only, as a consequence of precipitation. Considering the difficulties to diacylate 3,3'-diamino-2,2'-bipyridine with Boc$_2$O, the reaction was repeated with 1 equivalent of Boc$_2$O in order to obtain monoacylated **9c**. The ^{1}H-NMR spectra of several crude reaction mixtures showed reproducibly that the average ratio of mono- and diacylated 3,3'-diamino-2,2'-bipyridine was 85/15. Mono- and diacylated compounds were easily separated by column chromatography, and yields of up to 70% of the former were readily obtained. A survey of the monoacylated compounds **9a–c** and the yields obtained is given in table 2.2.
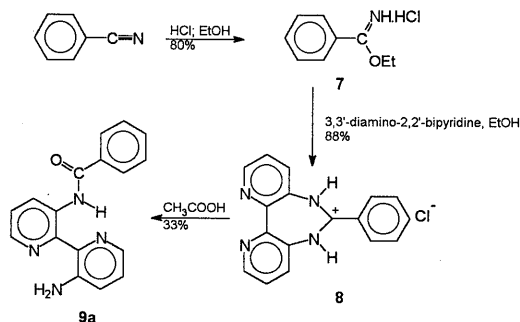
Scheme 2.2: Described synthesis of monoacylated diaminobipyridine[1c]

Table 2.2 *Acylated 3-aminopyridines and monoacylated 3,3'-diamino-2,2'-bipyridines: yields and relevant ^{1}H-NMR and IR data [a]*

Compound	6a	6b	6c	6d
R =	–CF$_3$	-Ph		
Yield (%)	50	60	60	46
δ(NH) (ppm)	9.40	8.43	8.24	13.88
δ(H4)(ppm)	8.35	8.35	8.14	8.52
ν(NH) (cm^{-1})	3416[b]	3430[b]	3402[b]	2910[c]

Compound	9a	9b	9c
R =	–Ph	-(R)-NHCH(CH$_3$)Ph	–OC(CH$_3$)$_3$
Yield (%)	33	87	70
δ(NH) (ppm)	14.74	12.70	12.42
δ(NH$_2$) (ppm)	6.62	6.45	6.35
δ(H4') (ppm)	9.30	8.84	8.76
δ(H4) (ppm)	7.11	7.08	7.10

[a] *All ^{1}H-NMR spectra were measured in CDCl$_3$;* [b] *IR spectra were taken in CDCl$_3$;* [c] *IR spectra were taken in KBr*

2.3 Spectroscopic studies: evidence for H-bond formation

2.3.1 ^{1}H-NMR spectroscopic data

The relevant ^{1}H-NMR data of diacylated compounds **3a–n** is summarised in table 2.1 and compared with the data of the parent 3,3'-diamino-2,2'-bipyridine, **2**. The latter shows a broad signal, centred around 6.26 ppm in CDCl$_3$ and assigned to the NH$_2$ protons. The corresponding amide-NH resonances of the diacylated compounds **3a–n** are located much more downfield, featuring sharp signals up to δ = 15.5 ppm. The shift in the NH absorption upon N-acylation is corroborated by a strong downfield shift of H-4: Δδ up to 2.4 ppm. Furthermore, the H-6 protons undergo the expected modest deshielding, due to the more electron withdrawing character of the C-3 substituent.

Noteworthy is the trend in the chemical shift of the amide-NH with the acid character of ROH, in which R represents the acylating group. Going from *t*-butoxycarbonyl (**3a**) to acetyl (**3b**), methoxycarbonylcarbonyl (**3e**) and trifluoroacetyl (**3c**), the acidity of the corresponding acids (table 2.3) increases steadily as does the δ value of the amide-NH. However, when phenyl groups are incorporated in the acylating group, this trend seems not to be followed. Finally, the chemical shifts of the NH's in the urea and acylurea derivatives (table 2.1) are found at slightly lower values than their amide counterparts (δ(NH) = 13.12 ppm for **3c** compared to δ(NH) = 12.57 ppm for **3l**).

Table 2.3 *pK$_a$ Values of acids corresponding to acylating groups and concomitant δ(NH) values*

Compound	acid	pK$_a$	δ(NH) (ppm)
3d	trifluoroacetic acid	0.23	15.55
3e	methoxycarbonylformic acid	1.23	15.18
3f	benzoic acid	4.19	14.59
3h	*(E)*-cinnamic acid	4.44	13.82
3b	acetic acid	4.75	13.15
3c	hexanoic acid	4.88	13.12
3a	*t*-butoxyformic acid	~7	12.16

In addition, we compared N,N'-diacylated 3,3'-diamino-2,2'-bipyridines with N-acylated 3-aminopyridines. Figure 2.3 shows the ^{1}H-NMR spectra of dibenzoyl derivative **3f** (table 2.1) and its "monomeric" counterpart **6b** (table 2.2). The amide protons in **3f** feature a relative deshielding of ~6.1 ppm while the H-4 protons show a relative deshielding of ~1.1 ppm.
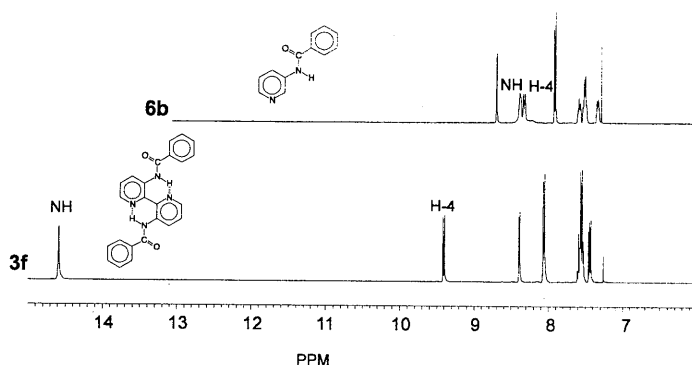
Figure 2.3: ^{1}*H-NMR spectrum of 3,3'-dibenzoylamino-2,2'-bipyridine **3f** compared to that of its monomeric counterpart **6b***

In the case of the 8-quinolinecarbonyl derivatives **3g** and **6d** the amide proton of the monomeric counterpart **6d** also features a low field resonance for the NH proton (δ = 13.88 ppm) (figure 2.4). More specific ^{1}H-NMR data, comparing **3g** to **6d**, is given in table 2.4. As expected, a strongly downfield absorption for H-4 in compound **3g** (δ = 9.31 ppm) is observed while in compound **6d** a normal chemical shift for H-4 at δ = 8.52 ppm is noticed. Another remarkable effect is the relative shielding of H-2' in **3g** when compared with the corresponding proton in **6d** (δ(H-2') = 8.55 ppm for **3g** *vs.* 9.04 ppm for **6d**).
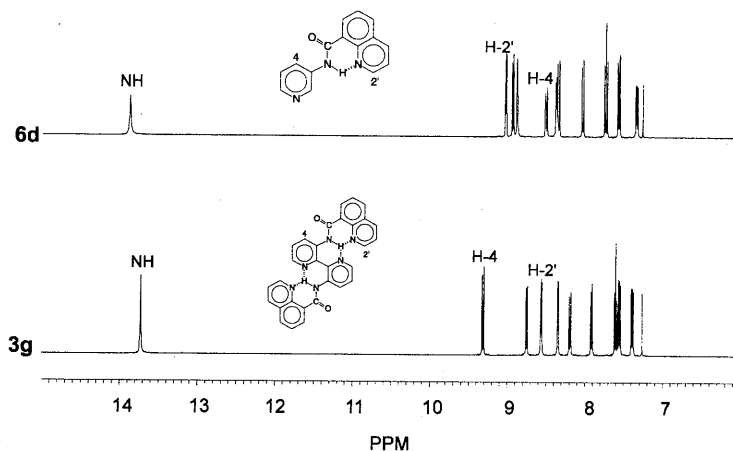
Figure 2.4: ^{1}*H-NMR spectrum of compound **3g** compared to that of its monomeric counterpart **6d***

Table 2.4 *Comparison of the ^1H NMR data of 3g and 6d^a*

	3g	6d
δ(NH)	13.74	13.88
δ(H-2)	/	8.89
δ(H-4)	9.31	8.52
δ(H-6)	8.35	8.39
δ(H-2')	8.55	9.04
δ(H-7')	8.75	8.95

3g   6d
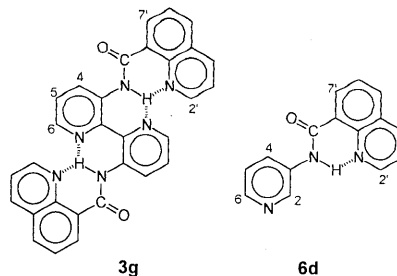
^{a}*All values are given in ppm and measured in CDCl$_3$*

The broad absorption of the NH$_2$ protons of compound **2** at 6.26 ppm in CDCl$_3$ indicates that the amine is not in a fixed conformation but slowly rotating and —as a consequence— H-bonding is marginally present on the NMR time scale. On the other hand, the observation that in a wide range of acylated 3,3'-diamino-2,2'-bipyridines **3a–n** sharp, low field NH absorptions are found, suggests that intramolecular H-bonding is operative in all these compounds. This is confirmed by comparison with their "monomeric" reference compounds, which lack the possibility of intramolecular H-bonding (figure 2.3). Apparently, the H-donor ability (acidity and orientation) of the amide moiety in the diacylated 3,3'-diamino-2,2'-bipyridines **3a–n** matches the H-acceptor behaviour of the pyridine-N-1 perfectly, resulting in intramolecular H-bonding in a six-membered conjugated array.

The downfield shift of H-4 in all acylated compounds **3a–n** can be explained by a planar orientation of the amide moiety with respect to the transoid bipyridine system, in which the carbonyl, pointing to H-4, exerts a downfield anisotropic effect. Therefore, not only the position of the NH signals is an important parameter in determining the presence of the H-bonding, but also the relative position of H-4 is indicative. Reichert *et al.*[4c] have suggested that strong deshielding effects in 2'-substituted anilides result from intramolecular H-bonding between Ar–H and C=O. Also in the present case, the strong deshielding of H-4 might be attributed to such intramolecular H-bonding. All the data are in agreement with the presence of intramolecular H-bonds between the amide function of one ring and the pyridine-N-1 of the other (and vice versa) and this H-bonding leads to a close to planar, transoid bipyridine system, favouring the Ar–H-4---C=O H-bonding.

It can be easily understood that the formation of a H-bond modifies the electron density around the NH proton and hence its shielding. In most cases this gives rise to a downfield shift in ^{1}H-NMR because the electron density in the immediate vicinity of the hydrogen is reduced. However, when anisotropic magnetic currents arise from the hydrogen acceptor, both shielding and deshielding effects can result[10c]. For intermolecular H-bonds, it has been

shown that H-bond strength and the position of the NH/OH signals in NMR are interrelated[10a]. Furthermore, in aromatic hydroxy compounds, correlation functions have been established that relate the acidity of the OH with the δ(OH) value[11]. Therefore, one can expect a relationship between δ(NH) and the pK_a of the acid derived from the acylating group in the bipyridine system. Such a relationship is indeed observed as can be deduced from table 2.3. When phenyl moieties are part of the acylating group, deviations occur due to additional anisotropic deshielding effects. This is exemplified by acetyl and benzoyl acylation: pK_a's are comparable in both cases, still the δ(NH) values differ significantly (> 1.4 ppm).

The relation between NH acidity, reflected by the pK_a of the carboxylic acid derived from the acylating group, and H-bond strength is further exemplified by comparing amide **3c** to urea **3l**. The amide protons in **3c** (δ(NH) = 13.12 ppm) are more acidic than the urea protons in **3l** (δ(NH) = 12.57 ppm) due to cross conjugation in the latter. As mentioned above, also the position of H-4 is an important probe to study planarity. In the amide group, the C–N bond has more double bond character than in the urea group. Therefore, the carbonyl in the latter features a lower degree of coplanarity with the pyridine ring as expressed by the δ values assigned to H-4 in compounds **3c** (δ = 9.06 ppm) and **3l** (δ = 8.86 ppm), respectively.

Finally, compound **3g** and monomeric reference compound **6d** both feature intramolecular H-bonds. In compound **6d**, however, the pyridine ring is free to rotate which is translated in the usual value for the chemical shift of H-4 (δ = 8.52 ppm). It is clear from the low field absorption of H-4 (δ = 9.31 ppm) in compound **3g** that the amide group is positioned in the plane of the pyridine unit. The relative shielding of H-2' in **3g** may result from some repulsion between H-6 of the pyridine and H-2' of the quinoline ring when compared with the corresponding proton in **6d**. This forces the quinoline ring out of planarity resulting in less deshielding of H-2' by the pyridine ring. This can explain to some extent the upfield shift from δ = 9.04 ppm in **6d** to δ = 8.55 ppm in **3g**. In contrast to H-2', the chemical shifts of H-7' in **3g** (δ = 8.75 ppm) and **6d** (δ = 8.95 ppm) do not differ significantly, presumably due to the smaller effect of rotation around the C-8' – C=O bond on the distance between H-7' and the carbonyl moiety. Based on the ^{1}H-NMR data, a structure incorporating bifurcated H-bonds is proposed for compound **3g** as shown in figure 2.4.

The discussion so far has focused on intramolecular H-bonding, ignoring the possibilities of intermolecular interactions. The urea and acylurea compounds may have the possibility to organise themselves into associates. No evidence for an association in solution in the ^{1}H-NMR spectra of urea derivatives has been observed. However, the broad peaks in ^{1}H-NMR of acylurea **3n** in toluene (see paragraph 2.5 for more information) and the complete insolubility

of dibenzoylurea **3m** in organic solvents indicate aggregation in solution and strong intermolecular interactions in the solid state.

2.3.2 Infrared spectroscopic data

In view of the sensitivity of the vibrational modes to the presence of H-bonding, the NH stretch frequencies of the amide derivatives are frequently used to confirm the presence of H-bonding. There is a common agreement that in most cases the NH stretch absorption (i) shifts to lower frequency (ii) becomes broader (iii) increases in intensity when a H-bond is present.

All IR data were obtained from KBr pellets or in CDCl$_3$ solutions (l = 0.1 mm, c ≈ 10 mmol) and are summarised in table 2.1 and 2.2. In KBr, diamino compound **2** shows two stretch frequencies at 3352 and 3221 cm^{-1}, indicating that in the solid state the amine-NH's are different. Also in CDCl$_3$, two NH stretch frequencies can be distinguished at 3471 and 3261 cm^{-1}.

All NH-stretch vibrations in KBr of compounds **3a–j** appear in the region of the CH stretch (around 3000 cm^{-1}) as broadened peaks and increased in intensity. A selection of compounds was also measured in solution and although differences between the solid state and the solution spectrum were present, the NH-stretch was still found in the region of CH stretch (compound **3f** in figure 2.5).

For the monomeric reference compounds **6a–c** , the IR spectra were taken in CDCl$_3$ and the NH-stretch could be clearly distinguished as a sharp peak around 3400 cm^{-1}. In KBr, on the other hand, the identification of the NH stretch is hampered again because of the CH stretch frequencies which are found in the same region. In figure 2.5 the IR spectra of compound **6b** are given both in the solid state as in solution.
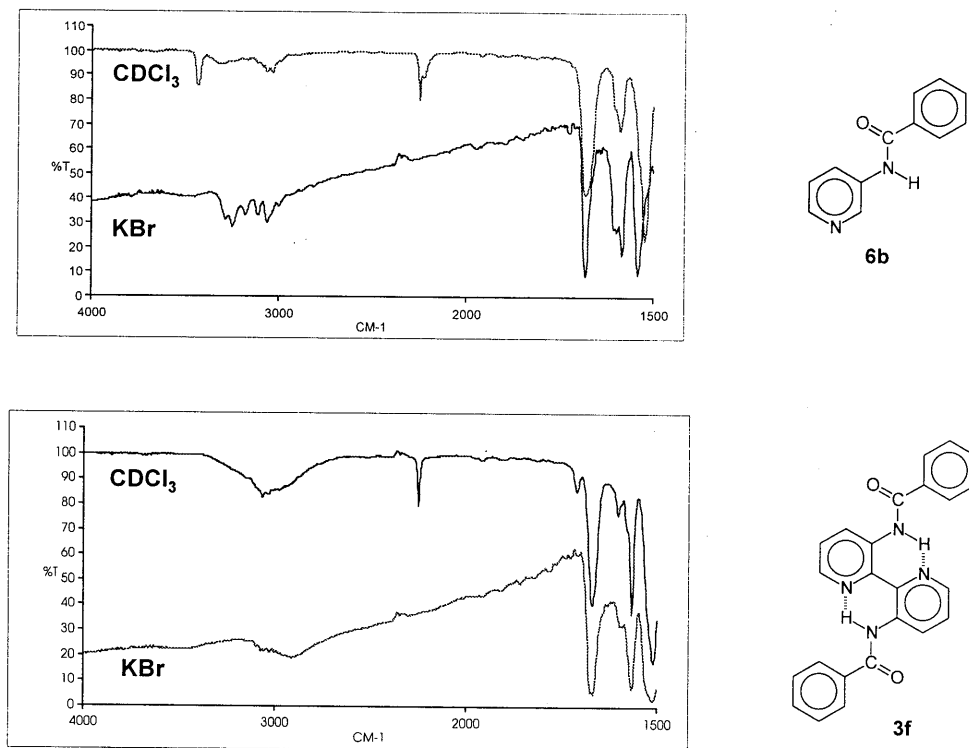
*Figure 2.5: IR spectra of compound **6b** and compound **3f** in CDCl₃ and in KBr pellets*

In the crystalline state (see paragraph 2.4) compound **2** is engaged in intramolecular as well as intermolecular H-bonds. This has been confirmed by the IR spectrum in KBr of compound **2**. The lower value (3221 cm^{-1}) can be attributed to the intramolecular H-bonded species while the higher value (3352 cm^{-1}) results from intermolecularly H-bonded species. In solution, the NH$_2$ in compound **2** is also engaged in intramolecular H-bonding, which can be deduced from the two NH stretch vibrations (3471 and 3261 cm^{-1}). The intermolecular H-bonding has, however, largely disappeared which can be concluded from the large differences in the higher NH-stretch values (3352 vs. 3471 cm^{-1}). This is in contrast with the observation in ^{1}H-NMR where only an average absorption peak for the NH$_2$ is found at room temperature in solution.

For the diacylated compounds **3a-j**, the IR spectra in solution and in the solid state resemble each other much more although differences are still present. Consequently, the intramolecular H-bonds in compounds **3a–j** are not significantly affected when the compounds are in solution. Unfortunately, the overlap of absorptions, both in the solid state and in solution, makes an exact assignment of the NH stretch difficult. Therefore, the values given in table 2.1 must be handled with some care. Due to the problems to unambiguously identify the NH

stretch vibration, IR spectroscopy is not a reliable technique to study intramolecular H-bonding in acylated diamino-bipyridines.

2.4 Single crystal X-ray diffraction studies

X-Ray quality crystals of three compounds were obtained: 3,3'-diamino-2,2'-bipyridine **2**, monobenzoyl compound **9a** and dicinnamoyl compound **3h** (figure 2.6). X-Ray quality crystals of compound **2** were obtained by slowly cooling a hot aqueous solution. Crystals of compound **9a** were grown by slow cooling of a hot, saturated solution in CH_3CN. Finally, crystals of compound **3h** were obtained from a slowly evaporating solution in $CHCl_3$. In table 2.5, the crystallographic data are collected. Table 2.6 summarises all the inter- and intramolecular interactions found in the crystal lattices.
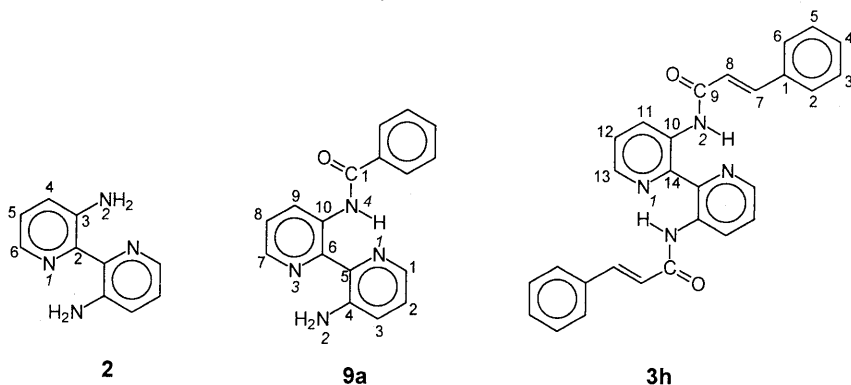
Figure 2.6: Compounds 2, 9a and 3h; the numbering of the atoms is in accordance with the numbering of the atoms in the X-ray structures as depicted in figures 2.7–2.9

Table 2.5   *Survey of the crystallographic data collected for compounds*
2, 9a and 3h

Data	2	9a	3h
formula	$C_{10}H_{10}N_4$	$C_{17}H_{14}N_4O$	$C_{28}H_{22}N_4O_2$
recrystallisation solvent	H_2O	CH_3CN	$CHCl_3$
formula weight	186.22	290.32	446.50
colour, habit	yellow plates	light yellow rhombs	yellow needles
lattice type	monoclinic	orthorhombic	monoclinic
space group	$P_{21/c}$	P_{na21}	$P_{21/c}$
cell dimensions			
a (Å)	7.781(5)	11.862(5)	11.228(10)
b (Å)	7.231(3)	6.027(5)	6.572(11)
c (Å)	12.056(6)	6.027(5)	6.572(11)
α (deg)	90	90	90
β (deg)	117.78(5)	90	119.47(7)
γ (deg)	90	90	90
V (Å^3)	433.77(5)	1412.79(16)	1070.40(2)
Z	2	4	2
D_c (g/cm^3)	1.4256(2)	1.3649(2)	1.3853 (3)
F (000)	196	608	468
μ (cm^{-1})	0.9	6.8	0.8
R1	0.044	0.036	0.043
wR2	/	0.092	0.112

Table 2.6   *Inter- and intramolecular interactions found in the crystal lattices of*
compounds 2, 9a and 3h

2	H-donor	H	H-acceptor	distance D–A (Å)	angle D–H–A (degrees)
intra	N(2)	H(21)	N(1)	2.66	132.0
inter	N(2)	H(22)	N(2')	3.23	164.6
9a					
intra	N(2)	H(2a)	N(3)	2.67	133.0
	N(4)	H(4a)	N(1)	2.60	147.0
	C(9)	H(9)	O(1)	2.86	121.9
inter	N(2)	H(2b)	O(1')	3.27	158.0
	C(3)	H(3)	O(1')	3.35	150.2
3h					
intra	N(1)	H(1a)	N(2)	2.61	142.9
	C(11)	H(11)	O(1)	2.86	122.7
inter	C(1)	H(1)	O(1')	3.34	140.5

The X-ray structure of compound **2** shows that the two pyridine rings are in an entirely planar, transoid conformation (figure 2.7). The pyridine-N as well as the amine-N act as H-bond acceptors and this allows all amine hydrogen atoms to be involved in H-bonding. Due to the presence of intermolecular H-bonds, infinite arrays of H-bonded molecules are formed. The presence of edge-to-face as well as face-to-face aromatic stacking interactions favours a structure resembling a herringbone (figure 2.7). The distance between two parallel stacks is 5.23 Å. From table 2.6 can be deduced that the intramolecular H-bonds are identical and the N–H---N distance is as short as 2.66 Å. All intermolecular bonds are also identical with a distance of 3.23 Å between donor and acceptor.
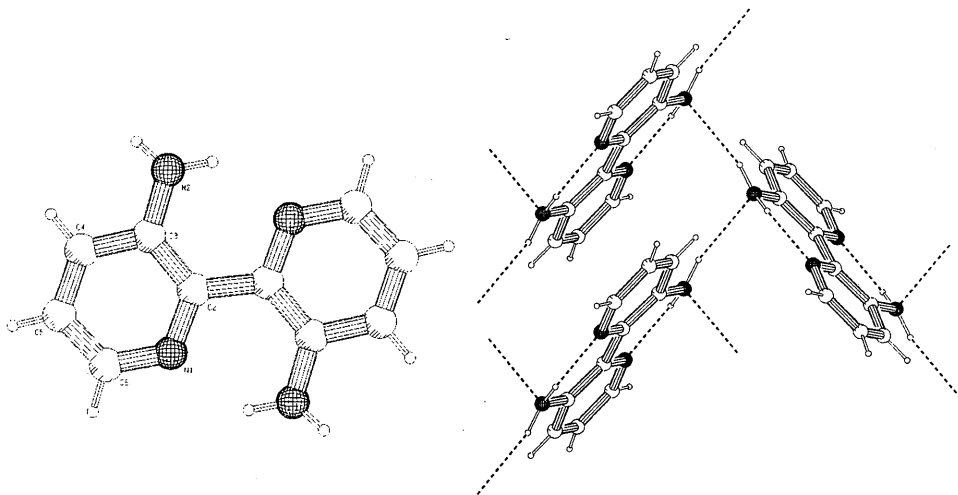
Figure 2.7: Crystal structure of 2 and its packing in the crystal lattice

In case of compound **9a**, the two pyridine rings deviate slightly from planarity: the torsion angle is 8°. The amide functionality is coplanar with the pyridine ring but not with the phenyl ring, which deviates 20° from the plane of the amide CONH–Py. Three intramolecular H-bonds are present. The amide-NH as well as one amine-NH act as H-donor. Furthermore, an intramolecular H-bond is found between C(9)–H(9) and O(1) as a result of the distance of 2.86 Å and the angle of 122 degrees between donor and acceptor. The remaining amine-NH is intermolecularly H-bonded to the C=O of the adjacent molecule, giving rise to infinite H-bonded chains (figure 2.8). A second intermolecular H-bond is marked between C(3)–H(3) and O(1'). Although assigning this intermolecular interaction to a H-bond is disputable, the distance between C(3) and O(1') is within the limits wherein H-bonds are considered to occur. In this case, the short distance between C(3) and O(1') probably originates from packing effects in the crystal lattice in combination with the intermolecular N–H---O(1') interaction.
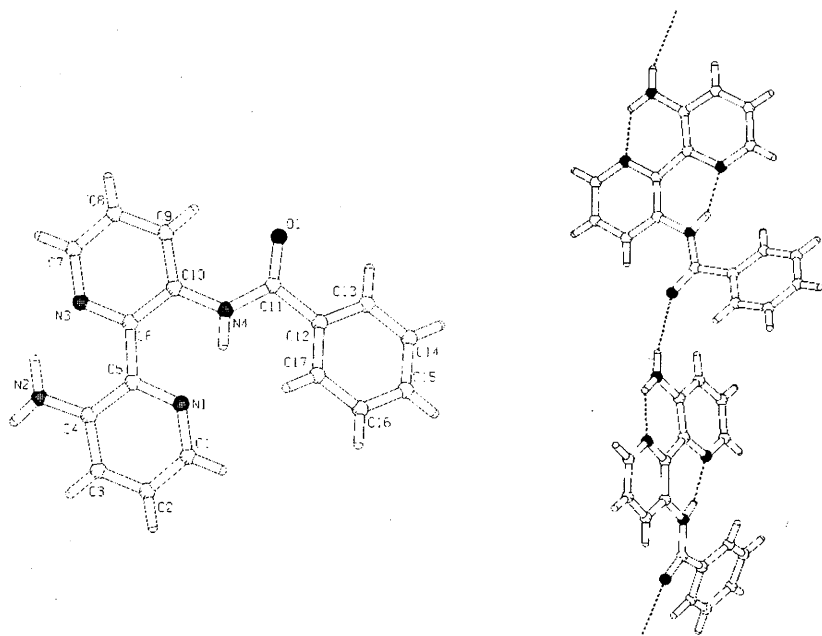
*Figure 2.8: Crystal structure of **9a** and the infinite H-bonded chains observed in the crystal lattice*

For compound **3h**, again, the torsion angle between the two pyridine rings is 0°, leading to a completely planar, centrosymmetric bipyridine system. The plane of the amide function, however, deviates 13.4° from the plane of the pyridine ring. Intramolecular H-bonding is present between the amide–NH and the pyridine-N and between the pyridine-H(11) and the C=O. Although disputable (vide supra), an intermolecular H-bond is marked between C(1)–H(1) and O(1') of an adjacent molecule. Figure 2.9 shows that the phenyl rings show edge-to-face stacking. Furthermore, the distance between two ethylenic bonds is approximately 6.5 Å, which implies that solid state photochemical dimerisation/polymerisation of the cinnamic acid derivative is not possible. According to Schmidt *et al.* distances should be within 3.5–4.7 Å for photochemical reactions to occur[12]. All our efforts to photochemically dimerise/polymerise **3h** failed accordingly.
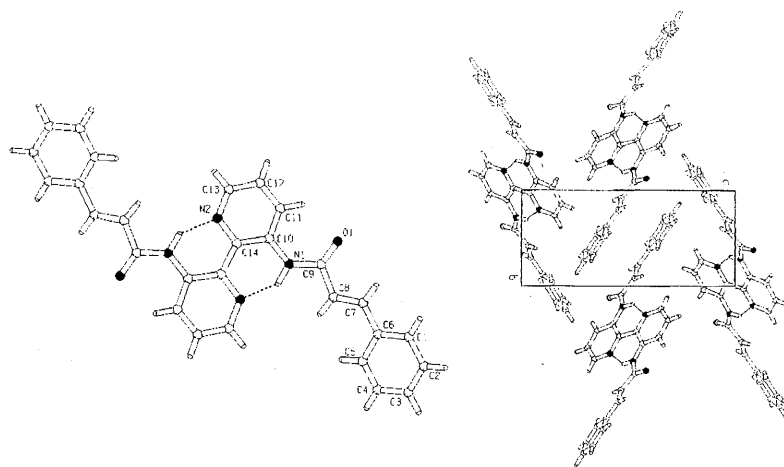
Figure 2.9: Crystal structure of 3h and view of the crystal lattice

In compound **2**, the dihedral angle of 0° suggests that the planar transoid conformation is energetically favoured which is in accordance with the statement that also in solution this conformation corresponds to an energy well. In compounds **3h** and **9a** the suggestion is confirmed that in solution intramolecular H-bonds might be present between C=O and H-4 of the pyridine ring. Considering the empirical rule discussed in Chapter 1 that if the difference between the sum of the van der Waals radii of donor and acceptor and the measured distance between H-bond donor and acceptor with X-ray diffraction is between the values of 0.25 and 0.5 Å, the H-bonds present can be considered as strong H-bonds and their energies range between 50 and 100 kJ/mol[10b]. For compounds **2**, **9a** and **3h**, these differences range from 0.436 to 0.50 Å. Hence, it is concluded that in the solid state strong intramolecular H-bonding is present between amine- or amide-NH and pyridine-N and that the binding energies will range from 50 to 100 kJ/mol.

2.5 Strength of H-bonding: medium and temperature effects

In order to evaluate qualitatively the strength of the intramolecular H-bonds of compounds **3a–n** in solution, the ^{1}H-NMR data were recorded as a function of concentration, medium and temperature. To investigate whether any concentration effect would occur, concentration dependent ^{1}H-NMR spectra of compound **3c** in CDCl$_3$ were taken. As can be expected for strong *intra*molecular H-bonds, no significant chemical shift variations of the δ(NH) and δ(H-4) were found: the δ values for NH and H-4 protons range from 13.197 (0.15 M) to 13.193 (0.015 M) ppm and 9.149 (0.15 M) to 9.150 (0.015 M) ppm, respectively.

The effect of various solvents on the ^{1}H-NMR spectra and hence on the secondary structure in this series of acylated bipyridines is exemplified for dibenzoyl compound **3f** in table 2.7. The position of the amide proton in **3f** is hardly affected by all solvents investigated with the exception of trifluoroacetic acid ($pK_a = 0.23$) and dichloroacetic acid ($pK_a = 1.48$). Strong proton acceptors like DMSO and HMPA are not capable of affecting the H-bonds. Neither acetic acid ($pK_a = 4.75$) and formic acid ($pK_a = 3.75$) nor strong bases as triethylamine (TEA) or 4-dimethylamino-pyridine (DMAP) influence the intramolecular H-bonding in **3f** significantly.

Table 2.7 *Influence of the medium on the H-bonding* [a]

3f	δ(NH)	δ(H-4)	δ(H-6)
CDCl₃	14.59	9.42	8.41
toluene-d8	14.70	9.70	8.00
DMSO-d6	14.24	9.25	8.63
CDCl₃/HMPA 9/1	14.58	9.40	8.35
CD₃COOD/CDCl₃ 3/1	(14.60)	9.37	8.46
CDCl₃/CF₃COOH 3/1	9.90	8.95	8.80
CDCl₃/HCOOH 3/1	14.50	9.38	8.47
CDCl₃/CHCl₂COOH 3/1	10.20	8.85	8.30
CDCl₃/DMAP 3/1	14.60	9.42	8.40
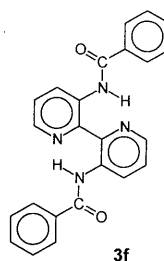
[a] All values are given in ppm; DMAP = 4-dimethylamino-pyridine; HMPA = hexamethylphosphortriamide

These results indicate that as long as the compounds are in a neutral state, the H-bond is retained. In contrast, the H-bonds do break due to salt formation in very strong acids such as trifluoroacetic acid (TFA). When a base like TEA was added to the solution, the H-bonds were restored immediately, confirming the reversibility of the H-bonding.

To evaluate the dependence of the strength of the intramolecular H-bonds in acylated bipyridines on the temperature of the medium, variable temperature ^{1}H-NMR measurements on compound **3i** in DMSO-*d6* were performed (figure 2.10). There is some weakening of the H-bonding, as expressed by the upfield shift of the amide-NH resonance with the increase of temperature ($\Delta\delta/\Delta T = 5.8 \times 10^{-3}$ ppm/K). However, the H-bonds do not collapse at higher temperatures (110°C). Other representatives of the **3** and **9** series were investigated as well and the results are summarised in table 2.8. A similar behaviour is found in all compounds except for acylurea **3n** where considerable changes for the additional imide-NH were noticed.
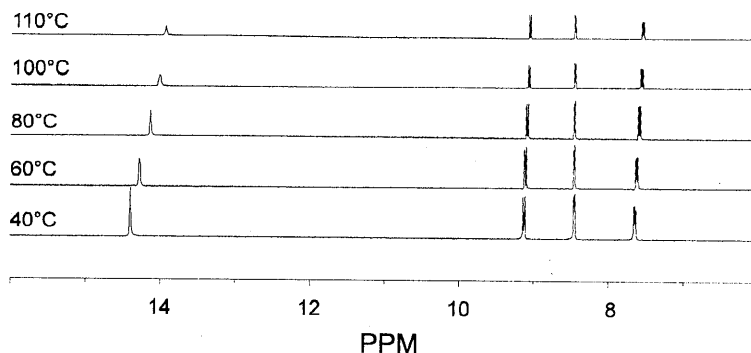
Figure 2.10: Variable temperature ^{1}H-NMR spectra of compound 3i in DMSO-d6

Table 2.8   *Variable ^{1}H-NMR data of acylated diaminobipyridines*

Compound	Solvent	$\Delta\delta/\Delta T$ (ppm/K)	Temperature range (°C)
3a	toluene-*d8*	4.6×10^{-3}	20–100
3f	toluene-*d8* DMSO-*d6*	3×10^{-3} 4.6×10^{-3}	20–70 20–90
3i	toluene-*d8* DMSO-*d6*	5.5×10^{-3} 5.8×10^{-3}	20–100 20–110
3n	toluene-*d8*	7×10^{-3} (amide-NH) 24×10^{-3} (imide-NH)	50–100
6d	DMSO-*d6*	2.9×10^{-3}	20–100
9a	DMSO-*d6*	5.1×10^{-3}	20–100
9b	DMSO-*d6*	3.7×10^{-3}	20–100

These data are in agreement with some temperature dependent measurements reported by Hamilton and co-workers[13] ($\Delta\delta/\Delta T$ = 3.0×10^{-3} and 1.5×10^{-3} ppm/K, in an unspecified temperature range). In our case, not the medium is responsible for the $\Delta\delta/\Delta T$ values but the intrinsic strength of the H-bond. The weaker H-bonding present in acylurea derivative **3n** induces more substantial changes in $\Delta\delta/\Delta T$ (7×10^{-3} ppm/K) compared to the relatively stronger H-bond of **3f** (3×10^{-3} ppm/K). The imide-NH in compound **3n** does undergo stronger changes ($\Delta\delta/\Delta T$ = 24×10^{-3} ppm/K) which can be explained by the break down of *inter*molecular H-bonds at elevated temperatures. In contrast to intramolecular H-bonds, intermolecular H-bonds are known to be highly temperature and concentration dependent[10c]. Variable temperature measurements from 0°C to –60°C on monobenzoyl derivative **9a** in acetone-*d6* (figure 2.11) were performed to investigate the behaviour of the amine at low temperatures. The amide-NH absorption is sharpened with the decrease of the temperature and shifts to lower field. Remarkable is the behaviour of the amine-NH protons, which are present as a broad singlet until 0°C. A dramatic change takes place at –50°C were two

singlets appear at δ = 6.4 and δ = 9.0 ppm, respectively, separated by 2.6 ppm. This large difference is attributed to restriction in conformational freedom of the amine and consequently the formation of a H-bond between one amine-NH and the pyridine-N of the adjacent ring. Compound **2** shows a similar behaviour. This phenomenon has also been reported for 3-amino-6,6'-dimethyl-2,2'-bipyridine[14].
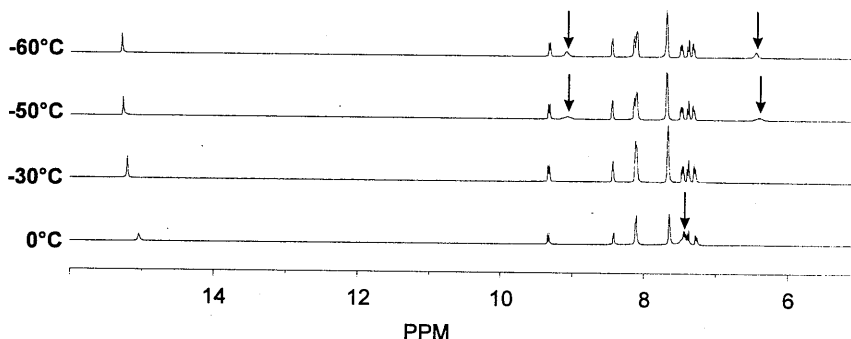
*Figure 2.11: Variable temperature ^{1}H-NMR spectra of compound **9a** in acetone-d6*

The results reveal that the intramolecular H-bonds in the conjugated, six-membered 4-acylamino-1-azadiene moiety, are not affected considerably either by temperature variations, or by solvent polarity. Therefore, the secondary structure of the diacylamino-bipyridine moiety is stable in a broad range of environments. On the other hand, it is possible to destroy the intramolecular H-bonds with the addition of strong acids, but H-bonding is restored after adding a base. This protonation/deprotonation might be a useful principle to reversibly induce the secondary structure in this diamino-bipyridine unit.

2.6 Optical activity of acylated 3,3'-diamino-2,2'-bipyridines

To investigate the degree of non-planarity of the bipyridines and the transfer of chirality in solution, UV and CD spectra of the enantiomeric bipyridine derivatives **3i** and **3j** (*see* p. 21) were recorded. Monoacylated bipyridine derivative **9b** and pyridine derivative **6c** were used as reference compounds (*see* p. 23).

The UV spectra of the bipyridines **3i–j** show three peaks in MeOH with λ_{max} at 226, 267 and 336 nm in MeOH. The λ_{max} at 336 nm is attributed to the transition of the bipyridine unit. The CD spectra of the four optically active products are recorded in MeOH and are represented in figure 2.12. The CD spectrum of compound **3i** shows one negative (λ_{max} = 226 nm) and two positive (λ_{max} = 267 and 336 nm) Cotton effects. The expected mirror image relationship between **3i** and **3j** is observed indeed. No evidence for exciton coupling can be found in the spectra. Monoacylated compound **9b** shows a similar behaviour: λ_{max} at 210, 265 and 361 nm

in MeOH and a Cotton effect in all three the absorption bands. Reference compound **6c**, on the other hand, does not exhibit any significant Cotton effect in the range of 225 to 400 nm.
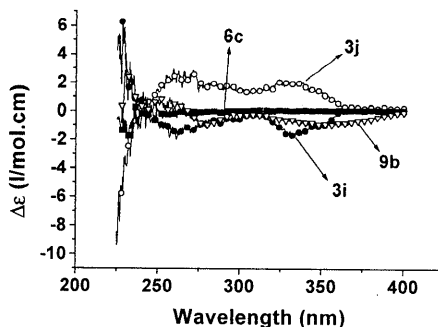
Figure 2.12: CD spectra of (+) and (–)-3,3'-dicamphanoylamino-2,2'-bipyridine, 3i–j, (–)-3-camphanoyl-amino-pyridine, 6c, and 3'-α-methylbenzylaminocarbonylamino-2,2'-bipyridine-3-amine 9b recorded in MeOH

The Cotton effects found at $\lambda = 336$ nm in compounds **3i–j** —corresponding to the transition of the bipyridine— are small but significant. The same holds for urea derivative **9b**. The effects are in agreement with the induction of chirality in the $\pi–\pi^*$ transition of the bipyridine due to local chirality and are not indicative for a strong preference of the bipyridine unit into an axial chiral conformation (see also Chapter 6).

2.7 Cooperativity in H-bonding

The presence or absence of cooperativity in the diacylated bipyridine system was analysed in more detail by ^{1}H-NMR spectroscopy. The ^{1}H-NMR spectra of dibenzoyl derivative **3f** and monobenzoyl derivative **9a**, recorded in CDCl$_3$, are compared in figure 2.13. The NH signal in **9a** appears at approximately the same chemical shift as that of diacylated compound **3f**. Variable temperature ^{1}H-NMR experiments of compound **9a** in DMSO ranging from 20 to 100°C (table 2.8) show a similar temperature independent behaviour as observed for compound **3f** ($\Delta\delta/\Delta T = 5.1\times10^{-3}$ ppm/K for **9a** and $\Delta\delta/\Delta T = 4.6\times10^{-3}$ ppm/K for **3f**). This implies that cooperativity is not needed for strong H-bonding and a preferred conformation of the bipyridine moiety. The NH resonance of **9a** ($\delta = 14.74$ ppm) is even somewhat more shifted downfield with respect to the NH resonance of **3f** ($\delta = 14.59$ ppm). One explanation emerges from considering H-donor and H-acceptor abilities of NH–CO and pyridine–N-1, respectively. Indeed, acylation of one aminopyridine ring diminishes the H-acceptor ability of that ring, which is reflected in a slightly less downfield NH absorption upon the second acylation.
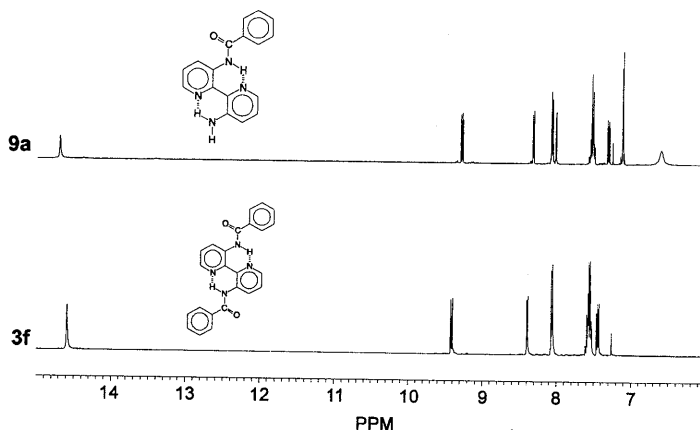
*Figure 2.13: ^{1}H-NMR spectra of compounds **3f** and **9a**: influence of single and double H-bonding in 3,3'-diamino-2,2'-bipyridines on chemical shifts*

2.8 Conclusions

^{1}H-NMR data regarding a series of mono- and diacylated 3,3'-diamino-2,2'-bipyridines unambiguously show the occurrence of intramolecular H-bonding, leading to a planar, transoid bipyridine system. Not only the position of the NH–CO proton absorption is indicative of H-bonding but also the deshielding of the H-4 proton as a result of a coplanar conformation of the NH–CO-group with respect to the bipyridine unit. Single crystal X-ray diffraction reveals that in the solid state this intramolecular H-bonding between the pyridine-N and the amide-NH can be considered to be "strong". In addition, there is also H-bonding present between the C=O and H-4 of the pyridine of an adjacent ring. The presence of H-bonds has also been studied using IR spectroscopy although the overlap of N–H stretch and C–H stretch vibration complicates a correct assignment.

Furthermore, the intrinsic strength of the intramolecular H-bonding and overall secondary structure in the bipyridine moiety in solution is demonstrated under various conditions like high temperatures and polar protic solvents. Only the addition of strong acids ($pK_a < 1.5$) leads to H-bond collapse due to protonation; the addition of a strong base restores the H-bonds. The reversible breaking and restoring of these order introducing H-bonds could be useful in further applications of the bipyridyl moiety in supramolecular chemistry.

Upon incorporation of the 8-quinolinecarbonyl group in the structure, the CO–NH group shares, as H-bond donor, its hydrogen with both the pyridine and the quinoline H-bond acceptors, leading to bifurcated H-bonding, which offers the possibility to extend the system to rigid-rod polymers.

No cooperativity is found to be operative in the H-bonded diacylated 3,3-diamino-2,2'-bipyridines. Due to its strength, one intramolecular H-bond is sufficient to force the bipyridine into planarity, as is demonstrated with monoacylated bipyridines.

The strong intramolecular H-bonding present in the 3,3'-di(acylamino)-2,2'-bipyridine moiety creates a structuring motif which can be incorporated in several supramolecular structures. Rigid-rod polymers can be conceived, in which one-dimensional ordering arises from bifurcated H-bonding or a preferred conformation (Chapter 3). Large disc-shaped molecules —in which rigidification of the central core results from intramolecular H-bonding in the bipyridine units— may lead to mesophases with enhanced temperature stability (Chapter 4). Finally, macrocycles can be envisaged for the construction of one-dimensional channels[15].

2.9 Experimental procedures

^{1}H-NMR and ^{13}C-NMR spectra were recorded on a Bruker AM-400 (400.13 MHz for ^{1}H-NMR and 100.62 for ^{13}C-NMR). UV spectra were taken on a Perkin Elmer Lambda 3B UV-VIS spectrophotometer. Infrared spectra were recorded on a Perkin-Elmer 1605 FT-IR. CD measurements were recorded on a Jasco J-600 spectropolarimeter. Optical rotations were recorded on a Jasco DIP-370 polarimeter at a wavelength of 589 nm (Na$_D$-line). Melting points were recorded with an Linkam THMS 600 hot stage. Elemental analyses were carried out using a Perkin Elmer 240. Single crystal X-ray crystallography data were obtained with an Enraf-Nonius CAD4 Turbo diffractometer on rotating mode: Mo Kα radiation, graphite monochromator, λ = 0.71073 Å in case of compounds **2** and **3h**, Cu Kα radiation, λ = 1.5418 Å in case of compound **9a**. Diethyl ether was dried on CaCl$_2$ and stored on Na-wire, THF was distilled from Na/benzophenone and CH$_2$Cl$_2$ was dried on CaCl$_2$ and destilled from P$_2$O$_5$. EtOH was dried by reflux during for 3 h in the presence of Mg followed by distillation.

3,3'-Dinitro-2,2'-bipyridine (1)[6]
Copper bronze (40 g, 0.63 mol) and 2-chloro-3-nitro-pyridine (40 g, 0.25 mol) in DMF (200 ml) were heated at 100°C. The reaction was monitored by TLC (eluent: toluene/EtOAc 1/1). When all starting material had disappeared, the reaction mixture was poured into water (300 ml), the remaining precipitates filtered off and washed with water (3x50 ml). Soxhlet extraction of the solid residue for 4 days with CH$_3$CN (500 ml), evaporation of the solvent *in vacuo* and treatment of the resulting solids with 10%- ammonia solution to remove Cu salts yielded after filtration **2** as a yellow powder (24 g, 78%, lit. 51%). Recrystallisation from CH$_3$CN gave an analytically pure sample. M.p. 210–211°C (lit. 206°C). ^{1}H-NMR (DMSO-*d6*): δ 8.94 (dd, 2H, *J* = 1.4 and 4.8 Hz, H-6); 8.72 (dd, 2H, *J* = 1.4 and 8.4 Hz, H-4); 7.89 (dd, 2H, *J* = 4.8 and 8.3 Hz, H-5). ^{13}C-NMR (DMSO-*d6*): δ 153.0 (C-6); 149.2 (C-3); 144.6 (C-2); 133.8 (C-4); 125.4 (C-5). Anal. calcd. for C$_{10}$H$_6$N$_4$O$_4$ (246.18): C, 48.79; H, 2.45; N, 22.76. Found: C, 48.9; H, 2.7; N, 22.9.

2,2'-Bipyridine-3,3'-diamine (2)[1a]
The synthesis was accomplished according to the previously described procedure. After recrystallisation from water pure **3** was obtained as yellow needles (3.17 g, 70%). M.p. 136.5–137.5°C (lit: 133–135°C). ^{1}H-NMR (CDCl$_3$): δ 7.96 (dd, 2H, *J* = 2.2 and 3.7 Hz, H-6); 7.02 (m, 4H, H-4 and H-5); 6.26 (bs, 2H, NH). ^{13}C-NMR (CDCl$_3$): δ 143.7 (C-3); 140.5 (C-2); 135.7 (C-6); 123.9

(C-4); 122.9 (C-5). Anal. calcd. for $C_{10}H_{10}N_4$ (186.22): C, 64.50; H, 5.41; N, 30.09. Found: C, 65.6; H, 5.4; N, 30.3.

3,3'-Di(t-butoxycarbonylamino)-2,2'-bipyridine (3a)

Compound **2** (0.6 g, 2.75 mmol) and Boc$_2$O (3 g) in THF (15 ml) were heated under reflux for 48 h. After cooling, the solvent was evaporated *in vacuo*. The crude compound was recrystallised from MeOH to yield pure **3a** as white plate-shaped crystals (0.7 g, 57%). M.p. 163.5–164.5°C. ^{1}H-NMR (CDCl$_3$): δ 12.16 (s, 2H, NHCO); δ 8.80 (dd, 2H, H-4); 8.26 (dd, 2H, H-6); 7.32 (dd, 2H, H-5); 1.52 (s, 18H, C(CH$_3$)$_3$).^{13}C-NMR (CDCl$_3$): δ 153 (C=O); 142.5; 139.7; 137.0; 128.3; 123.6; 28.32 (quat.C). Anal. calcd. for $C_{20}H_{26}N_4O_4$(386.45): C, 62.16; H, 6.78; N, 14.50. Found: C, 61.7; H, 6.9; N, 14.4.

3,3'-Di(acetylamino)-2,2'-bipyridine (3b)[1a]

The procedure was executed as described. M.p. 233–234°C (lit: 225–226°C).^{1}H-NMR (CDCl$_3$): δ 13.15 (s, 2H, NHCO); 9.10(dd, $J = 1.7$ and 8.5 Hz, 2H, H4); 8.34 (dd, $J = 1.6$ and 4.6 Hz, 2H, H-6); 7.38 (dd, $J = 4.5$ and 8.5, 2H, H-5); 2.24 (s, 6H, CH$_3$). Anal. calcd. for $C_{14}H_{14}N_4O_2$ (270.29): C, 62.21; H, 5.22; N, 20.73. Found: C, 61.7; H, 5.3; N, 21.5.

3,3'-Di(trifluoroacetylamino)-2,2'-bipyridine (3d)

To a solution of **2** (180 mg, 1 mmol) in dry THF (5 ml), trifluoroacetic anhydride (3 ml) was added. After boiling under reflux for 3 h, the mixture was evaporated *in vacuo*. The resulting solid was suspended in boiling MeOH, filtered and washed with hot MeOH. Pure **3d** was obtained as a cream-coloured powder (319 mg, 87%). M.p. 247–248°C. ^{1}H-NMR (CDCl$_3$): δ 15.55 (s, 2H, NHCO); 9.23 (dd, 2H, $J = 8.7$ and 1.4 Hz, H-4); 8.46 (dd, 2H, $J = 4.4$ and 1.2 Hz, H-6); 7.52 (dd, 2H, $J = 8.5$ and 4.7 Hz, H-5). Anal. calcd. for $C_{14}H_8F_6N_4O_2$ (378.23): C, 44.46; H, 2.13; N, 14.82. Found: C, 44.8; H, 2.4: N, 14.8.

General procedure for the acylation of 2 with acid chlorides

To an ice-cooled and stirred solution of **2** and TEA (2 eq.) in dry diethyl ether (0.1 M) under argon atmosphere, a solution of the acid chloride (2 eq) in dry diethyl ether (0.2 M) was added dropwise. After 1 h the ice bath was removed and stirring was continued until TLC showed the absence of the starting materials.

3,3'-Di(hexanoylamino)-2,2'-bipyridine (3c)

After stirring at room temperature for 2 h the precipitates were filtered, washed with water to remove the TEA salt, dried and recrystallised from MeOH to yield pure **3c** as cream coloured plates (0.3 g, 73%). M.p. 107–108°C. ^{1}H-NMR (CDCl$_3$): δ 13.12 (s, 2H, NH); 9.06 (dd, 2H, $J = 1.7$ and 8.5 Hz, H-4); 8.25 (dd, 2H, $J = 1.7$ and 4.3 Hz, H-6); 7.30 (dd, 2H, $J = 4.6$ and 8.5 Hz, H-5); 2.37 (t, 4H, COC$\underline{H}_2$); 1.70 (qui, 4H, COCH$_2$C$\underline{H}_2$); 1.31 (m, 4H, C$\underline{H}_2$CH$_2$CH$_3$); 0.82 (t, 6H, C$\underline{H}_3$).^{13}C-NMR (CDCl$_3$): δ 172.6 (C=O); 141.9 (C-2); 140.2 (C-6); 136.7 (C-3); 129.9 (C-4); 123.9 (C-5); 38.7 (CO$\underline{C}$H$_2$); 31.3 (COCH$_2$$\underline{C}H_2$); 25.2 ($\underline{C}H_2CH_2CH_3$); 22.4 ($\underline{C}H_2CH_3$); 13.9 ($\underline{C}H_3$). Anal. calcd. for $C_{22}H_{30}N_4O_2$(382.52): C, 69.08; H, 7.90; N, 14.65. Found: C, 68.6; H, 7.5; N, 14.8.

3,3'-Di(methoxycarbonylcarbonylamino)-2,2'-bipyridine (3e)

CH$_2$Cl$_2$ was used as solvent. After heating under reflux for 10 min the solution was cooled to room temperature and the resulting precipitate was filtered and washed with cold MeOH yielding pure **3e** (456 mg, 92%). M.p. 278–279°C. ^{1}H-NMR (CDCl$_3$): δ 15.18 (s, 2H, NH); 9.24 (dd, 2H, $J = 1.7$ and 7.6 Hz, H-4); 8.56 (dd, 2H, $J = 1.7$ and 4.4 Hz, H-6); 7.49 (dd, 2H, $J = 4.5$ and 8.5 Hz, H-5); 3.96 (s,

6H, OC$\underline{H}_3$). Anal. calcd. for $C_{16}H_{14}N_4O_6$ (358.31): C, 53.63; H, 3.94; N, 15.64. found: C, 53.2; H, 4.1; N, 15.5.

3,3'-Di(benzoylamino)-2,2'-bipyridine (3f)

After stirring at room temperature for 2 h the precipitates were filtered, washed with water to remove the TEA salt, dried and recrystallised from CH_3CN to yield pure **3f** as light yellow needles (0.26 g, 62%). M.p. 236.8–238.3°C. ^{1}H-NMR ($CDCl_3$): δ 14.59 (s, 2H, NH); 9.42 (dd, 2H, J = 1.7 and 8.5 Hz, H-4); 8.41(dd, 2H, J = 1.3 and 4.4 Hz, H-6); 8.07 (d, 4H, H-ortho); 7.58 (m, 6H, H-meta and para); 7.46 (dd, 2H, J = 4.4 and 8.5 Hz, H-5). ^{13}C-NMR ($CDCl_3$): δ 166.4 (C=O); 142.0 (C-2); 140.2 (C-6); 137.6 (C-2); 135.3 (C-ipso); 132.0 (C-para); 129.9 (C-4); 128.8 (C-ortho); 127.4 (C-meta); 124.2 (C-5). Anal. calcd. for $C_{24}H_{18}N_4O_2$ (394.72): C, 73.08; H, 4.60; N, 14.20. Found: C, 73.6; H, 5.1; N, 14.3.

8-Quinolinecarbonyl chloride (4)[7]

A mixture of anthranilic acid (12.85 g, 93.75 mmol), o-nitrobenzoic acid (9.4 g, 56.25 mmol), anhydrous glycerol (25 ml, 430 mmol) and concd. sulphuric acid (19 ml) was heated gently until a vigorous reaction took place. Then, the mixture was heated under reflux gently for 6 h (T_{bath} = 200°C). After cooling, the tar was poured onto ice (300 ml); when all the ice had melted, the pH was adjusted to 3–4 using concentrated ammonia. The resulting suspension was filtered and the filtrate was extracted with $CHCl_3$ (4×55 ml). The combined organic layers were dried with $MgSO_4$ and then evaporated *in vacuo*. Recrystallisation from EtOH (96%) yielded the pure acid (5.75 g, 35%). M.p. 186.5–189°C (lit. 187–189°C). ^{1}H-NMR ($CDCl_3$): δ 16.61 (s, 1H, COOH); 8.93 (dd, 1H, J = 4.3 and 1.7 Hz, H-2); 8.78 (dd, 1H, J = 7.3 and 1.3 Hz, H-7); 8.46 (dd, 1H, J = 8.3 and 1.6 Hz, H-4); 8.13 (dd, 1H, J = 8.2 and 1.4 Hz, H-5); 7.78 (t, 1H, J = 8 Hz, H-6); 7.66 (dd, 1H, J = 8.4 and 4.4 Hz, H-3).^{13}C-NMR ($CDCl_3$): δ 167.1 (C=O); aromatic carbons: 148.4; 145.1; 139.7; 135.2; 133.0; 128.1; 127.2; 124.4; 121.7. Anal. calcd. for $C_{10}H_7NO_2$ (173.17): C, 69.36; H, 4.07; N, 8.09. Found: C, 69.0; H, 4.7; N, 7.8. 8-Quinolinecarboxylic acid (2g, mmol) was heated under reflux in thionyl chloride (10 ml) for 1 h. The excess thionyl chloride was distilled and the crude acid chloride was flushed with pentane (2×10 ml) to yield a yellow solid (2.5 g, 95%). ^{1}H-NMR ($CDCl_3$) : δ 10.54 (bs, 1H, HCl); 9.33 (dd, 1H, J = 5.1 and 1.7 Hz, H-2); 9.20 (dd, 1H, J = 8.4 and 1.6 Hz, H-4); 8.71 (dd, 1H, J = 7.4 and 1.6 Hz, H-7); 8.60 (dd, 1H, J = 8.2 and 1.4 Hz, H-5); 8.10 (dd, 1H, J = 8.4 and 5.1 Hz, H-3); 7.99 (t, 1H, J = 7.3 Hz, H-6).^{13}C-NMR ($CDCl_3$): δ 166.8 (C=O); aromatic carbons: 148.5; 144.9; 139.4; 136.6; 134.6; 128.8; 128.5; 122.8; 121.5.

3,3'-Di(8-quinolinecarbonylamino)-2,2'-bipyridine (3g)

Due to the poor solubility of 8-quinolinecarbonyl chloride hydrochloride in diethyl ether, CH_2Cl_2 was used as solvent. 4 Equivalents of TEA were used. After stirring for 4 h at room temperature the suspension was extracted with water (3×35 ml) and brine (1×35 ml) and the organic phase was dried with $MgSO_4$ and evaporated *in vacuo*. The resulting oil was purified by column chomatography (SiO_2; first CH_3CN/CH_2Cl_2 1/1 to remove impurities, then CH_2Cl_2/MeOH 95/5 to elute the amide **3g**. Trituration with MeOH yielded pure **3g** (0.25g, 38%). M.p. 225–227°C.^{1}H-NMR ($CDCl_3$): δ 13.74 (s, 2H, NH); 9.31 (dd, 2H, J = 1.5 and 8.5 Hz, H-4); 8.76 (dd, 2H, J = 1.4 and 7.4 Hz, H-7'); 8.57 (dd, 2H, J = 1.4 and 4.6 Hz, H-2'); 8.35 (dd, 2H, J = 1.7 and 4.3 Hz, H-6); 8.20 (dd, 2H, J = 1.5 and 8.4 Hz, H-4'); 7.92 (d, 2H, J = 8.1 Hz, H-5'); 7.61 (t, 2H, J = 7.7 Hz, H-6'); 7.55 (dd, 2H, J = 4.6 and 8.4 Hz, H-3'); 7.40 (dd, 2H, J = 4.3 and 8.2 Hz, H-5).^{13}C-NMR ($CDCl_3$): δ 164.6 (C=O); aromatic carbons: 153.0; 149.0; 147.4; 145.0; 144.2; 137.6; 135.3; 134.0; 132.5; 130.3; 128.3; 126.4; 123.9; 120.9. Anal. calcd. for $C_{30}H_{20}N_6O_2$ (496.53): C, 72.57; H, 4.06; N, 16.92. Found: C, 72.0; H, 4.2; N, 17.0.

3,3'-Di((E)-cinnamoylamino)-2,2'-bipyridine (3h)

The mixture was stirred at room temperature for 3 h. The resulting solids were collected by filtration, the filtrate was evaporated *in vacuo* and triturated with CH_2Cl_2 (3x2 ml). The combined solids were suspended in water (100 ml), stirred for 15 min, filtered, washed with water (3x5 ml) and diethyl ether (2x5 ml) and dried. This yielded pure **3h** as a light yellow powder (1.98 g, 79%). An analytically pure sample was obtained by recrystallisation from DMSO. M.p. 260.5–262°C. ^{1}H-NMR (CDCl$_3$): δ 13.82 (s, 2H, NHCO); 9.34 (dd, 2H, J =1.5 and 8.5 Hz, H-4); 8.45 (dd, 2H, J = 1.3 and 4.4 Hz, H-6); 7.76 (d, 2H, J = 15.7 Hz, =CHPh); 7.60 (d, 4H, H-ortho); 7.45 (m, 8H, H-5 and H-meta and H-para); 6.62 (d, 2H, J = 15.7 Hz, =CHCO). Anal. calcd. for $C_{28}H_{22}N_4O_2$ (446.50): C, 75.32; H, 4.97; N,12.55. Found: C, 74.5; H, 5.4; N, 12.5.

(+)-3,3'-Di(camphanoylamino)-2,2'-bipyridine (3i)

The (–)-camphanic acid chloride was used. After stirring at room temperature for 2 h the solids were filtered and washed with hot diethyl ether. The filtrate was evaporated *in vacuo* and the resulting solid was recrystallised from MeOH to yield pure **3i** as light yellow needles (0.60 g, 68%). M.p. 281–282.5°C. $[\alpha]^{24}_D$ = 84.4° (CHCl$_3$, c = 0.64 g/dl).^{1}H-NMR (CDCl$_3$): δ 14.97 (s, 2H, NH); 9.22 (dd, 2H, J = 1.4 and 8.5 Hz, H-4); 8.58 (dd, 2H, J = 1.5 and 4.5 Hz, H-6); 7.40 (dd, 2H, J = 4.5 and 8.5 Hz, H-5); 2.64 (m, 2H); 2.02(m, 4H); 1.77(m, 1H); 1.16 (s, CH$_3$-syn); 1.14 (s, CH$_3$-anti); 0.93 (s, CH$_3$–C-3). ^{13}C-NMR (CDCl$_3$); δ 178.2 (C=O, lactone); 166.7 (C=O, amide); 141.6 (C-2); 141.3 (C-6); 135.9 (C-3); 129.2 (C-4); 124.2 (C-5); sp^3-carbons: 92.8; 55.4; 54.4; 30.1; 29.1; 16.7; 16.6; 9.8. Anal. calcd. for $C_{30}H_{34}N_4O_6$ (546.65): C, 65.91; H, 6.27; N, 10.24. Found: C, 66.3; H, 6.5; N, 10.3.

(–)-3,3'-Di(camphanoylamino)-2,2'-bipyridine (3j)

The (+)-camphanic acid chloride was used. Compound **3j** was obtained according to the procedure applied for **3i**. Yield: 0.17g (70%). M.p. 281–283°C. $[\alpha]^{24}_D$ = –83.7° (CHCl$_3$, c = 0.54 g/dl). Anal. calcd. for $C_{30}H_{34}N_4O_6$ (546.65): C, 65.91; H, 6.27; N, 10.24. Found: C, 65.6; H, 6.5; N, 10.1.

Procedures for the acylation of 2 with isocyanates

3,3'-Di(phenylaminocarbonylamino)-2,2'-bipyridine (3k)[1a]

Phenylisocyanate (0.4 g, 3.35 mmol) and **2** (0.2 g, 1.08 mmol) were dissolved in toluene (8 ml) and stirred for 30 min at 80°C. After cooling, the resulting precipitate was filtered and the solids were suspended in hot MeOH (50 ml), filtered and dried to give a white powder (0.48 g, 80%, lit.[1a] 94.3%). M.p. 221–224°C (lit. 207–209°C).^{1}H-NMR (DMSO-*d6*): δ 11.30 (s, 2H, NHCO); 9.65 (s, 2H, NHPh); 8.72 (dd, 2H, J = 1.6 and 8.5 Hz, H-4); 8.39 (dd, 2H, J = 1.4 and 4.6 Hz, H-6); 7.50 (m, 6H, H-5 and H-ortho); 7.31 (t, 4H, H-meta); 7.01 (t, 2H, H-para). ^{13}C-NMR (DMSO-*d6*): δ 152.5 (C=O); 142.3 (C-2); 140.7 (C-ipso); 139.5 (C-6); 136.0 (C-3); 129.8 (C-4); 128.7 (C-meta); 123.5 (C-5); 122.3 (C-para); 119.1 (C-ortho). Anal. calcd for $C_{24}H_{20}N_6O_2$ (424.46): C, 67.91; H, 4.75; N, 19.80. Found: C, 67.8; H, 4.7; N, 19.8.

3,3'-Di(n-butylaminocarbonylamino)-2,2'-bipyridine (3l)

n-Butylisocyanate (0.26 ml, 2.3 mmol) and **2** (0.2 g, 1.08 mmol) were dissolved in toluene and stirred for 3 h at 80°C. After cooling, pentane (5 ml) was added to the solution, the solids were filtered and recrystallised from toluene to give pure **3l** as yellow plates (0.13 g, 34%). M.p. 201.5–204°C.^{1}H-NMR (CDCl$_3$): δ 12.57 (bs, 2H, NHCO); 8.86 (dd, 2H, J = 1.3 and 7.8 Hz, H-4); 8.10 (dd, 2H, J = 1.4 and 4.5 Hz, H-6); 7.20 (dd, 2H, J = 4.5 and 8.5 Hz, H-5); 4.63 (bs, 2H, NHCH$_2$); 3.25 (qua, 4H, NHCH$_2$); 1.53 (qui, 4H, NHCH$_2$CH$_2$); 1.37 (se, 4H, CH$_2$CH$_3$); 0.90 (t, 6H, CH$_3$). ^{13}C-NMR (CDCl$_3$): δ 155.6 (C=O); 141.4 (C-2); 138.4 (C-6); 137.7 (C-3); 128.9 (C-4); 123.6 C-5); 40.6 (NHCH$_2$); 32.1

(NHCH$_2$CH$_2$); 20.1 (CH$_2$CH$_3$); 13.8 (CH$_3$). Anal. calcd. for C$_{20}$H$_{28}$N$_6$O$_2$ (384.48): C, 62.48; H, 7.34; N, 21.86. Found: C, 62.9; H, 7.3; N, 21.9.

Benzoylisocyanate (5a)[8]

To a solution of benzamide (3.75 g, 31 mmol) in 1,2-dichloroethane (30 ml), oxalyl chloride (6.7 g) was added dropwise under Ar. The mixture was stirred for 20 h at 40–50°C. The excess of oxalyl chloride and 1,2-dichloroethane were evaporated *in vacuo*. The residual oil was kept under Ar and used without further purification. ^{1}H-NMR (CDCl$_3$): δ 8.80 (d, 2H, H-ortho); 7.62 (t, 1H, H-para); 7.45 (t, 2H, H-meta). ^{13}C-NMR (CDCl$_3$): δ 165.0 (C=O); 131.1 (N=C=O); aromatic carbons: 134.5; 131.0; 130.3; 128.6.

3,3'-Di(benzoylaminocarbonylamino)-2,2'-bipyridine (3m)[1h]

To benzoylisocyanate (0.3 g, 2 mmol) in dry CH$_2$Cl$_2$ (6 ml), a solution of **2** (0.18 g, 1 mmol) in dry CH$_2$Cl$_2$ (6 ml) was added dropwise under argon. After stirring for 4 h at 30–40°C the solvent was evaporated *in vacuo* and the solids were triturated with hot CH$_3$CN (2x30 ml) to yield **3m** as a cream coloured powder (0.34 g, 70%). M.p. 279–282°C (dec.). ^{1}H-NMR (CDCl$_3$/trifluoroacetic acid 3/1): δ 10.18 (bs, 2H, NH); 9.23 (d, 2H, J = 8.6 Hz, H-4); 8.96 (d, 2H, J = 5.2 Hz, H-6); 8.28 (dd, 2H, J = 5.4 and 8.5 Hz, H-5); 7.88 (d, 4H, H-ortho); 7.72 (t, 2H, H-para); 7.56 (t, 4H, H-meta). ^{13}C-NMR (CDCl$_3$/trifluoroacetic acid 3/1): δ 171.0 (C=O); 154.3 (C=O); 142.4; 141.3; 137.3; 135.7; 135.1; 130.2; 129.7; 129.6; 128.3.

3,4,5-Tridodecyloxy-benzoylisocyanate (5b)

In a separatory funnel 3,4,5-tridodecyloxybenzoyl chloride[16] (2 g, 2.9 mmol) was dissolved in dry diethyl ether (15 ml). A 25% solution of NH$_3$ in water (20 ml) and ice (20 g) were added and the mixture was shaken vigorously. The resulting white precipitate was filtered, washed with water and dried to yield pure amide (1.84 g, 95%). M.p. 81–82.5°C. ^{1}H-NMR (CDCl$_3$): δ 7.08 (s, 2H, H-ortho); 4.07 (t, 6H, OCH$_2$); 1.85 (m, 6H, OCH$_2$CH$_2$); 1.53 (qui, 6H, OCH$_2$CH$_2$CH$_2$); 1.34 (bs, 48H, (CH$_2$)$_8$); 0.95 (t, 9H, CH$_3$). Anal. calcd. for C$_{43}$H$_{79}$NO$_4$ (674.1): C, 76.62; H, 11.81; N, 2.08. Found: C, 77.2; H, 12.4; N, 2.1. To a suspension of 3,4,5-tridodecyloxybenzamide (1 g, 1.48 mmol) in 1,2-dichloroethane (20 ml) oxalyl chloride (0.45 g) was added dropwise under argon. The resulting mixture was stirred at 40–45°C for 48 h. The solvent and excess of oxalyl chloride were evaporated *in vacuo* and the resulting oil was used without further purification. ^{1}H-NMR (CDCl$_3$): δ 7.17 (s, 2H, H-ortho); 4.05 (m, 6H, OCH$_2$); 1.78 (m, 6H, OCH$_2$CH$_2$); 1.49 (bs, 6H, OCH$_2$CH$_2$CH$_2$); 1.30 (bs, 48H, (CH$_2$)$_8$); 0.89 (t, 9H, CH$_3$).

3,3'-Di(3,4,5-tridodecyloxybenzoylaminocarbonylamino)-2,2'-bipyridine (3n)

To a solution of **5b** in dry CH$_2$Cl$_2$ (6 ml), a solution of **2** (79 mg, 0.42 mmol) in dry CH$_2$Cl$_2$ (3 ml) was added dropwise. After stirring for 1 h at room temperature the solvent was evaporated *in vacuo* and the remaining brown solid was purified by column chromatography (SiO$_2$; eluent: CH$_2$Cl$_2$/MeOH 97.5/2.5) to yield pure **3n** as a white powder (0.38 g, 57%). Recrystallisation from CHCl$_3$/EtOAc 1/1 afforded an analytically pure sample. T$_{cl}$ = 126–127.5°C. ^{1}H-NMR (CDCl$_3$): δ 13.28 (s, 2H, NHCO); 8.79 (dd, 2H, J = 1.2 and 8.4 Hz, H-4); 8.69 (dd, 2H, J =1.4 and 4.7 Hz, H-6); 8.29 (bs, 2H, CONHCO); 7.42 (dd, 2H, J = 4.5 and 8.4 Hz, H-5); 7.05 (s, 4H, H-ortho); 4.03 (t, 12H, OCH$_2$); 1.78 (m, 12H, OCH$_2$CH$_2$); 1.47 (qui, 12H, OCH$_2$CH$_2$CH$_2$); 1.27 (bs, 96H, (CH$_2$)$_8$); 0.88 (t, 18H, CH$_3$). Anal. calcd. for C$_{98}$H$_{164}$N$_6$O$_{10}$ (1586.43): C, 74.20; H, 10.42; N, 5.30. Found: C, 73.4; H, 10.1; N, 5.5.

Ethyl benzimidate (7)[9]

HCl-gas was bubbled though a solution of benzonitrile (22 g, 0.22 mol) in dry EtOH (10 g, 0.22 mol) for 2 h. The resulting crystals were suspended in dry EtOH (50 ml), filtered and dried to yield pure **7**

(32.6 g, 80%).^{1}H-NMR (CDCl$_3$): δ 12.56 (bs, 1H, HCl); 11.85 (bs, 1H, =NH); 8.38 (d, 2H, H-ortho); 7.72 (t, 1H, H-para); 7.56 (t, 3H, H-meta); 4.96 (qua, 2H, OCH$_2$); 1.63 (t, 3H, OCH$_2$CH$_3$). Anal. calcd. for C$_9$H$_{12}$ClNO (185.65): C, 58.22; H, 6.51; N, 7.54. Found: C, 57.7; H, 6.4; N, 7.7.

6-Phenyl-5H-dipyrido[3,2-d:2',3'-f]-[1,3]-diazepine (8)[1c]

A mixture of **2** (1 g, 5.37 mmol) and **7** (1.06 g, 5.37 mmol) in dry EtOH (11 ml) was stirred at room temperature for 3 h. Then, the mixture was heated under reflux for another 1 h. The resulting precipitates were filtered and washed with cold EtOH (3x5 ml) to yield pure **8** as a bright yellow powder (1.28 g, 88%). M.p. > 300°C. ^{1}H-NMR (CF$_3$COOD): δ 9.78 (d, 2H, H-6); 9.24 (d, 2H, H-ortho); 9.09 (t, 1H, H-para); 9.02 (d, 2H, H-4); 8.97 (dd, 2H, H-5); 8.84 (t, 2H, H-meta).

3'-Benzoylamino-2,2'-bipyridine-3-amine (9a)[1c]

Compound **8** (2.8 g, 10.3 mmol) was heated under reflux in acetic acid (50 ml) for 3 h. After cooling, the mixture was poured into water (100 ml) and neutralised with solid NaHCO$_3$. The mixture was then extracted with CH$_2$Cl$_2$ (3x100 ml). The combined organic layers were dried with MgSO$_4$ and evaporated *in vacuo*. The yellow solid was purified by column chromatography (SiO$_2$, eluent: CH$_2$Cl$_2$/MeOH 97.5/2.5, R$_f$ = 0.5). After recrystallisation from CH$_3$CN pure **9a** was obtained as light yellow crystals (1 g, 33%). M.p. 167.5–168.5°C.(Lit.[1c] 163–164°C). ^{1}H-NMR (CDCl$_3$): δ 14.74 (s, 1H, NHCO); 9.30 (dd, 1H, J = 1.5 and 8.3 Hz, H-4'); 8.32 (dd, 1H, J = 1.7 and 4.8 Hz, H-6'); 8.08 (dt, 1H, H-ortho); 8.00 (dd, 1H, J = 2.4 and 3.6 Hz, H-6); 7.55 (m, 3H, H-meta and H-para); 7.30 (dd, 1H, J = 4.6 and 8.4 Hz, H-5'); 7.11 (m, 2H, H-4 and H-5); 6.62 (bs , 2H, NH$_2$). ^{13}C-NMR (CDCl$_3$): δ 166.2 (C=O); aromatic carbons: 145.1; 143.5; 140.7; 138.4; 136.2; 135.6; 134.7; 131.6; 128.6; 128.4; 127.4; 125.2; 124.1; 122.6. Anal. calcd. for C$_{17}$H$_{11}$N$_4$O (290.32): C, 70.33; H, 4.86; N, 19.29. Found: C, 70.2; H, 4.6; N, 19.8.

3'-α-Methylbenzylaminocarbonylamino-2,2'-bipyridine-3-amine (9b)

R-(+)-α-Methylbenzylisocyanate (0.3 ml) was added to a solution of **2** (0.32 g, 1.72 mmol) in toluene (7 ml) at 80°C. The solution was stirred for 2 h. After cooling, the resulting solids were filtered, washed with cold toluene and recrystallised from CH$_3$CN to give orange crystals (0.49 g, 87%). M.p. 208–210°C. ^{1}H-NMR (CDCl$_3$): δ 12.70 (bs, 1H, NHCO); 8.84 (dd, 1H, J = 1.7 and 8.5 Hz, H-4'); 8.20 (dd, 1H, J = 1.4 and 4.5 Hz, H-6'); 7.86 (s, 1H, H-6); 7.40 (m, 4H, H-ortho and meta); 7.27 (t, 1H, H-para); 7.22 (dd, 1H, J = 4.8 and 8.5 Hz, H-5'); 7.08 (m, 2H, H-4 and H-5); 6.45 (bs, 2H, NH$_2$); 5.04 (qui, 1H, CH); 4.80 (d, 1H, NHCH); 1.55 (d, 3H, CH$_3$). Anal. calcd for C$_{19}$H$_{19}$N$_5$O (333.39): C, 68.45; H, 5.74; N, 21.01. Found: C, 68.3; H, 5.2; N, 21.1.

3'-t-Butoxycarbonylamino-2,2'-bipyridine-3-amine (9c)

A mixture of **2** (0.8 g, 4.3 mmol) and Boc$_2$O (0.95 g, 4.3 mmol) in dry THF (30 ml) was heated under reflux for 18 h. After cooling, the solution was poured into water (200 ml) and stirred for 10 min. The water phase was extracted with diethyl ether (3x100 ml). The combined organic layers were dried with MgSO$_4$, filtered, and evaporated *in vacuo*. The resulting yellow oil was purified by column chromatography. First the diacylated byproduct was eluted (eluent: hexane/EtOAc 95/5, R$_f$ = 0.12). Then, the desired monoacylated compound **9c** was eluted (eluent: CHCl$_3$/CH$_3$CN/hexane 1.8/2.5/3, R$_f$ = 0.6). After evaporation of the solvent *in vacuo*, pure **9c** was obtained as a yellow oil (0.87 g, 70%). ^{1}H-NMR (CDCl$_3$); δ 12.42 (s, 1H, NHCO);8.76 (d, 1H, H-4');8.24 (d, 1H, H-6'); 8.02 (d, 1H, H-6); 7.23 (dd, 1H, H-5'); 7.10 (m, 2H, H-5 and H-4); 6.35 (bs, 2H, NH$_2$); 1.53 (s, 9H, C(CH$_3$)$_3$). ^{13}C-NMR (CDCl$_3$): δ 153.5 (C=O); aromatic carbons:144.4; 139.6; 136.3; 135.5; 127.2; 124.8; 123.8; 122.6; 80.0 (quaternary C); 28.3 (CH$_3$).

45

3-Trifluoroacetylaminopyridine (N-3-pyridyl-trifluoracetamide) (6a)
A solution of 3-aminopyridine (1 g, 10.6 mmol) in $CF_3COOCOCF_3$ (7 ml) and dry THF (20 was heated under reflux for 2 h. The solvent was concentrated *in vacuo*. The resulting oil was dissolved in CH_2Cl_2 (30 ml) and extracted with saturated $NaHCO_3$ solution (30 ml) and water (30 ml). The organic layer was dried and evaporated *in vacuo* to yield a cream coloured solid. After recrystallisation from diethyl ether, pure white needle-like crystals of **6a** were obtained (0.7 g, 35%). M.p. 129–130°C. ^{1}H-NMR ($CDCl_3$): δ 9.40 (s, 1H, NH); 8.70 (s, 1H, H-2); 8.50 (s, 1H, H-6); 8.35 (d, 1H, $J = 8.4$ Hz, H-4); 7.40 (dd, 1H, $J = 4.7$ and 8.4 Hz, H-5). Anal. calcd. for $C_7H_5F_3N_2O$ (190.12): C, 44.22; H, 2.65; N, 14.73. Found: C, 44.0; H, 2.7; N, 14.6.

General procedure for the acylation of 3-aminopyridine with acid chlorides:
To an ice-cooled and stirred solution of 3-aminopyridine and TEA (1 eq.) under argon atmosphere in dry diethyl ether (0.2 M), a solution of the acid chloride (1 eq.) in dry diethyl ether (0.2 M) was added dropwise. After 1 h the ice bath was removed and stirring was continued until TLC showed the disappearance of the starting materials.

3-Benzoylaminopyridine (N-3-pyridyl-benzamide) (6b)
After stirring for 3 h the diethyl ether was evaporated *in vacuo*, CH_2Cl_2 (40 ml) was added and the solution was extracted with water (3x30 ml) and brine (1x20 ml). The solvent was evaporated *in vacuo* and the resulting solid was triturated with hot diethyl ether (2x10 ml) to remove impurities. Recrystallisation of the residue from water yielded pure **6b** as white needles (1.34 g, 60%). M.p. 118.3–119°C. ^{1}H-NMR ($CDCl_3$): δ 8.68 (d, 1H, $J = 2.4$ Hz, H-2); 8.43 (s, 1H, NH); 8.35 (dd, 2H, $J = 1.3$ and 4.7 Hz, H-6); 8.30 (ddd, 1H, $J = 1.5$ and 2.5 and 8.5 Hz, H-4); 7.90 (d, 2H, H-ortho); 7.58 (t, 1H, H-para); 7.49 (t, 2H, H-meta); 7.33 (dd, 1H, $J = 4.7$ and 8.5 Hz, H-5). ^{13}C-NMR ($CDCl_3$): δ 166.6 (C=O); 145.4 (C-6); 141.5 (C-2); 134.9 (C-ipso); 134.2 (C-3); 132.2 (C-para); 128.6 (C-ortho); 127.7 (C-4); 127.2 (C-meta); 123.7 (C-5). Anal. calcd. for $C_{12}H_{10}N_2O$ (198.22): C, 72.71; H, 5.08; N, 14.13. Found: C, 73.0; H, 5.3; N, 14.1.

(–)-3-Camphanoylaminopyridine (N-3-pyridyl-camphanicamide) (6c)
The (–)-camphanic acid chloride was used. The mixture was stirred at room temperature for 2 h and then filtered. The filtrate was evaporated *in vacuo* and purified by column chromatography (SiO_2; eluent: CH_3CN/CH_2CH_2 1/1) to give crude **6c**. The solids were washed with water to remove the TEA salt and gave a second crop of **6c**. The combined solids were recrystallised from water to give pure **6c** as white needles (0.70 g, 60%). M.p. 141.5–143°C. $[\alpha]^{25}_D = -25.6$ ° ($CHCl_3$, c = 1.69 g/dl). ^{1}H-NMR ($CDCl_3$): δ 8.72 (d, 1H, $J = 2.5$ Hz, H-2); 8.42 (dd, 1H, $J = 1.4$ and 4.7 Hz, H-6); 8.24 (s, 1H, NH); 8.14 (ddd, 1H, $J = 1.5$ and 2.6 and 8.4 Hz, H-4); 7.30 (dd, 1H, $J = 4.7$ and 8.4 Hz, H-5); 2.60 (m, 1H); 2.04 (m, 2H); 1.76 (m, 1H); 1.17 (s, CH_3); 1.16 (s, CH_3); 1.00 (s, CH_3). ^{13}C-NMR ($CDCl_3$): δ 177.7 (C=O, lactone); 165.8 (C=O, amide); 146.1 (C-6); 141.5 (C-2); 133.6 (C-3); 127.1 (C-4); 123.62 (C-5); sp^3 carbons: 92.2; 55.4; 54.5; 30.5; 29.0; 16.7; 16.5; 9.7. Anal. calcd. for $C_{15}H_{18}N_2O_3$ (274.32): C, 65.67; H, 6.61; N, 10.21. Found: C, 65.2; H, 7.0; N, 10.1.

3-(8-Quinolinecarbonylamino)-pyridine (N-3-pyridyl-8-quinolinecarbonamide) (6d)
THF was used instead of diethyl ether for reasons of low solubility and the acid chloride hydrochloride was used: hence 2 eq of TEA were needed. After stirring at 50–60°C for 5 h the precipitates were filtered and washed with THF. The combined filtrates were evaporated *in vacuo* and the remaining solid was purified by column chromatography (SiO_2; eluent: CH_2Cl_2/CH_3CN 1/1). Recrystallisation from water/MeOH 90/10 yielded **6d** as a white powder (0.15 g, 46%). M.p. 116.5–118.5°C. ^{1}H-NMR ($CDCl_3$): δ 13.88 (s, 1H, NH); 9.04 (dd, 1H, $J = 1.8$ and 4.2 Hz, H-2'); 8.95 (dd, 1H, $J = 1.3$ and 7.4 Hz, H-7'); 8.88 (d, $J = 2.2$ Hz, H-2); 8.52 (m, 1H, H-4); 8.37 (m, 2H, H-4' and H-

6), 8.05 (dd, 1H, J = 1.5 and 8.1 Hz, H-5'); 7.75 (t, 1H, J = 7.7 Hz, H-6'); 7.59 (dd, 1H, J = 4.3 and 8.4 Hz, H-3'); 7.35 (dd, 1H, J = 4.7 and 8.3 Hz, H-5). ^{13}C-NMR (CDCl$_3$): δ 164.2 (C=O); aromatic carbons: 149.2; 145.3; 144.9; 142.0; 138.2; 135.8; 134.4; 132.7; 128.6; 128.1; 127.5; 126.8; 123.7; 121.2. Anal. calcd. for C$_{15}$H$_{11}$N$_3$O (249.27): C, 72.28; H, 4.45; N, 16.86. Found: C, 71.9; H, 4.7; N, 16.6.

2.10 References and notes

[1] a) Kaczmarek, L.; Nantka-Namirski, P. *Acta Polon. Pharm.* **1979**, *6*, 629. b) Balicki, B.; Kaczmarek, L.; Sobotka, W.; Ejmocki, Z. *Journal f. Prakt. Chem.* **1989**, *331*, 995. c) Kaczmarek, L.; Nantka-Namirski, P. *Monatsh. Chemie* **1990**, *121*, 821. d) Kaczmarek, L. *Bull. Polish Acad. Sci. Chem.* **1985**, *33*, 402. e) Kaczmarek, L. *Polish J. Chem.* **1985**, *59*, 9. f) Kaczmarek, L. *Polish J. Chem.* **1985**, *59*, 1141.

[2] a) Bulska, H. *Chem. Phys. Lett.* **1983**, *98*, 398. b) Bulska, H.; Grabowska, A.; Grabowski, Z. *J. Lumin.* **1986**, *5*, 189. c) Sepiol, J.; Bulska, H.; Grabowska, A. *Chem. Phys. Lett.* **1987**, *140*, 607. d) Bulska, H. *J. Lumin.* **1988**, *39*, 293.

[3] a) Lipkowski, J.; Grabowska, A.; Waluk, J.; Calestani, G.; Hess Jr., B.A. *J. Cryst. and Spectr. Res.* **1992**, *22*, 563. b) Sitkowski, J.; Stefaniak, L.; Kaczmarek, L.; Webb, G.A. *J. Mol. Struct.* **1996**, *385*, 65.

[4] a) Reeves, L.W.; Allan, E.A.; Strømme, K.O. *Can. J. Chem.* **1960**, *38*, 1249. b) Bartels-Keith J.R.; Cieciuch, R.F.W. *Can. J. Chem.* **1968**, *46*, 2593. c) Andrews, B.D.; Rae, I.D.; Reichert, B.E. *Tetrahedron Lett.* **1969**, 1859. d) Andrews, B.D.; Poynton, A.J.; Rae, I.D. *Aust. J. Chem.* **1972**, *25*, 639. e) Dabrowski, J.; Zwitsun, Z.; Dabrowska, U. *Tetrahedron* **1973**, *29*, 2257. f) Kolodziejski, W.; Wawer, I.; Wozniak, K.; Klinowski, J. *J. Phys. Chem.* **1993**, *97*, 12147. g) Bertolasi, V.; Ferretti, V.; Gilli, P.; Gilli, G.; Issa, Y.M.; Sherif, O.E. *J. Chem. Soc. Perkin Trans. 2* **1993**, 2223. h) Boykin, D.W.; Chandrasekaran, S.; Bauwstark, A.L. *Magn. Reson. Chem.* **1993**, *31*, 489. i) Grecg, E.; Nowicka-Scheibe, J.; Olejnik, Z.; Lis, T.; Pawelka, Z.; Malarski, Z.; Sobczyk, L. *J. Chem. Soc. Perkin Trans. 2* **1996**, 343.

[5] a) Lehn J.-M.; Ziessel, R. *J. Chem. Soc., Chem. Commun.* **1987**, 1292. b) Zarges, W.; Hall, J.; Lehn, J.-M.; Bolm, C. *Helv. Chim. Acta* **1991**, *74*, 1843. c) Mihara, H.; Nishino, N.; Hasegawa, R.; Fujimoto, T.; Usui, S.; Ishida, H.; Ohkubo, K. *Chem. Lett.* **1992**, 1813. d) Pfeil, A.; Lehn, J.-M. *J. Chem. Soc., Chem. Commun.* **1992**, 838. e) Ghadiri, M.R.; Case, M.A. *Angew. Chem.* **1993**, *105*, 1663. f) Goulle, V.; Harriman, A.; Lehn, J.-M. *J. Chem. Soc., Chem. Commun.* **1993**, 1034. g) Krämer, R.; Lehn, J.-M.; de Cian, A.; Fischer, J. *Angew, Chem.* **1993**, *105*, 764. h) Eisenbach, C.D.; Schubert, U.S.; Baker, G.R.;Newkome, G.R. *J. Chem. Soc., Chem. Commun.* **1995**, 69. i) Smith, V.C M.; Lehn, J.-M. *Chem. Commun.* **1996**, 2733. j) Baxter, P.N.W.; Hanan, G.S.;Lehn, J.-M. *Chem. Commun.* **1996**, 2019. k) Hasenknopf, B.; Lehn, J.-M.; Kneissel, B.O.; Baum, G.; Fenske, D. *Angew. Chem.* **1996**, *108*, 1987. l) Woods, C.R.; Benaglia, M.; Cozzi, F.; Siegel, J.S. *Angew. Chem.* **1996**, *108*, 1977. m) Hasenknopf, B.; Lehn, J.-M. *Helv. Chim. Acta* **1996**, *79*, 1643.

[6] Etienne, A.; Izoret, G. *Fr. Pat. 1 369 401*, ref. *Chem. Abs.* **1965**, *62*, 570.

[7] Campbell, K.N.; Kerwin, J.F.; LaForge, R.A.; Campbell, B.K. *J. Am. Chem. Soc.* **1964**, *86*, 1844.

[8] Smith, L.R.; Speziale, A.J. *J. Org. Chem.* **1962**, *27*, 3742.

[9] Pinner, A.; Klein, F. *Ber.* **1877**, *10*, 1889.

[10] a) *Hydrogen Bonding*, (Eds. Joesten, M.D.; Schaad, L.J.) Marcel Dekker, Inc., New York, **1974**. b) *Advances in Physical organic Chemistry*; *Vol. 26*, (Ed. Bethell, D.), Academic Press, Ltd., London, **1990**, 225-381. c) *Hydrogen Bonding*, (Ed. Vinogradov, S.N.; Linnell, R.H.), Van Nostrand Reinhold Company, **1971**.

[11]   *See* reference 10a p 241.
[12]   a) Cohen, M.D.; Schmidt, G.M.J.; Sonntag, F.I. *J. Chem. Soc.* **1964**, *384*, 2000. b) Schmidt, G.M.J. *J. Chem. Soc.* **1964**, *385*, 2014. c) Schmidt, G.M.J. *Pure & Appl. Chem.* **1971**, *27*, 647.
[13]   Hamuro, Y.; Geib, S.J.; Hamilton, A.D. *Angew. Chem.* **1994**, *106*, 465.
[14]   Long, G.V.; Boyd, S.E.; Harding, M.M.; Buys, I.E.; Hambley, T.W. *J. Chem. Soc., Dalton Trans.* **1993**, 3175.
[15]   Many attempts have been undertaken to synthesise soluble macrocycli based on 3,3'-diamino-2,2'-bipyridine. However, solubility problems always hampered the formation of longer oligomers (discussed in Chapter 3). Suitable diacid dichlorides provided with sufficient lipophilic chains proved to be inaccessible.
[16]   The synthesis of 3,4,5-tridodecyloxybenzoyl chloride will be discussed in Chapter 4.

Chapter 3

The rigidity–solubility issue in systems incorporating the 3,3'-di(acylamino)-2,2'-bipyridyl unit

Abstract

The preferred planar conformation of the di(acylamino)-bipyridine moiety may provide structure in large molecules. Therefore, 3,3'-diamino-2,2'-bipyridine has been incorporated in oligomers/polymers based on terephthalic acid, 5-alkoxyisophthalic acid and phenazine-1,6-dicarboxylic acid. This affords mainly insoluble compounds unless the bipyridine unit is acylated with a strongly solubilising group such as the 3,4,5-tridodecyloxybenzoyl group. To improve the solubility of the diacylated bipyridine moiety itself, several approaches have been investigated for the introduction of lipophilic chains at the 5 and/or 5' positions of the bipyridine. Although none of them were successful, 5,5'-dimethoxy-3,3'-diamino-2,2'-bipyridine has been procured via a selective Ullmann coupling. This compound is a convenient new precursor molecule and may function as a reference compound to investigate the effect of small changes at the bipyridine substitution pattern on the properties upon introduction of this moiety in larger structures.

3.1 Introduction

Extended rigid-rod polymers have attained a lot of attention the last 20 years owing to their excellent properties. This has resulted in *e.g.* the development of high strength–high modulus fibers such as the polyaramides (figure 3.1.a) and poly(1,4-phenylene-2,6-benzobisthiazole)s (figure 3.1.b)[1,2]. The quality of the mechanical properties is directly related to the formation of lyotropic liquid crystalline phases which enhances ordering between the chains, resulting in the well-known high performance of the fibers. Interaction of the polymer with the solvent is needed to give rise to lyotropic systems. However, the notorious insolubility of highly ordered symmetrical systems capable of intermolecular interactions frequently hampers the formation

of mesophases. As a result all processes have to take place in strong acidic environments in which all intermolecular interactions are likely to be cancelled.

Recently, the 2,2'-bipyridine-5,5'-diyl unit has been incorporated in aromatic polyamides (figure 3.1.c). Apart from the high thermal stability of the resulting polymer and the formation of liquid crystalline mesophases upon addition of hexamethylphosphortriamide (HMPA), such polymers are interesting because of the complexing abilities with metal ions[3a]. Furthermore, a new rigid-rod polymer was recently introduced by Akzo–Nobel in which planarity is enforced by intramolecular H-bonding (figure 3.1.d)[3b]. The reversibility of such a non-covalent interaction might enhance processability and as a result lead to superior mechanical properties.
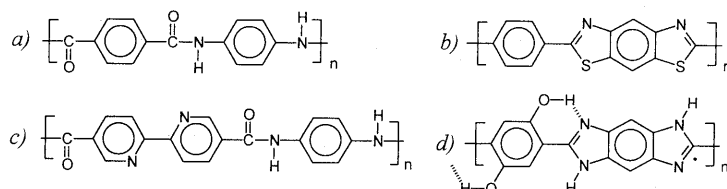
Figure 3.1: Rigid-rod polymers a) Kevlar b) poly(p-phenylene-benzobisthiazole) c) bipyridine containing aromatic polyamides d) intramolecularly H-bonded benzo-bisimidazole

In view of the previously discussed characteristics of N-acylated 3,3'-diamino-2,2'-bipyridines such as strong, reversible H-bonding and a planar, rigid system, the 3,3'-di(acylamino)-2,2'-bipyridine unit is attractive for incorporation in rigid-rod oligomers/polymers. Copolymers with terephthalic or isophthalic acid are envisaged and preliminary results will be discussed in paragraph 3.2. The intriguing bifurcated H-bonds found in 3,3'-di(8-quinolinecarbonylamino)-2,2'-bipyridine (Chapter 2), tempted us to design a rigid-rod polymer —shown in figure 3.2— being a copolymer of 3,3'-diamino-2,2'-bipyridine and phenazine-1,6-dicarboxylic acid. The synthesis of a model compound and the discussion of the planarity/rigidity in the system will be presented in paragraph 3.3.
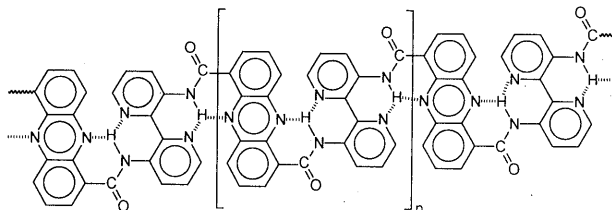
Figure 3.2: Design of a rigid-rod polymer incorporating the 3,3'-diamino-2,2'-bipyridyl unit

This study will also show whether the intramolecular H-bonds can be used to tune the processability of the polymers due to the reversibility of the H-bond formation. Otherwise, the introduction of lipophilic groups at the bipyridine moiety is necessary to enhance the characterisation of the polymers. Attaching the solubilising groups to the bipyridine moiety at the 5,5'-positions seems the most desirable as it will minimise unfavourable steric interactions. On the other hand, the double 2,3,5-substitution pattern in 2,2'-bipyridines is very uncommon and up to now only 5,5'-dimethyl-3,3'-dinitro-2,2'-bipyridine synthesised by Kazcmarek[4] was found to feature such a pattern. We will focus on the attempts to synthesise a modified version of the previously studied 3,3'-diamino-2,2'-bipyridine in paragraph 3.4. The major possibilities considered are depicted in figure 3.3.

$R = C_nH_{2n+1}$
or OC_nH_{2n+1}
or $NHCOalkyl$
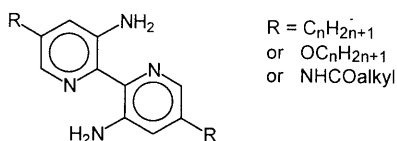
Figure 3.3: A modified bipyridine system with various substituents at the C-5,5' positions

3.2 Synthesis of oligomers based on 3,3'-diamino-2,2'-bipyridine and aromatic diacid dichlorides

The solubility of poly/oligoamides based on 3,3'-diamino-2,2'-bipyridine and diacid dichlorides was investigated by means of a number of model compounds. In analogy with the polyaramide fibers, model compounds were synthesised that derived from terephthaloyl chloride. Therefore, the previously described monoacylated 3,3'-diamino-2,2'-bipyridines **1a,b** (Chapter 2) were reacted with terephthaloyl chloride to give oligomers **2a,b** (figure 3.4).

1a : R = Ph

1b : R = *(R)*-NHCH(CH₃)Ph

2a : R = Ph

2b : R = *(R)*-NHCH(CH₃)Ph
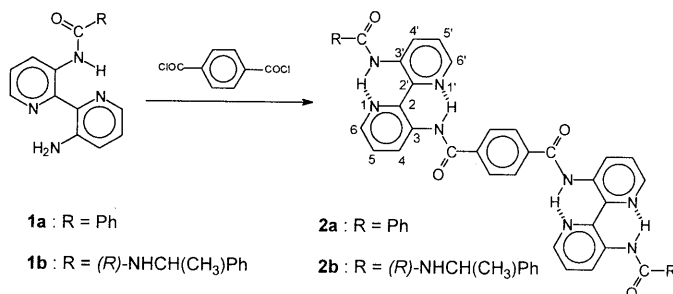
Figure 3.4: Oligomers based on terephthaloyl chloride

Oligomer **2a** can only be dissolved in strong acids such as trifluoroacetic acid. The formation of lyotropic liquid crystalline phases has not been observed. Oligomer **2b**, on the other hand, can be dissolved in polar aprotic solvents (DMF, DMSO, THF) at elevated temperatures.

Undoubtedly, the branching of the urea group improves solubility. In agreement with the results described in Chapter 2, high temperature ^{1}H-NMR data of compound **2b** in DMF-*d7* show little temperature dependence of the H-bonded N-H signals (7.5×10^{-3} ppm/K for the amide N-H and 6.3×10^{-3} ppm/K for the H-bonded urea N-H). Together with the strong deshielding of H-4 ($\delta = 9.29$ ppm), this confirms that strong H-bonding is present in DMF-*d7*.

Incorporating the diamino-bipyridine moiety in only small oligomers apparently leads to a severe reduction of the solubility of the compounds. As a result, the diacid dichloride has been modified by attaching an alkoxy chain. The 5-alkoxy-isophthaloyl chlorides **5a,b** proved to be easily accessible and their synthesis is depicted in scheme 3.1[5].
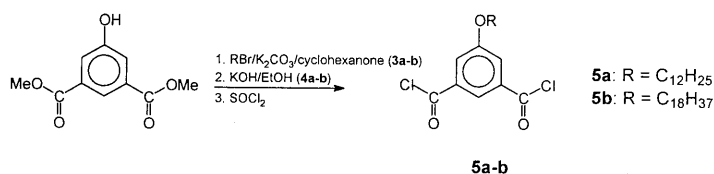
Scheme 3.1: Synthesis of 5-alkoxy-isophthaloyl chlorides

Dimethyl 5-alkoxy-isophthalates (**3a,b**) were obtained from the commercially available dimethyl 5-hydroxy-isophthalate in yields exceeding 75%. After quantitative saponification of the methyl ester and neutralisation, the dicarboxylic acids **4a,b** could easily be converted in the diacid dichlorides **5a,b** by treatment with thionyl chloride. Condensation of compound **5a** with monoacylated **1a** and **1c** gave rise to oligomers **6** and **7**, which were both soluble in chloroform (figure 3.5).
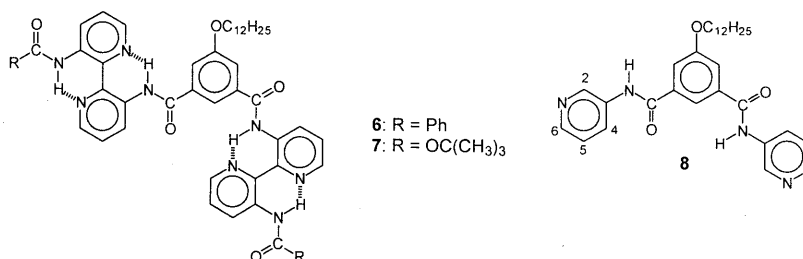
Figure 3.5: Oligomers based on compound 5a and reference compound 8

A polycondensation reaction was performed between 3,3'-diamino-2,2'-bipyridine and compound **5a** under high dilution conditions. A precipitate resulted which could not be dissolved in any of the usual solvents (*i.e.* DMSO, DMF, DMAA, NMP). The precipitate was only soluble when protonated with trifluoroacetic acid. Although the ^{1}H-NMR data suggested the formation of rather long oligomers (no end-groups were discerned), FAB-MS

demonstrated that the dispersity of the oligomers in the precipitate was high and that only short oligomers had been formed. Replacing the C_{12} chain for the longer C_{18} chain did not improve the solubility of the resulting oligomers. Methods to introduce more lipophilicity in the isophthaloyl moiety all failed.

Previous studies by Hunter[6] indicated that the preferred conformation in isophthaloyl diamides is the "trans-cis" conformation. In line with these results, we investigated whether such a preferred conformation also exists in compounds **6** and **7**. Therefore, we synthesised compound **8** for comparison. The ^{1}H-NMR spectra of compounds **6** and **8** are compared in figure 3.6. Although a relatively large difference is observed for the absorption of H-ortho and H-para between compounds **6** and **8**, there is only evidence that the H-ortho's are identical in both compounds. Even cooling of compound **6** to –60°C only resulted in sharp peaks and a symmetrical spectrum. From these results, it may be concluded that a high degree of rotational freedom around the Ph–C=O bond in compounds **6** and **8** exists. Although a more or less coplanar conformation of the isophthaloyl moiety with respect to the bipyridines might be preferred in the solid or liquid crystalline state, a substantial amount of conformational freedom seems to be present in solution.
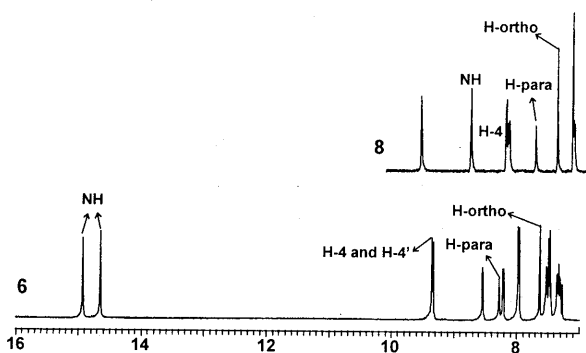
*Figure 3.6: ^{1}H-NMR data on compound **6** and reference compound **8** in CDCl$_3$*

To circumvent the insolubility resulting from incorporating the 3,3'-di(acylamino)-2,2'-bipyridine moiety in oligomers/polymers, two approaches can be conceived. One approach is to monoacylate 3,3'-diamino-2,2'-bipyridine with a strongly solubilising group such as the 3,4,5-trialkoxybenzoyl group. This may lead to disc-shaped compounds (see Chapter 4) which will be sufficiently soluble or to lath-like compounds in which an equilibrium between the aromatic/aliphatic content is achieved (see paragraph 3.3). The other approach is to attach the solubilising groups directly to the bipyridine ring without disturbing the intramolecular H-bonds (see paragraph 3.4).

3.3 Synthesis of a model compound for the phenazine-bipyridine rigid-rod copolymer

A most obvious model compound for the rigid-rod copolymer depicted in figure 3.3, is a condensation product of monoacylated 3,3'-diamino-2,2'-bipyridine and phenazine-1,6-dicarbonyl dichloride (figure 3.7). To ensure solubility, we opted for a monobenzoylated diamino-bipyridine, decorated with dodecyloxy chains (see Chapter 4). The co-trimer **9** is sufficiently long to study the degree of planarity and rigidity and to extrapolate the properties into that of the rigid-rod copolymer.

9
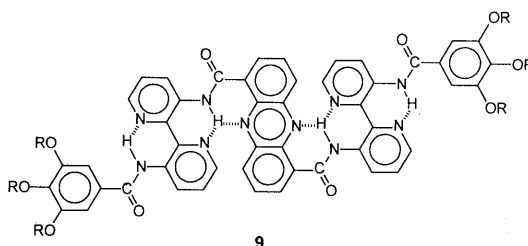
Figure 3.7: Model compound for a rigid-rod polymer based on 3,3'-diamino-2,2'-bipyridine

Although already in 1954 a simple synthesis for phenazine-1,6-dicarboxylic acid was described[7], we could not reproduce it[8]. The more elaborate method of Holliman *et al.*, however, did give satisfactory results[9]. Starting from 2-bromo-3-nitrobenzoic acid, **10**, an intermediate compound **11** was obtained via a nucleophilic aromatic substitution with *m*-aminobenzoic acid (scheme 3.2). The second step, a reductive ring closure, leads to the desired phenazine in a 12% overall yield (lit.[9] 14%). The low yield in the cyclisation step is mainly due to the formation of equal amounts of phenazine-1,6- and phenazine-1,8-dicarboxylic acid. Apparently, the reactivities of the 2- and 4-positions of *m*-aminobenzoic acid are comparable. Fortunately, the solubility of the unsymmetrical phenazine-1,8-dicarboxylic acid proved to be substantially higher in DMSO which made separation easy. The diacid **12** could be transformed quantitatively into the diacid dichloride **13** using SOCl$_2$. Subsequent coupling with 3-amino-3'-(3,4,5-tridodecyloxybenzoylamino)-2,2'-bipyridine **14**[#] leads to the desired model compound **9** which was obtained as a yellow powder in a 58% yield and showed sufficient solubility in organic compounds. Reaction of **13** with 3-aminopyridine, led to compound **15a** which is insoluble in organic solvents. Sufficient solubility was accomplished when **13** was reacted with *n*-octylamine, leading to compound **15b**. In view of the insolubility of **15a** in organic solvents, no polymerisation of 3,3'-diamino-2,2'-bipyridine with diacid dichloride **13** was attempted.

[#] The synthesis of compound **14** is described in Chapter 4 as compound **5b**
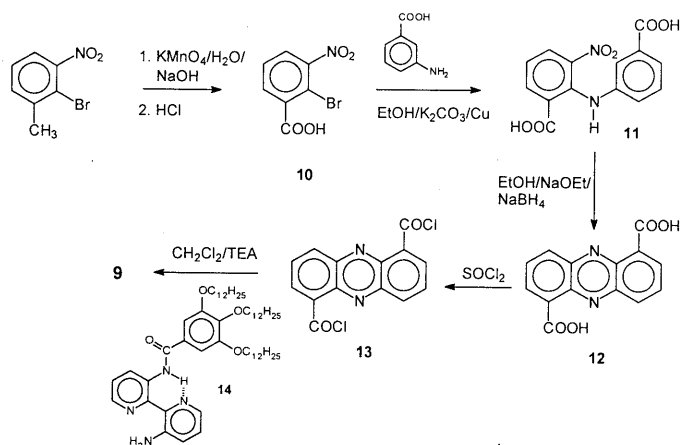
Scheme 3.2: Synthesis of compound 9, a model for a rigid-rod copolymer

Due to the combination of a rigid part and long flexible chains in compound **9**, we anticipated to find liquid crystalline behaviour in this compound. However, this was not the case. Only a sharp melting point was observed at 154–155°C.

Figure 3.8 shows the ^{1}H-NMR spectrum of model compound **9** in CDCl$_3$. Two sharp, downfield NH absorptions indicate the presence of intramolecular H-bonds. With the use of NMR decoupling techniques, all protons could be assigned. Variable temperature ^{1}H-NMR in toluene-*d8* gave $\Delta\delta/\Delta T = 5.3 \times 10^{-3}$ ppm/K for NH$_b$ and $\Delta\delta/\Delta T = 4.1 \times 10^{-3}$ ppm/K for NH$_a$ (measured in a temperature range of 20–75°C), comparable to the results obtained in Chapter 2. Finally, to get an impression of the sterical hindrance between H-9 and H-6", we performed NOE-experiments. Unfortunately, no NOE effects could be observed. However, a low value of the chemical shift in H-2 ($\delta = 8.91$ ppm) and a shielding effect on H-6" ($\delta = 7.63$ ppm) in compound **9** are notable (see below for more details).

The UV spectra of compound **9** and related **15b** gave no indication for conjugation between the bipyridine and the phenazine moiety. The UV spectrum of compound **9** seems to be a superposition of the UV spectra of a diacylated 3,3'-diamino-2,2'-bipyridine and N,N'-dioctyl-phenazine-1,6-dicarbonamide **15b**. This is consistent with the general observation that amides do not contribute significantly to the conjugation.
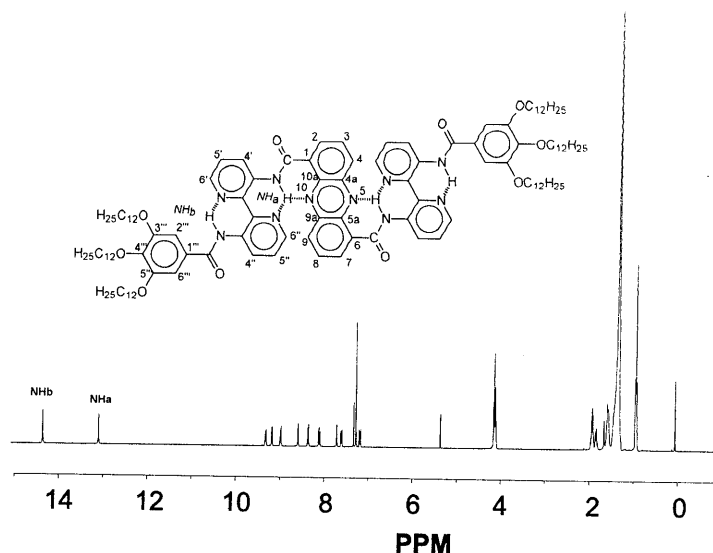
Figure 3.8: ^{1}H-NMR spectrum of compound 9 in CDCl$_3$

Although no evidence could be found for bifurcated H-bonding in the model compound **9**, it is highly unlikely that a bipyridine moiety would be perpendicular or even transoid with respect to the phenazine moiety. The comparison of the chemical shift of H-2 in compound **9** with the one in **15b**, δ = 8.91 and 9.08 ppm, respectively, may be indicative for a small rotation around the phenazine–CO bond. This is analogous to the results obtained in Chapter 2 where a similar decrease in the chemical shift of the proton adjacent to the carbonyl in quinoline derivatives has been attributed to a rotation around the Ph–CO bond. Furthermore, the chemical shift values of H-6 in the bipyridines studied so far are normally around δ ≈ 8.4 ppm (see Chapter 2) but the H-6 signals are now strongly shielded (δ = 7.63 ppm). This is indicative for the proximity of the phenazine ring and bipyridine moiety. A limited degree of out of plane conformation, on the other hand, does not exclude the presence of H-bonding. In a model system, 2-(2-*t*-butoxy-carbonyl-aminophenyl)-pyridine[10], a torsion angle of 37° between the phenyl and the pyridine ring in the crystal structure was found. Nevertheless, H-bonding was still present and a reasonable short distance d(N–H---N) = 2.78 Å was found. In this case, δ(NH) amounted to 11.06 ppm in CDCl$_3$.

Presumably, the lack of sufficient planarity in compound **9** leads to packing difficulties between the aromatic parts of different molecules. This might be an explanation for the absence of liquid crystallinity. The stability of compounds based on the phenazine moiety is exemplified when the melting point of **15a** is considered. The melting only takes place at 408°C and although simultaneously some decomposition is observed, the compound crystallises upon cooling.

3.4 Attempts to introduce lipophilic side chains at the 5,5'-positions of 2,2'-bipyridines

A number of coupling techniques is available to synthesise bipyridines. The Ullmann coupling which is a copper-mediated coupling of aromatic halides is frequently used. Although discovered at the end of the 19th century and despite extensive investigation in the past decades, the mechanism still has not been fully elucidated[11]. The reaction is believed to proceed via the formation of an organo-copper intermediate, but the exact nature of this intermediate and the way in which it is formed and consumed remains concealed. In the Ullmann reaction the reactivity increases in the series Cl<Br<I and highly electronegative groups, such as a nitro group, have an activating effect especially when positioned in *ortho* relative to the halide.

The synthesis of 2,6-dibromo-3-methoxy-5-nitropyridine **18** has been described and proceeds *via* a three step procedure in an overall yield of 15% (scheme 3.3)[12]. If this compound would undergo a selective Ullmann coupling, the desired 2,3,5-bipyridine substitution pattern would become accessible. To investigate the possibility of a selective Ullmann coupling in 2,6-dihalogenated pyridines, model studies have been conducted on 2,6-dichloro-3-nitropyridine. We found that using 1.1 equivalent of Cu-bronze instead of the usual large excess and lowering the temperature from 100°C to 80°C yielded mainly the symmetric Ullmann product by exclusive coupling at C-2. These reaction conditions were subsequently applied to 2,6-dibromo-3-methoxy-5-nitropyridine **18**. The desired coupling product **19** was obtained, indeed, in yields up to 75% after purification.

Furthermore, compounds **20** and **21** could be synthesised as well by using different reducing agents (scheme 3.3). The mild reducing agent $SnCl_2$ led to diamine **21** while the use of hydrazine and Pd/C catalyst produced its debrominated analogue **20**. Both compounds are interesting for comparison with 3,3'-diamino-2,2'-bipyridine and to study the influence of additional substituents on the pyridine ring on the intramolecular H-bonding properties. Crystals were obtained from compound **20** and revealed the similarity in the crystal structure of 3,3'-diamino-2,2'-bipyridine and its 5,5'-dimethoxy derivative **20**.
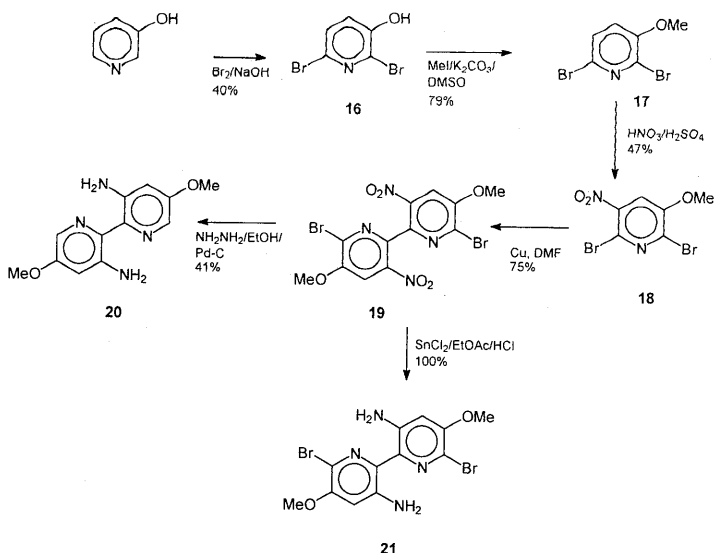
Scheme 3.3: Synthesis towards a 5,5'-substituted 3,3'-diamino-2,2'-bipyridine

As we were interested in long lipophilic chains at the 5,5'-positions, 2,6-dibromo-3-dodecyloxypyridine was synthesised in a procedure similar to that described for methoxy compound **17**. Unfortunately, all attempts to introduce a nitro group at the 5-position failed. Presumably, the lipophilic dodecyloxy group shields off the reactive site (as usually a polar medium is used in nitration reactions) thus preventing the attack of the NO_2^+ ion. Changing our strategy and introducing an alkyl chain in a later stage after demethylation of the methoxy group in compound **18** (or **19**) also failed: it proved to be impossible to obtain demethylated compounds derived from pyridine **18** or bipyridine **19**. Demethylating agents such as BBr$_3$, HBr (48%), AlCl$_3$ and NaSEt showed scarcely any reaction or no desired reaction on compound **18**. Attempted demethylation of compound **18** with LiI in pyridine did lead to a complete disappearance of the starting material and ^{1}H-NMR showed that indeed the Me-group was removed. However, investigation of the red-coloured end-product with ES-MS elucidated that only one bromine was left. From these results combined with the ^{1}H-NMR spectrum we could conclude that one bromine was displaced by pyridine resulting in an ionic compound as shown in figure 3.9. We have not been able to show unambiguously which of the two regio isomers is formed but in view of a higher electrophilicity of C-6, compound A seems most likely. Replacement of pyridine as solvent for a hindered solvent such as 2,6-dimethylpyridine didn't give satisfactory results. Treatment of compound **19** with LiI/pyridine also resulted in the formation of a red-coloured end-product which presumably indicates that again an ionic compound had been formed.
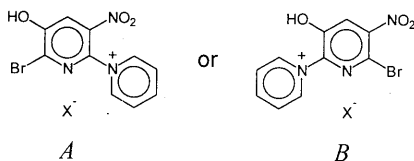
Figure 3.9: Possibilities for the undesired product obtained after reaction of 18 with LiI/pyridine

A number of other approaches could be envisaged to achieve a demethylated version of pyridine **18** or bipyridine **19**. However, due to the limited accessibility of these compounds (long synthesis) this approach was abandoned.

We then decided to concentrate on 5,5'-dimethyl-3,3'-dinitro-2,2'-bipyridine, **22**, which has been obtained in a 4-step procedure in an overall yield of 10%[4]. Several attempts to modify the methyl groups were performed. Oxidation of the methyl group with KMnO$_4$ led to a compound which could not be isolated from the water layer. Treatment with N-bromosuccinimide in CCl$_4$ did not result in any bromination of the methyl groups. Also oxidation with SeO$_2$, which led to excellent results in the oxidation of 6-methyl-2,2'-bipyridine[13], gave no reaction. A method described for the deprotonation of 5,5'-dimethyl-2,2'-bipyridine was applied[14]. The deprotonation did take place in our case. However, side reactions occurred and although all the starting material disappeared, no desired products could be identified. Finally we tried to do a simple condensation of 4-nitrobenzaldehyde with the slightly acidic methyl group in **22**. After 48 hours, no sign of the formation of double bonds was present in the ^{1}H-NMR spectrum. As a result, we also abandoned this approach. In essence, the problem with bipyridine **22** is the same as with compound **19**: a long synthesis with a low overall yield is required to have sufficient starting material available.
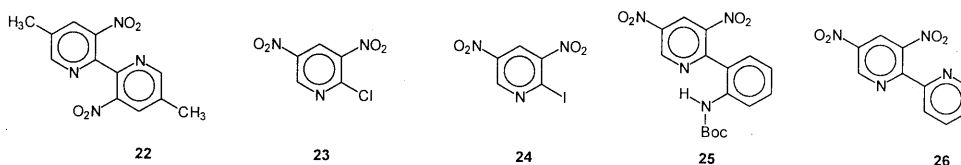
In our search for suitable monomers for 5,5'-disubstituted 3,3'-dinitro-2,2'-bipyridines, 2-chloro-3,5-dinitropyridine, **23**, was considered an interesting starting material. It is easily synthesised by a dinitration of 2-pyridinol using fuming sulphuric acid and fuming nitric acid[15]. The chlorine can be introduced by treating the hydroxy derivative with POCl$_3$ in DMF. Compound **23** was obtained in an overall yield of 40% (lit.[15] 66%). Strangely, all efforts to accomplish an Ullmann coupling with this material failed. Replacing the chlorine for a iodine using a Finkelstein reaction proved to be a highly efficient method to synthesise 2-iodo-3,5-dinitropyridine, **24**, but even this did not lead to a successful Ullmann coupling.

Most likely, an unreactive organocopper intermediate is formed. Unfortunately, this intermediate could not be isolated. If the 5-nitro group in compound **23** could be selectively reduced to an amine, the Ullmann coupling would again be feasible judged from the success in case of 2-chloro-3-nitropyridine and 2,6-dibromo-3-methoxy-5-nitropyridine. Preliminary experiments have indicated that selective reduction of the nitro groups in **23** is possible but no identification of the preferred regioisomer has been accomplished.

Finally, preliminary experiments showed that compound **23** is reactive in the Stille coupling[16,17]. Compound **23** gave rise to coupling products with N-(*t*-butoxycarbonyl)-2-trimethylstannyl-aniline[18] and 2-trimethylstannylpyridine[19] leading to compounds **25** and **26**, respectively, in reasonable yields.

3.5 Conclusions

The 3,3'-di(acylamino)-2,2'-bipyridine moiety is an interesting building block to be incorporated in larger molecules. However, this moiety is also introducing insolubility of the compounds due to the preferred, planar conformation. This has been exemplified when diamino-bipyridine was used to synthesise aromatic polyamides. Small oligomers based on terephthalic acid and 5-alkoxyisophthalic acid are scarcely soluble in organic solvents. Lyotropic liquid crystalline behaviour has not been observed. On the other hand, if the diamino-bipyridyl unit is provided with sufficient lipophilic chains, solubility is guaranteed. This was illustrated with a model compound for the bifurcated H-bonded rigid-rod polymer. Sufficient solubility is the direct result of the introduction of lipophilic chains. Although the preferred conformation of this model compound is deviating from planarity, ^{1}H-NMR results provide evidence that the conformation is not random.

Despite a great number of attempts to introduce lipophilic chains at the 5,5'-position of the bipyridine unit, none of them was successful. Of course, some possibilities remain to be tested. Promising building blocks such as 2-chloro-3,5-dinitropyridine were found to be unreactive in the Ullmann coupling, most likely due to the formation of an unreactive organo-copper intermediate. Despite the fact that making subtle changes at the bipyridine moiety provided more difficulties than initially conceived, 5,5'-dimethoxy-3,3'-diamino-2,2'-bipyridine is available. This building block can function as another moiety to be incorporated in larger structures, giving us the opportunity to study the structure/property relationship.

Although the strong intramolecular H-bonding in the 3,3'-di(acylamino)-2,2'-bipyridine moiety not only leads to rigidification of the molecules but also to a limited solubility, the concept of intramolecular H-bonding providing structure/preferred conformations has been

successfully extended to ladder-type polymers[10,18]. The pyrazine-phenylenediamine based copolymer shown in figure 3.10 is comparable to and designed by analogy of the diamino-bipyridine based rigid-rod polymers. As a result, *soluble* ladder-type polymers have become accessible in which an improved conjugation along the polymer backbone is arising from planarisation by intramolecular H-bonding. Most likely, these H-bonds are less strong than in case of the diamino-bipyridine based polymers, thus enabling a balanced ratio between the structuring capacities wanted and the solubility needed.
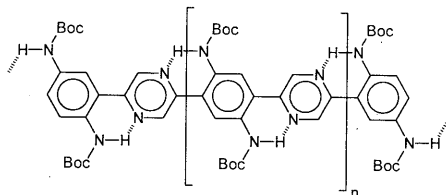
Figure 3.10: Ladder-type polymers in which planarity is enhanced by intramolecular H-bonding by Delnoye et al.[18]

3.6 Experimental procedures

General procedures
For a general section concerning purification of solvents and spectroscopic techniques: see chapter 2. Electrospray MS (ES-MS) was performed on a Perkin Elmer Sciex API-300 LC-MS/MS. Fast-atom bombardment mass spectra (FAB-MS) were recorded on a VG micromass VG 7070E using a Xe beam at 8 kV with nitrobenzyl alcohol (NOBA) as matrix.

N,N'-Bis-3-[3'-benzoylamino-2,2'-bipyridyl]-terephthaloyl diamide (2a)
To a solution of **1a** (*see* compound **9a**, Chapter 2 for the synthesis) (0.26 g, 1.0 mmol) and TEA (2 mmol, 0.15 ml) in dry THF (10 ml), a solution of terephthaloyl chloride (85 mg, 0.41 mmol) in dry THF was added dropwise under argon atmosphere. After stirring at room temperature for 2 h, the solution was heated (60°C) for 15 min. After cooling the precipitate was filtered, washed with THF (3x5 ml) and water (3x15 ml) and dried *in vacuo*. Pure **2a** was obtained as a light yellow powder (0.2 g, 73%). M.p. 382–388°C. ^{1}H-NMR (CDCl$_3$/ CF$_3$COOH 3/1): δ 10.72–9.83 (bs, 4H, NHCO); 8.97 (d, 2H, *J* = 8.4 Hz, H-4); 8.85 (m, 4H, H-4' and H-6'); 8.79 (d, 2H, *J* = 4.5 Hz, H-6); 8.15 (m, 4H, H-5 and H-5'); 7.89 (s, 4H, H-ortho); 7.70 (m, 6H, H'-ortho and H'-para); 7.50 (t, 4H, H'-meta). Anal. calcd. for C$_{42}$H$_{30}$N$_8$O$_4$ (710.75): C, 70.98; H, 4.25; N, 15.76. Found: C, 70.3; H, 4.2; N, 15.9.

N,N'-Bis-3-[3'-(R)-1-phenylethylamino-2,2'-bipyridyl]-terephthaloyl diamide (2b)
To a solution of **1b** (*see* compound **9b**, Chapter 2 for the synthesis) (0.2 g, 0.6 mmol) and TEA (0.1 ml, 1.2 mmol) in dry CH$_2$Cl$_2$/THF (1/1, 20 ml), a solution of terephthaloyl chloride (55 mg, 0.27 mmol) in dry THF (3 ml) was added dropwise under argon atmosphere. After stirring at room temperature for 16 h, the solution was evaporated *in vacuo* . The residue was suspended in a saturated NaHCO$_3$-solution, stirred for 30 min, filtered, washed thoroughly with water and dried. Recrystallisation from THF yielded pure **2b** as a white powder (0.1 g, 48%). T$_{dec}$ = 309°C. ^{1}H-NMR (DMF-*d7*): δ 14.49 (s, 2H, amide-NH); 12.28 (s, 2H, urea-NH); 9.29 (d, 2H, *J* = 8.5 Hz, H-4); 9.03

(d, 2H, J = 8.5 Hz, H-4'); 8.57 (dd, 2H, J = 3.8 and 1.4 Hz, H-6'); 8.53 (dd, 2H, J = 3.5 and 1.2 Hz, H-6); 8.33 (s, 4H, H-ortho); 8.02 (bs, 2H, N<u>H</u>CH(CH$_3$)Ph); 7.60 (dd, 2H, J = 4.5 and 8.5 Hz, H-5); 7.53 (dd, 2H, J = 4.5 and 8.5 Hz, H-5'); 7.44 (d, 4H, H'-ortho); 7.34 (t, 4H, H'-meta); 7.25 (t, 2H, H'-para); 5.01 (q, 2H, C<u>H</u>(CH$_3$)Ph); 1.47 (d, 6H, CH$_3$). Anal calcd. for C$_{46}$H$_{40}$N$_{10}$O$_4$ (796.88): C, 69.33; H, 5.06; N, 17.58. Found: C, 68.7; H, 5.4; N, 17.9.

5-Dodecyloxy-isophthaloyl chloride (5a)
A mixture of dimethyl 5-hydroxy-isophthalate (10 g, 47.6 mmol), 1-dodecyl bromide (11.85 g, 47.6 mmol) and K$_2$CO$_3$ (13.16 g) was heated under reflux in K$_2$CO$_3$ (400 ml) for 20 h. The mixture was cooled, the precipitate was filtered and the filtrate was evaporated *in vacuo*. The brown solid residue was recrystallised twice from EtOH (96%) to yield pure **3a** as a white solid (14.2 g, 79%). M.p. 55.7–57°C. ^{1}H-NMR (CDCl$_3$): δ 8.26 (s, 1H, H-2); 7.74 (2, 2H, H-4 and H-6); 4.03 (t, 2H, OCH$_2$); 3.94 (s, 6H, OCH$_3$); 1.82 (qui, 2H, OCH$_2$C<u>H</u>$_2$); 1.48 (qui, 2H, OCH$_2$CH$_2$C<u>H</u>$_2$); 1.30 (m, 16H, (C<u>H</u>$_2$)$_8$); 0.88 (t, 3H, CH$_3$). Anal. calcd. for C$_{22}$H$_{34}$O$_5$ (378.50): C, 69.81; H, 9.05. Found: C, 70.1; H, 9.2. A solution of KOH (1.77 g, 31.6 mmol) in EtOH (96%, 35 ml) was added dropwise to a suspension of **3a** (3 g, 7.9 mmol) in EtOH (96%, 35 ml). The mixture was heated under reflux for 3 h, cooled to room temperature and acidified with a concentrated HCl solution to pH = 2. Water (100 ml) was added and the resulting white precipitate was filtered, washed with H$_2$O and dried *in vacuo* to yield pure **4a** as a white powder (2.75 g, 99%). Recrystallisation from EtOH yielded an analytically pure sample. T_{cl} = 175°C. ^{1}H-NMR (DMSO-*d6*): δ 13.30 (bs, 2H, COOH); 8.05 (s, 1H, H-2); 7.61 (s, 2H, H-4 and H-6); 4.02 (t, 2H, OCH$_2$); 1.82 (qui, 2H, OCH$_2$C<u>H</u>$_2$); 1.38 (qui, 2H, OCH$_2$CH$_2$C<u>H</u>$_2$); 1.28 (m, 16H, (C<u>H</u>$_2$)$_8$); 0.87 (t, 3H, CH$_3$). Compound **4a** (2 g, 5.7 mmol) was heated under reflux in SOCl$_2$ (15 ml) for 3 h. The excess SOCl$_2$ was distilled off. The resulting solid was flushed with *n*-hexane (2x10 ml) to yield pure **5a** as a white powder (2.2 g, 100%). ^{1}H-NMR (CDCl$_3$): δ 8.45 (s, 1H, H-2); 7.88 (s, 2H, H-4 and H-6); 4.08 (t, 2H, OCH$_2$); 1.88 (qui, 2H, OCH$_2$C<u>H</u>$_2$); 1.50 (qui, 2H, OCH$_2$CH$_2$C<u>H</u>$_2$); 1.35 (m, 16H, (C<u>H</u>$_2$)$_8$); 0.88 (t, 3H, CH$_3$).

5-Octadecyloxy-isophthaloyl chloride (5b)
A mixture of dimethyl 5-hydroxy-isophthalate (10 g, 47.6 mmol), 1-octadecyl bromide (16.5 g, 47.6 mmol) and K$_2$CO$_3$ (14 g) was heated under reflux in DMF (100 ml) for 6 h. The hot mixture was poured into water, cooled and the resulting precipitate was filtered and dried. After recrystallisation from EtOH (96%) pure **3b** was obtained as a white solid (16.7 g, 76%). M.p. 70–71°C. ^{1}H-NMR (CDCl$_3$): δ 8.26 (s, 1H, H-2); 7.74 (2, 2H, H-4 and H-6); 4.04 (t, 2H, OCH$_2$); 3.93 (s, 6H, OCH$_3$); 1.83 (qui, 2H, OCH$_2$C<u>H</u>$_2$); 1.48 (qui, 2H, OCH$_2$CH$_2$C<u>H</u>$_2$); 1.35 (m, 28H, (C<u>H</u>$_2$)$_{14}$); 0.87 (t, 3H, CH$_3$). To a solution of KOH (5 g, 89 mmol) in EtOH (96%, 200 ml) and THF (100 ml), **3b** (10 g, 21 mmol) was added. The mixture was heated under reflux for 3 h. Water was added to the hot mixture until a clear solution was obtained. After acidification with concentrated HCl-solution, a white precipitate was formed which was filtered and washed with cold EtOH (96%). This afforded pure **4b** (8.95 g, 98%). M.p. 163–165°C. ^{1}H-NMR (CDCl3): δ 8.26 (s, 1H, H-2); 7.74 (2, 2H, H-4 and H-6); 4.04 (t, 2H, OCH$_2$); 1.83 (qui, 2H, OCH$_2$C<u>H</u>$_2$); 1.48 (qui, 2H, OCH$_2$CH$_2$C<u>H</u>$_2$); 1.35 (m, 28H, (C<u>H</u>$_2$)$_{14}$); 0.87 (t, 3H, CH$_3$). Compound **4b** (1.04 g, 2.39 mmol) was heated under reflux in SOCl$_2$ (20 ml) for 3 h. The excess SOCl$_2$ was distilled off. The resulting solid was flushed with *n*-hexane (2x10 ml) to yield pure **5b** as a white powder (1.12 g, 100%). ^{1}H-NMR (CDCl$_3$): δ 8.44 (s, 1H, H-2); 7.87 (s, 2H, H-4 and H-6); 4.08 (t, 2H, OCH$_2$); 1.85 (qui, 2H, OCH$_2$C<u>H</u>$_2$); 1.48 (qui, 2H, OCH$_2$CH$_2$C<u>H</u>$_2$); 1.31 (m, 28H, (CH$_2$)$_{14}$); 0.89 (t, 3H, CH$_3$). ^{13}C-NMR (CDCl$_3$): δ 167.3 (C=O); aromatic carbons: 159.83; 135.26; 125.85; 122.73. alphatic carbons: 62.24; 31.92; 31.59; 12 carbons between 29.69 and 28.90; 25.89; 22.66; 14.12.

General procedure for high dilution polymerisation of 3,3'-diamino-2,2'-bipyridine with diacid dichlorides 5a,b

To dry dichloromethane (100 ml) in a round-bottom flask under Ar atmosphere, two solutions were simultaneously added *via* a syringe at a rate of 0.15 ml/min. The first syringe contained a 33 mM solution of 3,3'-diamino-2,2'-bipyridine and TEA in dry dichloromethane (30 ml). The second syringe contained a 33 mM solution of diacid dichloride **5a** or **5b** in dry dichloromethane (30 ml). After 3.5 h the addition was completed and a finely powdered precipitate had formed. The mixture was stirred overnight. The precipitate was filtered (P4 glass filter) and dried to yield a cream-coloured powder. Reaction with **5a**: ^{1}H-NMR (CDCl$_3$/CF$_3$COOH): δ 10.20 (bs, 2H); 8.95 (d, 2H); 8.75 (s, 2H); 8.10 (s, 2H); 8.0 (s, 1H); 7.50 (s, 2H); 4.05 (bs, 2H, OCH$_2$); 1.90 (s, 2H, OCH$_2$C$\underline{H}_2$); 1.50 (bs, 18H, (CH$_2$)$_9$); 0.85 (s, 3H, CH$_3$). Reaction with **5b**: ^{1}H-NMR (CDCl$_3$/CF$_3$COOH): δ 8.95 (2xbs, 4H); 8.20 (bs, 3H); 7.60 (s, 2H); 4.05 (bs, 2H, OCH$_2$); 1.90 (s, 2H, OCH$_2$C$\underline{H}_2$); 1.50 (bs, 30H, (CH$_2$)$_{15}$); 0.85 (s, 3H, CH$_3$).

N,N'-Di[3-(3'-benzoylamino-2,2'-bipyridyl)]-5-dodecyloxy-isophthaloyl diamide (6)

To an ice-cooled solution of **1a** (0.18 g, 0.52 mmol) and TEA (0.1 ml) in dry CH$_2$Cl$_2$ (8 ml), a solution of **5a** (0.11 g, 0.26 mmol) in dry CH$_2$Cl$_2$ (4 ml) was slowly added under an Ar atmosphere. After the addition had been completed, stirring was continued at room temperature for 6 h. The precipitates were filtered and recrystallisation from CH$_2$Cl$_2$ yielded pure **6** as a white powder (50 mg, 22%). Monotropic: I 196°C M 170°C K. ^{1}H-NMR (CDCl$_3$): δ 15.01 (s, 2H, NHCO); 14.66 (s, 2H, NH'CO); 9.40 (m, 2H, H-4 and H-4'); 8.62 (d, 2H, H-6); 8.43 (s, 1H, H-para); 8.34 (d, 2H, H-6'); 8.04 (s, 4H, H'-ortho); 7.76 (s, 2H, H-ortho); 7.50 (m, 6H, H'-meta and H'-para); 7.4 (dd, 2H, H-5 and H-5'); 4.15 (t, 2H, OCH$_2$); 1.89 (qui, 2H, OCH$_2$C$\underline{H}_2$); 1.54 (qui, 2H, OCH$_2$CH$_2$C$\underline{H}_2$); 1.27 (m, 16H, (CH$_2$)$_8$); 0.88 (t, 3H, CH$_3$).

N,N'-Di[3-(3'-t-butoxycarbonylamino-2,2'-bipyridyl)]-5-dodecyloxy-isophthaloyl diamide (7)

To an ice-cooled solution of **1c** (0.6 g, 2.1 mmol) and TEA (0.6 ml) in dry diethyl ether (20 ml), a solution of **5a** (0.36 g, 1 mmol) in dry diethyl ether (10 ml) was slowly added under an Ar atmosphere. After the addition had been completed, the stirring was continued at room temperature for 12 h. Then, the diethyl ether was evaporated and the solid was solvated in CH$_2$Cl$_2$ (70 ml). The organic phase was extracted with sat. NaHCO$_3$ solution (2x70 ml), H$_2$O (2x70 ml), dried with MgSO$_4$ and dried *in vacuo*. Recrystallisation from EtOAc yielded pure **7** as a white powder (0.59 g, 74%). M.p. 189–191.5°C. ^{1}H-NMR (CDCl$_3$): δ 14.82 (s, 2H, NHCO); 12.61 (s, 2H, NH'CO); 9.40 (d, 2H, H-4); 8.89 (d, 2H, H-4'); 8.50 (d, 2H, H-6); 8.46 (s, 1H, H-para); 8.42 (d, 2H, H-6'); 7.80 (s, 2H, H-ortho); 7.44 (dd, 2H, H-5); 7.34 (dd, 2H, H-5'); 4.16 (t, 2H, OCH$_2$); 1.88 (qui, 2H, OCH$_2$C$\underline{H}_2$); 1.58 (bs, 20H, OCH$_2$CH$_2$C$\underline{H}_2$ and C(CH$_3$)$_3$); 1.35 (m, 16H, (CH$_2$)$_6$); 0.88 (t, 3H, CH$_3$). Anal. calcd. for C$_{50}$H$_{62}$N$_8$O7 (887.09): C, 67.70; H, 7.04; N, 12.63. Found: C, 67.6; H, 6.9; N, 12.5.

N,N'-Di(3-pyridyl)-5-dodecyloxy-isophthaloyl diamide (8)

The experiment was performed in a test tube at small scale by mixing in excess 3-aminopyridine with **5a** in the presence of TEA in CH$_2$Cl$_2$. Pouring the mixture in an excess of MeOH afforded a precipitate which was pure **8**. Crystals were grown by slow evaporation of a solution of compound **8** in CHCl$_3$/MeOH (3/1). M.p. 142–143°C. ^{1}H-NMR (CDCl$_3$): δ 9.50 (s, 2H, H-2); 8.74 (s, 2H, NHCO); 8.22 (d, 4H, H-4 and H-6); 7.81 (s, 1H, H-para); 7.48 (s, 2H, H-ortho); 7.26 (dd, 2H, H-5); 3.94 (t, 2H, OCH$_2$); 1.88 (qui, 2H, OCH$_2$C$\underline{H}_2$); 1.55 (qui, 2H, OCH$_2$CH$_2$C$\underline{H}_2$); 1.35 (bs, 16H, (CH$_2$)$_6$); 0.88 (t, 3H, CH$_3$).

2-Bromo-3-nitro-benzoic acid (10)

To a stirred suspension of 2-bromo-3-nitrotoluene (1.02 g, 4.7 mmol) in H_2O (4 ml), a solution of NaOH (0.4 g) in water (1 ml) was added. This mixture was then added to a stirred solution of $KMnO_4$ (1.66 g, 10 mmol) in water (35 ml). After heating under reflux for 3 h, the resulting solids were filtered over celite and washed with hot water. The filtrate was concentrated *in vacuo* to approx. 15 ml and acidified using concentrated HCl to pH = 2. The resulting precipitate was filtered and washed with water yielding pure **10** (0.66 g, 57%). M.p. 191°C.

2-(3-Carboxyanilino)-3-nitrobenzoic acid (11)

A mixture of **10** (1 g, 4 mmol), *m*-amino-benzoic acid (0.86 g, 6.2 mmol), K_2CO_3 (anhydrous, 0.9 g) and Cu-bronze (0.05 g) in dry EtOH (10 ml) was heated under reflux under an Ar atmosphere. After 24 h, the EtOH was removed *in vacuo* and water was added. The precipitate was filtered and the filtrate was acidified using concentrated HCl (pH = 2). The resulting filtrate was filtered and washed yield pure **11** (0.71 g, 59%, lit.[9] 63%). M.p. 264–265°C. ^{1}H-NMR (acetone-*d6*): δ 10.11 (s, 1H, NH); 8.38 (d, 1H, *J* = 7.8 Hz, H-4); 8.13 (d, 1H, *J* = 8.0 Hz, H-6); 7.71 (d, 1H, *J* = 7.6 Hz, H-4'); 7.62 (s, 1H, H-2'); 7.41 (t, 1H, *J* = 7.8 Hz, H-5); 7.26 (d, 1H, *J* = 7.8 Hz, H-6'); 7.17 (t, 1H, *J* = 7.8 Hz, H-5').

Phenazine-1,6-dicarboxylic acid (12)

A mixture of **3** (99 mg, 0.4 mmol), $NaBH_4$ (78 mg, 2.0 mmol) and NaOEt (97 mg, 1.5 mmol) was heated under reflux in dry EtOH (4 ml). After 30 h, the EtOH was removed *in vacuo* and sufficient water was added to dissolve the solid. After acidification with conc. HCl (pH = 2), the resulting precipitate was filtered and washed thoroughly with DMSO (to remove phenazine-1,8-dicarboxylic acid). The resulting solid was pure **12** (23 mg, 25%, lit.[9] 35%). ^{1}H-NMR ($CDCl_3/CF_3COOH$ 3/1): δ 9.27 (dd, 2H, *J* = 7.1 and 1.1 Hz, H-2 and H-7); 8.89 (dd, 2H, *J* = 8.8 and 1.1 Hz, H-4 and H-9); 8.47 (dd, 2H, *J* = 7.1 and 8.8 Hz, H-3 and H-8). ^{13}C-NMR ($CDCl_3/CF_3COOH$ 3/1): δ 169.2 (C=O); aromatic carbons: 140.8; 139.6; 139.0; 134.6; 133.2; 122.5.

Phenazine-1,6-dicarbonyl dichloride (13)

A solution of **12** (120 mg, 0.45 mmol) in $SOCl_2$ (4 ml) was heated under reflux for 3 h. Thionyl chloride was distilled of and the remaining solid was flushed with hexane (2x2 ml). The diacid dichloride was obtained in a quantitative yield (135 mg). ^{1}H-NMR ($SOCl_2/CDCl_3$): δ 8.64 (d, 2H, *J* = 7.2, H-2 and H-7); 8.59 (d, 2H, *J* = 7.6 Hz, H-4 and H-9); 8.02 (t, 2H, *J* = 7.6 Hz, H-3 and H-8).

N,N'-Di[3'-(3,4,5-tridodecyloxybenzoylamino)-2,2'-bipyridyl]phenazine-1,6-dicarbonamide (9)

Under Ar atmosphere, a solution of 3'-(3,4,5-tridodecyloxybenzoylamino)-2,2'-bipyridine-3-amine **14** (*see* compound **5b**, Chapter 4 for the synthesis) (1.01 g, 1.2 mmol) and TEA (0.2 ml) in dry CH_2Cl_2 (15 ml) was added dropwise to an ice-cooled solution of **13** (127 mg, 0.45 mmol) in dry CH_2Cl_2 (10 ml). When the addition was complete, the mixture was heated under reflux for 1 h. After cooling, the desired compound precipitated and was filtered. Recrystallisation from CH_2Cl_2 yielded pure **9** as a yellow powder (0.67 g, 65%). M.p. 154-155°C. ^{1}H-NMR ($CDCl_3$): δ 14.28 (s, 2H, $CONH_b$); 13.02 (s, 2H, $CONH_a$); 9.26 (dd, 2H, *J* = 8.7 and 1.6, H-4'); 9.12 (dd, 2H, *J* = 8.5 Hz, H-4"); 8.91 (dd, 2H, *J* = 7.3 and 0.9 Hz, H-2 and H-7); 8.52 (dd, 2H, *J* = 4.5 and 1.4 Hz, H-6'); 8.30 (dd, 2H, *J* = 8.6 and 1.1 Hz, H-4 and H-9); 8.05 (dd, 2H, *J* = 8,4 and 7.3 Hz, H-3 and H-8); 7.63 (dd, 2H, *J* = 4.6 and 1.4 Hz, H-6"); 7.55 (dd, 2H, *J* = 8.6 and 4.7 Hz, H-5'); 7.21 (s, 4H, H-ortho); 7.13 (dd, 2H, *J* = 8.5 and 4.6 Hz, H-5"); 4.08 (m, 12H, OCH_2); 1.87 (m, 8H, *m*-$OCH_2C\underline{H}_2$); 1.78 (m, 4H, *p*-$OCH_2C\underline{H}_2$); 1.50 (m, 108H, $(CH_2)_9$); 0.88 (t, 18H, CH_3). Anal. calcd. for $C_{120}H_{176}N_{10}O_{10}$ (1918.78): C, 75.11; H, 9.24; N, 7.30. Found: C, 74.7; H, 8.6; N, 7.5.

N,N'-Di-(3-pyridyl)-phenazine-1,6-dicarbonamide (15a)

To an ice cooled solution of **13** (448 mg, 1.4 mmol) in CH_2Cl_2 (10 ml), a solution of 3-aminopyridine (270 mg, 2.8 mmol) and TEA (1.0 ml) was added dropwise under an Ar atmosphere. After stirring for 1 h, the mixture was heated under reflux for another hour. After cooling, the precipitate was filtered and washed with CH_2Cl_2. Pure **15a** was thus obtained (410 mg, 70%). M.p. 409–410°C (slight decomposition). ^{1}H-NMR ($CDCl_3/CF_3COOH$ 3/1): δ 9.79 (s, 2H, H-2'); 9.25 (d, 2H, J = 7.2 Hz, H-2 and H-7); 9.14 (d, 2H, J = 8.1 Hz, H-4'); 8.87 (d, 2H, J = 8.9 Hz, H-4 and H-9); 8.75 (d, 2H, J = 5.4 Hz, H-6'); 8.43 (t, 2H, J = 7.5 and 8.3 Hz, H-3 and H-8); 8.23 (dd, 2H, J = 5.7 and 8.4 Hz, H-5').

N,N'-Dioctyl-phenazine-1,6-dicarbonamide (15b)

A mixture of **13** (42 mg, 0.1 mmol) and an excess of *n*-octylamine (3 ml) was heated at 80°C for 30 min. After cooling, the precipitate was filtered and washed with diethyl ether (57 mg, 85%). Recrystallisation from hexane afforded an analytically pure sample. M.p. 147.5–148.7°C. ^{1}H-NMR ($CDCl_3$): δ 10.75 (t, 2H, CONH); 9.08 (d, 2H, J = 7.2 and 1.0 Hz, H-2 and H-7); 8.35 (d, 2H, J = 8.5 and 1.0 Hz, H-4 and H-9); 8.08 (t, 2H, J = 8.6 and 7.3 Hz, H-3 and H-8); 3.50 (qua, 4H, NHC$\underline{H}_2$); 1.90 (qui, 4H, NHCH$_2$C$\underline{H}_2$); 1.37 (m, 20H, $(CH_2)_5$); 0.88 (t, 6H, CH_3).

2,6-Dibromo-3-methoxy-5-nitropyridine (18)

The title compound was synthesised according to literature procedures[12] in an overall yield of 15% (lit. 15%). M.p. 115.2–116.8°C (lit. 113–114°C). ^{1}H-NMR ($CDCl_3$): δ 7.64 (s, 1H, H-4); 4.02 (s, 3H, OCH_3). ^{13}C-NMR ($CDCl_3$): δ 153.0 (C-3), 145.4 (C-5), 135.0 (C-2), 121.8 (C-6), 115.7 (C-4), 57.4 (OCH_3).

Attempted demethylation of 18 with LiI/pyridine leading to 2-bromo-3-methoxy-5-nitro-6-N-pyridinium-pyridine

To compound **18** (1 g, 3.2 mmol) in pyridine (15 ml), LiI (0.5 g) was added. The mixture was heated under reflux for 3 h. The excess pyridine was distilled off under reduced pressure and the resulting brown oil was flushed with toluene (2x3 ml) to remove traces of pyridine. Ice-water (100 ml) was added to the oil and the mixture was extracted with $CHCl_3$ (3x50 ml). The organic layers were collected and evaporated *in vacuo* and yielded an orange-red solid. Recrystallisation from CH_3CN afforded orange-red plate-shaped crystals (0.3 g). ^{1}H-NMR (DMSO-*d6*): δ 9.65 (d, 2H); 8.60 (t, 1H); 8.15(t, 2H); 7.40 (s, 1H, H-4); 3.45 (s, 1H, OH). Calcd. for $C_{10}H_7N_3O_3Br$ (297.08) ES-MS (MeOH): m/z: 297.8 (d, 1:1 ratio caused by natural abundance of 1 Br, M$^+$); 614.5 (cluster); 759.9 (cluster); 909.8 (cluster).

6,6'-Dibromo-5,5'-dimethoxy-3,3'-dinitro-2,2'-bipyridine (19)

To a solution of **18** (1.10 g; 3.53 mmol) in DMF (3 ml), copper (0.25 g; 3.88 mmol) was added under an argon atmosphere. The suspension was stirred at 70°C during 24 h, after which it was poured into water (75 ml). The resulting precipitate was filtered, washed with water (2x20 ml), 25% ammonia (1x10 ml), 5% ammonia (5x20 ml) and water (2x20 ml). After drying *in vacuo* at 40°C, the resulting powder was repeatedly recrystallised from acetonitrile to give the pure title compound **19** (0.33 g; 40%). After evaporation of the mother liquor, column filtration of the residue (9 g SiO_2; eluent CH_2Cl_2; R_f = 0.50) yielded an additional amount of **19** (0.16 g, 20%; total yield 0.49 g, 60%). M.p. 242.7–244.0°C. ^{1}H-NMR ($CDCl_3$): δ 7.95 (s, 2H, H-4), 4.11 (s, 6H, OCH_3). ^{13}C-NMR ($CDCl_3$): δ 153.7 (C-5), 143.2 (C-2), 141.1 (C-3), 137.0 (C-6), 114.1 (C-4), 57.3 (OCH_3). Anal. calcd. for $C_{12}H_8Br_2N_4O_6$ (464.02): C, 31.06; H, 1.74; N, 12.07. Found: C, 31.5; H, 1.8; N, 12.2.

5,5'-Dimethoxy-2,2'-bipyridine-3,3'-diamine (20)

To a solution of **19** (0.60 g; 1.29 mmol) in ethanol (15 ml), hydrazine monohydrate (6 ml) and 10% Pd/C (0.25 g) were added under an argon atmosphere. After refluxing for 30 min, the suspension was filtered and the solution concentrated *in vacuo*. The residual powder was taken up in 13% ammonia (40 ml) and the suspension extracted with CH_2Cl_2 (4x40 ml). After drying with $MgSO_4$ and removal of the solvent *in vacuo*, a column separation of the residue (SiO_2; eluent $CHCl_3$/MeOH 97.5/2.5; $R_f =$ 0.33), followed by removal of an impurity by precipitation from acetone yielded analytically pure **20** (0.16 g, 41%). M.p. 190.1–191.6°C. ^{1}H-NMR ($CDCl_3$): δ 7.68 (d, 2H, J = 2.5 Hz, H-6); 6.54 (d, 2H, J = 2.6 Hz, H-4); 6.26 (s, 4H, NH_2); 3.83 (s, OCH_3). ^{13}C-NMR ($CDCl_3$): δ 154.8 (C-5); 144.4 (C-3); 134.6 (C-2); 123.3 (C-6); 107.7 (C-4); 55.4 (OCH_3). Anal. calcd. for $C_{12}H_{14}N_4O_2$ (246.26): C, 58.53; H, 5.73; N, 22.75. Found: C, 56.2; H, 5.7; N, 22.8.

6,6'-Dibromo-5,5'-dimethoxy-2,2'-bipyridine-3,3'-diamine (21)

To a solution of **19** (100 mg, 0.22 mmol) in EtOAc (10 ml), a solution of $SnCl_2$ (300 mg, 1.6 mmol) in 37% HCl solution was added in 15 min. When the addition was complete, EtOAc was evaporated *in vacuo* and the resulting suspension was heated. After 2 h. the mixture was poured into ice-water and the resulting precipitate was filtered and washed with cold water. Compound **21** was thus obtained in a quantitative yield. ^{1}H-NMR (DMSO-*d6*): δ 6.90 (s, 2H, H-4); 5.20 (bs, 4H, NH_2); 3.84 (s, 6H, OCH_3).

5,5'-Dimethyl-3,3'-dinitro-2,2'-bipyridine (22)

The compound was synthesised according to a modified procedure described by Kaczmarek[4]. 2-Amino-5-methylpyridine (3 g, 27.7 mmol) was dissolved in concentrated H_2SO_4 (15 ml) and cooled to −5°C. A mixture of concentrated sulphuric acid (2.5 ml) and nitric acid (2.5 ml) was slowly added, keeping the temperature below 10°C. After the addition was completed, the mixture was stirred at room temperature for 48 h. The mixture was poured into ice, neutralised and the resulting precipitate was filtered, washed with water and dried. This yielded 2-amino-5-methyl-3-nitropyridine (1.06 g, 25%). ^{1}H-NMR ($CDCl_3$): δ 8.95 (d, 1H, J = 1.9 Hz, H-6); 8.52 (bs, 2H, NH_2); 8.28 (d, 1H, J = 1.1 Hz, H-4); 2.51 (s, 3H, CH_3). Anal. calcd. for $C_6H_7N_3O_2$ (153.14): C, 47.06; H, 4.58; N, 27.45. Found: C, 47.4; H, 4.3; N, 28.2. Diazotisation of 2-amino-5-methyl-3-nitropyridine afforded 2-hydroxy-5-methyl-3-nitropyridine (2.07 g, 54%). M.p. 252–258°C. ^{1}H-NMR ($CDCl_3$/CF_3COOH 3/1): δ 8.74 (d, 1H, J = 1.4 Hz, H-6); 7.90 (s, 1H, H-4); 2.40 (s, 3H, CH_3). Anal. calcd. for $C_6H_6N_2O_3$ (154.12): C, 46.75; H, 4.55; N, 18.18. Found: C, 46.7; H, 4.2; N, 18.6. 2-Hydroxy-5-methyl-3-nitropyridine (1.01 g, 6.5 mmol) was treated with $POCl_3$ (10 ml) at reflux temperature for 6 h. The excess of $POCl_3$ was distilled off. Ice-water was added to the resulting oil and the mixture was extracted with diethyl ether. Evaporation of the solvent *in vacuo* afforded 2-chloro-5-methyl-3-nitropyridine (0.99 g, 89%). ^{1}H-NMR ($CDCl_3$/CF_3COOH 3/1): δ 8.60 (s, 1H, H-6); 8.30 (s, 1H, H-4); 2.46 (s, 3H, CH3). Anal. calcd. for $C_6H_5ClN_2O_2$ (172.57): C, 41.74; H, 2.90; N, 16.23. Found: C, 42.0; H, 3.3; N, 16.6. To a solution of 2-chloro-5-methyl-3-nitropyridine (8.6 g, 50 mmol) in DMF (42 ml) at 100°C, Cu (8 g) was added in small portions. After the addition was completed the mixture was stirred at 100°C until all starting material had disappeared. The mixture was poured into water and the precipitate was filtered. After Soxhlet extraction of the precipitate with CH_3CN, evaporation of the solvent *in vacuo* and treatment of the resulting solid with 5% NH_3-solution, pure compound **22** was obtained (5.9 g, 85%). Recrystallisation from CH_3CN afforded an analytically pure sample. M.p 197.5–199.5°C. ^{1}H-NMR ($CDCl_3$): δ 8.61 (d, 2H, J = 1.4 Hz, H-6); 8.29 (d, 2H, J = 1.4 Hz, H-4); 2.46 (s, 6H, CH_3). Anal. calcd. for $C_{12}H_{10}N_4O_4$ (274.23): C, 52.55; H, 3.68; N, 20.44. Found: C, 52.4; H, 3.9; N, 20.4.

2-Chloro-3,5-dinitropyridine (23)

2-Chloro-3,5-dinitropyridine was synthesised according to a literature procedure[15] (45%, lit. 66%). M.p. 62–63°C. ^{1}H-NMR (CDCl3): δ 9.44 (d, 1H, J = 2.4 Hz, H-6); 9.01 (d, 1H, J = 2.4 Hz, H-4). ^{13}C-NMR (CDCl3): δ 148.8; 147.0; 144.2; 142.8; 129.6.

2-Iodo-3,5-dinitropyridine (24)

A solution of **23** (0.30 g; 1.5 mmol) and sodium iodide (1.19 g; 7.94 mmol) in acetone (4 ml) was heated under reflux. After 6 h the acetone was removed *in vacuo* and the resulting solid taken up in diethyl ether. The diethyl ether was washed with water (2x20 ml) and the combined aqueous layers were extracted with diethyl ether (2x50 ml). The combined organic layers were dried over magnesium sulfate and concentrated *in vacuo*[#]. The resulting powder was subjected to recrystallisation from diisopropyl ether which yielded the title compound as a yellow powder (0.30 g, 69%). M.p. 101.0–101.7°C. ^{1}H-NMR (CDCl3): δ 9.35 (d, 1H, J = 2.4 Hz, H-6), 8.80 (d, 1H, J = 2.4 Hz, H-4).^{13}C-NMR (CDCl3): δ 147.2; 143.6; 142.7; 127.4; 117.5.

2-[2-(t-Butoxycarbonylamino)phenyl]-3,5-dinitropyridine (25)

2-Trimethylstannyl-(N-*t*-butoxycarbonyl)aniline[18] (0.175 g; 0.493 mmol), 2-chloro-3,5-dinitropyridine (0.100 g; 0.495 mmol), Cu2Br2 (6.2 mg; 22 μmol) and Pd(PPh3)2Cl2 (9.9 mg; 14 μmol) were added under argon to dry THF (5 ml). After 5 freeze-thaw cycles, the solution was heated under reflux. After 30 h, the solvent was removed *in vacuo*. The residue was dissolved in CHCl3 and washed with an aqueous 5% ethylenediamine solution (1x), water (3x) and brine (1x). After drying over MgSO4 and removal of the solvent *in vacuo*, column chromatography was carried out (SiO2; eluent *n*-hexane/ethyl acetate 4/1) to yield the pure title compound (R$_f$ = 0.23) as an orange solid (89 mg, 50%). M.p. 127.5–128.9°C. ^{1}H-NMR (CDCl3): δ 9.64 (d, 1H, J = 2.4 Hz, H-6), 8.96 (d, 1H, J = 2.1 Hz, H-4), 7.80 (d, 1H, J = 8.2 Hz, H-3') 7.66 (s, 1H, NH), 7.48 (td, 1H, J = 1.2 and 7.2 Hz, H-4'), 7.33 (dd, 1H, J = 1.2 and 6.6 Hz, H-6'), 7.20 (td, 1H, J = 0.8 and 7.4 Hz, H-5'), 1.40 (s, 9H, (CH3)3). ^{13}C-NMR (CDCl3): δ 157.3 (C=O), 152.6 (C-2), 146.3 (C-6), 145.2 (C-3), 141.8 (C-5), 136.2 (C-2'), 132.1 (C-1'), 129.7 (C-6'), 128.3 (C-4'), 125.5 (C-4), 124.4 (C-5'), 122.9 (C-3'), 81.1 (C-ipso), 28.1 (CH3)3. Anal. calcd. for C16H16N4O6 (360.33): C, 53.33; H, 4.48; N, 15.55. Found: C, 52.6; H, 4.5; N, 15.1.

3,5-Dinitro-2,2'-bipyridine (26)

A solution of 2-chloro-3,5-dinitropyridine (0.68 g; 3.3 mmol), Pd(PPh3)2Cl2 (0.11 g; 0.16 mmol), Cu2Br2 (47 mg; 0.16 mmol) and 2-trimethylstannylpyridine[19] (0.9 g; 3.7 mmol) in THF (30 ml) was degassed with three freeze-thaw cycles before heating overnight under reflux under an argon atmosphere. The resulting solution was concentrated *in vacuo*, suspended in CHCl3 (40 ml) and successively washed with an aqueous 5% ethylenediamine solution (1x40 ml), water (3x40 ml) and brine (1x40 ml) before being dried over magnesium sulfate and concentration *in vacuo*. A column filtration (eluent CHCl3/methanol 99/1) followed by crystallisation from CHCl3 resulted in the title compound (greenish needles) (0.30 g, 37%). M.p. 173.3–175.5°C.^{1}H-NMR (CDCl3): δ 9.60 (d, J = 2.2 Hz, 1H, H-6), 8.80 (d, 1H, J = 2.3 Hz, H-4), 8.64 (qd, 1H, J = 0.8 Hz, 1.0 Hz and 2.2 Hz, H-6'), 8.25 (td, 1H, J = 1.0 and 5.9 Hz, H-3'), 7.94 (td, 1H, J = 1.7 and 6.0 Hz, H-4'), 7.46 (qd, 1H, J = 1.2, 1.7 and 3.6 Hz, H-5').^{13}C-NMR (CDCl3): δ 154.5 (C-2), 151.8 (C-2'), 149.4 (C-6), 145.7 (C-6'), 145.4 (C-3), 142.6 (C-5), 137.3 (C-4'), 127.7 (C-4), 125.8 (C-3'), 124.1 (C-5'). Anal. calcd. for C10H6N4O4 (246.18): C, 48.79; H, 2.46; N, 22.76. Found: C, 48.6; H, 2.4; N, 22.6.

[#] Evaporation of the diethyl ether should be carried out at room temperature, as there seems to be a tendency of the product to undergo sublimation at elevated temperatures.

3.7 References and notes

[1] Baer, E.; Moet, A. *High Performance Polymers*, Carl Hanser Verlag, München, **1991**.

[2] a) Kwolek, S.L.; Morgan, P.W.; Sorenson, W.R. *U.S. Patent* **1962**, 3063966. b) Kwolek, S.L. *U.S. Patent* **1972**, 3671542. c) Kwolek, S.L.; Morgan, P.W.; Schaefgen, J.R.; Gulrich, L.W. *Macromolecules* **1977**, *10*, 1390.

[3] a) Chit, S.; Chan, W.K. *Polym. Prep.* **1997**, *38*, 123. b) *Personal communication.*

[4] Kazcmarek, L.; Nowak, B.; Zukowski, J.; Borowicz, P.; Sepiol, J.; Grabowska,A. *J. Mol. Structure* **1991**, *248*, 189.

[5] The 5-alkoxy isophthalic acids **4a,b** have been described previously: Valiyaveettil, S.; Enkelmann, V.; Müllen, K. *J. Chem. Soc., Chem. Commun.* **1994**, 2097.

[6] a) Carver, J.; Hunter, C.A.; Shannon, R.J. *J. Chem. Soc., Chem. Commun.* **1994**, 1277. b) Hunter, C.A. *J. Am. Chem. Soc.* **1992**, *114*, 5303.

[7] Birkover, L.; Widmann, A. *Chem. Ber.* **1953**, *86*, 1295.

[8] An analogous synthesis for phenazine-1-carboxylic acid (Kögl, F.; Postowski, J.J. *Liebigs. Ann.* **1930**, *480*, 280) was found not to be reproducible (Schales, O.; Schales, S.S.; Friedman, D.A. *Arch. Biochem.* **1945**, *6*, 329).

[9] Flood, M.E., Herbert, R.B.; Holliman, F.G. *J. Chem. Soc., Perkin Trans. 1* **1972**, *4*, 622.

[10] Delnoye, D.A.P., *Conjugated ladder polymers by intramolecular hydrogen bonding*, Post Graduate Report, T.U. Eindhoven, The Netherlands, ISBN 90-5282-600-5, **1996**.

[11] Goshaev, M.; Otroshenko, O.S.; Sadykov, A.S. *Russ. Chem. Rev.* **1972**, *41*, 1046.

[12] Clark, G.J.; Deady, L.W. *Aust. J. Chem.* **1981**, *27*, 81.

[13] Heirtzler, F.R.; Neuburger, M.; Zehnder, M.; Constable, E.C. *Liebigs Ann.* **1997**, 297.

[14] Douce, L.; Ziessel, R.; Seghrouchni, R.; Skoulios, A.; Campillos, E.; Deschenaux, R. *Liq. Cryst.* **1996**, *20*, 235.

[15] Bashkir, E.A. *Chem. Abs. 79*, 91945g.

[16] Stille, J.K. *Angew. Chem.* **1986**, *98*, 504.

[17] The synthesis of the asymmetrical 3-amino-6,6'-dimethyl-2,2'-bipyridine *via* a Stille coupling has been described: Long, G.V.; Boyd, S.E.; Harding, M.M.; Buys, I.E.; Hambley, T.W. *J. Chem. Soc., Dalton Trans.* **1993**, 3175.

[18] a) Delnoye, D.A.P.; Sijbesma, R.P.; Vekemans, J.A.J.M.; Meijer, E.W. *J. Am. Chem. Soc.* **1996**, *118*, 8717. b) Vekemans, J.A.J.M.; Groenendaal, L.; Palmans, A.R.A.; Delnoye, D.A.P.; van Mullekom, H.A.M.; Meijer, E.W. *Bull. Soc. Chim. Belg.* **1996**, *105*, 659.

[19] Yamamoto, Y.; Yanagi, A. *Chem. Pharm. Bull.* **1982**, *30*, 1731.

Chapter 4

Extended-core discotic liquid crystals based on the intramolecular H-bonding in the 3,3'-di(acylamino)-2,2'-bipyridine unit

Abstract

*A new type of disc-shaped molecules, **1a–d** and **2**, has been synthesised and characterised. The molecules are built up by linking monoacylated 2,2'-bipyridine-3,3'-diamines to a central 1,3,5-benzenetricarbonyl core. ^1H-NMR results show that the interior of compounds **1** and **2** preferentially adopts a mainly planar conformation resulting in an extended core. This large core gives rise to strong intermolecular interactions. All molecules show thermotropic liquid crystalline behaviour as confirmed by DSC, polarisation microscopy and X-ray diffraction. The mesophase has been identified as a D_{ho} phase in all compounds **1** and **2**. For compounds **1a–c** and **2** this mesophase is already present at room temperature. Furthermore —as a result of the large aromatic core— the D_{ho} phase extends over a broad temperature range (> 250 K) in all compounds. Apparently, the presence of six additional methoxy groups in the interior of the disc-shaped molecules does not influence the thermotropic behaviour dramatically. However, the intracolumnar helical superstructure found in the D_{ho} phase of compounds **1a–d**, seems not to exist in case of compound **2**.*

4.1 Introduction

The use of the 2,2'-bipyridyl unit in metal-ligated liquid crystals is not unexpected. The transition metal–complexing capacities of 2,2'-bipyridine derivatives are well-known[1] and elaborate research has led to a wide range of paramagnetic and luminescent complexes[2]. The incorporation of the bipyridyl moiety in liquid crystalline derivatives can, therefore, lead to new types of mesomorphic materials that integrate novel structural elements and physical properties. Some examples of liquid crystalline 2,2'-bipyridine derivatives and their metal–

ion complexes are shown in figure 4.1[3]. Up to now, no examples of columnar mesophases based on the 2,2'-bipyridyl moiety have been presented.
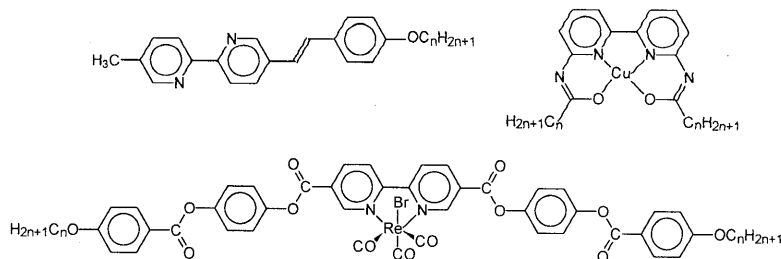
Figure 4.1: Mesomorphic 2,2'-bipyridines[3]

Lately, there has been an increasing interest in discotic liquid crystals with extended aromatic cores (diameter > 20 Å)[4]. The main interest of such extended disc-shaped cores rests on the broadening of the temperature window in which the mesophase is present. This will facilitate future applications —*e.g.* in one-dimensional charge transport— in which an enhanced temperature stability of the mesophases is desirable[5]. An innovative field of research applies secondary interactions to build up cores of enlarged dimensions. Secondary interactions such as H-bonding[6] and metal–ion complexation[7] may become powerful and flexible tools to facilitate the synthesis of these large cores.

Although a wide variety of central cores is currently known to induce discotic liquid crystalline behaviour, only few reports have appeared in which planarity of the discotic core is induced by *intra*molecular H-bonding in an otherwise flexible core[8]. On the contrary, examples have been presented in which *inter*molecular H-bonding between wedges is used to create large discs. For those compounds columnar mesophases have been observed, indeed[9].

In Chapter 2, we have shown that strong intramolecular H-bonding is present in N-acylated 3,3'-diamino-2,2'-bipyridines. We intended to use the structuring 3,3'-di(acylamino)-2,2'-bipyridine moiety as a building block to design a new class of large disc-shaped molecules (figure 4.2). Here, the synthesis and properties of compounds **1a–d** and **2** is discussed, in which three rigid bipyridine units connected with a central benzene ring *via* amide linkages give rise to a large aromatic core.
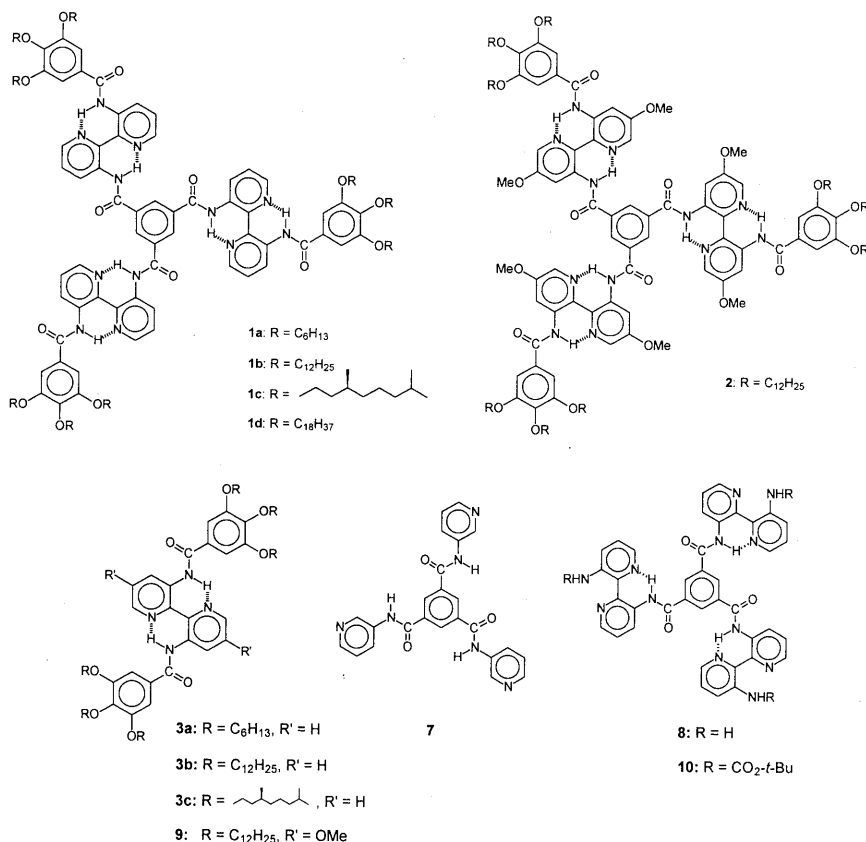
*Figure 4.2: Disc-shaped compounds based on 3,3'-diamino-2,2'-bipyridine (**1a–d** and, 5,5'-dimethoxy-3,3'-diamino-2,2'-bipyridine (**2**), together with precursors (**8, 10**) and reference compounds (**3, 7** and **9**)*

4.2 Synthesis of disc-shaped compounds 1 and 2

Disc-shaped molecules **1** and **2** have been synthesised by a convergent approach[10] and the synthesis is depicted in scheme 4.1. The synthesis of 3,3'-diamino-2,2'-bipyridine and 5,5'-dimethoxy-3,3'-diamino-2,2'-bipyridine has been described in Chapters 2 and 3, respectively, while the acid chlorides **4a–d** are obtained from the commercially available methyl 3,4,5-trihydroxybenzoate upon modification of previously described procedures[11]. The chiral side-chain in **4c** was derived from *(S)*-citronellol, which was first catalytically hydrogenated and then brominated giving rise to *(S)-(+)*-1-bromo-3,7-dimethyloctane, **11**[12]. Monoacylations were carried out by adding a dilute solution of the acid chlorides **4a–d** ($\approx$ 0.1 M) to an ice-cooled and dilute solution ($\approx$ 0.1 M) of the diamine and triethylamine (TEA). This ensures a high degree of monoacylation in the condensation reaction. Typical product ratios of mono-

/diacylated compounds of 85/15 were found, regardless of the acid chloride used. Column chromatography proved to be an effective technique to separate the monoacylated compounds **5a–c** and **6** quantitatively from the less polar diacylated compounds **3a–c** and **9**[13]. In case of compound **5d** however, solubility problems and identical R_f values for the mono- and diacylated products hampered separation with column chromatography. Compound **5d** could be purified, however, up to a purity of 95% and was used as such. In the final step —a linkage of the monoacylated bipyridine-diamines **5a–d** and **6** with benzene-1,3,5-tricarbonyl trichloride—it was crucial to use a slight excess of the monoacylated bipyridine-diamines **5a– d** and **6** to ensure that no acid chloride group would remain unreacted. Although acid chlorides are reactive, long reaction times —in case of compound **5d** even elevated temperatures— were used to drive the reaction to completion. The crude compounds **1a–d** and **2** were thoroughly purified and finally precipitated from a $CHCl_3$ solution with acetone. The desired compounds **1a–d** were thus procured in reasonable to good yields (54–82%). The disappointing yield of 19% obtained for compound **2** was mainly due to difficulties during work up as a result of the small scale of the reaction. Compounds **1a–c** and **2** were obtained as waxy, strongly birefringent substances at room temperature indicating the presence of a mesophase (vide infra). Compound **1d** was obtained as a white powder.
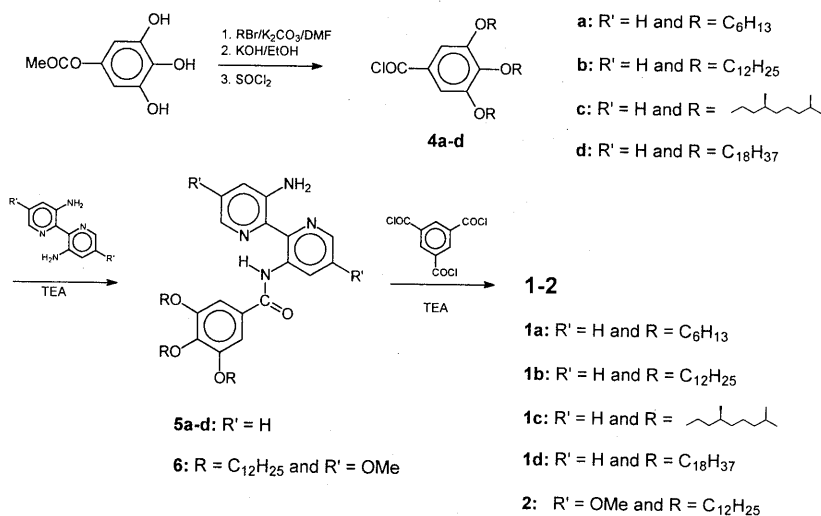
Scheme 4.1: Synthesis of disc-shaped compounds 1a–d and 2

Compounds **3** and **7–9** have been synthesised as reference and for additional studies (figure 4.2). Reference compound **7** was obtained by condensation of 3-aminopyridine with benzene-1,3,5-tricarbonyl trichloride in a yield of 79%. Precursor **8** has been acquired by a quantitative deprotection of the corresponding Boc-protected triamine **10** with trifluoroacetic acid. Compound **10** has been derived from a condensation of 3'-*t*-butoxycarbonylamino-2,2'-

bipyridine-3-amine (see Chapter 2) with benzene-1,3,5-tricarbonyl trichloride in a similar procedure as discussed for compounds **1–2**. Compounds **7** and **8** were hardly soluble in common organic solvents except for DMSO and DMF.

All new compounds **1–3** and **9** were fully characterised with NMR and IR spectroscopy and gave satisfactory elemental analyses. GPC measurements were conducted on compounds **1a– d** and **2** and confirmed the high purity (> 99.5%) with respect to higher and lower molecular weight substances.

4.3 ^{1}H-NMR spectroscopy

As has been shown in Chapter 2, strong intramolecular H-bonding in the 3,3'-di(acylamino)-2,2'-bipyridine moiety leads to a planar, transoid bipyridine system. Its conformation is characterised in the ^{1}H-NMR spectra by low field amide-NH absorptions (around δ = 14 ppm), concurrent with downfield absorptions of the H-6 protons (δ = 8.25–8.6 ppm) and the H-4 protons of the pyridine ring (around δ = 9.2 ppm). The latter is a consequence of the anisotropic deshielding exerted by the carbonyl of the adjacent amide.
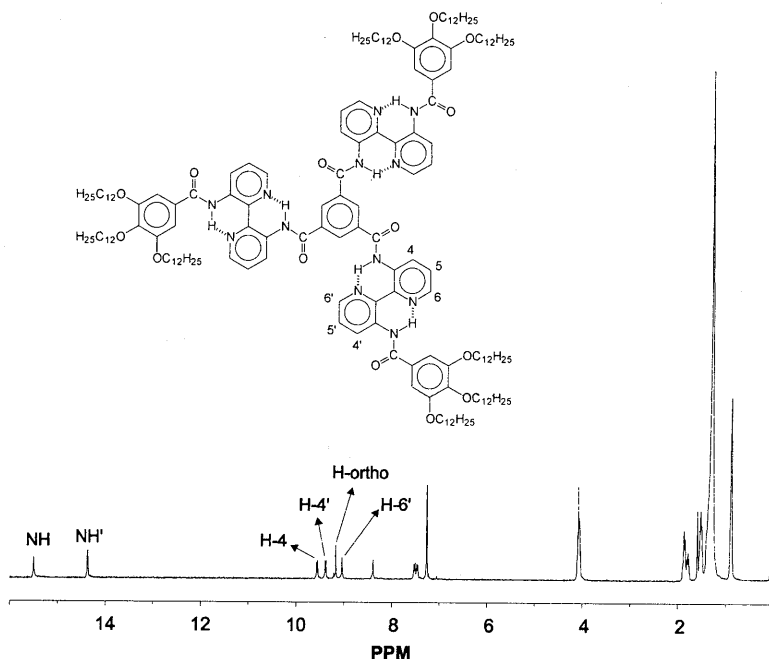
Figure 4.3: ^{1}H-NMR spectrum of compound **1b** in CDCl$_3$

73

The ^{1}H-NMR spectra of disc-shaped compounds **1a–d** were taken in CDCl$_3$ and follow the pattern described above, although the inner proton signals are significantly more deshielded than the corresponding signals in the linear compounds. For example, in compound **1b** two low field NH-absorptions (δ = 15.49 and 14.36 ppm, respectively) are present (figure 4.3). Furthermore, the absorptions of pyridine protons H-4 and H-4' are found at δ = 9.56 and 9.38 ppm, respectively. Remarkable is the more downfield position of the H-6' signal (pointing inside), δ = 9.03 ppm, with respect to the corresponding H-6 signal (pointing outside), δ = 8.38 ppm. Also, the chemical shift of δ = 9.16 ppm for the ortho hydrogens of the central benzene ring is high compared to other trimesic amides. Similar high values for H-ortho protons are found in compounds **1a, 1c** and **1d** at δ = 9.25 ppm, 9.25 ppm, and 9.22 ppm, respectively.
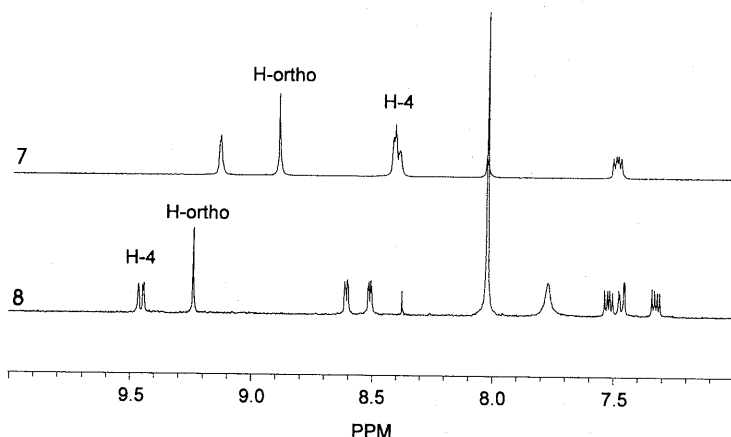
Figure 4.4: Comparison of the ^{1}H-NMR spectra of precursor 8 and reference compound 7, both spectra are taken in DMF-d7

To clarify the origin of these strong deshieldings, reference compound **7** was synthesised and compared to its bipyridyl analogue **8**. Both compounds are insoluble in CDCl$_3$, and DMF-*d7* was used for their ^{1}H-NMR spectra; these are compared in figure 4.4. A large difference between the chemical shifts of the amide-NH signal for compounds **8** (δ = 15.79 ppm) and **7** (δ = 10.94 ppm) is observed. In addition, proton H-4 in compound **8** appears strongly deshielded compared to the corresponding proton in compound **7**, (δ = 9.46 and δ = 8.40 ppm, respectively). Furthermore, a substantial difference in chemical shift of H-ortho protons of the central benzene ring is present for compounds **7** (δ = 8.88 ppm) and **8** (δ = 9.23 ppm).

Concentration dependent ^{1}H-NMR data were gathered to get an impression of association and π-stacking in solution. A concentration effect was noticed for compounds **1a–d** in CDCl$_3$. Going from higher concentration (31 mmol/l) to lower concentrations (1.55 mmol/l) the ^{1}H-

NMR signals of compound **1a** in CDCl$_3$[14] sharpened substantially and all aromatic peaks showed some deshielding (figure 4.5.a). The effect was most pronounced for H-ortho of the central benzene ring and other protons in the interior of the molecule: NHCO, H-4 and H-6'.
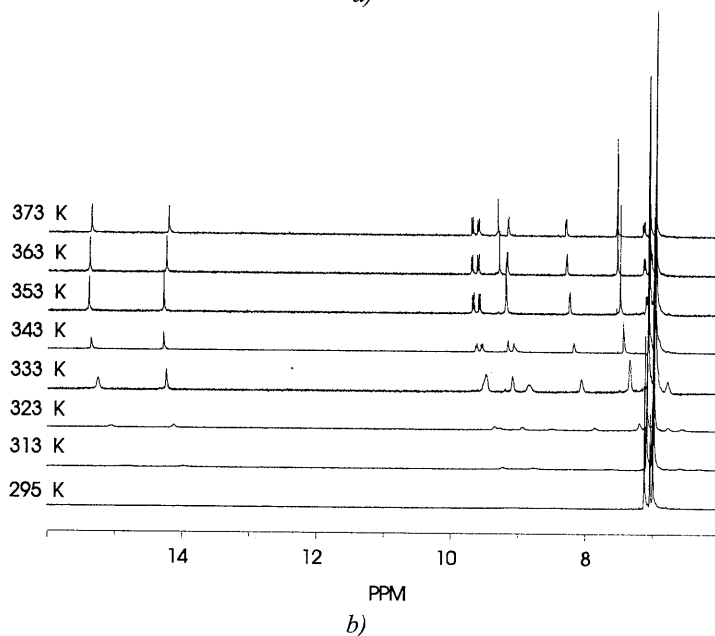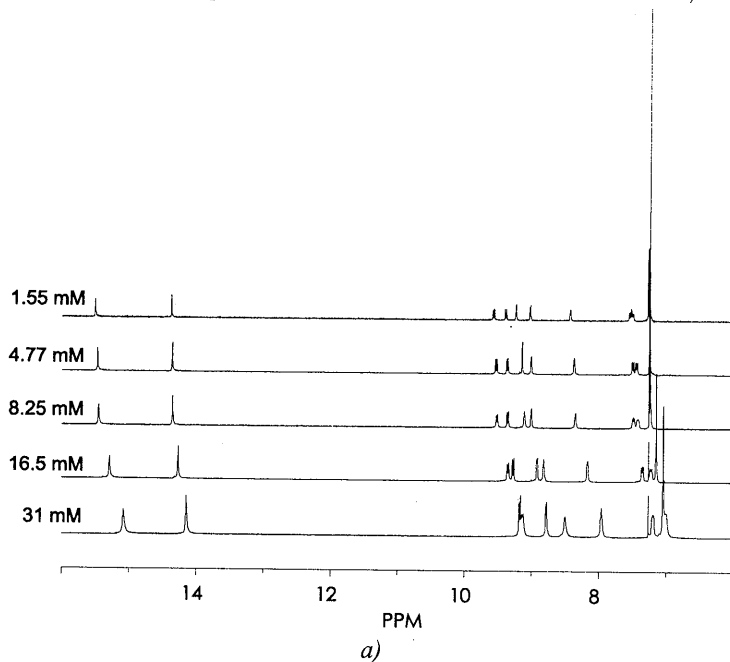
Figure 4.5: a) Variable concentration ^{1}H-NMR data of compound **1a** in CDCl$_3$; b) variable temperature ^{1}H-NMR of compound **1a** in toluene-d8 (2.8 mmol/l)

A similar effect was encountered when a 2.8 mM solution of **1a** in toluene-*d8* was heated from room temperature to 100°C (figure 4.5.b). At room temperature, the peaks were extremely broad but at 80°C they started sharpening with concomitant deshielding of the aromatic protons. Finally, it was found that when very apolar solvents were used (hexane and cyclohexane), compounds **1a–d** did not really dissolve but formed stable gels, as discussed further in Chapter 5.

Compound **2** showed only broad signals in the ^{1}H-NMR spectrum, although it was soluble in CDCl$_3$. This indicates that the molecules are aggregated at room temperature. Also at elevated temperatures, only broad peaks could be observed. Therefore, 1,1,2,2-tetrachloroethane-*d2* was used as a solvent because of the larger temperature window. Indeed, at 110°C an interpretable ^{1}H-NMR spectrum was obtained (figure 4.6). H-Ortho in compound **2** was found at a somewhat lower δ-value: δ = 9.17 ppm for **2** in 1,1,2,2-tetrachloroethane-*d2* and δ = 9.27 ppm for **1a** in 1,1,2,2-tetrachloroethane-*d2*, both at 110°C. The addition of trifluoroacetic acid to a solution of **2** in CDCl$_3$ resulted in sharpening of the peaks at room temperature but with concomittant collapse of the H-bonding. In alkane solvents, the formation of viscous solutions has been observed for compound **2** as well.
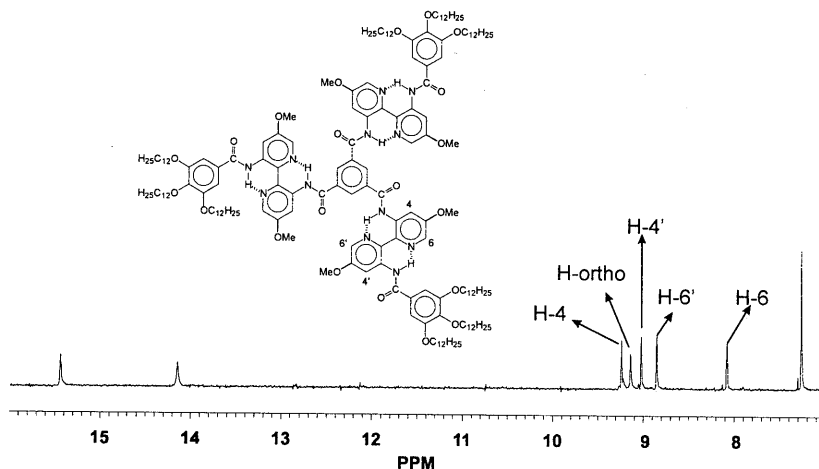
Figure 4.6: ^{1}H-NMR data of compound 2 in 1,1,2,2-tetrachloroethane-d2 at 110°C

The strong, multiple intramolecular H-bonding in acylated 3,3'-diamino-2,2'-bipyridines favours a rigid, planar, transoid bipyridine system. The deshielding of the amide-NH and H-4/H-4' protons in compounds **1a–d** points to the presence of such a rigid transoid conformation. The low field chemical shift of the H-ortho protons of the central benzene ring in all compounds **1a–d** can only be rationalised by adopting a mainly planar orientation of the

bipyridine moiety with regard to the central benzene ring. Indeed, the carbonyl and pyridyl units would induce a relative deshielding on the protons of the central benzene ring. This is clearly demonstrated when reference compound **7** is compared to compound **8**. The large $\Delta\delta$ of 0.35 ppm between the H-ortho protons can not be attributed to electronic effects but rather to more pronounced rotational freedom around the Ph–C=O in case of model compound **7**. In compound **8** a mainly coplanar orientation of the bipyridine units with the central benzene ring would indeed induce a relative deshielding of the protons belonging to the trimesic core. If such a phenomenon occurs in compound **8**, then the rotational freedom around the Ph–C=O bond will certainly be restricted in compounds **1a–d**. This hindered rotation is illustrated in a CPK model of compound **1b** in figure 4.7 from which it is also obvious that the coplanarity of the central benzene ring with one bipyridine unit requires C_3-symmetry due to the space availability.

1b   **2**
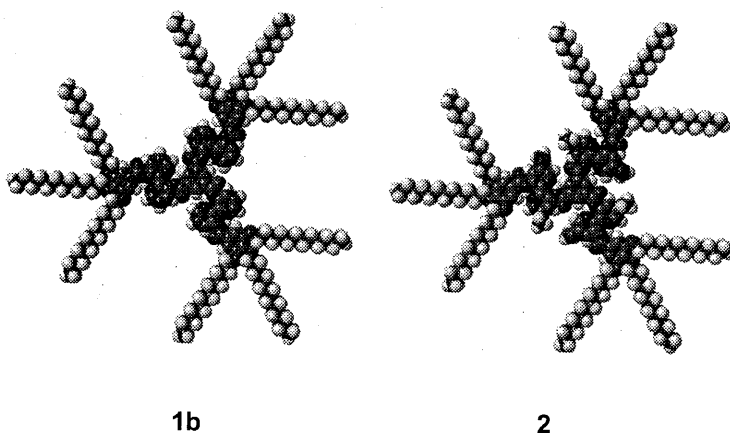
Figure 4.7: CPK models of compounds 1b and 2

The consequence of the preferred, concerted, mainly planar orientation of the aromatic interior is a large rigid core with a diameter of approximately 28 Å in compounds **1a–d**. The observation that these disc-like molecules show a strong tendency to aggregate in solution —promoted by less polar solvents, higher concentrations and lower temperatures— indicates a strong driving force for phase separation. The stacking effects influence the δ-values for the protons at the inside of the molecule as is shown in figure 4.5.a. H-ortho, H-4, NH and H-6' protons are the most affected by variations in concentration. Although less obvious, the same holds for temperature dependent measurements in toluene-*d8* (figure 4.5.b). The conclusion is that the discs must stack on top of each other. The tendency for phase separation ultimately leads to liquid crystalline behaviour in the absence of solvent.

There are no indications that there is less coplanarity of the bipyridine wedges with respect to the central trimesic core in compound **2**, although the presence of six methoxy groups might

suggest so. This can be deduced from the similar δ(H-ortho) of compound **2** compared to compound **1a**. Indeed, it seems possible for all the wedges in compound **2** to fit in plane with the central core when CPK models of compound **1b** and **2** are compared (figure 4.7). It is peculiar that —instead of hindering optimal packing between subsequent molecules and thus disturbing aggregation— the methoxy groups seemingly stabilise the aggregated species. The stronger aggregation observed for compound **2** in CDCl$_3$ is not fully understood. A more detailed investigation to explain these unexpected differences in aggregation behaviour will be presented in Chapter 6.

4.4 Characterisation of the mesophases of compounds 1 and 2

4.4.1 DSC analyses

The phase transition temperatures and corresponding enthalpies of compounds **1** and **2** were determined using DSC. The heating and cooling rates were 10 K/min. All samples were dried in a vacuum stove before use. The data are collected in table 4.1. Although not discussed in detail, DSC was also performed on linear compounds **3a–c** and **9** for comparison. The transition temperatures and enthalpies are included in table 4.1.

Table 4.1 *Transition temperatures (°C) and corresponding enthalpies (kJ/mol) of disc-shaped compounds **1a–d** and **2**, and reference compounds **3a–c** and **9***

Compound	K	T (ΔH)	M	D$_{ho}$	T (ΔH)	I
1a	–[a]	–	–	●	383 (17)[c]	●
1b	●	9 (56)	–	●	355 (27)[c]	●
1c	–[a]	–	–	●	373 (28)[c]	●
1d	●	62 (172)	–	●	308 (30)[c]	●
2	●	13 (33.0)	–	●	>400 (dec.)	–
3a	●	53 (38)	●	–	108 (2.5)	●
3b	●	38 (79)	●	–	110 (2.5)	●
3c	–[b]	–	●	–	123 (7.8)	●
9	●	12 (49.3)	●	–	191 (7.6)	●

●: *phase is observed; –: phase is not observed; K = crystalline phase; M = unidentified mesophase; D$_{ho}$ = hexagonally ordered columnar phase; I = isotropic phase;* [a] *cooling the sample down to –80°C did not show any transition;* [b] *cooling the sample down to –20°C did not show any transition;* [c] *the clearing is accompanied by some decomposition of the sample making the accuracy of the calculated enthalpies less reliable.*

Due to the high clearing temperatures of compounds **1a–d** and the presence of air in the sealed pans, slight decomposition took place in all samples starting from 250°C. Compound **1a** was heated in a first run from −40°C to 200°C and subsequently cooled to −80°C. No K–D_{ho} transition could be observed. In a second run the sample was heated to 400°C and a D_{ho}–I transition was visible at 383°C. Due to decomposition of the sample the cooling run was rather unreliable although a I–D_{ho} transition seemed present at 340°C. For compound **1c** similar observations were made: no K–D_{ho} transition and an irreversible D_{ho}–I transition at 373°C.

Compound **1b** was heated and cooled in a first run from −20 to 200°C. In the heating run a K–D_{ho} transition was present at 9°C and a D_{ho}–K transition in the cooling run at −3°C. A second heating and cooling run from −20 to 200°C gave the same results. In a last run the sample was heated from 20 to 380°C and showed a D_{ho}–I transition at 355°C and, upon cooling, an I–D_{ho} transition at 333°C. Also compound **1d** showed a reversible K–D_{ho} transition at 62°C and a D_{ho}–K transition at 54°C, the latter being followed by a second transition at 47°C. A second heating and cooling run gave the same results. In the third run the sample was heated up to 330°C and a D_{ho}–I transition was observed at 308°C. The cooling run showed a I–D_{ho} transition at 302°C.

Compound **2** was heated and cooled in a first run from −20 to 200°C and a K–D_{ho} was observed at 13°C and a D_{ho}–K transition at 10°C. A second heating run to 400°C only led to decomposition of the sample starting from 300°C. No D_{ho}–I transition could be discerned during this run.

4.4.2 Polarisation microscopy

In order to study the thermal behaviour of the compounds with polarisation microscopy, samples of compounds **1a–d** and **2** were prepared on a glass plate. A strongly birefringent texture was observed for **1a–c** and **2**, indicating that these compounds were already in a mesophase at room temperature. This was confirmed by the fact that upon heating (around 200°C) the samples slowly became mobile —*i.e.* sensitive towards pressure changes— while remaining strongly birefringent. Compounds **1a–c** exhibited a permanent mesophase starting from room temperature up to the clearing temperatures at 389, 373 and 383°C[16] for **1a, 1b** and **1c**, respectively. In all cases, the isotropic state had a low viscosity. Typical textures — showing a digitated growth pattern— were grown for compounds **1a–c** by slowly cooling the isotropic liquid (1 K/min). An example is presented in figure 4.8.a. No textures could be grown for compound **2** because of severe decomposition above 300°C.

Compound **1d**, on the contrary, showed a different behaviour. It was obtained as a white powder that changed around 58°C into a liquid crystalline phase. The clearing temperature was substantially lower, 320°C, compared to the other representatives. The fast reappearance of the liquid crystalline phase at 317°C indicates a high degree of pre-orientation in the isotropic state. Again, typical textures could be grown by slowly cooling the isotropic liquid (figure 4.8.b). Large homeotropic monodomains were present in the liquid crystalline state. Upon further cooling, a gradual transition into the crystalline state was observed around 45°C.

a)   *b)*
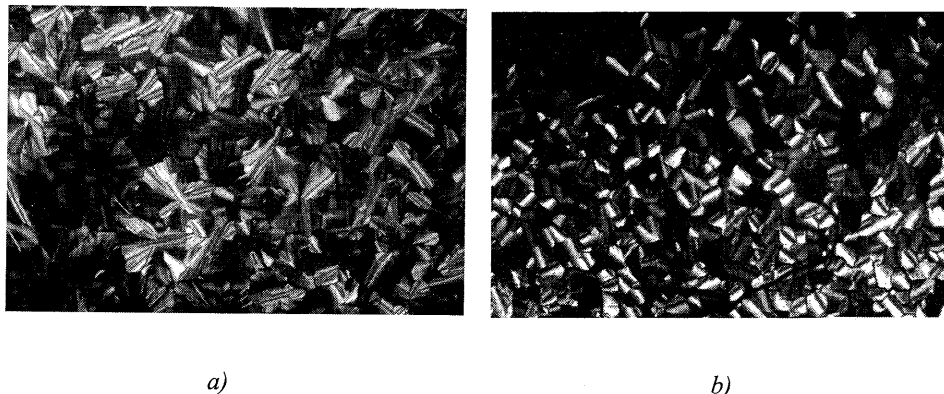
Figure 4.8: Textures grown for a) compound 1b and b) compound 1d

4.4.3 X-Ray diffraction

The structures of the mesophases of compounds **1a–d** were examined with X-ray diffraction. Compound **1d** was heated in a glass capillary to the clearing point and was then slowly cooled into the liquid crystalline state at a rate of 5 K/min. At 120°C the sample was screened to find suitably large monodomains. In figure 4.9.a the obtained diffraction pattern is shown and the calculated diffraction spacings are collected in table 4.2. The diffraction pattern as shown in figure 4.9.a points unambiguously to a hexagonal columnar packing of the molecules. Furthermore, two monodomains can be distinguished: the first, most prevalent one in which the columns are in the direction of the X-rays and a second, less pronounced one in which the columns are perpendicular to the X-rays. The reflections in the wide-angle area originate from the second monodomain. A sharply defined reflection at 3.5 Å and a broad ring at 4.7 Å can be assigned to the disc–disc distance and the disorder of the aliphatic chains, respectively. In the small angle area (figure 4.9.b) two clear reflections at 40 and 23 Å are present in a hexagonal distribution. The reflections are assigned to the 100 and 110 reflection, respectively. Finally, two less intense reflections at 20 and 13.8 Å are observed which derive from the 200 and 210 reflections. The hexagonal distribution of the 100 and 110 reflection clearly points to a hexagonal packing of the columns in the liquid crystalline state with an

intercolumnar distance of approximately 46 Å. When compound **1d** was heated and sheared/pressed on a Be-surface[15], another diffraction pattern could be distinguished. In this side-on view, a characteristic reflection with a pattern splitting in a quadruplet is observed (figure 4.9.c).

Compounds **1a–c** were shear aligned on a Be-surface at room temperature. The three compounds showed similar diffraction patterns. A characteristic pattern splitting in a quadruplet is present in all three compounds. The diffraction pattern of chiral compound **1c** is shown in figure 4.9.d and the calculated diffraction spacings of compounds **1a–c** are summarised in table 4.2. The diffraction pattern shown in figure 4.9.d indicates that the molecules are packed in columns. In the small angle area, two clear reflections are present: a first order reflection at 32.7 Å and a quadruplet splitting reflection at 17.4 Å. In the wide angle area, the disorder of the aliphatic chains at 4.7 Å, a sharp reflection at 3.5 Å and a more diffuse reflection at 3.6 Å are noticed. Comparison of the diffraction pattern of the side-on view of compound **1d** (figure 4.9.c) with the diffraction pattern obtained for compound **1c** (figure 4.9.d) reveals their similarity.

Compound **2** was shear aligned on a Be surface and the obtained diffraction spacings are summarised in table 4.2. In the small angle area a first order reflection at 36.7 Å and a second order, but very weak reflection at 18.4 Å are found. In the wide angle area, a sharp reflection at 3.5 Å and a diffuse reflection at 4.4 Å are discerned. No quadruplet splitting diffraction peak has been observed in this case.

Table 4.2   *Diffraction spacings obtained for compounds **1a–c** and **2** at 20°C and for compound **1d** at 120°C*

	Diffraction spacings (Å)[a]				
hkl	1a[b]	1b	1c	1d	2
100	25.4	34.1	32.7	40.0 *(40.1)*	36.7
110	–	–	–	23.2	–
200	–	–	16	20.0	18.4
210	–	–	–	13.8	–
?	–	17.4[c]	17.4[c]	*(20)*[c]	–
?	–	3.6	3.6	*(14.5)*[c]	–
halo	4.7	4.7	4.7	4.7 *(4.7)*	4.4
inter-disc distance	3.3	3.4	3.5	3.5 *(3.5)*	3.5
inter-column distance	30	40	38	46	42.3

[a] the spacings found for the side-on oriented sample of **1d** are given between brackets; [b] the quality of this picture was very low; [c] quadruplet splitting pattern
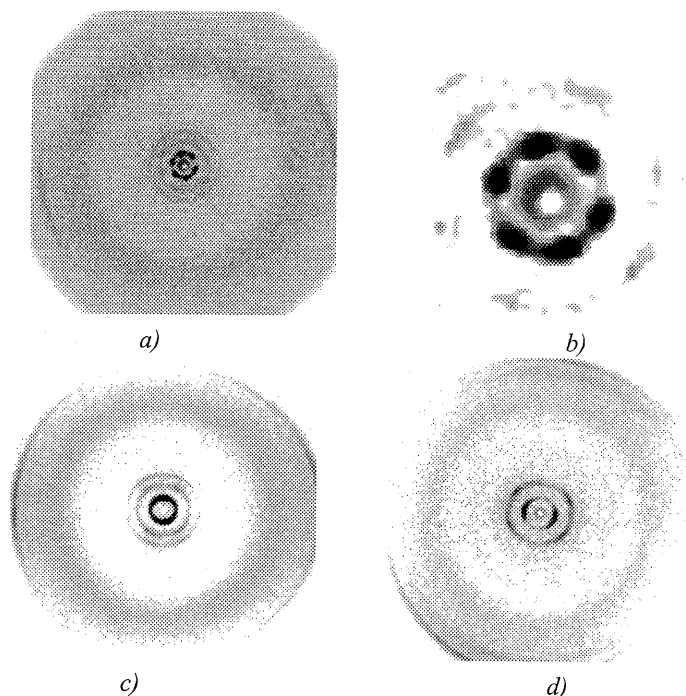
*Figure 4.9: Diffraction patterns observed for compound **1d** a) overall picture b) small angle area enlarged c) side-on view; d) diffraction pattern for compound **1c**, shear aligned at 20°C*

4.4.4 Discussion

As is shown by DSC and polarisation microscopy, compounds **1a–c** and **2** show only one mesophase from room temperature to their clearing points[16] while compound **1d** shows a mesophase from 62°C to 308°C. The expected increase in $\Delta H_{K\text{-}Dho}$ with increasing molecular weight is observed[12b]. The large difference in the transition enthalpies $\Delta H_{K\text{-}Dho}$ of the C_{12} and the C_{18} derivatives **1b** and **1d**, can be explained assuming that the interior methylenes of the alkoxy chain are less prone of participation in the crystallisation process. This is supported by the observation that **1a** does (can?) not crystallise. The lack of crystallisation in **1c** can be rationalised by the presence of the branching 3-methyl group, which is well known to lower the K–D_h transition[17]. The transition enthalpies ΔH_{Dho-I} in compounds **1a–d** are notably larger than in *e.g.* triphenylene and dibenzopyrene based liquid crystals[18]. The investigation of mesomorphic compounds incorporating an amide moiety revealed that intermolecular H-bonding stabilises the columnar structure and significantly higher ΔH_{Dh-I} enthalpies were found[19]. Intermolecular H-bonding might also contribute to the large ΔH_{Dho-I} in the columnar mesophases of compounds **1–2**. Unfortunately, the differences in C=O stretch vibration of compound **1b** as a pure compound or molecularly dissolved in $CDCl_3$ were too small to draw any conclusions concerning this intermolecular H-bonding. However, preliminary modelling

studies show that when the bipyridine wedges are tilted with respect to the central benzene ring and the discs are mutually rotated, the spatial arrangement of the amide-NH allows for bifurcated H-bonding with a carbonyl of the next molecule.

Digitated growth of the textures of **1a–c** and the presence of large homeotropic areas in compound **1d** are characteristic for the presence of orthogonal phases. For compound **1d**, evidence for this proposal is found in the diffraction pattern where a characteristic hexagonal pattern is present (figure 4.9.a). Two reflections in the hexagonal array are more pronounced due to the overlapping second monodomain which increases the intensity. The sharpness of the 3.5 Å reflection indicates an ordered packing of the discs in the columns. The nature of the liquid crystalline state present can thus be designated as a D_{ho} phase.

The similarity between the diffraction patterns of compounds **1a–c** points to similar structures in the liquid crystalline state. The mesophase present is most likely to be a D_{ho} phase because of the similarities between the X-ray diffraction pattern obtained for **1d** (side-on view) and the diffraction patterns found for compounds **1a–c**. We propose that the remarkable quadruplet splitting pattern in the X-ray patterns of compounds **1a–d** most likely arises from a helical superstructure present in the columns. The periodicity of this helix then amounts to 17.4 Å for compounds **1b,c** and 20 Å for **1d**. This is in accordance with the observation of a quadruplet splitting reflection in mesomorphic alkyl-substituted 1,3-diaminobenzenes, which has been attributed to a helical intracolumnar ordering[19b]. When considering the CPK model in figure 4.7, compound **1** is not perfectly disc-shaped but possesses a more or less trefoiled shape. Together with a slightly tilted orientation of the bipyridine wedge with respect to the central benzene ring and the rotation of one disc with respect to the other, this might explain the origin of the extra order in the lattice. A more detailed proposal for the superstructure in columnar aggregates of these compounds will be given in Chapter 6.

In compound **2**, the perpendicular orientation of the [100] reflection with respect to the [001] reflection indicates a columnar packing of the discs. Furthermore, the sharpness of the reflection corresponding to the disc–disc distance indicates that the molecules are orderly stacked. Again, all evidence points to the presence of a D_{ho} phase in compound **2**. As can be expected, the intercolumnar distance in compound **2** is slightly larger than in its methoxy-free analogue: 42.3 Å in **2** compared to 40 Å in **1b**. This is presumably due to better space filling of the aromatic interior. An equal disc–disc distance of 3.5 Å remains present. The absence of the quadruplet splitting diffraction peak in the diffraction pattern points to an absence of a helical superstructure within the columns.

There is a striking difference in the stability of the mesophases of the linear reference compounds **3a,b** and the disc-shaped analogues. While the temperature range in which compounds **3a,b** display liquid crystallinity is limited to approximately 60 K, the temperature range in which compounds **1a,b** exhibit liquid crystallinity is more than 350 K. Furthermore, the introduction of methoxy groups at the bipyridine moiety leads obviously to a stabilisation of the mesophase: the temperature range in which linear compound **9** exhibits a mesophase is nearly 100 K broader than for compound **3b**. Although all textures and X-ray diffraction data point to the presence of columnar mesophases in compounds **3a–c** and **9**, the exact nature of the mesophases in these model compounds remains concealed.

4.5 One-dimensional charge transport in disc-shaped derivative 1d

Pulse radiolysis time-resolved microwave conductivity (PR-TRCM) is a powerful technique to study the one-dimensional mobility of charge carriers in discotic liquid crystals. A detailed description of this technique and the measurements has been described elsewhere[20]. Primary ions were created by irradiation of the sample with 20 ns pulses of 3 MeV electrons from a Van der Graaff accelerator. The radiation-induced conductivity was monitored as the absorption of microwaves at 30 GHz. The conductivity measured at the end of an ionising pulse, $\Delta\sigma_{eop}$, is related to the sum of the mobilities of the charge carriers present.

Compound **1d** has been selected because the phase transition temperatures (K 62 D_{ho} 308) allow to monitor the conductivity in the crystalline as well as in the D_{ho} phase. The sample was heated from room temperature to 100°C and subsequently cooled. The temperature dependence of the dose normalised end-of-pulse conductivity ($\Delta\sigma_{eop}/D$) of compound **1d** is summarised in figure 4.10.
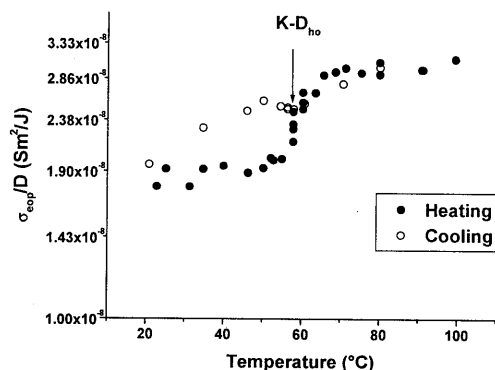
Figure 4.10: First heating and cooling scan of compound 1d

Compared to previously studied liquid crystalline phthalocyanine (Pc) derivatives, the $\Delta\sigma_{eop}/D$ of compound **1d** is lower in the crystalline phase than that of PcOC$_{12}$ and PcOC$_{18}$ in the crystalline phase. In the mesophase, on the contrary, the values are comparable[21]. It is remarkable that the $\Delta\sigma_{eop}/D$ increases going from K→D$_{ho}$. This has never been observed in related systems such as phthalocyanines or triphenylenes. Furthermore, the transient decays faster. In the D$_{ho}$ phase, the kinetics of the short time transient changes in time: a faster decaying transient can be measured while the end-of-pulse height stays the same. On cooling, the D$_{ho}$→K transition doesn't occur at a distinctive temperature but the short time transient decays slower and the end-of-pulse value decreases gradually.

Normally, long range columnar order is essential for the conductive properties of discotic liquid crystals. Going from a crystalline to a liquid crystalline phase, there is an increase of the positional disorder in the columns along the stacking axis when the alkoxy chains become liquid-like. Therefore, the $\Delta\sigma_{eop}/D$ decreases upon passing the K→D$_{ho}$ transition. This effect has been observed repeatedly in liquid crystalline phthalocyanines, porphyrines and triphenylenes.

The increase in $\Delta\sigma_{eop}/D$ going from the K to the D$_{ho}$ phase for compound **1d** may rest on more efficient macroscopic packing in the columns in the D$_{ho}$ phase than in the K phase, generating a more efficient path for charge migration. Unfortunately, we have not been able to elucidate the nature of the K phase in disc-shaped compounds **1a–d**[22]. Therefore we can only assume that very small monodomains are present in the K phase, while substantially larger monodomains are formed in the D$_{ho}$ phase, giving rise to favourable one-dimensional charge migration.

4.6 Conclusions

A new class of discotic liquid crystals based on 3,3'-diamino-2,2'-bipyridine has been synthesised and characterised. The convergent approach towards molecules **1** and **2** proves to be an easy and accessible strategy to synthesise large, disc-shaped molecules in relatively high yields and at reasonable scale. The key step, monoacylation of the diamino-bipyridines, proceeds highly selective. This is a consequence of the formation of an intramolecular H-bond upon the first acylation. By varying the acid chloride a wide range of disc-shaped compounds becomes accessible. One drawback is the limited accessibility of compound **2** due to a long and tedious synthetic route —with a rather low overall yield— towards 5,5'-dimethoxy-3,3'-diamino-2,2'-bipyridine.

¹H-NMR has revealed that in compounds **1** and **2** the whole interior prefers a mainly planar conformation in solution as a result of the intramolecular H-bonding present in acylated 3,3'-diamino-2,2'-bipyridines. As a consequence, an extended aromatic core is present with a diameter of approximately 28 Å. It has been deduced from variable concentration and temperature ¹H-NMR measurements that the molecules feature a strong tendency to aggregate in solution which is promoted by less polar solvents, higher concentrations and lower temperatures.

All compounds **1** and **2** show thermotropic liquid crystalline behaviour in a broad temperature range. The stability of the D_{ho} phase in compounds **1** and **2** is a direct result of the large aromatic core pre-organised by intramolecular H-bonding. Furthermore, secondary interactions within the columns such as π-stacking interactions and possibly intermolecular H-bonding add to this stability. Modifications in the aromatic core, such as adding methoxy groups to the bipyridine moiety, do not affect the liquid crystalline behaviour dramatically. The mesophase in compounds **1** and **2** has been designated as a D_{ho} phase. Interestingly, the X-ray diffraction results point to the presence of an intra-columnar helical superstructure in case of compounds **1a–d**. On the contrary, the columnar mesophase of compound **2** does not show this characteristic.

The liquid crystalline behaviour in this new class of discotic liquid crystals relies on several cooperative processes. First, strong intramolecular H-bonding in the 3,3'-di(acylamino)-2,2'-bipyridine moiety planarises the bipyridine unit in a transoid conformation. Secondly, the central benzene-1,3,5-tricarbonyl unit preferentially adopts an almost planar conformation in which all carbonyl groups are pointing to the same direction giving rise to C_3-symmetry and —together with the bipyridine system— to an extended, mainly planar core. Thirdly, the presence of peripheral lipophilic non-aromatic side-chains induces liquid crystalline behaviour.

Finally, one-dimensional charge transport was measured in the K as well as the D_{ho} phase of compound **1d**. Unexpectedly, the end-of-pulse conductivity increases at the K–D_{ho} transition. Therefore, we may conclude that the migration of charges appears to be more efficient in the mesophase than in the crystalline phase, indicating that compound **1d** features a highly ordered, well-defined mesophase.

4.7   Experimental procedures

For a general section concerning purification of solvents and spectroscopic techniques: see chapter 2. For a general section concerning mass spectroscopy techniques (ES-MS and FAB-MS): see chapter 3. GC-MS was performed on a HP 5790 GC. Optical properties of the materials were studied using a

Jenaval polarisation microscope equipped with a Linkam THMS 600 heating device, with crossed polarisers. Melting points of all compounds except for compounds **1a–d** were recorded on an Linkam THMS 600 heating device. The clearing points of compounds **1a–d** were determined with DSC. DSC scans were taken using a Perkin-Elmer DSC–7 under a nitrogen atmosphere with heating and cooling rates of 10 K/min. X-ray diffraction patterns of oriented and non-oriented samples were taken using a multi-wire area detector X-1000 coupled with a graphite monochromator and a Linkam THM 600 hot stage at elevated temperatures or by a flat film camera at room temperature (Ni filtered, $Cu_{K\alpha}$-radiation) The temperature accuracy was ± 0.5 K. For the GPC measurements a column with PL gel (5µl particles and 500 Å pore size) was used with chloroform as eluent and a flow of 1 ml/min. A UV detector was used at a wavelength of 254 nm.

3,4,5-Trihexyloxybenzoyl chloride (4a)

A mixture of methyl 3,4,5-trihydroxy-benzoate (10 g, 54.3 mmol), 1-bromohexane (29 g, 175 mmol) and anhydrous K_2CO_3 (40 g) was stirred under Ar atmosphere in DMF (200 ml) at 75°C for 6 h. After cooling, the reaction mixture was poured into water and extracted with *n*-hexane (2x250 ml). The combined organic layers were consecutively extracted with HCl (1 M, 200 ml), saturated $NaHCO_3$ solution (200 ml), dried with $MgSO_4$, filtered and evaporated *in vacuo*. The resulting yellow oil was purified by column chromatography (SiO_2). First, impurities were eluted (eluent: *n*-hexane), then, the desired ester was eluted (eluent: hexane/EtOAc 85/15, R_f = 0.50). This afforded a colourless oil (20.3 g, 85%). ^{1}H-NMR ($CDCl_3$): δ 7.22 (s, 2H, H-ortho); 4.03 (m, 6H, OCH_2); 3.88 (s, 3H, OCH_3); 1.80 (m, 6H, $OCH_2C\underline{H}_2$); 1.48 (qui, 6H, $OCH_2CH_2C\underline{H}_2$); 1.30 (bs, 12H, $(CH_2)_2$); 0.90 (t, 9H, CH_3). A mixture of the ester (10 g, 23.6 mmol) and KOH (2.7 g) in EtOH (96%, 200 ml) was heated under reflux for 4 h. Then, concentrated HCl (6 ml) was added to the hot solution, followed by the addition of H_2O (200 ml). Extraction with diethyl ether (3x200 ml) yielded the crude acid which was purified by column chromatography (SiO_2). First, impurities were removed (eluent: CH_2Cl_2), then the acid was eluted (eluent: CH_2Cl_2/CH_3CN 1/1, R_f = 0.62). The acid was obtained as a slowly solidifying white solid (7.35 g, 76%). M.p. 41–42.5°C. ^{1}H-NMR ($CDCl_3$): δ 7.27 (s, 2H, H-ortho); 4.02 (m, 6H, OCH_2); 1.80 (m, 6H, $OCH_2C\underline{H}_2$); 1.46 (qui, 6H, $OCH_2CH_2C\underline{H}_2$); 1.30 (bs, 12H, $(CH_2)_2$); 0.88 (t, 9H, CH_3). Anal. calcd. for $C_{25}H_{42}O_5$ (422.60): C, 71.05; H, 10.01. Found: C, 71.0; H, 9.9. The acid (4.1 g, 9.7 mmol) was treated with thionyl chloride (50 ml) at reflux temperature for 3 h. The excess thionyl chloride was distilled off and the resulting brown oil was flushed with *n*-hexane (2x10 ml). The brown oil was dissolved in *n*-hexane and filtered. After evaporation of the filtrate *in vacuo*, **4a** was obtained as a yellow oil (3.65 g, 85%). ^{1}H-NMR ($CDCl_3$): δ 7.30 (s, 2H, H-ortho); 4.02 (t, 2H, OCH_2-para); 3.98 (t, 4H, OCH_2-meta); 1.80 (m, 6H, $OCH_2C\underline{H}_2$); 1.48 (m, 6H, $OCH_2CH_2C\underline{H}_2$); 1.28 (m, 12H, $(CH_2)_2$); 0.88 (t, 9H, CH_3).

3'-(3,4,5-Trihexyloxybenzoylamino)-2,2'-bipyridine-3-amine (5a)

To an ice-cooled solution of 3,3'-diamino-2,2'-bipyridine (1.49 g, 8 mmol) and TEA (1.3 ml) in dry diethyl ether (70 ml), a solution of **4a** (3.54 g, 8 mmol) in dry diethyl ether (70 ml) was added dropwise under an Ar atmosphere. After complete addition, the ice bath was removed and the mixture was stirred at room temperature for 16 h. The resulting suspension was extracted with saturated $NaHCO_3$ solution (2x100 ml) and the organic layer was dried with $MgSO_4$, filtered and evaporated *in vacuo*. Purification by column chromatography (SiO_2; eluent: hexane/EtOAc 9/1, R_f = 0.23 of by-product **6a**, R_f = 0.05 of compound **5a**) followed by recrystallisation from *n*-hexane at 0°C afforded pure **5a** as yellow needles (3.15 g, 66%). T_{cl} = 119-121°C. ^{1}H-NMR ($CDCl_3$): δ 14.28 (s, 1H, NH'CO); 9.25 (dd, 1H, H-4'); 8.33 (dd, 1H, H-6'); 8.00 (dd, 1H, H-6); 7.32 (dd, 1H, H-5'); 7.12 (m, 2H, H-4 and H-5); 6.56 (bs, 2H, NH_2); 4.07 (m, 6H, OCH_2); 1.88 (m, 6H, $OCH_2C\underline{H}_2$); 1.49 (qui, 6H, $OCH_2CH_2C\underline{H}_2$); 1.32 (bs, 12H, $(CH_2)_2$); 0.88 (t, 9H, CH_3). Anal. calcd. for $C_{35}H_{50}N_4O_4$ (590.80): C, 71.15; H, 8.53; N, 9.48. Found: C, 71.3; H, 8.3; N, 9.3.

87

3,3'-Bis(3,4,5-trihexyloxybenzoylamino)-2,2'-bipyridine (3a)

The compound with R_f value of 0.23 (vide supra) was isolated and an analytically pure sample was obtained after recrystallisation from CH_2Cl_2/MeOH 8/2. K 53°C M 110°C I. IR (nujol): $v = 2928$ (C–H), 2856 (C–H), 1668 (C=O), 1578, 1459, 1375, 1333, 1225, 1112 cm^{-1}. ^{1}H-NMR (CDCl$_3$): δ 14.15 (s, 2H, NH); 9.40 (dd, 2H, J = 1.6 and 8.5 Hz, H-4); 8.38 (dd, 2H, J = 1.4 and 4.6 Hz, H-6); 7.50 (dd, 2H, J = 4.6 and 8.5 Hz, H-5); 7.25 (s, 4H, H-ortho); 4.05 (m, 12H, OCH$_2$); 1.80 (m, 12H, OCH$_2$CH$_2$); 1.50 (qui, 12H, OCH$_2$CH$_2$CH$_2$); 1.31 (bs, 24H, (CH$_2$)$_2$); 0.88 (t, 18H, CH$_3$). Anal. calcd. for C$_{60}$H$_{90}$N$_4$O$_8$ (995.39): C, 72.39; H, 9.11; N, 5.63. Found: C, 72.6; H, 9.3; N, 5.7.

N,N',N''-Tris{3[3'-(3,4,5-trihexyloxybenzoylamino)-2,2'-bipyridyl]}benzene-1,3,5-tricarbonamide (1a)

To a solution of **5a** (2 g, 3.39 mmol) and TEA (0.75 ml) in dry CH$_2$Cl$_2$ (40 ml) a solution of benzene-1,3,5-tricarbonyl trichloride (0.29 g, 1.12 mmol) in dry CH$_2$Cl$_2$ (10 ml) was added dropwise under an Ar atmosphere. After stirring at room temperature for 16 h, the resulting precipitate was filtered (P4 glass filter) and washed extensively with a mixture of acetone/CHCl$_3$ 1/1 yielding pure **1a** as a white sticky solid (1.79 g, 82%). T$_{cl}$ = 383°C (dec.). IR (nujol): $v = 2892$ (C–H), 1668 (C=O), 1572, 1459, 1375, 1291, 1243, 1112 cm^{-1}. ^{1}H-NMR (CDCl$_3$): δ 15.51 (s, 3H, NHCO); 14.38 (s, 3H, NH'CO); 9.59 (d, 3H, H-4); 9.40 (d, 3H, H-4'); 9.25 (s, 3H, H-ortho); 9.04 (d, 3H, H-6'); 8.44 (d, 3H, H-6); 7.50 (dd, 6H, H-5 and H-5'); 7.26 (s, 6H, H'-ortho); 4.02 (m, 18H, OCH$_2$); 1.80 (qui, 18H, OCH$_2$CH$_2$); 1.51 (qui, 18H, OCH$_2$CH$_2$CH$_2$); 1.32 (m, 36H, (CH$_2$)$_2$); 0.88 (t, 27H, CH$_3$). Anal. calcd. for C$_{114}$H$_{150}$N$_{12}$O$_{15}$ (1928.50): C, 71.00; H, 7.84; N, 8.71. Found: C, 70.8; H, 7.3; N, 8.6.

3,4,5-Tridodecyloxybenzoyl chloride (4b)

A mixture of methyl 3,4,5-trihydroxy-benzoate (3.5 g, 19 mmol), 1-bromododecane (14.5 g, 57 mmol) and K$_2$CO$_3$ (13 g) was heated under reflux in cyclohexanone (160 ml) for 40 h. After cooling, the precipitates were removed and the filtrate was evaporated *in vacuo*. The resulting brown solid residue was purified by column chromatography (flash SiO$_2$; eluent: petroleum ether (60–80)/EtOAc (96/4)) which afforded the pure ester as a white powder (12.6 g, 90%). An analytically pure sample was obtained after recrystallisation from EtOH (96%). M.p. 43.2–43.8°C. ^{1}H-NMR (CDCl$_3$): δ 7.22 (s, 2H, H-ortho); 4.03 (m, 6H, OCH$_2$); 3.88 (s, 3H, OCH$_3$); 1.80 (m, 6H, OCH$_2$CH$_2$); 1.48 (qui, 6H, OCH$_2$CH$_2$CH$_2$); 1.30 (bs, 48H, (CH$_2$)$_8$); 0.90 (t, 9H, CH$_3$). Anal. calcd. for C$_{44}$H$_{80}$O$_5$ (689.11): C, 76.70; H, 11.70. Found: C, 77.3; H, 11.8. To a mixture of the ester (5 g, 7.25 mmol) in EtOH (96%, 50 ml), a solution of KOH (0.9 g) in EtOH (96%, 28 ml) was added dropwise. The mixture was heated under reflux for 4 h. After cooling and acidification with conc. HCl-solution to pH = 2–3, the reaction mixture was poured into water (200 ml). The resulting white precipitate was filtered and recrystallised from EtOH (96%) to yield a white powder (4 g, 82%). M.p. 57.5–58°C. ^{1}H-NMR (CDCl$_3$): δ 7.31 (s, 2H, H-ortho); 4.02 (m, 6H, OCH$_2$); 1.80 (m, 6H, OCH$_2$CH$_2$); 1.46 (qui, 6H, OCH$_2$CH$_2$CH$_2$); 1.30 (bs, 48H, (CH$_2$)$_8$); 0.88 (t, 9H, CH$_3$). Anal. calcd. for C$_{43}$H$_{78}$O$_5$ (675.10): C, 76.50; H, 11.65. Found: C, 77.2; H, 11.7. The acid (2 g, 2.96 mmol) was treated with thionyl chloride (10 ml) at reflux temperature for 3 h. The excess thionyl chloride was distilled off and the resulting solid was flushed with *n*-hexane (2x10 ml) to give pure **4b** as a white solid in quantitative yield (2.07 g, 100%). ^{1}H-NMR (CDCl$_3$): δ 7.32 (s, 2H, H-ortho); 4.05 (m, 6H, OCH$_2$); 1.80 (m, 6H, OCH$_2$CH$_2$); 1.46 (qui, 6H, OCH$_2$CH$_2$CH$_2$); 1.30 (bs, 48H, (CH$_2$)$_8$); 0.88 (t, 9H, CH$_3$).

3'-(3,4,5-Tridodecyloxybenzoylamino)-2,2'-bipyridine-3-amine (5b)

To an ice-cooled solution of 3,3'-diamino-2,2'-bipyridine (0.5 g, 2.6 mmol) and TEA (0.5 ml) in dry diethyl ether (25 ml), a solution of **4b** (1.8 g, 2.6 mmol) in dry diethyl ether (20 ml) was added dropwise under an Ar atmosphere. After complete addition, the ice bath was removed and the mixture was stirred at room temperature for 4 h. The mixture was evaporated *in vacuo* and purification by

column chromatography (SiO$_2$; eluent: CHCl$_3$; R$_f$ = 0.55 for by-product **3b** and R$_f$ = 0.28 for **5b**) yielded pure **5b** as a yellow powder (1.27 g, 58%). Recrystallisation from *n*-hexane yielded an analytically pure sample. T$_{cl}$ = 64-65°C. ^{1}H-NMR (CDCl$_3$): δ 14.28 (s, 1H, N$\underline{H}$CO); 9.25 (dd, 1H, H-4'); 8.33 (dd, 1H, H-6'); 8.00 (dd, 1H, H-6); 7.32 (dd, 1H, H-5'); 7.12 (m, 2H, H-4 and H-5); 6.56 (bs, 2H, NH$_2$); 4.07 (m, 6H, OCH$_2$); 1.88 (m, 6H, OCH$_2$C$\underline{H}_2$); 1.49 (qui, 6H, OCH$_2$CH$_2$C$\underline{H}_2$); 1.32 (bs, 48H, (CH$_2$)$_8$); 0.88 (t, 9H, CH$_3$). Anal. calcd. for C$_{53}$H$_{86}$N$_4$O$_4$ (843.30): C, 75.48; H, 10.28; N, 6.64. Found: C, 75.8; H, 10.2; N, 6.6.

3,3'-Bis(3,4,5-tridecyloxybenzoylamino)-2,2'-bipyridine (**3b**)

The compound with R$_f$ = 0.55 (vide supra) was isolated and an analytically pure sample was obtained after recrystallisation from EtOAc. K 38°C M 110°C I. IR(nujol): ν = 2928 (C–H), 2856 (C–H), 1656 (C=O), 1572, 1459, 1369, 1333, 1225, 1123 cm^{-1}. ^{1}H-NMR (CDCl$_3$): δ 14.11 (s, 2H, NH); 9.35 (dd, 2H, *J* = 1.6 and 8.5 Hz, H-4); 8.38 (dd, 2H, *J* = 1.4 and 4.6 Hz, H-6); 7.44 (dd, 2H, *J* = 4.6 and 8.5 Hz, H-5); 7.25 (s, 4H, H-ortho); 4.05 (m, 12H, OCH$_2$); 1.85 (qui, 8H, OCH$_2$C$\underline{H}_2$-meta); 1.77 (qui, 4H, OCH$_2$C$\underline{H}_2$-para); 1.50 (qui, 12H, OCH$_2$CH$_2$C$\underline{H}_2$); 1.31 (bs, 96H, (CH$_2$)$_8$); 0.88 (t, 18H, CH$_3$). Anal. calcd. for C$_{96}$H$_{162}$N$_4$O$_8$ (1500.36): C, 76.85; H, 10.88; N, 3.73. Found: C, 76.4; H, 11.1; N, 3.4.

N,N',N''-Tris{3[3'-(3,4,5-tridecyloxybenzoylamino)-2,2'-bipyridyl]}benzene-1,3,5-tricarbonamide (**1b**)

To a solution of **5b** (1.27 g, 1.5 mmol) and TEA (0.3 ml) in dry CH$_2$Cl$_2$ (15 ml) a solution of benzene-1,3,5-tricarbonyl trichloride (0.13 g, 0.48 mmol) in dry CH$_2$Cl$_2$ (5 ml) was added dropwise. The mixture was heated under reflux for 18 h and, after cooling, evaporated *in vacuo*. To remove the salts, the solids were triturated with MeOH (2x20 ml). After purification by column chromatography (SiO$_2$, eluent: CHCl$_3$, R$_f$ = 0.50) the oil was dissolved in CHCl$_3$ (20 ml) and cooled (0°C). Acetone (15 ml) was added dropwise until a white solid precipitated. The precipitates were filtered and washed with acetone to yield pure **1b** as a sticky solid (0.76 g, 56%). T$_{cl}$ = 368°C. IR (nujol): ν = 2911 (C–H), 1668 (C=O), 1579, 1502, 1377, 1300, 1250, 1111 cm^{-1}. ^{1}H-NMR (CDCl$_3$): δ 15.49 (s, 3H, NHCO); 14.36 (s, 3H, NH'CO); 9.56 (d, 3H, H-4); 9.38 (d, 3H, H-4'); 9.16 (s, 3H, H-ortho); 9.03 (d, 3H, H-6'); 8.38 (d, 3H, H-6); 7.52 (dd, 3H, H-5); 7.48 (dd, 3H, H-5'); 7.26 (s, 6H, H'-ortho); 4.05 (m, 18H, OCH$_2$); 1.85 (qui, 18H, OCH$_2$C$\underline{H}_2$); 1.50 (qui, 18H, OCH$_2$CH$_2$C$\underline{H}_2$); 1.31 (bs, 144H, (CH$_2$)$_8$); 0.88 (t, 27H, CH$_3$). Anal. calcd. for C$_{168}$H$_{258}$N$_{12}$O$_{15}$ (2685.98): C, 75.12; H, 9.68; N, 6.25. Found: C, 75.1; H, 9.6; N, 6.2.

(S)-(+)-1-Bromo-3,7-dimethyloctane (**12**)

(S)-citronellol (25 g, 150 mmol) in EtOAc (150 ml) was catalytically hydrogenated in the presence Pd/C (10%, 1g) using a Parr apparatus. When no more H$_2$ was consumed, the catalyst was filtered and the filtrate was evaporated *in vacuo* yielding the corresponding saturated alcohol in a quantitative yield as a colourless oil. The alcohol (15.4 g, 97.8 mmol) and triphenylphosphine (28.3 gr, 108 mmol) were dissolved in dry CH$_2$Cl$_2$ (100 ml) and the solution was cooled to 0°C. In small portions, solid N-bromosuccinimide (18.4 g, 103 mmol) was added and the temperature was kept below 20°C during the addition. After stirring overnight at room temperature, the CH$_2$Cl$_2$ was evaporated *in vacuo* and *n*-hexane (200 ml) was added. The precipitates were filtered and thoroughly washed with *n*-hexane. The combined *n*-hexane layers were evaporated *in vacuo* and the resulting yellow oil was distilled under reduced pressure yielding a clear liquid (18.1 g, 84%). T$_b$ = 55°C/8.8x10^{-2} mbar. [α]$_D^{20}$ = +5.5° (CHCl$_3$, c = 17 g/dl). ^{1}H-NMR (CDCl$_3$): δ 3.45 (m, 2H, BrCH$_2$); 1.88 (m, 1H, C$^*\underline{H}$CH$_3$); 1.65 (m, 2H, BrCH$_2$C$\underline{H}$); 1.55 (m, 1H, C$\underline{H}$(CH$_3$)$_2$);1.25 (m, 3H, CH$_2$); 1.15 (m, 3H, CH$_2$); 0.90 (t, 9H, CH$_3$). ^{13}C-NMR (CDCl$_3$): δ 40.13; 39.19; 38.74; 31.8; 31.7; 27.9; 24.5; 22.6; 22.5; 18.9.

3,4,5- Tri-((S)-3,7-dimethyloctyloxy)benzoyl chloride (4c)
A mixture of methyl 3,4,5-trihydroxybenzoate (4 g, 21.7 mmol), *(S)*-1-bromo-3,7-dimethyloctane **12** (15 g, 68.1 mmol) and anhydrous K_2CO_3 (12 g) was stirred under an Ar atmosphere in DMF (80 ml) at 75°C for 18 h. After cooling, the reaction mixture was poured into water (150 ml) and extracted with *n*-hexane (3x100 ml). The combined organic layers were washed with aqueous HCl solution (1 M, 200 ml), H_2O (200 ml), saturated aqueous $NaHCO_3$ (200 ml) and brine (200 ml). After drying with $MgSO_4$, filtration and evaporation of the solvent *in vacuo*, the resulting oil was dried under high vacuum for 10 h to remove traces of bromine. The ester was obtained as a yellow oil (12.35 g, 94.5%) which was used without further purification. ^{1}H-NMR ($CDCl_3$): δ 7.22 (s, 2H, H-ortho); 4.03 (m, 6H, OCH_2); 3.88 (s, 3H, OCH_3); 1.88 (m, 3H, $OCH_2C\underline{H}$); 1.75 (bs, 3H, $OCH_2C\underline{H}$); 1.55 (m, 6H, $C^*HCH_3C\underline{H}_2$);1.33 (m, 9H, C^*H and $C^*HCH_3CH_2C\underline{H}_2$); 1.15 (m, 9H, $C\underline{H}(CH_3)_2$ and $C\underline{H}_2CH(CH_3)_2$); 0.95 (m, 9H, C^*CH_3); 0.88 (dd, 18H, CH_3). ^{13}C-NMR ($CDCl_3$): δ aromatic carbons: 166.9 (C=O); 152.6; 142.2; 124.6; 107.8. aliphatic carbons:71.6; 67.4; 52.1; 39.3; 39.2; 37.4; 37.3; 36.3; 29.8; 29.6; 27.9; 24.7; 22.7; 22.6; 19.5.$[\alpha]^{20}_D = -2.45$ ($CHCl_3$, c = 8.4 g/dl). A mixture of the ester (5.06 g, 8.3 mmol) and KOH (1 g) was heated under reflux in EtOH (96%) (100 ml) for 3 h. After cooling and acidification with conc. HCl-solution to pH = 2–3, H_2O (100 ml) was added. Extraction with $CHCl_3$ (3x100 ml), drying of the combined organic layers with $MgSO_4$ and evaporation of the solvent *in vacuo*, yielded the acid as a light yellow oil (4.98 g, 100%). An analytically pure sample was obtained by purification of the crude compound with column chromatography (SiO_2; eluent: CH_3CN/CH_2Cl_2 1/1). M.p. 57.5–58°C. ^{1}H-NMR ($CDCl_3$): δ 7.35 (s, 2H, H-ortho); 4.05 (m, 6H, OCH_2); 1.88 (m, 3H, $OCH_2C\underline{H}$); 1.75 (bs, 3H, $OCH_2C\underline{H}$); 1.55 (m, 6H, $C^*HCH_3C\underline{H}_2$);1.33 (m, 9H, C^*H and $C^*HCH_3CH_2C\underline{H}_2$); 1.15 (m, 9H, $C\underline{H}(CH_3)_2$ and $C\underline{H}_2CH(CH_3)_2$); 0.95 (m, 9H, C^*CH_3); 0.88 (dd, 18H, CH_3).^{13}C-NMR ($CDCl_3$): δ 171.5 (C=O); 152.8; 142.9; 123.7; 108.4. aliphatic carbons: 71.7; 67.4; 58.4; 39.3; 39.2; 37.4; 37.3; 36.2; 29.6; 29.5; 27.9; 24.7; 22.7; 22.6; 19.5. Anal. calcd. for $C_{37}H_{66}O_5$ (590.92): C, 75.20; H, 11.25. Found: C, 75.8; H, 11.4. $[\alpha]^{20}_D = -2.98$ ($CHCl_3$, c = 7.83 g/dl). The acid (1.13 g, 1.92 mmol) was treated with thionyl chloride (10 ml) at reflux temperature for 3 h. The excess thionyl chloride was distilled off and the resulting oil was flushed with *n*-pentane (2x10 ml) to give pure **4c** as a yellow oil in quantitative yield (1.16 g, 100%). ^{1}H-NMR ($CDCl_3$): δ 7.32 (s, 2H, H-ortho); 4.05 (m, 6H, OCH_2); 1.88 (m, 3H, $OCH_2C\underline{H}$); 1.75 (bs, 3H, $OCH_2C\underline{H}$); 1.55 (m, 6H, $C^*HCH_3C\underline{H}_2$);1.33 (m, 9H, C^*H and $C^*HCH_3CH_2C\underline{H}_2$); 1.15 (m, 9H, $C\underline{H}(CH_3)_2$ and $C\underline{H}_2CH(CH_3)_2$); 0.95 (m, 9H, C^*CH_3); 0.88 (dd, 18H, CH_3).

3'-[3,4,5-Tri((S)-3,7-dimethyloctyloxy)benzoylamino]-2,2'-bipyridine- 3-amine (5c)
To an ice-cooled solution of 3,3'-diamino-2,2'-bipyridine (0.3 g, 1.6 mmol) and TEA (0.3 ml) in dry diethyl ether (40 ml), a solution of **4c** (1 g, 1.6 mmol) in dry diethyl ether (15 ml) was added dropwise under an Ar atmosphere. After complete addition, the mixture was stirred at room temperature for another 4 h. Then, CH_2Cl_2 (50 ml) was added and the mixture was extracted with H_2O (3x50 ml). The organic layer was dried with $MgSO_4$, filtered and evaporated *in vacuo*. The resulting crude compound was purified with column chromatography (SiO_2; eluent: hexane/EtOAc 85/15, R_f = 0.21) yielding pure **5c** as a sticky yellow solid (1g, 80%). T_{cl} = 68.5-69.5°C. ^{1}H-NMR ($CDCl_3$): δ 14.31 (s, 1H, NHCO); 9.26 (dd, 1H, H-4'); 8.33 (dd, 1H, H-6'); 8.00 (dd, 1H, H-6); 7.32 (dd, 1H, H-5'); 7.25 (s, 2H, H-ortho) 7.12 (m, 2H, H-4 and H-5); 6.56 (bs, 2H, NH_2); 4.07 (m, 6H, OCH_2); 1.88 (m, 3H, $OCH_2C\underline{H}$); 1.75 (bs, 3H, $OCH_2C\underline{H}$); 1.55 (m, 6H, $C^*HCH_3C\underline{H}_2$);1.33 (m, 9H, C^*H and $C^*HCH_3CH_2C\underline{H}_2$); 1.15 (m, 9H, $C\underline{H}(CH_3)_2$ and $C\underline{H}_2CH(CH_3)_2$); 0.95 (m, 9H, C^*CH_3); 0.88 (dd, 18H, CH_3). Anal. calcd. for $C_{47}H_{74}N_4O_4$ (759.12): C, 74.36; H, 9.82; N, 7.38. Found: C, 74.5; H, 9.8; N, 7.1.

3,3'- Bis[3,4,5-tri((S)-3,7-dimethyloctyloxy)benzoylamino]-2,2'-bipyridine (3c)

To an ice-cooled solution of 3,3'-diamino-2,2'-bipyridine (0.13 g, 0.7 mmol) and TEA (0.3 ml) in dry diethyl ether (20 ml), a solution of **4c** (0.9 g, 1.48 mmol) in dry diethyl ether (20 ml) was added dropwise under an Ar atmosphere. After complete addition, the mixture was stirred at room temperature for another 4 h. The solution was extracted with $NaHCO_3$ solution (2x50 ml) and H_2O (50 ml) and the organic layer was dried with $MgSO_4$, filtered, washed with diethyl ether and evaporated *in vacuo*. The crude product was purified using column chromatography (eluent: hexane/ EtOAc 95/5) yielding pure **3c** as a sticky white solid (0.53 g, 58%). T_{cl} = 126-126.5°C. ^{1}H-NMR ($CDCl_3$): δ 14.15 (s, 2H, NHCO); 9.37 (dd, 2H, H-4); 8.38 (dd, 2H, H-6); 7.44 (dd, 2H, H-5); 7.26 (s, 4H, H-ortho); 4.13 (m, 12H, OCH_2); 1.89 (m, 6H, $OCH_2C\underline{H}$); 1.75-1.15 (m, 56H, CH_2 and CH); 0.88 (dt, 56H, CH_3). Anal. calcd. for $C_{84}H_{138}N_4O_8$ (1332.05): C, 75.74; H, 10.44; N, 4.21. Found: C, 74.7; H, 10.3; N, 4.1.

N,N',N"-Tris{3[3'-(3,4,5-tri((S)-3,7-dimethyloctyloxy)benzoylamino)-2,2'-bipyridyl]}benzene-1,3,5-tricarbonamide (1c)

To a solution of **5c** (0.73 g, 0.96 mmol) and TEA (0.2 ml) in dry CH_2Cl_2 (20 ml) a solution of benzene-1,3,5-tricarbonyl trichloride (80 mg, 0.30 mmol) in dry CH_2Cl_2 (4 ml) was added dropwise under an Ar atmosphere and heated under reflux for 16 h. The resulting clear solution was cooled to room temperature and acetone (10 ml) was added slowly until a white solid precipitated. The precipitate was filtered off (P4 glass filter) and washed with acetone yielding pure **1c** as a sticky white solid (0.6 g, 82%). T_{cl} = 373°C. $[\alpha]^{20}_D$ = –8.23 (CHCl$_3$, c = 0.51 g/dl). ^{1}H-NMR ($CDCl_3$): δ 15.52 (s, 3H, NHCO); 14.40 (s, 3H, NH'CO); 9.60 (dd, 3H, H-4); 9.40 (dd, 3H, H-4'); 9.25 (s, 3H, H-ortho); 9.05 (d, 3H, H-6'); 8.44 (d, 3H, H-6); 7.54 (m, 6H, H-5 and H-5'); 7.32 (s, 6H, H-ortho');4.07 (m, 18H, OCH_2); 1.88 (m, 9H, $OCH_2C\underline{H}$); 1.75 (bs, 9H, $OCH_2C\underline{H}$); 1.55 (m, 18H, C*HC$\underline{H}_3$C$\underline{H}_2$);1.33 (m, 27H, C*H and C*HCH$_3$CH$_2$C$\underline{H}_2$); 1.15 (m, 27H, C$\underline{H}$(CH$_3$)$_2$ and C$\underline{H}_2$CH(CH$_3$)$_2$); 0.95 (m, 27H, C*CH$_3$); 0.88 (dd, 54H, CH$_3$). Anal. calcd. for $C_{150}H_{222}N_{12}O_{15}$ (2433.47): C, 74.03; H, 9.19; N, 6.91. Found: C, 73.8; H, 9.3; N, 6.8.

3,4,5-Trioctadecyloxybenzoyl chloride (4d)

A mixture of methyl 3,4,5-trihydroxy-benzoate (5 g, 27.15 mmol), 1-bromooctadecane (29 g) and anhydrous K_2CO_3 (20 g) was stirred under an Ar atmosphere in DMF/THF 1/1 (200 ml) at 80°C for 24 h. After cooling, the reaction mixture was poured into water (200 ml) and the precipitate was filtered and washed with toluene (100 ml). The ester was used without further purification (11.65 g, 91%). An analytically pure sample was obtained by recrystallisation from diethyl ether. M.p. 61– 63°C. ^{1}H-NMR ($CDCl_3$): δ 7.25 (s, 2H, H-ortho); 4.03 (m, 6H, OCH_2); 3.88 (s, 3H, OCH_3); 1.80 (m, 6H, $OCH_2C\underline{H}_2$); 1.48 (qui, 6H, $OCH_2CH_2C\underline{H}_2$); 1.30 (bs, 84H, $(CH_2)_{14}$); 0.90 (t, 9H, CH_3). Anal. calcd. for $C_{62}H_{116}O_5$ (941.59): C, 79.08; H, 12.41. Found: C, 79.2; H, 12.4. A mixture of the ester (5.75 g, 6.1 mmol) and KOH (2 g) was heated under reflux in EtOH (96%)/dioxaan 1/1 (200 ml) for 4 h. After cooling and acidification with conc. HCl-solution to pH = 2–3, the resulting white precipitate was filtered and washed with EtOH. After recrystallisation from EtOAc, the acid was obtained as a white powder (4.66 g, 82%). M.p. 86.5–87.2°C. ^{1}H-NMR ($CDCl_3$): δ 7.31 (s, 2H, H-ortho); 4.02 (m, 6H, OCH_2); 1.80 (m, 6H, $OCH_2C\underline{H}_2$); 1.46 (qui, 6H, $OCH_2CH_2C\underline{H}_2$); 1.30 (bs, 84H, $(CH_2)_{14}$); 0.88 (t, 9H, CH_3). Anal. calcd. for $C_{61}H_{114}O_5$ (927.56): C, 78.99; H, 12.38. Found: C, 79.1; H, 12.7. The acid (2.05 g, 5.39 mmol) was treated with thionyl chloride (40 ml) at reflux temperature for 3 h. The excess thionyl chloride was distilled off and the resulting solid was flushed with *n*-hexane (2x10 ml) to give pure **4d** as a white solid in quantitative yield (2.1 g, 100%). ^{1}H-NMR ($CDCl_3$): δ 7.32 (s, 2H, H-ortho); 4.05 (m, 6H, OCH_2); 1.80 (m, 6H, $OCH_2C\underline{H}_2$); 1.46 (qui, 6H, $OCH_2CH_2C\underline{H}_2$); 1.30 (bs, 84H, $(CH_2)_{14}$); 0.88 (t, 9H, CH_3).

3'-(3,4,5-Trioctadecyloxybenzoylamino)-2,2'-bipyridine-3-amine (5d)

To an ice-cooled solution of 3,3'-diamino-2,2'-bipyridine (0.5 g, 2.6 mmol) and TEA (0.5 ml) in dry THF (80 ml), a solution of **4d** (2.45 g, 2.6 mmol) in dry THF (40 ml) was added dropwise under an Ar atmosphere. After complete addition, the mixture was stirred at room temperature for another 16 h. The mixture was poured into H_2O (100 ml) and extracted with diethyl ether (3x100 ml). The solvent was removed *in vacuo* and the crude product was recrystallised from CH_2Cl_2 yielding **5d** with a 95% purity (the impurity being the diacylated compound) (2.18 g, 74%). Due to solubility difficulties, no further purification was attempted and the compound was used as such. ^{1}H-NMR (CDCl$_3$): δ 14.22 (s, 1H, NH'CO); 9.25 (dd, 1H, H-4'); 8.33 (dd, 1H, H-6'); 8.00 (dd, 1H, H-6); 7.32 (dd, 1H, H-5'); 7.12 (m, 2H, H-4 and H-5); 6.56 (bs, 2H, NH$_2$); 4.07 (m, 6H, OCH$_2$); 1.88 (m, 6H, OCH$_2$CH$_2$); 1.49 (qui, 6H, OCH$_2$CH$_2$CH$_2$); 1.32 (bs, 84H, (CH$_2$)$_{14}$); 0.88 (t, 9H, CH$_3$).

N,N',N''-Tris{3[3'-(3,4,5-trioctadecyloxybenzoylamino)-2,2'-bipyridyl]}benzene-1,3,5-tricarbon-amide (1d)

To a solution of **5d** (0,85 g, 0.68 mmol) and TEA (0.15 ml) in dry CH_2Cl_2 (40 ml) a solution of benzene-1,3,5-tricarbonyl trichloride (60 mg, 0.22 mmol) in dry CH_2Cl_2 (4 ml) was added dropwise under an Ar atmosphere and heated under reflux for 16 h. The resulting white precipitate was filtered off (P4 glass filter) and washed with cold CH_2Cl_2. The crude product was purified by column chromatography (SiO$_2$). First the impurities were eluted with CH_2Cl_2 in which compound **1d** is hardly soluble at room temperature. Then, extensive elution with CHCl$_3$ yielded **1d**. After evaporation of the solvent, compound **1d** was dissolved in CHCl$_3$ (15 ml) and cooled (0°C). Acetone was slowly added until a white solid precipitated. The precipitate was filtered and washed with acetone to yield **1d** as a white powder (0.46 g, 54%). T$_{cl}$ = 308°C (dec.). IR (nujol): v = 2926 (C–H), 2856 (C–H), 1668 (C=O), 1578, 1459, 1375, 1303 cm^{-1}. ^{1}H-NMR (CDCl$_3$): δ 15.49 (s, 3H, NHCO); 14.39 (s, 3H, NH'CO); 9.55 (d, 3H, H-4); 9.40 (d, 3H, H-4'); 9.22 (s, 3H, H-ortho); 9.04 (d, 3H, H-6'); 8.42 (d, 3H, H-6); 7.55 (dd, 3H, H-5); 7.49 (dd, 3H, H-5'); 7.26 (s, 6H, H'-ortho); 4.05 (m, 18H, OCH$_2$); 1.85 (qui, 18H, OCH$_2$CH$_2$); 1.50 (qui, 18H, OCH$_2$CH$_2$CH$_2$); 1.31 (bs, 252H, (CH$_2$)$_{14}$); 0.88 (t, 27H, CH$_3$). Anal. calcd. for C$_{222}$H$_{366}$N$_{12}$O$_{15}$ (3443.45): C, 77.43; H, 10.71; N, 4.88. Found: C, 77.3; H, 10.7; N, 5.1.

5,5'-Dimethoxy- 3'-(3,4,5-tridodecyloxybenzoylamino)-2,2'-bipyridine-3-amine (6)

To a stirred solution of 5,5'-dimethoxy-2,2'-bipyridine-3,3'-diamine (0.17 g; 0.68 mmol) and TEA (0.5 ml; 3.6 mmol) in THF (10 ml) at −10°C, **4b** (0.43 g; 0.62 mmol) in THF (10 ml) was added dropwise in 1h. After continued stirring of the solution at room temperature for 18 h, the solvent was removed *in vacuo*, the residue dissolved in CH_2Cl_2 and washed with saturated aqueous NaHCO$_3$ (3x25 ml) and brine (1x25 ml). The product was purified by column chromatography (18 g silica gel; eluent: CHCl$_3$/methanol 97/3) followed by column filtration (13 g silica gel, gradient CH_2Cl_2/hexane 5/2 to pure CH_2Cl_2), resulting in pure **6** (0.34 g; 62%).^{1}H-NMR (CDCl$_3$): δ 14.32 (s, 1H, NHCO), 8.99 (d, J = 2.8 Hz, 1H, H-4'), 8.00 (d, J = 2.8 Hz, 1H, H-6'), 7.70 (d, J = 2.5 Hz, 1H, H-6), 7.26 (s, 2H, H-ortho), 6.58 (d, J = 2.5 Hz, 1H, H-4), 6.53 (s, 2H, NH$_2$), 4.06 (m, 6H, OCH$_2$), 3.93 (s, 3H, 5'-OCH$_2$), 3.83 (s, 3H, 5-OCH$_3$), 1.81 (m, 6H, OCH$_2$CH$_2$), 1.48 (m, 6H, O(CH$_2$)$_2$CH$_2$), 1.26 (bs, 48H, (CH$_2$)$_8$), 0.88 (t, 9H, CH$_3$).^{13}C-NMR (CDCl$_3$): δ 166.4 (C=O); aromatic carbons: 155.5 154.2; 153.1; 145.7; 141.6; 136.5; 136.5; 132.8; 130.5; 129.1; 123.1; 111.9; 107.9; 106.5; aliphatic carbons: 73.5; 69.5; 55.5; 55.3; 31.9; 30.3; 29.5; 26.3; 22.6; 14.1.

3,3'-Bis(3,4,5-tridodecyloxybenzoylamino)-5,5'-dimethoxy-2,2'-bipyridine (9)

A solution of 5,5'-dimethoxy-3,3'-diamino-2,2'-bipyridine (54 mg; 0.22 mmol) and TEA (0.5 ml; 3.6 mmol) in THF (10 ml) was stirred at −10°C. Compound **4b** (0.31 g; 0.44 mmol) was dissolved in THF (4 ml) and added dropwise to the solution. After the addition was complete, the solution was

stirred at room temperature for 18 h. The solvent was then removed *in vacuo*, the residue dissolved in dichloromethane and washed with a saturated aqueous solution of NaHCO$_3$ (3x) and brine (4x). The product was further purified by column chromatography (5 g silica gel; eluent hexane/CHCl$_3$ 1/2; R$_f$= 0.30) and precipitation from CHCl$_3$/acetone, which yielded the pure title compound (0.14 g; 41%). T$_{cl}$ = 191.0°C. ^{1}H-NMR (CDCl$_3$): δ 14.24 (s, 1H, NH), 9.09 (d, J = 2.5 Hz, 2H, H-4), 8.07 (d, J = 2.5 Hz, 2H, H-6), 7.26 (s, 4H, H-ortho), 4.07 (m, 12H, OCH$_2$), 3.96 (s, 6H, OCH$_3$), 1.86 (m, 12H, OCH$_2$C$\underline{H}_2$), 1.50 (m, 12H, O(CH$_2$)$_2$C$\underline{H}_2$), 1.26 (bs, 96H, (CH$_2$)$_8$), 0.88 (t, J = 6.4 Hz, 18H, CH$_3$). ^{13}C-NMR (CDCl$_3$): δ 166.6 (C=O); aromatic carbons: 155.2; 153.2; 141.9; 137.8; 135.1; 130.1; 112.5; 106.5; aliphatic carbons: 73.6; 69.6; 55.9; 31.9; 29.7; 29.4; 26.1; 22.7; 14.1.

N,N',N''-Tris{3[3'-(3,4,5-tridodecyloxybenzoylamino)-5,5'-dimethoxy-2,2'-bipyridyl]}benzene-1,3,5-tricarbonamide (2)

A solution of **6** (0.27 g; 0.28 mmol) and TEA (0.1 ml; 0.7 mmol) in THF (0.8 ml) under argon was cooled to −10°C. A solution of benzene-1,3,5-tricarbonyl trichloride (23 mg; 86 μmol) in THF (0.5 ml) was added, where after the resulting suspension was stirred for 2 h at 40°C and overnight at room temperature. The suspension was then filtered, the solid washed with acetone and further purified by precipitation from acetone/CHCl$_3$. Additional purification by column filtration (7 g silica gel; eluent: CHCl$_3$/EtOAc 98/2; R$_f$ = 0.47) resulted in pure **2** (47 mg, 19%). ^{1}H-NMR ((CDCl$_2$)$_2$): δ 15.45 (s, 3H, NHCO); 14.16 (s, 3H, NH'CO); 9.26 (s, J = 2.6 Hz, 3H, H-4); 9.16 (s, 3H, H-ortho); 9.04 (s, J = 2.6 Hz, 3H, H-4'); 8.87 (s, J = 2.7 Hz, 3H, H-6'); 8.10 (s, J = 2.3 Hz, 3H, H-6); 7.28 (s, 6H, H-ortho'); 4.14 (m, 18H, OCH$_2$); 3.85 (s, 18H, OCH$_3$); 1.80 (m, 18H, OCH$_2$C$\underline{H}_2$); 1.48 (m, 18H, O(CH$_2$)$_2$C$\underline{H}_2$); 1.30 (bs, 144H, (CH$_2$)$_8$); 0.90 (bs, 27H, CH$_3$).

N,N',N''-Tris(3-pyridyl)-benzene-1,3,5-tricarbonamide (7)

Dropwise addition of a solution of trimesic chloride (0.90 g, 3.39 mmol) in THF (10 ml) to an ice-cold solution of 3-pyridylamine (1.00 g, 10.6 mmol) and TEA (1.6 ml, 1.13 g, 11.2 mmol) in THF (10 ml) afforded a milky suspension. After 2 h stirring at 0°C, the reaction mixture was allowed to attain room temperature overnight. Then the precipitate was filtered, taken up in saturated aqueous NaHCO$_3$ (30 ml), re-filtered and washed with water (3x20 ml) and diethyl ether (20 ml) and finally dried *in vacuo* to give crude **7** (1.18 g, 79%) as a white solid. Recrystallisation from methanol (200 ml) afforded large, transparent hexagonal crystals, which lost their transparency in air. M.p. 287–289°C. ^{1}H NMR (DMSO-*d6*): δ 10.87 (NH), 9.01 (H-2'), 8.82 (H-2, 4, 6), 8.39 (H-6'), 8.26 (H-4'), 7.47 (H-5'), 4.1 (OH), 3.19 (CH$_3$). ES-MS (MeOH + HCOOH): 439.1, (M+H)$^+$ and 219.9 (M+2H)$^{++}$.

N,N',N''-Tris[3(3'-t-butoxycarbonylamino-2,2'-bipyridyl)]benzene-1,3,5-tricarbonamide (10)

To an ice-cooled solution of 3'-*t*-butoxycarbonylamino-2,2'-bipyridine-3-amine (*see* compound **9c**, Chapter 2 for the synthesis) (1.4 g, 4.8 mmol) and TEA (0.7 ml) in dry THF (50 ml), a solution of benzene-1,3,5-tricarbonyl trichloride (0.39 g, 1.5 mmol) was added slowly. The reaction was carried out under Ar atmosphere. After complete addition, the ice bath was removed and the mixture was stirred at room temperature for another 18 h. The resulting white precipitates were filtered and washed with cold THF (3x5 ml), H$_2$O (3x10 ml) and saturated NaHCO$_3$ solution (2x10 ml). The resulting white solid was suspended in MeOH to remove last traces of TEA.HCl. After filtration and drying of the residue, pure **9** was obtained as a white powder (1.36 g, 83%). M.p. 265°C (dec.). ^{1}H-NMR (CDCl$_3$): δ 15.33 (s, 3H, NHCO); 12.77 (s, 3H, NHBoc); 9.44 (d, 3H, H-4); 9.10 (s, 3H, H-ortho); 8.90 (m, 6H, H-6 and H-4'); 8.38 (d, 3H, H-6'); 7.41 (m, 6H, H-5 and H-5'); 1.57 (s, 27 H, C(CH$_3$)$_3$). FAB-MS: m/z (%): 1037 (42) [MNa$^+$]; 1015 (83) [MH$^+$]; 941 (52) [MH$^+$− C(CH$_3$)$_3$O]; 914 (55) [MH$^+$− C(CH$_3$)$_3$OCO].

N,N',N''-Tris[3(3'-amino -2,2'-bipyridyl)]benzene-1,3,5-tricarbonamide (8)
To a solution of **10** (1 g, 1 mmol) in CH$_2$Cl$_2$ (10 ml), TFA (10 ml) was added carefully. The yellow solution was stirred for 18 h at room temperature. Then, TEA (10 ml) was cautiously added through a dropping funnel (this addition gave rise to aggressive fumes). The resulting yellow precipitate was filtered, washed with CH$_2$Cl$_2$/TEA (1/1, 3x5 ml) and suspended in CH$_2$Cl$_2$ (20 ml). After filtration and drying of the precipitates, **8** was obtained as a yellow powder (0.7 g, 99%). ^{1}H-NMR (DMF-*d7*): δ 15.79 (s, 3H, NHCO); 9.46 (dd, 3H, H-4); 9.23 (s, 3H, H-ortho); 8.60 (dd, 3H, H-6'); 8.50 (dd, 3H, H-6); 7.77 (bs, 6H, NH$_2$); 7.51 (dd, 3H, H-5'); 7.47 (dd, 3H, H-4'); 7.32 (dd, 3H, H-5).

4.8   References and notes

[1]   Constable, E.C. *Adv. Inorg. Chem.* **1989**, *34*, 1 and references cited herein.

[2]   For some recent examples see a) Araki, K.; Mutai, T.; Shigemitsu, Y.; Yamada, M.; Nakajima, T.; Kuroda, S.; Shimao, I. *J. Chem. Soc., Perkin Trans. 2* **1996**, 613. b) Issberner, J.; Vögtle, F.; De Cola, L.; Balzani, V. *Chem. Eur. J.* **1997**, *3*, 707. c) Palmans, R.; MacQueen, D.B.; Pierpont, C.G.; Frank, A.J. *J. Am. Chem. Soc.* **1996**, *118*, 12647.

[3]   a) Kuboki, T.; Araki, K.; Yamada, M.; Shiraishi, S. *Bull. Chem. Soc. Jpn.* **1994**, *67*, 948. b) Rowe, K.E.; Bruce, D.W. *J. Chem. Soc., Dalton Trans.* **1996**, 3913. c) L. Doucce, L.; Ziessel, R.; Seghrouchni, R.; Skoulios, A.; Campillos, E.; Deschenaux, R. *Liq. Cryst.* **1996**, *20*, 235. d) El-Ghayoury, A.; Douce, L.; Ziessel, R.; Seghrouchni, R.; Skoulios, A. *Liq. Cryst.* **1996**, *21* 143. e)Yu, S.C.; Chan, W.K. *Polym. Prep.* **1997**, *38*, 123.

[4]   a) Mertsendorf,C.; Ringsdorf, H. *Mol. Eng.* **1992**, *2*, 189; b) Bauer, S.; Plesnivy, T.; Ringsdorf, H.; Schuhmacher, P. *Makromol. Chem. Macromol. Symp.* **1992**, *64*, 19; c) Zhang, J.; Moore, J. *J. Am. Chem. Soc.* **1994**, *116*, 2655; d) Kretschmann, H.; Müller, K.; Kolshorn, H.; Schollmeyer, D.; Meier, H. *Chem. Ber.* **1994**, *127*, 1735; e) Stabel, A.; Herwig, P.; Müllen, K.; Rabe, J.P. *Angew. Chem., Int. Ed. Engl.* **1995**, *34*, 1609; f) Mohr, B.; Wegner, G.; Ohta, K. *J. Chem. Soc., Chem. Commun.* **1995**, 995; g) Plesnivy, T.; Ringsdorf, H.; Schuhmacher, P.; Nütz, U.; Diele, S. *Liq. Cryst.* **1995**, *18*, 185.

[5]   a) Adam, D.; Schuhmacher, P.; Simmerer, J.; Häussling, L.; Siemensmeyer, K.; Etzbach, K.H.; Ringsdorf, H.; Haarer, D. *Nature* **1994**, *371*, 141; b) van Nostrum, C.F.; Picken, S.J.; Schouten, A-J.; Nolte, R.J.M. *J. Am. Chem. Soc.* **1995**, *117*, 9957.

[6]   Paleos, C.M.; Tsiourvas, D. *Angew. Chem., Int. Ed. Engl.* **1995**, *34*, 1696.

[7]   a) Barbera, J.; Cativiela, C.; Serrano, J.L.; Zurbano, M.M. *Adv. Mater.* **1991**, *3*, 602. b) Serrette, A.G.; Swager, T.M. *Ang. Chem., Int. Ed. Engl.* **1994**, *33*, 2342. c) Fischer, H.; Plesnivy, T.; Ringsdorf, H.; Seitz, M. *J. Chem. Soc., Chem. Commun.* **1995**, 1615. d) Zheng. H.; Xu, B.; Swager, T.M. *Chem. Mater.* **1996**, *8*, 907. e) Thompson, N.J.; Serrano, J.L.; Baena, M.J.; Espinet, P. *Chem. Eur. J.* **1996**, *2*, 214. f) Kroczynski, A.; Pociecha, D.; Szydlowska, J.; Przedmojski, J.; Gorecka, E. *Chem. Commun.* **1996**, 2731.

[8]   a) Paulus, W.; Ringsdorf, H.; Diele, S.; Pelzl, G. *Liq. Cryst.* **1991**, *9*, 807. b) Van der Auweraer, M.; Catry, C.; Feng Chi, L.; Karthaus, O.; Knoll, W.; Ringsdorf, H.; Sawodny, M.; Urban, U. *Thin Solid Films* **1992**, *210/211*, 39. c) Gorecka, E.; Pyzuk, W.; Krowczynski, A.; Przedmojski, J. *Liq. Cryst.* **1993**, *14*, 1837.

[9]   a) Kleppinger, R.; Lillya, C.P.; Yang, C. *Angew. Chem.* **1995**, *107*, 1762; b) Koh, K.N.; Araki, K.; Komori, T. ; Shinkai, S. *Tetrahedron Lett.* **1995**, *36*, 5191; c) Ebert, M.; Kleppinger, R.; Soliman, M.; Wolf, M.; Wendorf, J.H.; Lattermann, G.; Staufer, G. *Liq. Cryst.* **1990**, *7*, 553; d) Serrette, A.G.; Swager, T. *Angew. Chem., Int. Ed. Engl.* **1994**, *33*, 2342. e) Ungar G.; Abramic, D.; Percec, V.; Heck, J.A. *Liq. Cryst.* **1996**, *21*, 73.

[10]   Initial efforts to synthesise disc-shaped derivative **1b** were based on a divergent approach. Therefore, a selective monoacylation of 3,3'-diamino-2,2'-bipyridine with Boc$_2$O was

developed leading to compound **8**. However, only low yields of the desired disc-shaped compound **1b** were obtained (5%).

[11]   a) J. Malthête, A.M. Levelut and N.H. Tihn, *J. Phys. Lett.,* **1985**, *46*, L875. b) H. Meier, E. Praß, G. Zerban and F. Kosteyn, *Z. Naturforsch.,* **1988**, *43B*, 889.

[12]   a) P.G. Schouten, J.F. van der Pol, J.W. Zwikker, W. Drenth, Picken, S.J. *Mol. Cryst. Liq. Cryst.* **1991**, *195*, 291. b) Van Nostrum, C.F. *Supramolecular assemblies from phthalocyanine building blocks*, PhD thesis, University of Nijmegen, The Netherlands, **1995**.

[13]   The diacylated compounds **3a–c** were also isolated and purified. A full characterisation of these compounds is included in the experimental part. As expected, they also show liquid crystalline behaviour. Preliminary X-ray results suggest the presence of a D_{ho} phase in all compounds.

[14]   Compounds **1b–d** also show a concentration effect. Due to their high molecular weights, the effect of change in weight concentration is less pronounced compared to compound **1a**. Therefore, only the results of concentration and temperature variation of compound **1a** are discussed.

[15]   Fischer, H.; Karasz, F.E. *Liq. Cryst.* **1993**, *15*, 513.

[16]   The differences in the clearing temperatures between DSC and polarisation microscopy are due to the fact that at high temperatures the heat transfer in the heating stage of the microscope is not so efficient.

[17]   Collard, D.M.; Lillya, C.P. *J. Am. Chem. Soc.* **1991**, *113*, 8577.

[18]   Discotic liquid crystals with an aromatic core of comparable size as present in compounds **1** and **2** often do not show a D_{ho}–I transition due to decomposition of the sample (see references 4f and 12b) or the corresponding enthalpies are not mentioned in the reference (see for example references 4d,e). a) Destrade, C.; Thin, N.H.; Gasparoux, H. *Mol. Cryst. Liq. Cryst.* **1981**, *71*, 111. b) Zamir, S.; Singer, D.; Spielberg, N.; Wachtel, E.J.; Zimmerman, H.; Poupko, R.; Luz, Z. *Liq. Cryst.* **1996**, *21*, 39.

[19]   a) Harada, H.; Matsunaga, Y.; *Bull. Chem. Soc. Jpn.* **1988**, *61*, 2739. b) Malthête, J.; Levelut, A.-M.; Liébert, L. *Adv. Mater.* **1992**, *1*, 37. c) see reference 9e.

[20]   Schouten, P.G. *Charge carrier dynamics in pulse-irradiated columnar aggregates of mesomorphic porphyrins and phthalocyanines*, PhD thesis, University of Delft, The Netherlands, ISBN 90-73861-22-5, **1994**.

[21]   In this respect it can be noted that hexa-hexylthiotriphenylene (HHTT) shows a slightly larger value of the one-dimensional, intra-columnar mobility ($\sum\mu_c = 0.08\times10^{-4}$ m²/V.s) than the average values found for the ordered columnar mesophases of alkoxysubstituted phthalocyanines ($\sum\mu_c = 0.06\times10^{-4}$ m²/V.s). $\sum\mu_c$ can be estimated from the dose normalised end-of-pulse conductivity, *see* reference 20 for more details.

[22]   A methoxy derivative (N,N',N''-tris{3[3'-(3,4,5-trimethoxybenzoylamino)-2,2'-bipyridyl]}-benzene-1,3,5-tricarbonamide) and a chainless derivative (N,N',N''-tris[3(3'-benzoylamino)-2,2'-bipyridyl]benzene-1,3,5-tricarbonamide) of compounds **1** were synthesised in order to obtain crystals. Unfortunately, both compounds proved to be highly insoluble in organic solvents. Boc-derivative **10** was, in fact, soluble in various organic solvents but all attempts to grow crystals failed.

Chapter 5

Lyotropic liquid crystalline behaviour in disc-shaped amide derivatives of 3,3'-diamino-2,2'-bipyridine

Abstract

Highly stable lyotropic liquid crystalline mesophases are found when extended-core disc-shaped compounds 1a,b are dissolved in alkane solvents. At low concentrations (5–28% w/w) all evidence points to the presence of an N_C phase. In concentrated samples (55% w/w), a D_{ho} phase is observed in which the helical superstructure found for the thermotropic liquid crystalline phase of compounds 1a,b is retained. Preliminary rheology measurements on anisotropic and isotropic solutions reveal that the viscosity of the dodecane solutions increases drastically upon the addition of only 1% w/w of compound 1a. Furthermore, both solutions show visco-elastic behaviour. The lyotropic liquid crystalline phases can be oriented in a planar alignment —in which the columnar axis is parallel to the glass surface— by uniaxially rubbing the samples between glass plates. Switching this orientation into a homeotropic alignment —in which the columnar axis is perpendicular to the glass surface— has been achieved by applying an electrical field over the samples.

5.1 Introduction

Lyotropic liquid crystalline behaviour has been elaborately studied in rigid-rod polymers such as polyaramides and poly(γ-benzyl-L-glutamate)[1]. The formation of mesophases in these systems is a direct consequence of the molecular asymmetry of the molecules as there is a limit to the number of rod-like chains that can be accommodated in a random arrangement in solution[2]. Rheology measurements on lyotropic solutions of rod-like polymers[3] have revealed a peculiar shear-thinning behaviour[4]. This behaviour is characterised by a three region flow behaviour as depicted in figure 5.1: shear-thinning at low shear rates (region I), a plateau of approximately constant shear-thinning with increasing shear rate (region II) and an additional region of shear-thinning at high shear rates (region III). The three region behaviour

has been explained by a polydomain structure of the liquid crystal. In moving from region I to region II, the liquid crystal evolves from a piled polydomain to a dispersed polydomain. In region III, the texture has finally evolved in a monodomain.
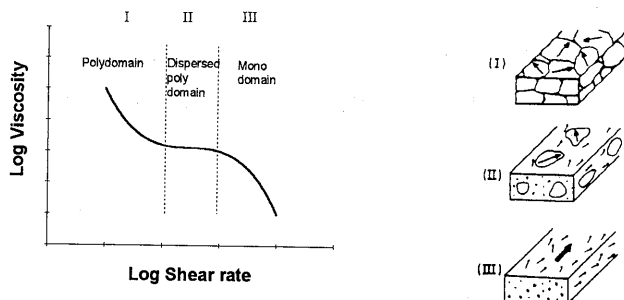

Figure 5.1: Three region flow behaviour as observed in lyotropic liquid crystals

In contrast with the well-studied lyotropic liquid crystalline behaviour of rod-like molecules, lyotropic liquid crystalline behaviour in disc-shaped molecules is not frequently observed[5,6]. Even more limited is the number of disc-shaped molecules exhibiting both thermotropic and lyotropic liquid crystalline behaviour[7]. This is a consequence of the limited stability of columnar phases to support the formation of lyotropic columnar mesophases. Enhanced π–stacking interactions arising from extended cores, strong phase separation of the core from the solvent[8], intermolecular H-bonding[9] or metal-ligand interactions[10] can, however, overcome the stability problem (figure 5.2) and encourage the formation of columnar phases.
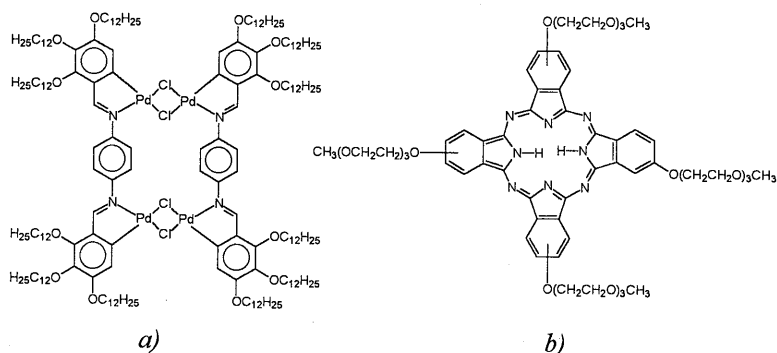

Figure 5.2: Examples of disc-shaped molecules exhibiting both thermotropic and lyotropic mesomorphism a) Pd-complexes by Usel'tseva et al.[5b] b) phthalocyanines provided with hydrophilic chains by Painter et al.[6d]

When the columnar aggregates only possess partial orientational order, they have been designated as nematic columnar mesophases (N_C). In more concentrated solutions, mostly a hexagonal packing of these columnar aggregates has been observed called a D_h phase. In figure 5.3 both the N_C and the D_{ho} phase are represented.

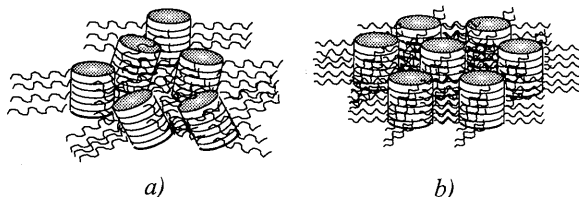*a)*   *b)*

Figure 5.3: Lyotropic mesophases a) lyotropic N_C phase: the columnar stacking of discs is retained and only partial orientational ordering of the columns is present b) lyotropic D_{ho} phase: the solvent increases the distance between the columns

In Chapter 4, we have introduced a new class of disc-shaped C_3-symmetrical compounds **1a,b** (figure 5.4). These compounds have an extended aromatic core giving rise to strong π-stacking interactions and additionally intermolecular H-bonding may stabilise the columnar structure. As a result, compounds **1a,b** might sustain lyotropic mesomorphism. Furthermore, the molecular characteristics of compounds **1a,b** (C_3-symmetry, amide bonds, long alkoxy chains) resemble those discussed for the C_3-symmetrical molecular gelators[11] in Chapter 1. The possible presence of intermolecular H-bonding[12] in the columnar stacks of compounds **1a,b** together with π-stacking interactions[13] between the discs, makes them promising candidates to function as a molecular gelator.

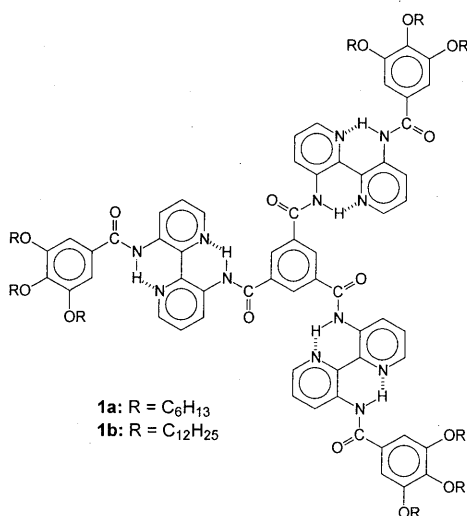
1a: R = C_6H_{13}
1b: R = $C_{12}H_{25}$

*Figure 5.4: Disc-shaped compounds **1a,b***

In this chapter, we will focus on the characterisation of the highly viscous solutions when compounds **1a,b** are treated with alkane solvents. The lyotropic mesomorphism in the birefringent solutions will be addressed. Furthermore, the visco-elastic behaviour of the viscous solutions will be evaluated. Finally, preliminary results of the response of the columnar mesophases to an applied electrical field are discussed.

5.2 Characterisation of the lyotropic liquid crystalline mesophases in compounds 1a,b

Compounds **1a,b** give rise to viscous solutions when dissolved in alkane solvents such as hexane, cyclohexane and dodecane starting from concentrations of approximately 1 mg/ml[14]. The solution becomes birefringent starting from approximately 5% w/w of compound **1a** in dodecane. Although aggregation is also observed in aromatic organic solvents (toluene-*d8*, *o*-dichlorobenzene-*d4*) as evidenced by ^{1}H-NMR, no unusual viscosity behaviour was perceived in these solvents. Chapter 6 will concentrate on this aggregation behaviour in more detail. In long chain alcohols (citronellol) and bromides (citronellyl bromide), compounds **1a,b** do not dissolve at room temperature.

5.2.1 *Polarisation microscopy and DSC*

A detailed description of the preparation of the lyotropic solutions and the analysis of the composition is given in the experimental section. Solutions of compound **1a** in dodecane were prepared in concentrations between 5–55% w/w and the clearing temperatures of the birefringent solutions were determined with polarisation microscopy. To analyse whether the transition into the isotropic state was depending only on the aromatic core, also birefringent solutions based on **1b** were studied. DSC scans were taken for some of the solutions and they confirmed the transition temperatures observed with polarisation microscopy. However, the transitions in the DSC scans were very broad and difficult to distinguish. Table 5.1 summarises the transitions into the isotropic state (T_{cl}) as determined with polarisation microscopy and the results are visualised in figures 5.5.a and 5.5.b.

Table 5.1   *Composition of the solutions of **1a,b** in dodecane and the corresponding clearing temperatures*

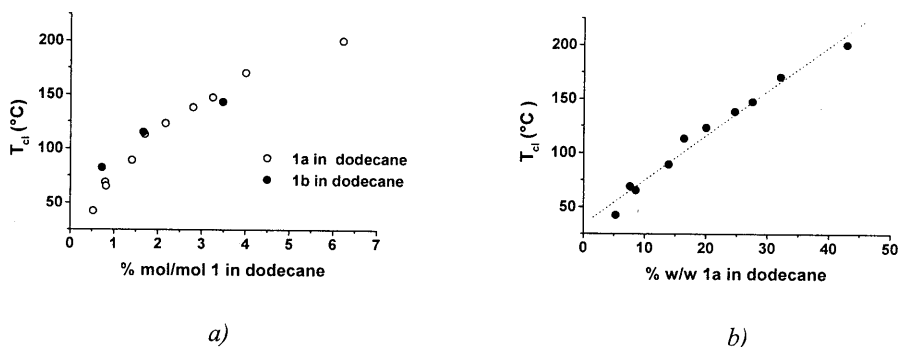| Compound 1a in dodecane			Compound 1b in dodecane		
%w/w	%mol/mol	T_{cl}(°C)	%w/w	%mol/mol	T_{cl}(°C)
5.3	0.53	42	10.2	0.72	82
7.6	0.80	68.5	21.0	1.66	115
8.54	0.82	65	36.3	3.48	143
13.9	1.41	89			
16.4	1.70	113			
20.0	2.17	123			
24.6	2.80	138			
27.5	3.25	147			
32.0	4.01	170			
42.8	5.06	200			

*Figure 5.5: Dependence of the clearing temperatures on the composition of the samples a) expressed in mol% compound **1a/1b** in moles dodecane b) linear relation between T_{cl} and the weight fraction of **1a** in dodecane, the line is a guide to the eye*

Lyotropic mesomorphism is observed starting from approximately 5% w/w solutions and is, as a result, present in a wide concentration range. The temperature range in which the mesophase is displayed is rather broad: a 25% w/w (= 2.8% mol/mol) solution of compound **1a** shows a transition into the isotropic state at a temperature as high as 138°C. When this clearing temperature is compared to, for example, the Pd-complex discussed in figure 5.2.a[5b] —in which $T_{cl} \approx 60$°C for a 30% w/w (~ 2.6% mol/mol) solution in pentadecane— it may be concluded that the lyotropic mesophases in solutions of **1a** in dodecane are indeed stable over a broad temperature range. This stability may find its origin in the strong π–stacking interactions between the discs as a result of the extended aromatic core, together with a strong phase separation of the aromatic core with respect to the solvent used. Furthermore, intermolecular H-bonding —which might be present according to the DSC results discussed in Chapter 4— may lead to an additional stabilisation of the columnar structure.

The results shown in figure 5.5.a demonstrate that the clearing temperatures of the lyotropic solutions based on compounds **1a** and **1b** are similar when based on the molar ratios between compound and solvent. Therefore, one can conclude that the transition into the isotropic state is determined by the aromatic core. Furthermore, the relationship between the amount of **1a** in dodecane —expressed in %w/w— and the clearing temperature T_{cl} seems to be linear (figure 5.5.b).

Textures could be grown by slowly cooling isotropic samples of **1** in dodecane between glass slides. For 5–13.9% w/w samples the presence of threaded textures and a low viscosity at higher temperatures might point to the presence of a nematic phase. In this case, this suggests a nematic packing of the columns (see figure 5.3). Samples ranging from 17 to 25% w/w also showed threaded textures just beneath T_{cl}. Although no changes in the textures were observed upon heating the sample, changes did occur upon cooling from the isotropic state. Growing textures for the more concentrated samples (> 30% w/w) was difficult due to evaporation of dodecane. A more precise assignment of the mesophase present can be accomplished by X-ray diffraction.

5.2.2 *X-Ray diffraction measurements*

The characterisation of the mesophase formed in the lyotropic liquid crystalline state was further investigated with X-ray diffraction. All measurements were performed on solutions of compound **1a** in dodecane. The samples were prepared by flow alignment of the viscous solutions into a capillary. Only the 55% w/w solution, which was highly viscous, was prepared by shear/pressing on a Be-surface.

Figure 5.6 shows the diffraction pattern obtained for the 15.7% w/w solution of **1a** in dodecane. A spontaneous orientation —induced by the flow of the sample into the capillary— is clearly discerned. The orientation of the columns is parallel to the flow direction as can be deduced from the orientation of both two splitting reflections. This orientation was quite stable and endured for time periods of several hours. In the wide angle area, a sharp reflection at 3.5 Å and a broad reflection at 4.7 Å are present. The former can be attributed to the disc–disc distance while the latter results from the disorder of the aliphatic chains and the solvent. In the small angle area, only a broad reflection is found. Higher order reflections in the small angle area have not been discerned unequivocally. The inter-disc reflection has a perpendicular orientation with respect to the broad reflection arising from the inter-columnar distance. This indicates that a columnar packing of the discs as present in neat compound **1a** is retained.
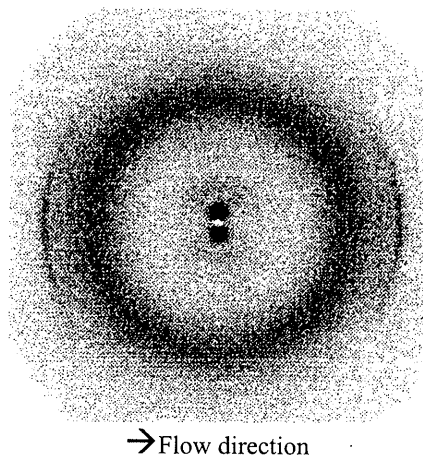
→ Flow direction

Figure 5.6: Diffraction pattern of 15.7% w/w 1a in dodecane

A more detailed investigation was performed on the dependence of the inter-disc and inter-columnar distances on the amount of dodecane present. Similarly, spontaneously oriented diffraction patterns as depicted in figure 5.6 were found for all 7.6% to 28% w/w solutions measured. Only the 6.7% w/w solution did not show an oriented diffraction pattern. Figure 5.7.a shows the inter-disc distance as a function of the amount of dodecane present in the solutions that can be derived from the diffraction patterns. The inter-disc distance approaches 3.4 Å in all samples, except for the 6.7% solution in which this reflection was not present. In the small angle area, only one broad reflection can be discerned for all samples. Because of the broadness, it was impossible to make a correct attribution of the peak maximum. The diffraction patterns in the solutions between 7.6 and 28% w/w are identical to the one discussed for the 15.7% w/w solution. Therefore, the mesophases are likely to be similar.

The temperature dependence of this mesophase has been investigated by measuring the X-ray diffraction patterns at different temperatures. For this purpose, the 20% w/w solution of **1a** in dodecane was used. The form of the diffraction pattern as well as the orientation of the columns is retained up to 100°C, then the orientation vanishes. The inter-disc reflection remains visible (although diminishing in intensity) up to 120°C. At 140 °C de sample has become isotropic, which is in accordance with the polarisation microscopy results. After cooling, the orientation of the columns has disappeared. The dependence of the inter-disc distance on the temperature is presented in figure 5.7.b. No evidence was found for another mesophase at higher temperature during the heating scan.
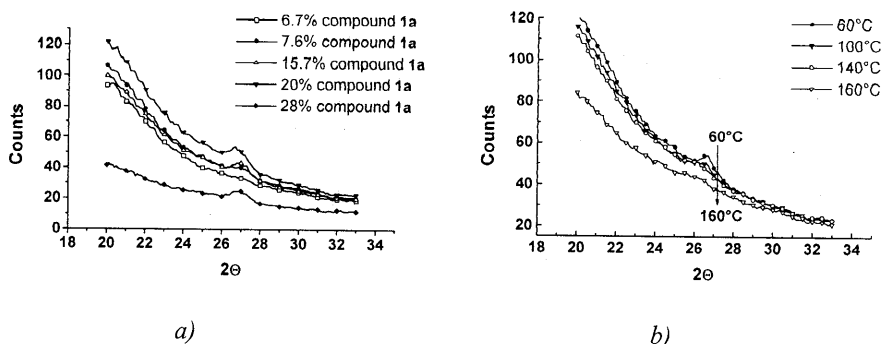
a)   b)

Figure 5.7: Dependence of inter-disc distance a) on the amount of dodecane at 25°C and b) on the temperature (20% w/w solution)

An oriented sample was also present for the 55% w/w solution which was prepared on Be. The diffraction pattern for the sample differed completely from the patterns described for 7.6–28% w/w samples. Now, the diffraction pattern resembled the pattern found for neat **1b**. Figure 5.8 shows an integrated intensity plot of the 55% w/w solution of **1a** in dodecane. In the wide angle area, two sharp two splitting reflections at 3.4 and 3.7 Å together with a broad non-oriented halo ring at 4.7 Å are present. The reflection at 3.4 Å is attributed to the inter-disc distance while the broad halo is resulting from the disorder of the alkyl chains. The reflection at 3.7 Å was also found in neat **1b**, but the origin of this reflection could not be rationalised. In the small angle area, two reflections can be discerned: a first order reflection at 38.4 Å and a higher order reflection at 17.6 Å. From the first order reflection, an inter-columnar distance of 44 Å can be calculated The higher order reflection shows the characteristic quadruplet splitting pattern, which was also found in case of pure compound **1b**. The sharpness of the reflection at 38.4 Å and the similarity between the diffraction patterns of neat compound **1b** and the 55% w/w solution suggest that the mesophases are similar.
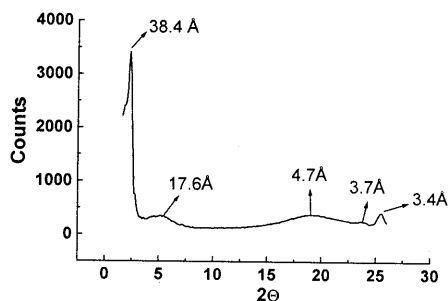

*Figure 5.8: Integrated plot of the diffraction pattern obtained from a 55% w/w solution of **1a** in dodecane*

The textures obtained from the birefringent solutions below 28% w/w, point to the existence of an N_C phase. X-Ray diffraction results show the broadness of the small angle reflection and the sharp inter-disc reflection at 3.4 Å. This might confirm that to this mesophase an N_C phase can be assigned. More dilute solutions (< 7.6% w/w) did not give an inter-disc reflection. This can either be due to the lack of orientation in the sample —which leads to weaker reflections— or because of another type of mesophase. However, also in this case the textures point to a nematic packing of the columns. The 55% w/w sample, on the other hand, shows sharp reflections in the small angle area and a sharp inter-disc reflection. The similarity between this diffraction pattern and that of pure **1b**, together with the sharp reflection in the small angle area indicates that a D_{ho} phase is retained. An inter-columnar distance of 44 Å is present. When compared to the inter-columnar distance of 30 Å found for pure compound **1a**, this illustrates that indeed the dodecane is separating the columns from each other. Furthermore, the inter-columnar distances in neat compound **1b** and its C_{18} homologue were found at 38 and 46 Å, respectively. A calculation reveals that in a 55% w/w sample, approximately 9.2 molecules of dodecane are available for each molecule **1a**. Interestingly, the inter-columnar distance of **1a**, 55% w/w in dodecane, matches the inter-columnar distance of the neat C_{18} homologue[15].

5.2.3 NMR spectroscopy

NMR spectroscopy was performed on a 1% w/w solution of **1a** in octane-*d18* to have an indication of the temperature effect on the columnar packing of the molecules. ^{1}H-NMR spectra were recorded between 20 and 110°C. Up to 110°C, no peaks could be discerned, indicating that strong aggregation remains until at least 110°C. ^{13}C-NMR spectra, also recorded between 20 and 110°C, did not feature any aromatic signals in this temperature window. Therefore, it may be concluded that compound **1a** can not be molecularly dissolved in an alkane solvent at or below 110°C (at this concentration) and that the tendency for molecules **1a** to remain stacked in columns is very strong.

5.3   Visco-elastic behaviour of compound 1a in dodecane

We have performed preliminary investigations of the visco-elastic properties of isotropic as well as anisotropic solutions of compound **1a** in dodecane by means of rheology measurements. For this purpose, a 1.2% w/w and a 5.3% w/w solution (T_{cl} = 42°C) were prepared. Rheology measurements were performed with a cone-on-plate geometry, more detailed information is given in the experimental part.

Figure 5.9 summarises the steady shear viscosity as a function of shear rate for the isotropic sample and for the anisotropic sample under (25°C) and above (65°C) T_{cl}. The viscosity of the solutions, $\eta \approx 10$ and $\eta \approx 0.3$ Pa.s for the anisotropic and the isotropic samples at room temperature, respectively, is very high compared to the viscosity of neat dodecane ($\eta = 1.35 \times 10^{-3}$ Pa.s). Such enormous increases in viscosity —a factor ~220 for the isotropic and a factor ~7400 for the anisotropic sample— upon the addition of only a small amount of a compound may point to a "gelation" of the solvent[11c]. The isotropic sample shows shear-thinning behaviour starting from a shear rate of 10 s^{-1}. The shear-thinning behaviour in the anisotropic sample, on the other hand, starts earlier, around 0.15 s^{-1}. In the latter case, some resemblance seems present with the three region flow behaviour discussed in case of lyotropic liquid crystalline polymers. Above the T_{cl}, a "normal" shear-thinning behaviour, as observed for the isotropic sample, is resumed.
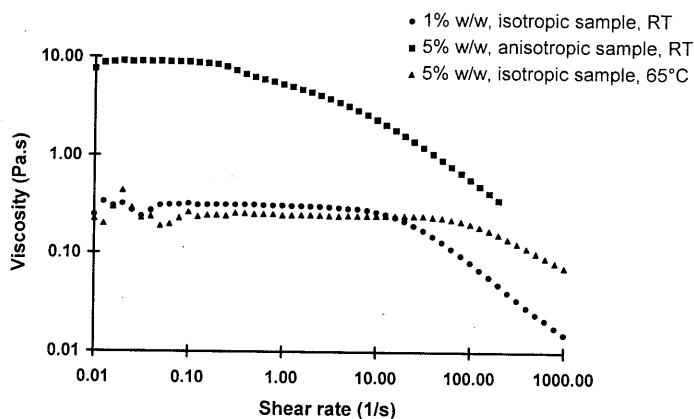

Figure 5.9: Steady shear viscosity as a function of shear rate for a 1% w/w and 5% w/w sample

The shear-thinning behaviour in the isotropic solutions of compound **1a** indeed suggests the presence of visco-elastic properties. This behaviour may be rationalised by several explanations. Firstly, the columnar stacks may be so long that a molecular weight is reached above which entanglements of the polymer chains —in this case the columnar stack— are present. Shear-thinning behaviour can then be rationalised in terms of breaking up entanglements between the polymer chains. In fact, when the association constant of 10^8 l/mol—which will be derived in Chapter 6— is taken into consideration, it can be estimated that one stack in the 1% w/w sample consists of approximately 700 molecules. Secondly, it may be considered that the columnar stacks formed by molecules **1a**, behave analogously to rigid-rod polymers. The sharp increase in viscosity and visco-elastic behaviour can then be explained by the large volume occupied by a random arrangement of one "polymer chain". In the anisotropic sample, some resemblance with the three region flow behaviour discussed for

LCP's may be discerned. It is reasonable to assume that in a fresh, birefringent sample, a polydomain structure will be present (region I). At low shear rates, the liquid crystal features shear-thinning behaviour. At increasing rate, the viscosity seems to level off and the polydomain is transferred in a dispersed polydomain (region II). At higher shear rates, shear-thinning is resumed (region III). Thirdly, there is a striking resemblance between the molecular characteristics of compounds **1** and those of the C_3-symmetrical molecular gelators[11] discussed in Chapter 1. It may therefore be assumed that the columnar stacks of **1a** in dodecane build up fiber-like structures with van der Waals contacts between the long alkoxy chains connecting different fibers. This may lead to the formation of a network. Shear-thinning may now be explained by breaking up the network and, possibly, the columnar structure leading to a loss in viscosity.

However, it must be emphasised, that these rheology experiments are preliminary and definite conclusions of the behaviour of these systems can only be drawn when more detailed measurements will be conducted. Presumably, sophisticated measurements such as rheology in combination with SAXS or SANS could give more detailed information about the structural features of these viscous solutions. The combination of these techniques has been used in other systems with notable results[16].

5.4 *Applications of the lyotropic liquid crystalline solutions*

During X-ray diffraction measurements, we observed that the birefringent solutions could be oriented in a planar alignment by uniaxial rubbing on Be or by flow alignment in a capillary. This prompted us to investigate the feasibility of switching between different orientations of the columns using an external electrical field.

5.4.1 *Abbe refractometer results*

The Abbe refractometer was used to determine the orientation of thermotropic and lyotropic liquid crystalline phase of compounds **1** on a glass surface. For neat compound **1b**, two refractive indices could be clearly distinguished which is indicative for a planar orientation of the columns, in which the columnar axis is parallel to the glass plate, with respect to the surface.

Two birefringent solutions of compound **1a** in dodecane were investigated. The 7.6% w/w as well as the 20% w/w solution showed two refractive indices at room temperature. Again, this indicates that a planar orientation is present. Heating the 7.6% w/w solution, led to the disappearance of the birefringence around 60°C (figure 5.10.a). This coincides with the

transition into the isotropic state as shown with polarisation microscopy. The 20% w/w solution (T_{cl} = 123°C) did not show such a disappearance between 25 and 85°C, but only a linear decrease of both refractive indices (figure 5.10.b).

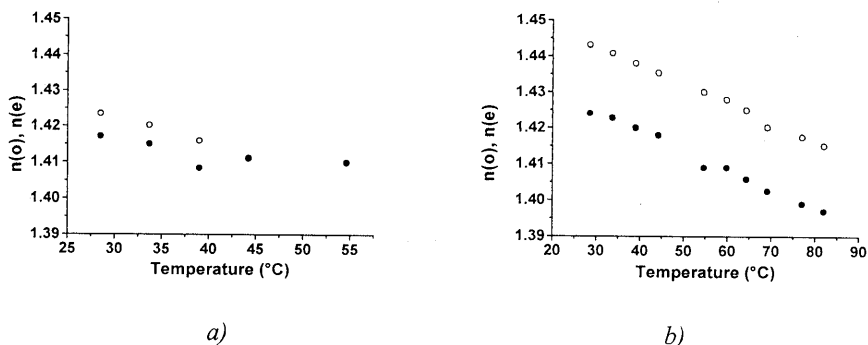a)   b)

Figure 5.10: Abbe refractometer results as a function of temperature of a) a 7.6% w/w sample in dodecane b) 20% w/w sample in dodecane

The optical properties of the birefringent solutions are further investigated in the forthcoming section.

5.4.2 Switching of the columns in the lyotropic mesophase

As it became clear that lyotropic solutions of compound **1a** preferentially adopt a planar alignment on a glass surface, we investigated the possibility of switching the columns to a homeotropic alignment by means of an electrical field. In order to induce a uniaxial, planar orientation, a lyotropic solution was sheared between electron conducting indium-tinoxide (ITO) coated glass plates. The distance between the glass plates was kept constant using spacers (glass fibers or polymer film).

A polarisation microscope provided with a photo-multiplier was used to follow the response of the columns oriented in a planar orientation on an electrical field. As a homeotropically aligned sample is not birefringent between crossed polarisers, the transmitted intensity of the light is expected to decrease upon switching the orientation of the sample. Preliminary experiments with a 20% w/w solution and a distance between the ITO coated glass plates of 7 μm, showed that switching only occurred when a direct current (DC) voltage was used. The threshold voltage for switching was found to be 10 V. Upon application of a DC voltage of 10 V, the expected decrease in time of the transmission of light was indeed observed.

The influence of the voltage applied over the cell as well as the temperature of the sample on the speed of the switching process have been investigated. First, the transmission of light was

measured as a function of various DC voltages (30–70 V) applied over a uniaxial, planar oriented sample. The results are summarised in figure 5.11.a. It is obvious that the switching process is faster when higher voltages are applied. Apparently, this is not a linear process. Secondly, the influence of the temperature on the speed of switching was investigated in a more concentrated sample (32% w/w, figure 5.11.b). The switching process becomes faster with increasing temperature. This may be explained by the reduction in the viscosity of the sample with increasing temperatures, which facilitates a reorientation of the columns. Unfortunately, when the DC voltage is switched off, the planar alignment is only retaken after applying some pressure on the sample.
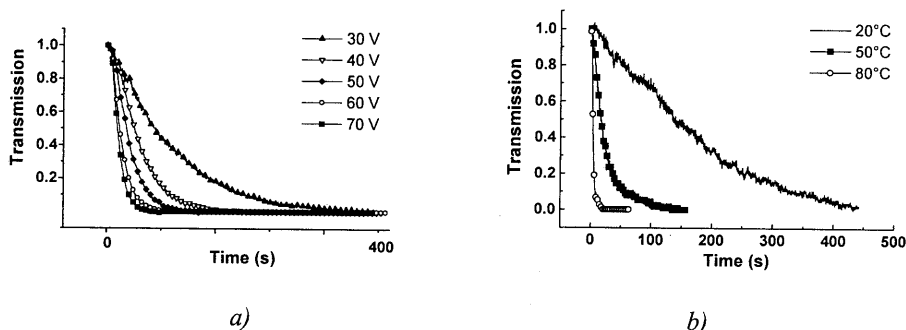

a)   b)

*Figure 5.11:Dependence of the switching process on a) the DC voltage applied over a cell with a 20% w/w solution of **1a** in dodecane, 7μm spacer b) the temperature of a 32% w/w solution of **1a** in dodecane, 6 μm spacer, V≈15 V*

UV-VIS measurements were performed in order to confirm the orientation induced by applying an electrical field over the sample,. A large difference is expected between the absorption of light in a homeotropically oriented sample and a planar oriented sample. This is schematically shown in figure 5.12. In the case of a planar orientation the interaction of the plane polarised light with the π-conjugated system will depend on the polarisation direction with respect to the columnar axis. In situation *A,* the polarisation direction and the columnar axis are parallel. Therefore, the interaction of the plane polarised light with the π-conjugated system is not very large and as a result the absorption will be low. In situation *B* on the other hand, the polarisation direction and the columnar axis are perpendicular. A large interaction of plane polarised light with the π-conjugated system can be expected and therefore a large absorption will result. In a homeotropically aligned sample —as depicted in situation *C*— the absorption will not be influenced by the direction of polarisation and will be approximately comparable to situation *B*.
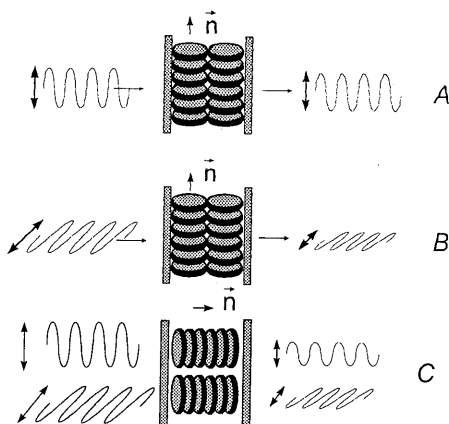
Figure 5.12: Different situations of the orientation of plane polarised light with respect to the columnar axis. Situation A: parallel orientation of the direction of plane polarised light to the columnar axis. Situation B: perpendicular orientation of the direction of plane polarised light to the columnar axis. Situation C: homeotropically oriented sample

Figure 5.13.a shows the differences in absorption of plane polarised light when planar oriented rods of **1a** in dodecane (20% w/w) are placed between glass plates. As expected, the absorption is substantially lower when the direction of polarisation is parallel to the columnar axis (situation *A*) than when the direction of polarisation is perpendicular to the columnar axis (situation *B*). Subsequently, a cell was prepared in situation *A* and a DC voltage of 28 V was applied over the cell. Figure 5.13.b shows the evolution of the absorption as a function of time. Immediately after turning on the DC voltage, the absorption increases. Already after 30 s, a clear difference between the absorption of a planar aligned sample and a partially reoriented sample can be distinguished. Finally, after approximately 5 min the absorption does not increase further and the homeotropic alignment (situation *C*) has been attained.

a)   *b)*
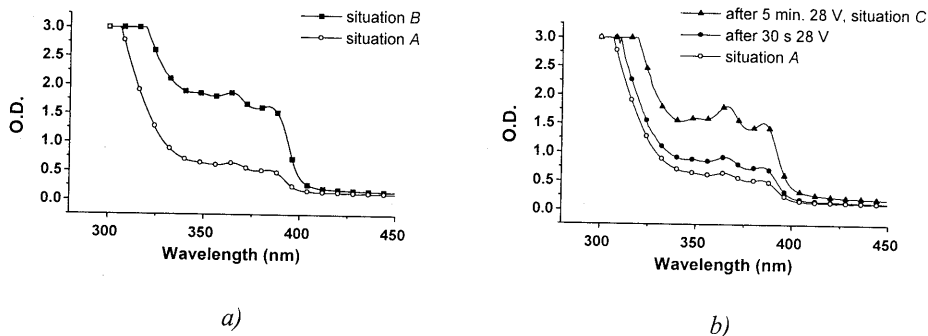
Figure 5.13: a) Differences in absorption between the direction of polarisation parallel to the columnar axis (situation A) and the direction of polarisation perpendicular to the columnar axis (situation B), the cell had a thickness of 6 μm and was filled with a 20% w/w sample; b) the absorption as a function of time when a DC of 28 V was applied over a sample with orientation A

From the results shown in figure 5.13.a, an anisotropy value (A_B/A_A) can be derived of 2.89 and 3.09 at λ_{max} of 364 nm and 383 nm, respectively. These values are rather low when compared to values usually found in thermotropic nematic liquid crystals. Apart from the quality of the alignment, this can be further rationalised by the fact that compound **1a** possesses C_3-symmetry. Additionally, a deviation of the transition moment of the bipyridine chromophore from the plane of the disc may be present. Furthermore, although these columns can be oriented mechanically on a glass surface, an extra interaction with the surface to obtain a homogeneous, planar alignment is probably useful. Maybe this can also result in a spontaneous relaxation to a planar alignment when the DC voltage is turned off.

5.5 Conclusions

Lyotropic mesomorphism is observed when compounds **1a,b** are dissolved in alkane solvents. In birefringent solutions of **1a** with concentrations varying between 7.6% w/w and 28% w/w in dodecane, all evidence points to the presence of an N_C phase. Concentrated samples, such as the 55% w/w sample, on the other hand, show that the hexagonal packing of the columns —as observed in the neat compound— as well as the helical superstructure within the columns are retained. A D_{ho} phase can thus be assigned. This lyotropic mesomorphism originates from strong π–stacking interactions between the large discs, a strong phase separation of the aromatic core with respect to the solvent and presumably intermolecular H-bonding within the columns. As a result, compound **1** is one of the few disc-shaped compounds that exhibit both lyotropic and thermotropic mesomorphism.

In the isotropic state, all evidence is in agreement with a preservation of the columnar structure. Preliminary results show that anisotropic as well as isotropic solutions of **1a** in dodecane show shear-thinning behaviour. Unfortunately, the exact origin of the shear-thinning behaviour has not been elucidated yet. However, the similarity in structure and properties of our system with the recently studied C_3-symmetrical molecular gelators might indicate that the shear-thinning behaviour is the result of a breaking down of a network structure.

Upon mechanical orientation of the birefringent solutions between glass plates, the lyotropic solutions adopt a uniaxial, planar orientation. Polarisation microscopic studies as well as UV measurements confirm that when a DC electrical field is applied over the cell, the columns can be switched into a homeotropic alignment. This switching process is accelerated when higher temperatures and higher DC voltages are used. Unfortunately, the planar orientation is only retaken when some pressure is applied over the sample. Nevertheless, this ability to induce the formation of large monodomains simply by applying an electrical field might be

very interesting when applications —such a 1D charge transport of ions[17] or electrons— are considered.

5.6 Experimental procedures

For a general section concerning NMR spectroscopy, polarisation microscopy, DSC measurements and X-ray diffraction techniques: see Chapters 2 and 4. The synthesis and characterisation of compounds **1a,b** has been described in Chapter 4. Lyotropic solutions of compound **1a** were prepared by dissolving an amount of **1a** in $CHCl_3$. An appropriate amount of dodecane was added and the $CHCl_3$ was removed using a rotary evaporator ($T_{bath} < 50°C$). ^{1}H-NMR spectroscopy was used to verify the absence of $CHCl_3$ and to measure the exact composition of the solutions. The composition was derived from the integration of the OCH_2 proton signals attached to the benzoyl group and all CH_2 proton signals belonging to the alkoxy chains and the dodecane. Samples for polarisation microscopy were prepared by putting a sample between 2 glasses. The X-ray diffraction measurements were performed on aligned samples. Alignment was brought about either by shear/pressing on Be or by drawing the lyotropic solution in a capillary. Rheology measurements were performed on a Rheometrics RFSII with a cone-on-plate geometry (diameter = 5 cm, gap = 0.046 mm). The temperature was controlled in all measurements. Between each steady state measurement, the cone and the plate were removed from each other and the sample was left for approximately 5 min. to attain a random starting situation. All measurements were recorded in triplo, the differences between different measurements were negligible. The refractive index measurements were carried out using an Abbe refractometer which could be thermostated up to 100°C. Cells were prepared using electron conducting ITO coated glass plates. To ensure a constant distance between the plates, a spacer of 6–7 μm was used which consisted of glass fibers or a polymer film. The switching of the columns was followed by placing the cell between crossed polarisers. To obtain a maximum transmission the cell was placed in a position between the polarisers so that the orientation of the rods had an angle of 45° with respect to the polarisers. A DC current was needed to observe a change in orientation. The transmitted light intensity was followed as a function of time by coupling the polarising microscope to a photomultiplier. The temperature was controlled by a Mettler hot stage. UV spectroscopy was carried out using a Philips PU 8740 spectrometer. All UV spectra were recorded using a plane polarised light beam.

5.7 References and notes

[1]   a) Baer, E.; Moet, A. *High Performance Polymers*, Carl Hanser Verlag, München, **1991**. b) Kwolek, S.L.; Sorenson, W.R. *U.S. Patent* **1962**, 3063966. c) Kwolek, S.L.; Morgan, P.W.; Schaefgen, J.R.; Gulrich, L.W. *Macromolecules* **1977**, *10*, 1390. d) Blair, T.I.; Morgan, P.W.; Killian, F.L. *Macromolecules* **1977**, *10*, 1396. e) Robinson, C. *Trans. Faraday Soc.* **1954**, *52*, 571. f) Robinson, C. *Tetrahedron Lett.* **1961**, *13*, 219.

[2]   *Encyclopedia of Polymer Science and Engineering*, *Vol. 9*, John Wiley and Sons, New York, **1987**, 1–57.

[3]   a) Onogi, S; Asada, T. *Rheology*, *Vol. I*, (Eds. Astarita G.; Marucci, G.; Nicolais, L.), Plenum, New York, **1980**, b) Wissbrun, K.F. *J. Rheol.* **1981**, *25*, 619.

[4]   Visco-elasticity indicates the simultaneous existence of viscous and elastic properties in a material. Common liquids, water for example, show pure Newtonian behaviour when a deformation is applied. This is expressed by a complete absence of an elastic component. As a consequence, the viscosity is independent of the shear rate. Polymers, on the other hand, exhibit also an elastic component which accounts for the properties so desired in polymers. In

the vast majority of cases, the viscosity in polymers is found to decrease with increasing shear rate, giving rise to what is generally called "shear-thinning" behaviour. For an introduction into this topic *see*: Barnes, H.A.; Hutton, J.F.; Walters, K. *An Introduction to Rheology*, Elsevier Science Publishers B.V., Amsterdam, **1989**.

[5]   Disc-shaped molecules showing lyotropic mesomorphism in apolar solvents: a) Kohne, B.; Praefcke, K.; Derz, T.; Hoffmann, T.; Schwander, B. *Chimia* **1986**, *40*, 171. b) Usel'tseva, N.; Praefcke, K.; Singer, D.; Gündogan, B. *Liq. Cryst.* **1994**, *16*, 601.

[6]   Disc-shaped molecules showing lyotropic mesomorphism in water a) Keller-Griffith, R.; Ringsdorf, H.; Vierengel, A. *Colloid & Polymer Sci.* **1986**, *264*, 924. b) Boden, N.; Bushby, R.J.; Hardy, C.; Sixl, F. *Chem. Phys. Lett.* **1986**, *123*, 359. c) Zimmermann, H.; Poupko, R.; Luz, Z.; Billard, J. *Liq. Cryst.* **1989**, *6*, 151. d) Mckeown, N.B.; Painter, J. *J. Mater. Chem.* **1994**, *4*, 1153.

[7]   Thermotropic as well as lyotropic mesomorphism has been described for disc-shaped compounds presented in references 1b and 2c,d.

[8]   *See for example*: references 2a–d

[9]   *See for example*: a) Bauer, S. PhD thesis, Johannes Guteberg Universtity of Mainz, Germany, **1994**, 74-80. b) reference 1a.

[10]   *See for an example*: reference 1b.

[11]   a) Yasuda, Y.; Takebe, Y.; Fukumoto, M.; Inada, H.; Shirota, Y. *Adv. Mater.* **1996**, *8*, 740. b) Yasuda, Y.; Iishi, E.; Inada, H.; Shirota, Y. *Chem. Lett.* **1996**, 575. c) Hanabusa, K.; Koto, C.; Kimura, M.; Shirai, H.; Kakehi, A. *Chem. Lett.* **1997**, 429. d) Zhang, S.; Zhang, D.; Liebeskind, L.S. *J. Org. Chem.* **1997**, *62*, 2312.

[12]   For intermolecular H-bonding contributing to gel formation: *see:* a) Hanabusa, K.; Tange, J.; Tagushi, Y.; Koyama, T.; Shirai, H. *J. Chem. Soc., Chem. Commun.* **1993**, 390. b) Keller, U.; Müllen, K.; De Feyter, S.; De Schryver, F.C. *Adv. Mater.* **1996**, *8*, 490. c) Jokic, M.; Makarevic, J.; Zinic, M. *J. Chem. Soc., Chem. Commun.* **1995**, 1723. d) Jeong, S.W.; Murata, K.; Shinkai, S. *Supramolecular Sci.* **1996**, *3*, 83. e) Hanabusa, K.; Miki, T.; Tagushi, Y.; Koyama, T.; Shirai, H. *J. Chem. Soc., Chem. Commun.* **1993**, 1382. f) Hanabusa, K.; Yamada, M.; Kimura, M.; Shirai, H. *Angew. Chem.* **1996**, *108*, 2086.

[13]   For π-stacking interactions contributing to gel formation: *see:* a) Lin, Y.; Kachar, B.; Weiss, R.G. *J. Am. Chem. Soc.* **1989**, *111*, 5542. b) Brotin, T.; Untermöhlen, R.; Fages, F.; Bouas-Laurent, H.; Desvergne, J.-P. *J. Chem. Soc., Chem. Commun.* **1991**, 416. c) Snijder, C.S.; de Jong, J.C.; Mettsma, A.; van Bolhuis, F.; Feringa, B.L. *Chem. Eur. J.* **1995**, *1*, 594. d) Placin, F.; Colomés, M.; Desvergne, J.-P. *Tetrahedron Lett.* **1997**, *38*, 2665.

[14]   The apparent viscosity of **1a** in cyclohexane is lower than in hexane and related alkane solvents. A detailed investigation of the viscosity as a function of solvent has not yet been conducted.

[15]   A formula has been derived (Seitz, M. PhD thesis, Johannes Guteberg Universtity of Mainz, Germany, **1996**) to calculate the inter-columnar distance in a hexagonally packed lyotropic system starting from the inter-columnar distance of the pure compound and the amount of solvent added. Application of this formula in our case leads to a calculated inter-columnar distance of 41 Å, which is slightly lower than the experimental value (44 Å). This may be rationalised by some evaporation of dodecane during the measurements and integration errors to determine the composition of the sample from the ^{1}H-NMR spectra.

[16]   a) Grizutti, N.; Moldenaers, P.; Mewis, J. *Rheol. Acta* **1993**, *32*, 218. b) Odell, J.A.; Ungar, G.; Feijoo, J.L. *J. Pol. Sci., B, Polym. Phys.* **1993**, *31*, 141. c) Walker, L.M.; Wagner, N. *J. Rheol.* **1994**, *38*, 1525. d) Dammer, C.; Maldivi, P.; Terech, P.; Guenet, J.-M. *Langmuir*, **1995**, *11*, 1500. e) Walker, L.M.; Wagner, N.; Larson, R.G.; Mirau, P.A.; Moldenaers, P. *J. Rheol.* **1995**, *39*, 925. f) Prud'homme, R.K.; Wu, G.; Schneider, D.K. *Langmuir* **1996**, *12*,

4651. g) Montalvo, G.; Valiente, M.; Rodenas, E. *Langmuir* **1996**, *12*, 5202. h) Ugaz, V.M.; Cinader Jr., D.K.; Burghardt, W.R. *Macromolecules* **1997**, *30*, 1527.

[17]   Preliminary experiments have revealed that when the alkoxy chains in compounds **1** are replaced by oligoethylene glycol chains, relatively high ion-conductivities are measured upon mixing these compounds with Li salts. *See:* Brunsveld, L. *Disc-like liquid crystals: aggregation and ion-conductivity*, Under-graduation Report, T.U. Eindhoven, The Netherlands, **1997**.

Chapter 6

Aggregation behaviour of extended-core disc-shaped compounds: a UV and CD spectroscopic study

Abstract

The aggregation behaviour of three disc-shaped compounds 1–3 —all pre-organised by intramolecular H-bonding— has been studied by means of UV and CD spectroscopy. All compounds show a strong tendency to aggregate in columnar stacks when dissolved in alkanes. Compounds 2 and 3 also strongly aggregate in more polar solvents such as chloroform and o-dichlorobenzene. CD measurements revealed the tendency of the columnar stacks built up by molecules 1a,b in alkane solvents to be chiral. One handedness of the stack could be favoured by attaching chiral peripheral side-chains as in 1a or by using a chiral alkane solvent. The "Sergeants-and-Soldiers" principle was found to be applicable to this system. From a theoretical treatment of the experimental results it could be deduced that the organisation within the aggregates consists of at least 80 molecules with an association constant between the molecules of approximately 10^8 l/mol.

6.1 Introduction

Extensive studies to understand the underlying principles of chirality in stiff helical polymers have led to unique observations referred to as "Majority Rule" and the "Sergeants-and-Soldiers" principle[1]. It has been shown that poly(*n*-alkylisocyanates) adopt an extended helical conformation in which long stretches of one handedness —referred to as the cooperative length L_c— are separated by high-energy reversals. When small portions of external chirality are added, cooperative effects strongly favour one helical sense. This external chirality can arise from the use of a chiral solvent[1f] or even the replacement of one hydrogen by a deuterium as in poly[*(R)*-1-deuterio-*n*-hexyl-isocyanate][1d].

Recently, it has been shown that these effects are operative in several polymers with stiff helical backbones[2]. Also in polymers such as polythiophene and poly(*p*-phenylenevinylene) which do not have a stiff helical backbone, chiral —presumably helical— packing has been observed in the aggregated polymer[3]. In all systems studied so far, circular dichroism (CD) spectroscopy has proved to be an indispensable tool.

In low molecular weight compounds helical stacking of molecules has been observed as well, the most famous examples being cholesteric liquid crystals[4]. In nematic liquid crystals, the induction of chirality is complex but predominantly linear or additive[5]: the more chiral molecule is added to a nematic liquid crystal the shorter the helical pitch of the induced cholesteric phase will be. A number of low molecular weight substances such as folic acid salts[6], cholesteryl derivatives[7] and others[8] show helical stacking of the molecules in solution. However, to our knowledge, neither the "Majority Rule" principle —in which a slight excess of one enantiomer leads to a strong preference of the helical sense preferred by the major enantiomer— nor the "Sergeants-and-Soldiers" principle —in which only a few chiral units (the sergeants) control the movements of large numbers of cooperative achiral units (the soldiers)— have been studied in these low molecular weight systems.

As disc-shaped compounds **1a** (chiral) and **1b** (achiral) (figure 6.1) have been found to stack helically in the thermotropic liquid crystalline state (Chapter 4) and to form columnar stacks in alkane solutions (Chapter 5), a detailed investigation of the aggregation behaviour of these molecules is presented here. Chiral compound **1a** is decorated with 9 chiral C_{10} alkoxy chains while compound **1b** is an achiral C_6 alkoxy chain analogue. For comparison, extended disc-shaped achiral molecules **2** and **3**[9] and a number of reference compounds were included in the study. In disc-shaped compound **2**, 6 methoxy groups have been added to the central aromatic core at the 5 and 5' positions of the bipyridine units. Replacement of the diamino-bipyridine units by 2,5-bis(2-aminophenyl)-pyrazine units —which are planarised by intramolecular H-bonds as well— has led to compound **3**. As reference compounds, compound **4** —precursor for the synthesis of compound **1**— and linear analogue **5** of compound **1** have been selected (figure 6.1).
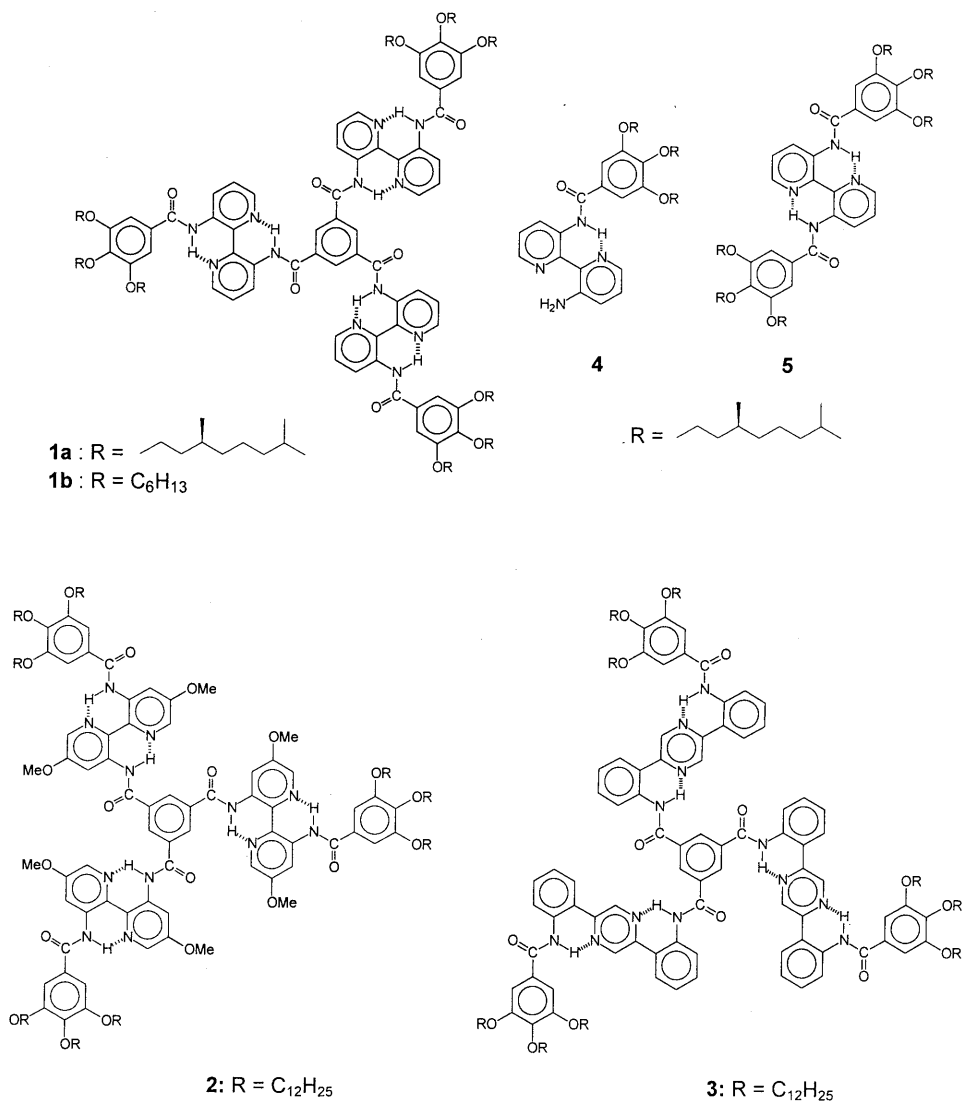
1a : R = (branched alkyl chain)
1b : R = C_6H_{13}

4

5

R = (branched alkyl chain)

2: R = $C_{12}H_{25}$

3: R = $C_{12}H_{25}$

Figure 6.1: Disc-shaped compounds 1–3, precursor 4 and reference compound 5

6.2 Spectroscopic studies

6.2.1 UV spectroscopy

The UV spectra of the mono- and diacylated bipyridine-diamines **4** and **5** were recorded in hexane and CHCl$_3$ and compared to that of disc-shaped derivative **1a**. The relevant data are summarised in table 6.1 and the corresponding spectra are depicted in figure 6.2.

Table 6.1 *Relevant UV data of compounds 1–5*

	1a		4		5		2		3	
	λ_{max}	ε	λ_{max}	ε	λ_{max}	ε	λ_{max}	ε	λ_{max}	ε
hexane	364	3.2×10^4	364	1.4×10^4	352	1.3×10^4	/	/	/	/
	384	2.3×10^4								
dodecane	364	3.2×10^4	/	/	/	/	/	/	393	5×10^4
	384	2.3×10^4								
CHCl$_3$	351	5.4×10^4	363	1.3×10^4	348	1.5×10^4	~350[a]	/	388	3.8×10^4
ODCB	357	5.2×10^4	/	/	/	/	~365[a]	/	391	3.3×10^4

[λ] = nm; [ε] = l/mol.cm. ODCB = o-dichlorobenzene. [a] As the OMe groups influence the shape of the UV spectra in compound 2, these λ$_{max}$ values (present as a shoulder in the spectra) are merely an approximation

For monoacylated compound **4**, the values of λ_{max} at 364 nm and 363 in hexane and CHCl$_3$, respectively, are comparable and are attributed to the π–π* transition of the bipyridine. Also for diacylated compound **5**, only minor differences have been observed in the π–π* transition of the bipyridine at λ_{max} of 352 and 348 nm in hexane and CHCl$_3$, respectively. The spectra of disc-shaped compound **1a** and its diacylated reference compound **5** are similar in shape in CHCl$_3$ and comparable values of λ_{max} have been found. In hexane, on the contrary, there is a substantial difference in the shape and λ_{max} values of the spectra of **1a** and **5**. This becomes more obvious when we focus on the effect of the solvent on the UV spectra of compounds **1a** and **1b** (figure 6.3). In CHCl$_3$, λ_{max} amounts to 351 nm, whereas in dodecane[#] a significant red shift of 13 nm is observed for λ_{max} to 364 nm. Furthermore, a shoulder in the CHCl$_3$-spectrum, has developed into a peak at 384 nm in dodecane. The spectrum of **1a** in dodecane resembles the UV spectrum of a sheared film of neat **1a** which is in a D$_{ho}$ phase at room temperature (figure 6.3). Heating the solution in dodecane to 100°C (figure 6.3), leads to a blue shift of the λ_{max} to 357 nm and the disappearance of the fine structure.

[#] Dodecane and hexane give identical spectra and extinction coefficients, however, for variable temperature measurements dodecane is more suitable
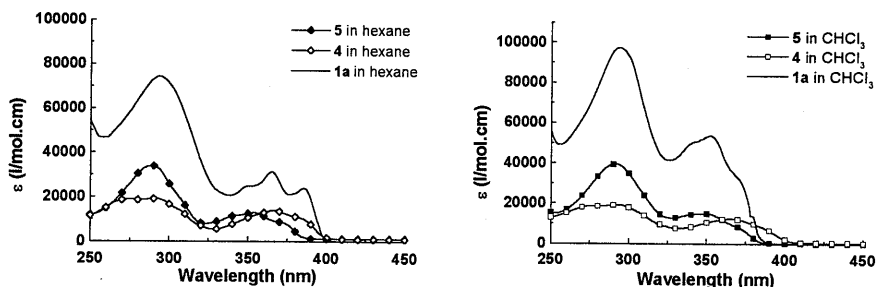
Figure 6.2: UV spectra of compounds 1a, 4 and 5 in CHCl₃ and hexane

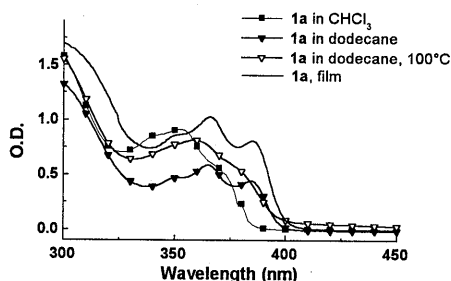*Figure 6.3: UV spectra of compound 1a in CHCl₃ (c = 1.7x10⁻⁵ mol/l, l = 1 cm), in dodecane (c = 1.8x10⁻⁵, l = 1 cm) and as a solid sheared film*

The UV results found for **1a,b** imply that these compounds are molecularly dissolved in CHCl₃ at room temperature (and in dodecane at 100°C), while in dodecane (and related alkane solvents) the packing of the molecules in columns, as present in the thermo- and lyotropic liquid crystalline state, is retained up to very low concentrations (~10^{-6} mol/l). Compared to the well studied hexakis(*n*-alkoxytriphenylenes) where aggregation starts at concentrations of 10^{-3} mol/l in alkane solvents[10], compounds **1a,b** start aggregating at astonishingly low concentrations. This can be explained by the larger aromatic core and the stronger tendency to phase separate. The model compounds **4** and **5,** on the other hand, are molecularly dissolved in both chloroform and hexane at 10^{-5} mol/l.

In contrast to compounds **1a,b,** ¹H-NMR results show that compounds **2,3** are also in an aggregated state at room temperature in polar solvents such as CDCl₃ and ODCB-*d4* (see also Chapter 4). This has been concluded from the broad signals in ¹H-NMR at room temperature for compounds **2** and **3** in CDCl₃ and ODCB-*d4*. As discussed in Chapter 4, compound **2** can be molecularly dissolved in 1,1,2,2-tetrachloroethane at 110°C. Also for compound **3** sharp peaks have been obtained at 110°C in 1,1,2,2-tetrachloroethane.

The UV spectra at room temperature in various solvents of compound **2**, bearing six additional methoxy substituents compared to **1**, are depicted in figure 6.4.a. The shape of the UV spectra of compound **2** in CHCl$_3$ and hexane differs substantially from the shape of the spectra of compound **1** in these solvents. This may be attributed to the effect of the methoxy group on the bipyridine ring. However, this has not been investigated in more detail. In CHCl$_3$, the shoulder around 350 nm may correspond to λ_{max} of the bipyridine transition. In dodecane and ODCB, this shoulder is shifted towards higher wavelengths, indicating aggregation of the molecules. No significant shift in λ_{max} of the bipyridine transition is found when compound **2** is heated in dodecane. In ODCB, however, the onset of the shoulder around 350 nm at room temperature develops into a peak at 349 nm at 90°C (figure 6.4.b).
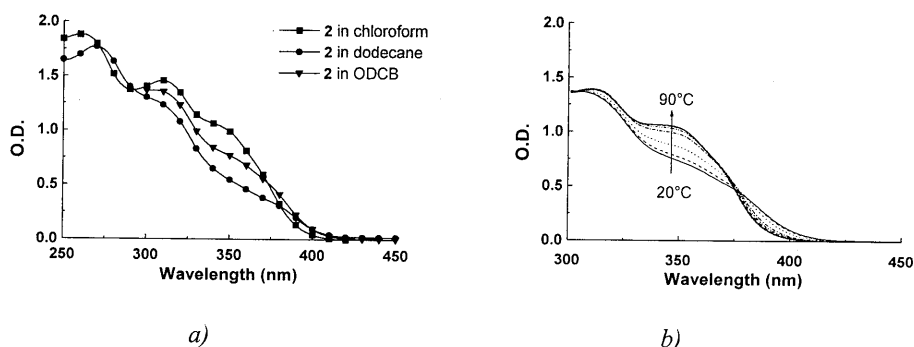

Figure 6.4: a) UV spectra of compound 2 in various solvents; b) variable temperature UV spectra of compound 2 in ODCB

For compound **3**, λ_{max} is found at comparable wavelengths in dodecane and ODCB, 393 nm and 391 nm, respectively (figure 6.5.a). No change in the dodecane spectrum can be observed upon heating of the solution from 20 to 100°C. However, a considerable shift in λ_{max} from 391 nm at 20°C to 380 nm at 90°C and an isosbestic point at λ = 390 nm are found when a solution of compound **3** in ODCB is heated (figure 6.5.b).
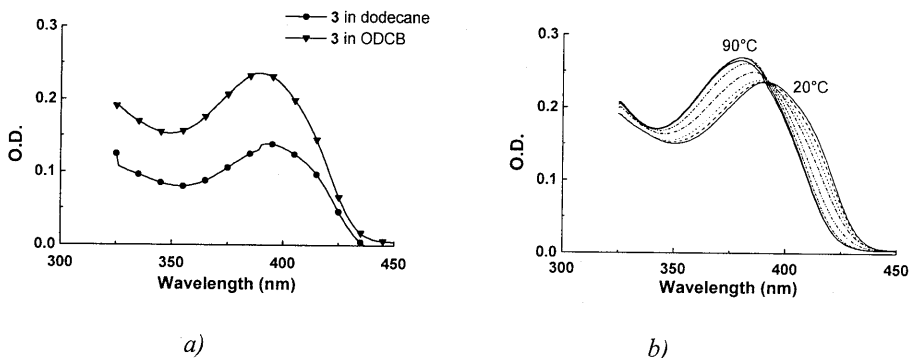

Figure 6.5: a) UV spectra of compound 3 in various solvents; b) variable temperature UV spectra of compound 3 in ODCB

From these combined ^{1}H-NMR (Chapter 4) and UV results it is obvious that for compounds **2** and **3** aggregation is also observed in CHCl₃ and ODCB at room temperature. The aggregation can be cancelled by heating up the solutions in ODCB but not in dodecane. This suggests that the tendency to aggregate is much stronger for compounds **2** and **3** than for compounds **1a,b**. For compound **3** this can be rationalised by the significantly larger aromatic core, leading to stronger π-stacking interactions. For compound **2**, this explanation is not satisfactory. However, it has been shown in triphenylene derivatives that replacing one alkoxy chain by an alkanoyloxy chain results in a dramatic stabilisation of the D_{ho} phase[11]. This has tentatively been explained by the out of plane position of the C=O, which causes an entanglement between the discs, thus stabilising the columnar structure. A similar effect might be presumed by replacing a hydrogen at the bipyridine by a methoxy group, as is the case in compound **2**.

6.2.2 CD spectroscopy

The aggregation behaviour of compounds **1–3** was studied in more detail using CD spectroscopy. The CD spectra of chiral reference compounds **4** and **5** were recorded in hexane as well as in CHCl₃, but no Cotton effects were found in the bipyridine transition. CD spectra of compound **1a** recorded in CHCl₃ did not show a significant Cotton effect as well. In dodecane, however, compound **1a** featured a negative Cotton effect for the π–π* absorption band of the bipyridine moiety at λ = 387 (Δε = –35.6 l/mol.cm) and 369 nm (Δε = –23.6 l/mol.cm) with chiral anisotropy factors g[12] of –1.5x10⁻³ and –7.4x10⁻⁴, respectively (figure 6.6).

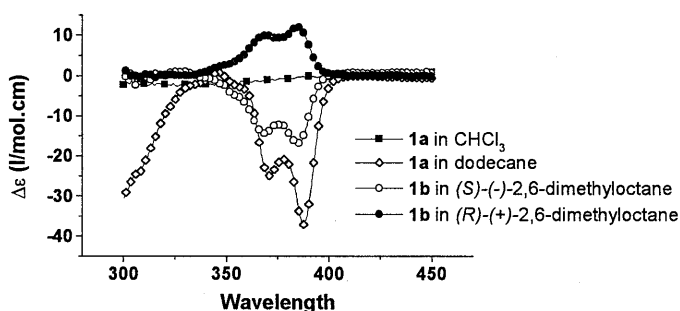*Figure 6.6: CD spectra of compound **1a** recorded in CHCl₃ (c = 1.7x10⁻⁵ mol/l, l = 1 cm), compound **1a** in dodecane (c =1.8x10⁻⁵ mol/l, l = 1 cm), compound **1b** in (R)-(–)-2,6-dimethyloctane (c = 1.9x10⁻⁴ mol/l, l = 1 mm) and compound **1b** in (S)-(+)-2,6-dimethyloctane (c = 3.4x10⁻⁴ mol/l, l = 1 mm)*

The Cotton effects observed in the solution of **1a** in dodecane are relatively small when compared to the Cotton effects found in *e.g.* chiral polythiophenes, where values of *g* as high as 2x10^{-2} have been found for the π–π* transition[3b]. On the other hand, the Δε observed in this system is 10 to 100 times higher than the values found in chiral bipyridines (see Chapter 2, Δε ≈ 2 l/mol.cm), chiral aggregates of folic acids (Δε ≈ 2 l/mol.cm)[6] and CT complexes of hexakis(*n*-alkoxy-triphenylenes) and *(–)*-menthol-dinitrobenzoate (Δε ≈ –0.18 l/mol.cm)[8]. From this comparison it is obvious that in case of compound **1a**, the chirality of the side chain can be transferred quite efficiently to the central core.

Heating the solution of compound **1a** in dodecane caused a gradual decrease of the Cotton effect which vanished at 100°C. However, upon cooling the Cotton effect was immediately restored. The temperature dependence of the Cotton effect at λ = 387 nm has been investigated for different concentrations of **1a** in dodecane and is summarised in figure 6.7. At low temperatures, all curves seem to converge to one point. These results, together with variable temperature UV experiments of compound **1a** in dodecane point to the breaking down of columnar aggregates at higher temperatures. This is a concentration dependent process as for the lowest concentration (10^{-6} mol/l) the CD effect disappears more rapidly than for the higher concentration (10^{-4} mol/l) (figure 6.7). In a ^{1}H-NMR experiment with a 4x10^{-3} mol/l solution of **1b** in octane-*d18,* no peaks were discerned up to 110°C, suggesting that at these higher concentrations, the molecules remain aggregated up to relatively high temperatures (110°C). The convergence into one point as observed in figure 6.7 might be an indication for the existence of fairly long aggregates below a certain temperature. However, a halledecisive conclusion can only be drawn when experiments can be conducted at still lower temperatures and in a wider concentration range.
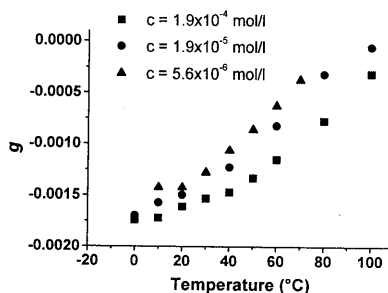

Figure 6.7: Temperature dependence of the Cotton effect, expressed as the anisotropy factor g

Previous results on chiral solvation[1f] prompted us to investigate whether in this case chirality can also be transferred from the solvent to the bipyridine moiety. Therefore, *(R)-(–)-2,6-*

dimethyloctane and *(S)-(+)-*2,6-dimethyloctane were synthesised by catalytic hydrogenation of α- and β-citronellyl bromide. The UV spectra of achiral compound **1b** in both enantiomers of 2,6-dimethyloctane are identical to the spectra of chiral compound **1a** in dodecane. The CD spectra of achiral **1b** in *(R)-(–)-*2,6-dimethyloctane and *(S)-(+)-*2,6-dimethyloctane show the expected mirror-image relationship (figure 6.6). The anisotropy factors *g*, however, are somewhat lower (-8.5×10^{-4} and $+5.7 \times 10^{-4}$ at $\lambda = 386$ nm, respectively, and -5.3×10^{-4} and $+3.5 \times 10^{-4}$ at $\lambda = 367$ nm, respectively) than in the corresponding chiral **1a** in dodecane. Again, heating the samples led to a decrease of the Cotton effects, vanishing around 100°C.

Transfer of chirality from the solvent to the bipyridine moiety is less efficient than the transfer of chirality from the chiral side chain, as is evidenced by the smaller *g* values of the former. Nonetheless, the efficiency of transferring the chirality from the solvent to the achiral stack seems to be better than in case of the achiral polyisocyanates studied by Green *et al*[11]. They observed effects between 0.5 and 2 mdeg while in our case the Cotton effect in *(S)-(+)-*2,6-dimethyloctane amounts to –15 mdeg. An honest comparison is not possible in this case as the reference neither gives the optical path length nor an exact molar concentration. However, the concentration by weight used is relatively large, so we may assume that the effects in polyisocyanates are relatively small.

The results on chiral solvation indicate strong cooperative effects, suggesting a tendency of the stack to be chiral. Therefore, we attempted to apply the "Sergeants-and-Soldiers" experiment on mixtures of chiral compound **1a** with its achiral analogue **1b** in hexane. As expected, compound **1b** did not show any Cotton effect in hexane (figure 6.8.a). However, upon addition of only 1.25% of chiral compound **1a** to the achiral solution of **1b** in hexane, a Cotton effect was immediately generated. Already at 2.5% chiral compound added, the Cotton effect in the bipyridine transition was similar in magnitude as for pure **1a** in hexane. Remarkably, starting from pure chiral **1a** the Cotton effect even increases with increasing amount of achiral compound until a maximum is reached (when approximately 75% achiral compound **1b** is added), then it diminishes again (figure 6.8.b).
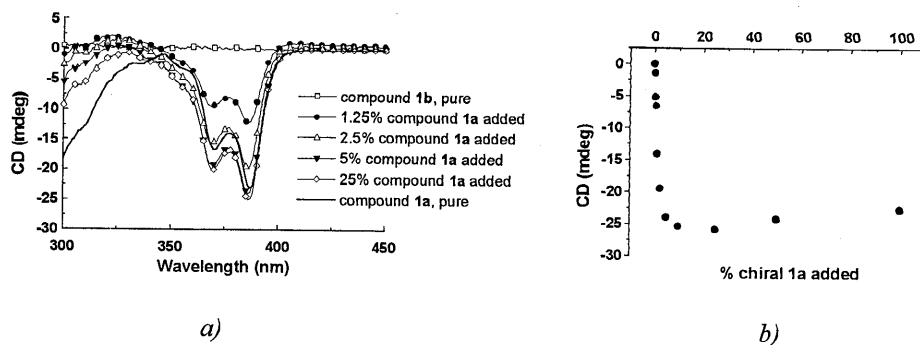
a)

b)

*Figure 6.8: Amplification of chirality: a) mixing hexane solutions of compound **1a** (c = 1.9x10^{-5} mol/l) and compound **1b** (c = 1.9x10^{-5} mol/l) b) the non-linear relationship between the Cotton effect and the amount of chiral compound added to a solution of achiral **1b** in hexane*

The mixing experiment was repeated with solutions of different concentrations of compounds **1a,b** in hexane. The dependence of the *g* values on the amount of chiral compound **1a** added to a solution of the achiral compound **1b** is summarised in figure 6.9[13]. The curves show the same trends, although the effect is smaller for the lowest concentration (1.9x10^{-6} mol/l). We also found that the Cotton effects in the bipyridine transition are relatively independent from the concentration of pure compound **1a** in hexane within the range of 10^{-6} to 10^{-3} mol/l although a slight deviation at the low concentration end can be discerned (figure 6.9, inset).
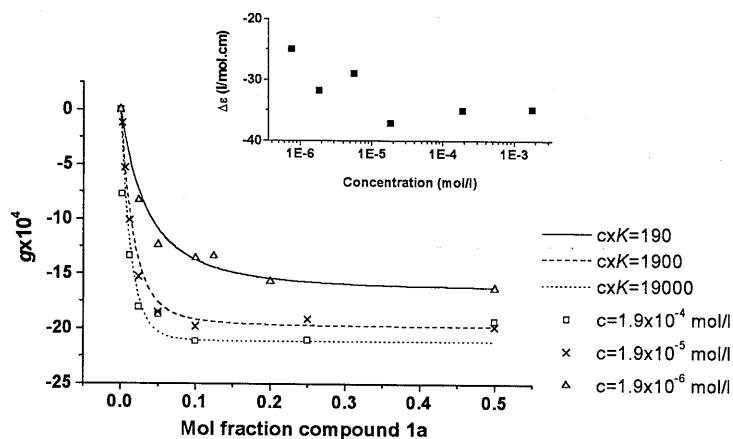

*Figure 6.9: Anisotropy value g as a function of the amount of compound **1a** added to the achiral solution of **1b** in hexane in 1 mm (□), 1 cm (x) and 10 cm (△) cells; the fitted lines represent the theoretically predicted development of g as a function of the mol fraction of chiral compound **1a** present in the mixture in which an association constant K of ±10^{8} mol/l and a cooperative length of 81 gave the optimal fit; the inset gives the molar ellipticity Δε at λ = 387 nm as a function of the concentration of **1a** in hexane*

In the "Sergeants-and-Soldiers" experiment, unexpectedly, the Cotton effects increase with increasing amount of achiral compound **1b** in the hexane solution in the concentration range of 0–75%. This is tentatively explained by a more efficient packing between achiral molecules **1b** the chiral molecules **1a**, as in the former no branching methyl group is present at the C–3 position. Additional evidence can be offered by evaluating 10^{-3} mol/l solutions of **1a,b** in hexane: the solution of compound **1a** shows a substantial lower viscosity, indicating less efficient packing.

When compounds **2** and **3** are dissolved in *(R)-(–)-2,6-dimethyloctane*, surprisingly, no Cotton effects have been found in the π–$\pi*$ transitions. On the other hand, the X-ray diffraction patterns of neat compounds **2** and **3** do not show —in contrast to compounds **1**— the characteristic four splitting diffraction peak, which has been assigned to a helical superstructure within the columns (Chapter 4). Apparently, there is a connection between the thermotropic liquid crystalline phase and the aggregation behaviour of compounds **1–3**. Presumably, a delicate equilibrium exists between the freedom of the wedges in the disc-shaped compounds and the strength of the secondary interactions between the discs in the columns. This may be decisive for the discs to be able to attain a chiral conformation within the columns and, as a result, determine the transfer of the chirality from the solvent to the molecule[14].

6.2.3 Theoretical approach of the "Sergeants-and-Soldiers" experiment

To interpret the experimental results presented in figure 6.8 more quantitatively, E. Havinga developed a theoretical model to fit the data. In this model, the association constant K between the discs and the cooperative length L_c can be varied. We assume that in solution various lengths of stacks are present. Then, the following equilibrium is operational:

$$M_1 + M_{i-1} \Leftrightarrow M_i \quad i = 2,.... \infty$$
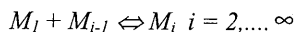
With equilibrium constants

$$\frac{[M_i]}{[M_1][M_{i-1}]} = K_i$$

The simplest assumption is that all equilibrium constants are equal or $K_i = K$

Then, by putting $K[M_1] = a$

one gets for the concentration of a stack consisting of i discs $K[M_i] = a^i$

If the starting concentration of monomeric discs is c, $c = \sum_{i=1}^{\infty} i[M_i]$

which leads to the relation
$$cK = \sum_{i=1}^{\infty} ia^i = \sum_{i=1}^{\infty}\sum_{j=i}^{\infty} a^j = \frac{a}{(1-a)^2}$$

then, solving this equation for a gives[15]
$$a = 1 + \frac{1 - \sqrt{1 + 4Kc}}{2Kc}$$

The Cotton effect in the $\pi-\pi*$ absorption band of stacks consisting of i molecules is approximated as follows. The contribution to the Cotton effect in the bipyridine transition of a stack is proportional to the number of monomeric units in the stack and remaining non-associated species do not contribute to the Cotton effect. Furthermore, the association constant K of chiral and achiral monomers is equal and if a stack contains a chiral monomer, the latter will induce chirality in other molecules in the stack. We denote the starting concentration of monomeric units by c, as before, and the relative concentration of chiral monomeric unit by x, leaving $q = 1-x$ as the relative concentration of non-chiral monomeric unit. For mixed stacks in equilibrium we can then deduce the following equation:

$$\frac{g}{g_0} = \frac{\sum_{n=2}^{\infty}[M_n]n(1-q^n)}{\sum_{n=2}^{\infty}[M_n]n}$$

In which q is the chance that a monomer is non-chiral and q^n is the chance that a combination of n monomeric units, i.e. the n-mer has no chiral element at all. Hence $(1-q^n)$ is the chance that the n-mer has at least 1 chiral element, which stacks according to our assumption in a completely chiral stack. Furthermore, g is the anisotropy factor for a mixture with a mol fraction x of chiral **1a** in a solution of **1b**, g_0 is the anisotropy factor for the solution of pure **1a**[16].

However, a probably more realistic approximation is that the chiral monomer will induce chirality to other molecules in a stack which are not further remote than say s places. Then, the equation becomes:

$$\frac{g}{g_0} = \frac{\sum_{n=2}^{\infty}[M_n]n(1-q^n) + \sum_{n=s+1}^{2s}[M_n](n - \sum_{i=1}^{n/2}2q^{s+i}) + \sum_{n=2s+1}^{\infty}[M_n](n - \sum_{i=1}^{s}2q^{i+s} - \sum_{i=s+1}^{n-s}q^{2s+1})}{\sum_{n=2}^{\infty}[M_n]n}$$

Evaluation gives:
$$\frac{g}{g_0} = 1 - \frac{(2-t)(\frac{t}{1-t})^2 - \frac{s(1-t)+1}{(1-t)^2}t^{s+1} + \frac{2(t^{s+1}-t^{2s+1})}{(1-a)(1-q)} + \frac{t^{2s+1}}{(1-a)^2} - \frac{2(qr)^{s+1}(1-r^s)}{(1-q)(1-r)}}{(2-a)(\frac{a}{1-a})^2}$$

in which $t = aq$ and $r = a\sqrt{q}$. A fit of this model to the experimental data (figure 6.9) leads to $K = 10^8$ l/mol and $s = 40$, which leads to a cooperative length $L_c = 2s+1$ of approximately 80 molecules.

6.2.4 A molecular model for the chiral aggregation of compounds 1

To explain the cooperative response of compounds **1** on external chiral information, the following hypothesis is proposed.

First, the Cotton effect in the π–$\pi*$ transition of the bipyridine moiety —observed for compound **1a** in dodecane (figure 6.6)— may result from a helical stacking of the bipyridine moieties[17], as the absence of a Cotton effect in CHCl$_3$ shows that the bipyridine moiety of an individual molecule is not affected intramolecularly by the chirality of the side chains. In case of achiral compound **1b**, this means that in hexane equal amounts of P and M helical columns will be present, so no Cotton effect can be observed. However, in case of the chiral compound **1a**, one of the helical senses will be favoured for sterical reasons (the 3-methyl attached to the chiral centre pointing preferentially in one direction), leading to a Cotton effect. Therefore, we assume that associates of C$_3$-symmetrical molecules of type **1** adopt a propeller conformation in which the bipyridine wedges are tilted with respect to the central trimesic core. In hexane, molecules **1** are aggregated in columnar stacks and the packing between subsequent molecules will be optimal when all bipyridine wedges are tilted in the same direction which results in a preferred stable chiral conformation of the disc-shaped molecule. This can be compared with propellers being piled on top of each other. Rotating the first with respect to the second will improve the packing but will also give rise to a helix. This is tentatively illustrated in a cartoon, figure 6.10. In such a conformation intermolecular H-bonds might stabilise the columnar stacks[18].
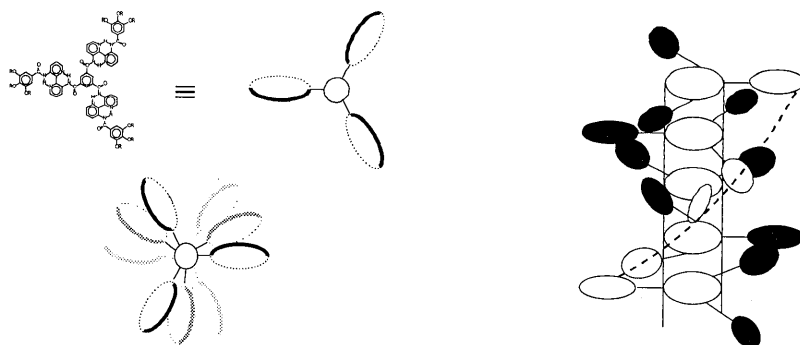
Figure 6.10: Cartoon representing the chiral stacks built up by compound 1 in alkane solvents; the degree of rotation of the molecules with respect to each other and the tilt angle of the wedges are arbitrary and have no physical meaning

Secondly, mixing hexane solutions of chiral **1a** and achiral **1b**, will lead to a random distribution of chiral and achiral molecules in one stack. The instantaneous observation of Cotton effects when small amounts of **1a** are added to **1b** points to dynamic processes and an exchange of the molecules between different stacks. The stack length is concentration dependent and corresponds to a $K_{ass} \approx 10^8$ l/mol, while the cooperative length of one helical sense between helical reversals is concentration independent and corresponds to an $L_c \approx 80$. By introducing on average one molecule of chiral **1a** per 80 molecules achiral **1b**, the chiral component (the sergeant) will dictate the helical sense of the total stack (the soldiers).

Thirdly, that also a chiral alkane solvent can dictate the sense of helicity of a stack of achiral molecules presumably means that the first layer of solvent organises itself along the peripheral alkoxy chains of the molecules. Again sterical reasons will dictate which helical sense will lead to the most favourable interactions between subsequent molecules. In fact, the *S* configuration of the alkoxy chain (derived from *(S)*-citronellol) corresponds to the *R* configuration of the alkane solvent; in both cases a negative Cotton effect is observed.

6.3 Conclusions

At low concentrations ($\sim 10^{-5}$ mol/l), disc-shaped compounds **1–3** show strong aggregation behaviour in alkane solvents. The aggregates are built up by stacking of the discs in columnar stacks. This is a result of the strong π–stacking interactions between the extended aromatic cores and the solubility of the alkoxy chains in alkane solvents. In addition, compounds **2** and

3 also show strong aggregation in more polar solvents such as chloroform and ODCB. This is tentatively explained by the presence of a larger aromatic core in compound **3** and a "clicking" together of the discs in compound **2** due to the methoxy groups that are located out-of-plane.

CD spectroscopy has allowed for a more detailed study of the columnar aggregates formed by compound **1** in alkane solvents, and has revealed a strong tendency of the stacks to be chiral. A model is proposed in which the discs adopt a chiral propeller conformation. In the propellers, the direction of the tilt is imposed by the chiral side chains or by the chiral alkane solvent. Piling up of these propellers leads to a columnar stack with a helical packing of the bipyridine sub-units. Mixing chiral and achiral molecules has revealed that the —for polymers with stiff helical backbones well-known— "Sergeants-and-Soldiers" principle is also applicable to the dynamic stacks of compound **1**. A theoretical model to fit the experimental results shows that the cooperative length in the stack corresponds to approximately 80 molecules and the association constant between the discs amounts to 10^8 l/mol.

6.4   Experimental procedures

General procedures
The synthesis of compounds **1, 2, 4** and **5** has been described in chapter 4. The synthesis of 2,5-bis(2-*t*-butoxycarbonylaminophenyl)-pyrazine has been described elsewhere[19]. A detailed description of the spectroscopic techniques used is given in Chapter 2. GC/MS measurements were performed on a Shimadzu GC/MS-QP5000.

(R)-(–)-2,6-Dimethyloctane
In a Parr apparatus *(S)-(+)*-citronellyl bromide (25.3 g, 115 mmol) was catalytically hydrogenated in the presence of MeOH (150 ml), K_2CO_3 (32 g) and 5% Pd/C (0.68 g). After 24 h, no more H_2 was taken up and the suspension was filtered over celite and washed with MeOH. The filtrate was poured into water and the upper organic layer was separated, dried with $MgSO_4$ filtered and concentrated to yield 7.75 g of mainly the alkene. This was hydrogenated again with 5% Pd/C (0.11 g) in MeOH (25 ml) until no more H_2 was consumed. The solution was poured into water and the upper organic layer was separated, dried with $MgSO_4$ and filtered to yield the title compound as a clear liquid (7.5 g, 46%). ^{13}C-NMR (CDCl$_3$): δ 39.4; 36.9; 34.5; 29.5; 28.0; 24.9; 22.7; 22.6; 19.2; 11.4. GLC-EI-MS: (M$^+$): 142; (M$^+$-CH$_3$): 127; (M$^+$-CH$_2$CH$_3$): 113; 85; 71; 57; 43; 29. $[\alpha]^{20}_D = -5.5°$ (neat)

(S)-(+)-2,6-Dimethyloctane
The same procedure was followed as for the *(R)*-enantiomer, but now with *(R)-(–)*-citronellyl bromide as the starting material. The *(S)-(+)*-2,6-dimethyloctane was obtained in a yield of 2.32 g (36%). $[\alpha]^{20}_D = +5.4°$ (neat). (lit. +6.3)[20]

Synthesis of compound 3

 # 2-(2-t-Butoxycarbonylaminophenyl)-5-(2-aminophenyl)-pyrazine (6)

A solution of 2,5-bis(2-*t*-butoxycarbonylaminophenyl)-pyrazine (0.43 g, 0.93 mmol) and trifluoroacetic acid (0.205 ml, 0.30 g, 2.66 mmol) in chloroform (3.5 ml) was stirred at room temperature for 24 h and subsequently stirred at 50°C for 12 h. The solution was cooled, diluted with chloroform and neutralised with a diluted sodium bicarbonate solution. The organic layer was then washed with a sat. $NaHCO_3$ solution (2x), water (1x), brine (1x) and dried over Na_2SO_4. Evaporation of the filtrate gave the crude product which consisted of 3 products: 2,5-bis(2-aminophenyl)-pyrazine (R_f =0.10; EtOAc/CHCl$_3$ 1/25), the title compound (R_f = 0.24; EtOAc/CHCl$_3$ 1/25) and the starting material (R_f = 0.39; EtOAc/CHCl$_3$ 1/25). Separation and purification of these products was accomplished by column chromatography (first: silica, EtOAc/CHCl$_3$ 1/25; second: EtOAc/CHCl$_3$ 6/94) and gave **6** (0.11 g, 30%) which was used without further purification. ^{1}H-NMR (CDCl$_3$) δ 10.55 (s, 1H, NHBoc); 8.99 (s, 1H, H-3 pyrazine); 8.92 (s, 1H, H-6 pyrazine); 8.33 (d, 1H, J = 8.3 Hz, H-3'); 7.65 (2xdd, 2H, H-6' and H-6''); 7.43 (td, 1H, J = 1.4 and 8.0 Hz, H-4'); 7.23 (td, 1H, J = 1.5 and 7.9 Hz, H-4''); 7.13 (td, 1H, J = 1.1 and 7.6 Hz, H-5'); 6.84 (d, 1H, J = 8.3 Hz, H-3''); 6.80 (t, 1H, J = 8.2 Hz, H-5''); 5.78 (s, 2H, NH$_2$); 1.52 (s, 9H, C(CH$_3$)$_3$).

 # 2-(2-t-Butoxycarbonylaminophenyl)-5-[2-(3,4,5-tridodecyloxybenzoylaminophenyl)]-pyrazine (7)

To an ice-cooled solution of **6** (0.11 g, 0.30 mmol) and TEA (0.06 ml, 0.3 mmol) in dry CH$_2$Cl$_2$ (3 ml), a solution of 3,4,5-tridodecyloxybenzoyl chloride (0.21 g, 0.30 mmol) in dry CH$_2$Cl$_2$ (2 ml) was added dropwise via a syringe. After addition, stirring at room temperature was continued for 16 h. Then, the solvents were evaporated *in vacuo* and the reaction mixture was purified by column chromatography (silica, THF/ CHCl$_3$ 4/96). The compound was further purified by dissolving it in CHCl$_3$ and adding MeOH until a precipitate appeared. Filtration over a P$_4$ filter yielded pure **7** (0.10g, 33%). M.p. 187°C. ^{1}H-NMR (CDCl$_3$): δ 12.29 (s, 1H, NH''); 10.50 (s, 1H, NH'); 9.13 (s, 1H, H-6 pyrazine); 8.96 (s, 1H, H-3 pyrazine); 8.78 (d, 1H, J = 8.0 Hz, H-3''); 8.37 (d, 1H, J = 8.6 Hz, H-3'); 7.85 (d, 1H, J = 7.9 Hz, H-6''); 7.64 (d, 1H, J = 7.9 Hz, H-6'); 7.56 (t, 1H, J = 7.9 Hz, H-4''); 7.47 (t, 1H, J = 7.9 Hz, 1H, H-4'); 7.28 (t, 1H, H-5''); 7.22 (s, 2H, *ortho*-H); 7.15 (t, 1H, J = 7.6 Hz, H-5'); 4.07 (t, 4H, *meta*-COCH$_2$); 4.03 (t, 2H, *para*-COCH$_2$); 1.84 (m, 6H, OCH$_2$CH$_2$); 1.52 (s, 9H, C(CH$_3$)$_3$); 1.47 (m, 6H, OCH$_2$CH$_2$CH$_2$); 1.26 (m, 48H, (CH$_2$)$_8$); 0.88 (t, 9H, CH$_3$). ^{13}C-NMR (CDCl$_3$): δ 165.4 (C=O''); 153.2 (C=O'). Aromatic carbons: 153.0; 151.2; 150.7; 141.6; 141.3; 140.4; 138.8; 138.5; 131.3; 130.1; 128.5; 123.8; 122.5-122.3 (3C); 121.7; 121.0; 106.2. Aliphatic carbons: 80.4 (C-*ipso*, Boc); 73.6; 69.5; 31.9; 30.4; 29.7; 29.7; 29.6; 29.4; 29.4; 28.3; 26.1; 22.7; 14.1. IR (KBr): ν = 3281 (N-H); 2917 (C=C-H); 2850 (C-H); 1715 (C=O); 1660 (C=O); 1584; 1532; 1439; 1334; 1164; 1112; 754.

 # 2-(2-Aminophenyl)-5-{2-(3,4,5-tridodecyloxybenzoylaminophenyl)}-pyrazine (8)

To a solution of **7** (0.10 g, 0.098 mol) in CH$_2$Cl$_2$ (3 ml), TFA (1.5 ml) was added and the solution was heated under reflux for 10 min. The organic layer was cooled, diluted with CH$_2$Cl$_2$, washed first with a diluted sodium bicarbonate solution and then with water (3x) and brine (1x). The organic layer was dried over Na$_2$SO$_4$ and then evaporated *in vacuo* to yield the title compound (0.088 g, 98%). The product was used without further purification. ^{1}H-NMR (CDCl$_3$): δ 12.37 (s, 1H, NH''); 9.01 (s, 1H, H-6 pyrazine); 8.94 (s, 1H, H-3 pyrazine); 8.78 (d, 1H, J = 8.4 Hz, H-3''); 7.77 (dd, 1H, J = 0.9 and 8.0 Hz, H-6''); 7.58 (dd, 1H, J = 0.8 and 7.9 Hz, H-6'); 7.51 (td, 1H, J = 1.0 and 7.9 Hz, H-4''); 7.22 (m, 4H, H-5''and H-4' and *ortho*-H); 6.78 (m, 2H, H-3' and H-5'); 5.60 (s, 2H, NH$_2$); 4.07 (t, 4H, *meta*-OCH$_2$); 4.03 (t, 2H, *para*-OCH$_2$); 1.84 (m, 6H, OCH$_2$CH$_2$); 1.47 (m, 6H, OCH$_2$CH$_2$CH$_2$); 1.26 (m, 48H, (CH$_2$)$_8$); 0.88 (t, 9H, CH$_3$). ^{13}C-NMR (CDCl$_3$): δ 165.4 (C=O). Aromatic carbons: 153.1; 152.2; 149.4; 147.4; 141.5; 141.3; 139.4; 138.4; 131.3; 130.9; 130.2; 128.3; 123.7; 122.7; 122.1; 117.6 (3C); 106.1. Aliphatic carbons: 73.5; 69.4; 31.9; 30.3; 29.7; 29.7; 29.6; 29.4; 29.4; 26.1; 22.7;

14.1. IR (KBr): $\nu = 3431$ (N-H); 3330 (N-H); 2920 (C=C-H); 2851 (C-H); 1654 (C=O); 1584; 1437; 1336; 1121; 748. UV (CHCl$_3$): $\lambda_{max} = 384$ nm.

 # N,N',N''-Tris{2[2(5[2{3,4,5-tridodecyloxybenzoylaminophenyl}] pyrazinyl)phenyl]}benzene-1,3,5-tricarbonamide (3)

A solution of **8** (0.088 g, 0.096 mmol), TEA (0.02 ml) and trimesic chloride (5.4 mg, 0.020 mmol) in dry CH$_2$Cl$_2$ (1 ml) was stirred at room temperature for 14 h. CH$_2$Cl$_2$ was added to the reaction mixture and the organic layer was extracted with water (3x) and brine (1x) and dried over Na$_2$SO$_4$. The crude product was purified by column chromatography twice (first: silica, EtOAc/CHCl$_3$ 4/96; second: silica, EtOAc/hexane 1/2). The title compound was obtained as a sticky yellow solid (50 mg, 86%). T$_{cl,dec}$ = 430°C. ^{1}H-NMR (110°C, C$_2$D$_2$Cl$_4$): δ 13.61 (s, 3H, NH'); 12.22 (s, 3H, NH''); 10.02 (s, 3H, H-6-pyrazine); 9.25 (s, 3H, H-*ortho*); 9.11 (s, 3H, H-3-pyrazine); 9.09 (d, 3H, H-3'); 8.76 (d, 3H, H-3''); 8.35 (d; 3H; H-6''); 7.89 (d, 3H, H-6'); 7.58 (t, 3H, H-4'); 7.50 (t, 3H, H-4''); 7.26 (t, 6H, H-5' and H-5''); 7.19 (s, 6H, H-*ortho*-benzoyl); 4.03 (t, 18H, OCH$_2$); 1.77 (m, 18H, OCH$_2$C<u>H</u>$_2$); 1.44 (m, 18H, OCH$_2$CH$_2$C<u>H</u>$_2$); 1.20 (m, 144H, (CH$_2$)$_8$); 0.79 (t, 27H, CH$_3$). IR (KBr): ν = 2923 (C=C-H); 2852 (C-H); 1676 (C=O); 1582; 1436; 1332; 1119; 752. UV (CHCl$_3$): λ_{max} = 388 nm, ε = 3.8·10^4 l·mol^{-1}·cm^{-1}.

6.5   References and notes

[1]   a) Green, M.M.; Peterson, N.C.; Sato, T.; Teramoto, A.; Cook R.; Lifson S. *Science* **1995**, *268*, 1860. b) Lifson, S.; Andreola, C.; Peterson, N.C.; Green, M.M. *J. Am. Chem. Soc.* **1989**, *111*, 8850. c) Green, M.M.; Sato, T.; Teramoto, A.; Lifson, S. *Macromol. Symp.* **1996**, *101*, 363. d) Green, M.M.; Andreola, C.; Muñoz, B.; Reidy, M.P.; Zero, K., *J. Am. Chem. Soc.* **1988**, *110*, 4063. e) Green, M.M.; Reidy, M.P. ; Johnson, R.D.; Darling, G.; O'Leary, D.J. *J. Am. Chem. Soc.* **1989**, *111*, 6452. f) Green M.M.; Khatri, C.A.; Peterson, N.C. *J. Am. Chem. Soc.*, **1993**, *115*, 4941. g) Green, M.M.; Khatri, C.A.; Reidy, M.P.; Levon, K. *Macromolecules*, **1993**, *26*, 4723.

[2]   a) Schlitzer, D.S.; Novak, B.M. *Pol. Prep.* **1997**, *38*, 296. b) Hu, Q.-S.; Vitharana, D.; Liu, G.-Y.; Jain, V.; Wagaman, M.W.; Zhang, L.; Randall Lee, T.; Pu, L. *Macromolecules* **1996**, *29*, 1082. c) Ramos, E.; Bosch, J.; Serrano, J.L.; Sierra, T; Veciana, J. *J. Am. Chem. Soc.* **1996**, *118*, 4703 and refs. cited therein.

[3]   a) Bouman M.M.; Meijer, E.W. *Adv. Mater.* **1995**, *7*, 385. b) Langeveld-Voss, B.M.W.; Janssen, R.A.J.; Christiaans, M.P.T.; Meskers, S.C.J.; Dekkers, H.P.J.M.; Meijer, E.W. *J. Am. Chem. Soc.* **1996**, *118*, 4908.

[4]   For an overview: Collings, P.J. *Liquid Crystals*, IOP Publishing Ltd, Princeton University Press, New Jersey, **1990**.

[5]   a) Nakagiri, T.; Kodama, H.; Kobayashi, K.K. *Phys. Rev. Lett.* **1971** *27*, 564. b) Partyka, J.; Hiltrop, K. *Liq. Cryst.* **1996**, *20*, 611.

[6]   a) Bonazzi, S.; de Marcus, M.M.; Gottarelli, G.; Mariani, P.; Spada, G.P. *Angew. Chem. Int. Ed. Engl.* **1993**, *32*, 248. b) Ciuchi, F.; Di Nicola, G.; Franz, H.; Gottarelli, G.; Mariani, P.; Ponzi Bossi, M.G.; Spada, G.P. *J. Am. Chem. Soc.* **1994**, *116*, 7064.

[7]   a) Terech, P.; Ostuni, E.; Weiss, R.G. *J. Phys. Chem.* **1996**, *100*, 3759. b) Lin, Y.; Kachar, B.; Weiss, R.G. *J. Am. Chem. Soc.* **1989**, *111*, 5542. c) Murata, K.; Aoke, M.; Suzuki, T.; Harada, T.; Kawabata, H.; Komori, T.; Ohseto, F.; Ueda, K.; Shinkai, S. *J. Am. Chem. Soc.* **1994**, *116*, 6664.

[8]   a) Hanabusa, K.; Yamada, M.; Kimura, M.; Shirai, H. *Angew. Chem.* **1996**, *108*, 2086. b) Gallivan, J.P.; Schuster, G.B. *J. Org. Chem.* **1995**, *60*, 2423. c) Kimikuza, N.; Fujikawa, S.;

Kuwahara, H.; Kunitake, T.; Marsh, A.; Lehn, J.-M. *J. Chem. Soc., Chem. Commun.* **1995**, 2103.

[9]   Compound **3** shows a D_{ho} phase from –9 to 430°C. Upon addition of alkane solvents, highly viscous solutions are formed. Unfortunately, due to an elaborate synthesis, no substantial amount of this compound was available for more detailed investigations.

[10]   In hexakis(*n*-alkoxy)triphenylenes neutron scattering experiments (Sheu, E.Y.; Liang, K.S.; Chiang, L.Y. *J. Phys. Fr.* **1989**, *50*, 1279) showed that the molecules only aggregated starting from 10^{-3} mol/l solutions in alkane solvents.

[11]   Werth, M.; Vallerien, S.U.; Spiess, H.W. *Liq. Cryst.* **1991**, *10*, 759. A similar explanation was given in perylene derivatives which were entangled due to a non-planar structure, resulting in an increased mesophase range: Göltner, C.; Pressner, D.; Müllen, K.; Spiess, H.W. *Angew. Chem. Int. Ed. Engl.* **1993**, *32*, 1660.

[12]   A measure for the induced chirality is given by the chiral anisotropy factor g (= $\Delta\varepsilon/\varepsilon$) in which $\Delta\varepsilon$ can be calculated as follows: $\Delta\varepsilon = CD\text{-}effect/(32980 x c x l)$, [CD-effect] = mdeg, [c] = l/mol.cm and [l] = cm.

[13]   The g value is used here as a concentration independent value and as such small concentration differences in the solutions are taken into account.

[14]   Unfortunately, we did not acylate 5,5'-dimethoxy-3,3'-diamino-2,2'-bipyridine and 2,5-bis(2-*t*-butoxycarbonyl-aminophenyl)-pyrazine with chiral acid chlorides in analogy with diamino-bipyridine (Chapter 2) to study the CD behaviour of these more simple compounds. Neither did we attach the chiral 3,4,5-trialkoxy group to compounds **2** and **3**. Possibly, in these cases, small Cotton effects might be detected.

[15]   Bruce Martin, M. *Chem. Rev.* **1996**, *96*, 3043.

[16]   For the constant g_0, the g value of a mixture 10/90 **1a/1b** was used in the fit to compensate for packing effects. This proved to be necessary because of the approximation that K_{ass} is equal for **1a** and **1b**.

[17]   From the appearance of a strong CD effect in cholesteryl 4-(2-anthryloxy)butanoate (CAB) in the gel phase it was suggested that the aromatic moieties are helically packed. No exciton coupling was present in the CD spectra. See ref. 7b.

[18]   a) Yasuda, Y.; Takebe, Y.; Fukumoto, M.; Inada, H.; Shirota, Y. *Adv. Mater.* **1996**, *8*, 740. b) Yasuda, Y.; Iishi, E.; Inada, H.; Shirota, Y. *Chem. Lett.* **1996**, 575. c) Zhang, S.; Zhang, D.; Liebeskind, L.S. *J. Org. Chem.* **1997**, *62*, 2312.

[19]   a) Delnoye, D.A.P.; Sijbesma, R.P.; Vekemans, J.A.J.M.; Meijer, E.W. *J. Am. Chem. Soc.* **1996**, *118*, 8717. b) Delnoye, D.A.P. *Conjugated ladder polymers by intramolecular hydrogen bonding*, Post Graduate Report: T.U. Eindhoven, The Netherlands, ISBN 90-5282-600-5, **1996**.

[20]   Kishner, N.M. *J. Russ. Phys. Chem. Soc.* **1913**, *45*, 1786.

Chapter 7

# Organic zeolites by serendipity

Abstract

*N,N',N''-Tris(3-pyridyl)-trimesic amide, **1**, forms a unique P₋₃ symmetrical crystal containing pores with a mean diameter > 8 Å. These pores are the result of a superimposed, hexagonal bilayer structure built up by intermolecular N–H---N H-bonding, a concomitant cyclic arrangement of six 3-aminopyridyl units, and the template activity of methanol. The result is an open channel molecular network, in which non-destructive exchange of methanol for tetradeuteriomethanol could be accomplished. This can be considered as an example of an organic zeolite, not designed by crystal engineering but found by serendipity.*

7.1   Introduction

Crystal engineering has received considerable attention lately[1] with highlights in the construction of rosettes[2], tapes[3], tubular superstructures[4] and porous solids[5]. One of the challenging goals is to gain access to molecular analogues of inorganic zeolites, in which pores of uniform size from rigid aluminosilicate networks provide tailored reaction environments. However, the forces holding the molecular lattices together are generally weak and as nature doesn't like void space, the formation of pores similar in size as those of zeolites is highly unfavourable.

Obviously, this has not withheld chemists from pursuing these networks and as the knowledge of the relation between molecular and crystal structure —more specifically the prediction of the crystal structures— is increasing, the formation of a real porous structure with channels of nanometer scale diameter and millimeter scale length is within reach[6]. One of the major tools to achieve the desired order is the use of suitable tectons, in which H-bonding groups often provide the desired directionality, strength and reliability[7].

In Chapter 4, the synthesis of compound **1**, serving as a model for comparison with intramolecular H-bonded disc-shaped structure **2**, has been discussed[8]. The beautiful hexagon-shaped crystals obtained after recrystallisation prompted us to investigate them more elaborately with single crystal X-ray diffraction. To our surprise, up to now no X-ray data are available on symmetrical secondary trimesic amides[9]. Trimesic acid, on the other, hand has been studied in depth, and interpenetration of two-dimensional layers composed of three parallel molecules is observed[10], unless guests like pyrene and ethanol are built in[11]. In the case of trimesic acid salts, trivalent metal cations will assemble and fill the crystal structure[12], while dicyclohexylammonium salts form hexagonal sheets incorporating methanol[6c]. The closely related N,N',N''-tris-(2-picolyl)-cyclohexane-*cis*,*cis*-1,3,5-tricarbonamide gave an intriguing helical structure owing to intermolecular α-helix type H-bonding perpendicular to the average plane of the cyclohexane ring with the help of additional C–H---N interactions[13].
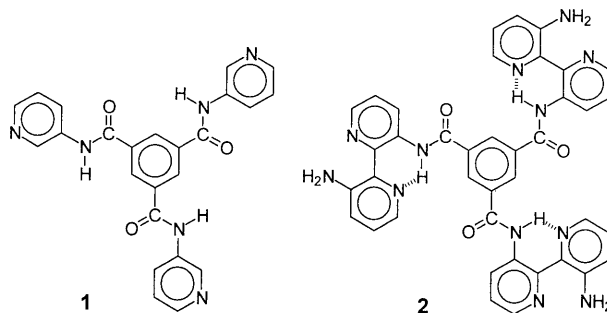
7.2   Results and discussion

The synthesis of compound **1** has been presented in Chapter 4. The large (diameter = 1–2 mm), transparent, hexagon-shaped crystals of **1** were obtained by slowly cooling[14] a hot solution in MeOH. In air and solvents such as toluene, the crystals became opaque and disintegrated. In pentane, by contrast, the crystals were stable. Although removal of the solvent led to disintegration of the crystals, the single crystal X-ray structure could be obtained and the relevant data are summarised in table 7.1. The asymmetric unit comprises only one third of a molecule, while the unit cell is populated by two molecules.

Table 7.1   *Crystallographic details: data collection and refinement parameters*

Data	1
formula	$C_{24}H_{18}N_6O_3$
solvent	MeOH
formula weight	438.45
colour, habit	colourless, block shaped crystals
crystal size (mm)	0.3 x 0.3 x 0.5
lattice type	trigonal
space group	P_{-3}
cell dimensions	
a (Å)	13.8732 (10)
b (Å)	13.8732 (10)
c (Å)	8.4005 (5)
α (deg)	90
β (deg)	90
γ (deg)	120
Z	2
D_c (g/cm^3)	1.039
F(000)	456
μ (cm^{-1})	0.7
θ range (deg)	1.7–27.5
no. of unique reflections	
measured	4819
observed, $F_0 > 4\sigma(F_0)$	1727
R1	0.0376
wR2	0.0973
intermolecular interactions	d(NH---N): 2.909 Å
	α(NH---N): 164°
	d(CH---O): 3.387 Å
	α(CH---O): 175°

As indicated in figure 7.1.a, the molecules have adopted a propeller-shaped conformation in which all pyridyl nitrogens point to the same direction. A torsion angle of 26.6° is found between the amide and the central benzene ring. Intermolecular H-bonding between the pyridyl nitrogens and the amide-NH's of adjacent molecules leads to a macrocyclic organisation in a rosette-like structure (figure 7.1.b)[15]. Owing to the propeller shape of a single molecule, a 30-membered macrocycle is formed with participation of six molecules. As a result, the 3-aminopyridyl units constitute the walls of a cavity with a mean diameter of 8.26 Å.

a)   *b)*
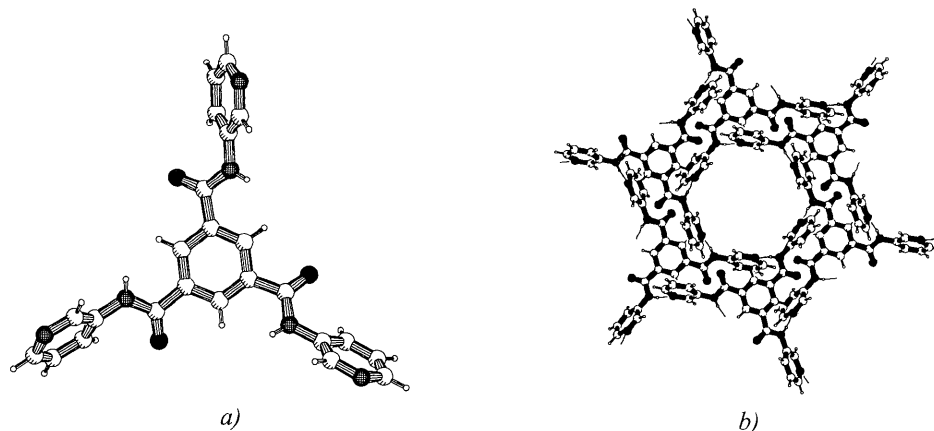
*Figure 7.1: a) Conformation of compound **1** in the crystal lattice; b) macrocyclic arrangement of the pyridylunits leading to a rosette-like structure*

The C_3-symmetry of the molecule allows for the creation of an infinite two-dimensional honeycomb grid with repeating units at 13.9 Å distance in six directions and with a thickness of approximately 8.4 Å (figure 7.2).
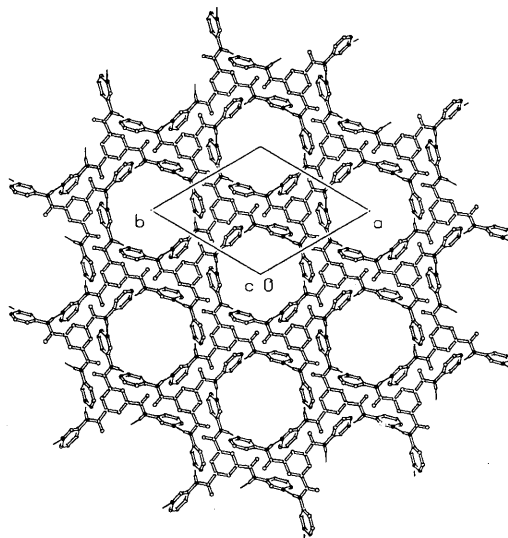

*Figure 7.2: Infinite honeycomb grid of **1***

Closer inspection reveals the bilayer structure of an ensemble of molecules in one sheet (figure 7.3.a). The benzene units occupy alternating up and down positions with all amide carbonyls pointing outwards. The pyridyl units orient their nitrogens inwards in the bilayer structure. The distance between the bilayers is surprisingly small. As shown in figure 7.3.a, the infinite bilayer sheets are themselves belonging to a three dimensional superstructure in

which all the sheets are in fact repeating units placed exactly on top of each other. This results in the formation of a real porous structure with channels of nanometer scale diameter and millimeter scale length (figure 7.3.b). The formation of this 3D structure may rest simply on optimal packing. Alternatively, the 3D structure can be rationalised by cooperative C–H---O interactions[16] (total length 3.39 Å) between each amide oxygen and a pyridyl C4–H4 belonging to an adjacent bilayer. The amide carbonyl dipoles of one trimesic unit —all located on one side of the aromatic ring— are compensated by carbonyl dipoles belonging to three different trimesic units of an adjacent layer, although the latter carbonyls are slightly more remote from the centre. This implies that although the crystal as a whole is achiral, the unit cell as depicted in figure 7.2 is in fact a combination of three trimesic units with *P*-helicity (on top of the bilayer) with three units with *M*-helicity (at the bottom). By consequence, the construction of the 3D structure from achiral bilayers necessitates proper orientation of the latter.
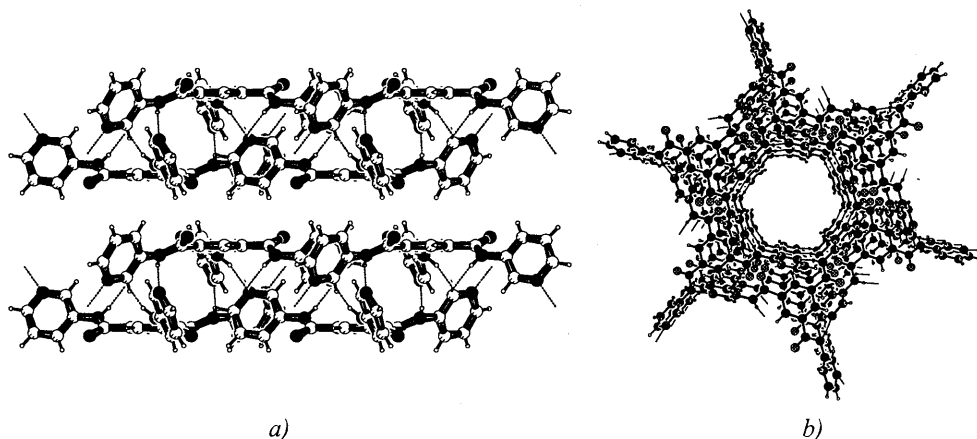

a)   *b)*

Figure 7.3: a) Superimposed bilayer structure of 1; b) channels created by superimposed bilayers

Methanol is essential to guarantee the stability of the crystals, undoubtedly due to its role as a template and guest filling the void space in the interior of the channels —more specifically in the cavity surrounded by the six pyridyl units. The X-ray determination does not allow accurate localisation of methanol. However, the electron density in the cavity amounts to 111 electrons, which is in accordance with the presence of approximately six molecules of MeOH in the cavity. As a result, a molecular ratio of 3 between MeOH and triamide **1** can be deduced. From ^{1}H-NMR spectra in DMSO-*d6* of the crystals which were washed with pentane to remove methanol on the surface— a molecular ratio ranging from 1.5 to 3 has been found between methanol and triamide **1**. The variation in the ^{1}H-NMR results probably arises from the sample treatment. This may also account for the difference between X-ray diffraction and NMR results[17].

To provide evidence for the porous structure of the crystals and the accessibility of the channels for external molecules, a methanol–tetradeuteriomethanol exchange experiment was conducted and the ^{1}H-NMR spectrum in DMSO-*d6* unambiguously demonstrates the complete disappearance of non-deuteriated methanol from the crystals. Analogous experiments have been conducted in other trimesic acid derivatives and in other tectonic molecules [3a, 4e, 10d]. The calculated density of **1** without guests amounts to 1.0395 g/cm^3 and of **1•**3 MeOH to only 1.267 g/cm^3. This relatively low density contrasts with the high density of many trimesic derivatives including the parent acid (1.449 g/cm^3).[10]

7.3 Conclusions

Crystals of **1**, obtained by serendipity, were found to exhibit a P_{-3} symmetrical crystal structure with an open channel structure in which the pores are filled with MeOH. The presence of C$_3$-symmetry tends to induce void space in crystals, which is not preferred for energetic reasons. In this case, Nature compensates for this by stabilising the pores with MeOH. A crystal pattern as the one found in compound **1**, has to our knowledge never been described. It seems that in this particular structure an acceptable compromise is found between void space, concatenation of molecules and inclusion of guests.

7.4 Experimental procedures

Single crystal X-ray crystallography
An Enraf-Nonius CAD4 Turbo diffractometer on rotating mode was used (Mo Kα radiation, graphite monochromator, λ = 0.71073 Å, T = 150 K). Data were corrected for L$_p$ effects and for linear instability of 1% of the reference reactions, but not for absorptions. Data collection and refinement parameters are given in Table 7.1. The structure was solved for automated directed methods (SHELXS96); no observance criterion was applied during refinement. Electron density in a disordered solvent area (the unit cell contains a channel parallel to the *c*-axis, through the origin, with a volume of 450Å^3 and containing 111 electrons per *c*-translation period) was taken into account in the refinement via PLATON/SQUEEZE. Where relevant, data cited are given without the disordered solvent contribution. Positional parameters for hydrogen atoms were included in the refinement; initial values were obtained from a difference Fourier map. Refinement converged at a final wR_2 value of 0.0973, R$_1$ = 0.0376 (for 1727 reflections with $F_0 > 4\sigma (F_0)$), S = 1.071, for 118 parameters. A final difference Fourier showed no residual density outside –0.20 and 0.24 e Å^{-3}.

N,N',N'-Tris(3-pyridyl)-benzene-1,3,5-tricarboxamide (1)
The synthesis and analytical data of compound **1** have been described in Chapter 4 under compound **7**.

CH$_3$OH–CD$_3$OD exchange experiment
Crystals of **1** in methanol were removed from the mother liquor and unloaded from exterior methanol by repetitive immersion in pentane. A crystal was subsequently dissolved in DMSO-*d6* as a blank. The rest of the crystals was washed twice with tetradeuteriomethanol and finally kept in this solvent

for four days. The crystals remained intact and were then filtered and washed with pentane. ^{1}H-NMR in DMSO-*d6* then indicated the complete replacement of methanol by tetradeuteriomethanol.

7.5   References and notes

[1]   Desiraju, G.R. *Angew. Chem., Int. Ed. Engl.* **1995**, *34*, 2311.

[2]   a) Matthias, J.P.; Simanec, E.E.; Whitesides. G.M. *J. Am. Chem. Soc.* **1994**, *116*, 4326. b) Funeriu, D.P.; Lehn, J.-M.; Baum, G.; Fenske, D. *Chem. Eur. J.* **1997**, *3*, 99. c) Yang, J.; Marendaz, J.-L.; Geib, S.J.; Hamilton, A.D. *Tetrahedron Lett.* **1994**, *35*, 3665. d) Timmerman, P.; Reinhoudt, D.N. *Chem. Eur. J.* **1997**, in press

[3]   a) Zerkowski, J.A. ; Seto, C.T,; Wierda, D.A.; Whitesides, G.M. *J. Am. Chem. Soc.* **1990**, *112*, 9025. b) Zerkowski, J.A. ; Matthias, J.P.; Whitesides, G.M. *J. Am. Chem. Soc.* **1994**, *116*, 4305. c) Zerkowski, J.A.; Whitesides, G.M. *J. Am. Chem. Soc.* **1994**, *116*, 4298. d) Zerkowski, J.A.; MacDonald, J.C.; Seto, C.T,; Wierda, D.A.; Whitesides, G.M. *J. Am. Chem. Soc.* **1994**, *116*, 2382. e) MacDonald, J.C.; Whitesides, G.M. *Chem. Rev.* **1994**, *94*, 2383 and references cited herein. f) Reddy, D.S.; Paneerselvam, K.; Pilati, T.; Desiraju, G.R. *J. Chem. Soc., Chem. Commun.* **1993**, 661.

[4]   a) Weber, E.; Pollex, R.; Czugler, M. *J. Org. Chem.* **1992**, *57*, 4068. b) Venkataraman D.; Lee, S.; Zhang, J.; Moore, J.S. *Nature* **1994**, *371*, 591. c) Ghadiri M.R. *Adv. Mater.* **1995**, *7*, 675.

[5]   a) Gardner, G.B.; Venkataraman, D.; Moore, J.S.; Lee S. *Nature* **1995**, *374*, 792. b) Brunet, P.; Simard, M.; Wuest, J.D. *J. Am. Chem. Soc.* **1997**, *119*, 2737.

[6]   a) Khazanovich, N.; Granja, J.R.; McCree, D.E.; Milligan, R.E.; Ghadiri, M.R. *J. Am. Chem. Soc.* **1994**, *116*, 6011. b) Ward, M.D. *Nature* **1995**, *374*, 764. c) Melendez, R.E.; Krishnamohan, C.V.; Zarawotko, M.J.; Bauer, Rogers, R.D. *Angew. Chem., Int. Ed. Engl.* **1996**, *35*, 2213. d) Mascal, M.; Hext, N.M.; Warmuth, R.; Moore, M.H.; Turkenburg, J.P. *Angew. Chem., Int. Ed. Engl.* **1996**, *35*, 2204. e) Wang, X.; Simard, M.; Wuest, J. D. *J. Am. Chem. Soc.* **1994**, *116*, 12119.

[7]   a) Russell V.A.; Ward, M.D. *Chem. Mater.* **1996**, *8*, 1654. b) Fan, E.; Vicent, C.; Geib, S.J.; Hamilton, A.D. *Chem. Mater.* **1994**, *6*, 1113.

[8]   Palmans, A.R.A.; Vekemans, J.A.J.M.; Fischer, H.; Hikmet R.A.; Meijer, E.W. *Chem. Eur. J.* **1997**, *3*, 300.

[9]   One symmetric tertiary amide derivative of trimesic acid has been described: a) Azumaga, I.; Kageshika, H.; Yamaguchi, K.; Sheido, K. *Tetrahedron* **1995**, *51*, 5277. b) Yamaguchi, K.; Matsumura, G.; Kageshika, H.; Azumaga, I.; Ito, Y.; Itai, A.; Sheido, K. *J. Am. Chem. Soc.* **1991**, *113*, 5474. Recently, the crystal structure of a secondary amide of trimesic acid (trimethyl-1,3,5-benzenetricarboxamide) has been discussed but there is no C_3-symmetry in the crystal: Hanabusa, K.; Koto, C.; Kimura, M.; Shirai, H.; Kakehi, A. *Chem. Lett.* **1997**, 429.

[10]   Duchamp, D.J.; Marsh, R.E. *Acta Cryst.* **1969**, *B25*, 5.

[11]   Kolotuchin, S.V.; Fenlon, E.E.; Wilson, S.R.; Loweth, C.J.; Zimmerman, S.C. *Angew. Chem.* **1995**, *107*, 2873.

[12]   a) Gutschke, S.O.H.; Molinier, M.; Powell, A.K.; Winpenny, R.E.P.; Wood, P.T. *Chem. Commun.* **1996**, 823. b) Yaghi, O.M.; Li, H.; Groy, T.L. *J. Am. Chem. Soc.* **1996**, *118*, 9096. c) Yaghi, O.M.; Davis, C.E.; Li, G.; Li, H. *J. Am. Chem. Soc.* **1997**, *119*, 2861. d) Yaghi, O.M.; Li G.; Li, H. *Nature* **1995**, *378*, 704.

[13]   Fan, E.; Yang, J.; Geib, S.J.; Stoner, T.C.; Hopkins, M.D.; Hamilton, A.D., *J. Chem. Soc., Chem. Commun.* **1995**, 1251.

[14]   Slow cooling was accomplished by putting the flask in a water bath of ~60°C. This was essential as rapid cooling only furnished a micro-crystalline powder.

[15]   According to Etter's graph set analysis the nitrogen H-bond donors and acceptors are involved in a $R_6^6(30)$ pattern. a) Etter, M.C. *Acc. Chem. Res.* **1990**, *23*, 120. b) Bernstein, J.E.; Davis, R.E.; Shimoni, L.; Chang, N.-L. *Angew. Chem., Int. Ed. Engl.* **1995**, *36*, 1555.

[16]   a) Berkovich-Yellin, Z.; Leiserowitz, L. *Acta Cryst.* **1984**, *B40*, 1596. b) Desiraju, G.R. *Acc. Chem. Res.* **1996**, *29*, 441.

[17]   In this respect, we noticed that it was very difficult to obtain a satisfactory elemental analysis of these crystals. Only after exhaustive drying at 150°C in a vacuum stove —after which all MeOH was removed as indicated by ^{1}H-NMR— and a fast sample preparation, reasonable analytical data were obtained. Apparently, this compound attracts atmospheric water to compensate for the loss of MeOH. Anal. calcd. for $C_{24}H_{18}N_6O_3$ (438.44): C, 65.75; H, 4.14; N, 19.17. Found: C, 64.8; H, 4.2; N, 18.8.

Summary

Intramolecular H-bonds pre-organise the 3,3'-di(acylamino)-2,2'-bipyridine moiety in a planar, transoid conformation. Therefore, this moiety is suitable to provide structure when incorporated in larger molecules. This thesis deals with (i) the synthesis and characterisation of various acylated 3,3'-diamino-2,2'-bipyridines, focusing on the intramolecular H-bonding present in these molecules, and (ii) the incorporation of the 3,3'-di(acylamino)-2,2'-bipyridine moiety in disc-shaped structures which leads to a new class of extended-core liquid crystalline materials. As a result of these studies, 3,3'-di(acylamino)-2,2'-bipyridines show promising opportunities as a new type of valuable building blocks for the construction of supramolecular assemblies.

The acylated 3,3'-diamino-2,2'-bipyridines are introduced in Chapter 2. A large number of derivatives has been synthesised and characterisation with ^{1}H-NMR spectroscopy, IR spectroscopy and single crystal X-ray diffraction reveals the presence of intramolecular H-bonding, which can be considered to be strong. Furthermore, the intramolecular H-bonds are stable in a variety of conditions such as high temperatures and polar solvents. The consequence of this strong H-bonding is that the bipyridine resides in a planar, transoid conformation.

The incorporation of the aforementioned bipyridine moiety in larger molecules and the study of the solubility/rigidity relationship are evaluated in Chapter 3. Even small oligo-amides based on 3,3'-diamino-2,2'-bipyridine become sparingly soluble in common organic solvents. Although the synthesis of aromatic polyamides might be envisaged, our priority has been to provide the bipyridine moiety with lipophilic chains to ensure solubility. The synthesic steps towards the desired compounds have proved to be complex and laborious, however, a convenient method is described for the synthesis of 5,5'-dimethoxy-3,3'-diamino-2,2'-bipyridine; a model and precursor of the pursued lipophilic bipyridines.

The synthesis of C_3-symmetrical, disc-shaped compounds based on 3,3'-diamino-2,2'-bipyridine is addressed in Chapter 4. To circumvent solubility issues, the diamino-bipyridyl unit has been monoacylated with the strongly solubilising 3,4,5-trialkoxybenzoyl group. This monoacylation proceeds with high selectivity which can be attributed to the formation of a H-bond upon the first acylation. Five disc-shaped derivatives **1a–d** and **2** differing in chain length (compounds **1a–d**) or aromatic core (compound **2**) have been synthesised in a convergent approach. ^{1}H-NMR results have revealed the strong tendency of the aromatic interior to adopt a mainly planar conformation in solution. Compounds **1a–d** and **2** all show thermotropic liquid crystalline behaviour in an extended temperature range (> 250 K). From combined results of differential scanning calorimetry (DSC), polarisation microscopy and X-ray diffraction, it has been concluded that all compounds **1** and **2** show an ordered columnar mesophase (D_{ho}). Additionally, a helical superstructure has been observed within the columns of compounds **1a–d**.

The distinctive aromatic–aliphatic part in compounds **1a–d** and **2** and the strong secondary interactions within the columnar stacks result in lyotropic mesomorphism as well. Chapter 5 reports on the lyotropic mesomophism for compounds **1a,b** in alkane solvents. At low concentrations (< 28% w/w) in dodecane, evidence points to the presence of an N_C phase whereas in a higher concentration (55% w/w), a D_{ho} phase has been assigned. Visco-elastic properties are found in the anisotropic as well as the isotropic solutions of compound **1a** in dodecane. Upon shear/pressing between glass plates, the lyotropic columnar mesophase orients in a planar alignment. When a DC electrical field is applied over the cell, the columns re-orient into a homeotropic alignment. The speed of the switching process in the orienation of the columns is depending on the temperature and the voltage applied.

1   **2**   **3**
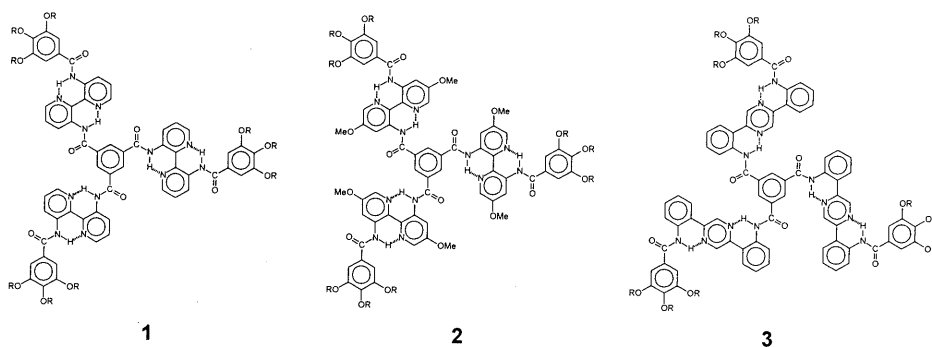
The aggregation behaviour of three disc-shaped compounds **1–3** in dilute solutions (~10^{-5} mol/l) is described in Chapter 6. All compounds show a strong tendency to aggregate in columnar stacks when dissolved in alkanes as evidenced by UV and CD spectroscopy. Compounds **2** and **3** also strongly aggregate in more polar solvents such as chloroform and o-dichlorobenzene. Circular dichroism measurements have revealed that the columnar stacks of compound **1** in alkane solvents are inclined to be chiral. One handedness of the stack can be favoured by attaching chiral peripheral side chains or by using a chiral alkane as solvent. The "Sergeants-and-Soldiers" principle has been found to be applicable in this system. A theoretical treatment of the experimental results shows that the persistence length within the aggregates is approximately 80 molecules with an association constant between the molecules of ~10^8 l/mol.

By serendipity, hexagon-shaped crystals have been obtained for N,N',N''-tris(3-pyridyl)trimesic amide, a model compound for the previously mentioned disc-shaped derivatives. Chapter 7 deals with the unique P_{-3} symmetrical crystal containing pores with a mean diameter of ~8.3 Å. These pores are the result of a superimposed, hexagonal bilayer structure built up by intermolecular N–H---N hydrogen bonding, concomitant cyclic arrangement of six 3-aminopyridyl units, and template activity of methanol. The result is an open channel molecular network, in which non-destructive exchange of MeOH for MeOD has been accomplished.

Samenvatting

Intramoleculaire waterstofbruggen pre-organiseren de 3,3'-di(acylamino)-2,2'-bipyridine eenheid in een vlakke, transoïde conformatie. Deze eenheid lijkt daarom geschikt voor de inbouw in grotere moleculen waardoor supramoleculaire structurering optreedt. Dit proefschrift concentreert zich enerzijds op de synthese van een reeks geacyleerde 3,3'-diamino-2,2'-bipyridines waarbij de nadruk ligt op de karakterisering van de intramoleculaire waterstofbruggen en anderzijds op het inbouwen van de 3,3'-di(acylamino)-2,2'-bipyridine eenheid in schijfjesvormige structuren. Dit leidt tot een nieuwe klasse van vloeibaar kristallijne materialen. De behaalde resultaten laten zien dat de 3,3'-di(acylamino)-2,2'-bipyridine eenheid kan worden gebruikt als een nieuwe bouwsteen voor de supramoleculaire chemie.

De geacyleerde 3,3'-diamino-2,2'-bipyridines worden geïntroduceerd in Hoofdstuk 2. Een brede variëteit aan derivaten is gesynthetiseerd en uit de karakterisering m.b.v. ^{1}H-NMR spectroscopie, IR spectroscopie en kristalstructuur analyse blijkt dat de intramoleculaire waterstofbruggen sterk zijn en stabiel in een scala van condities zoals hoge temperaturen en polaire oplosmiddelen. Het gevolg van de waterstofbrugvorming is dat de bipyridine eenheid preferentieel een vlakke, transoïde conformatie aanneemt.

Het inbouwen van bovengenoemde bipyridine eenheid in grotere moleculen en het bestuderen van de oplosbaarheids-/rigiditeitsrelatie worden geëvalueerd in Hoofdstuk 3. Zelfs kleine oligo-amides gebaseerd op 3,3'-diamino-2,2'-bipyridine blijken slecht oplosbaar te zijn in de gangbare organische oplosmiddelen. Ofschoon de synthese van aromatische polyamides zeker tot de mogelijkheden behoort, hebben we ons toegespitst op het voorzien van de bipyridine eenheid met lipofiele ketens om aldus oplosbaarheid te garanderen. De synthese naar de gewenste verbindingen is gecompliceerder dan initieel gedacht, echter een goed uitvoerbare procedure voor de synthese van 5,5'-dimethoxy-3,3'-diamino-2,2'-bipyridine —een modelverbinding en precursor voor de gewenste lipofiele bipyridines— is uitgewerkt.

De synthese van C$_3$-symmetrische, schijfjesvormige moleculen gebaseerd op 3,3'-diamino-2,2'-bipyridine wordt behandeld in Hoofdstuk 4. Om oplosbaarheidsproblemen te vermijden is het diamine eenmaal geacyleerd met de sterk solubiliserende 3,4,5-trialkoxybenzoyl groep. Deze monoacylering verloopt onverwacht selectief, hetgeen kan worden toegeschreven aan de invloed van de waterstofbrugvorming. Vijf schijfjesvormige verbindingen **1a–d** en **2** — verschillend in ketenlengte (verbindingen **1a–d**) en aromatische kern (verbinding **2**)— zijn gesynthetiseerd via een convergente methode. Uit ^{1}H-NMR resultaten is de sterke neiging van de aromatische kern om een bijna vlakke conformatie aan te nemen in oplossing gebleken. Thermotroop vloeibaar kristallijn gedrag is waargenomen in alle verbindingen **1a–d** en **2** in een breed temperatuur gebied (>250 K). Uit de gecombineerde resultaten van polarisatiemicroscopie, DSC metingen en X-ray diffractie is geconcludeerd dat de mesofase van alle verbindingen van het geordende columnaire type is (D$_{ho}$). Additioneel zijn in verbindingen **1** aanwijzingen gevonden voor heliciteit binnen de kolommen.

De aanwezigheid van uitgesproken aromatische en alifatische gedeelten in **1a–d** en **2** en de sterke secundaire interacties in de columnaire stapeling resulteren eveneens in lyotroop vloeibaar kristallijn gedrag. Hoofdstuk 5 beschrijft het lyotrope mesomorfisme van verbindingen **1a,b** in dodecaan. In lage concentraties (< 28% w/w in dodecaan) is waarschijnlijk een N_C fase aanwezig. In hogere concentraties (55% w/w in dodecaan) kan een D_{ho} fase worden waargenomen. Zowel anisotrope als isotrope oplossingen van **1a** in dodecaan vertonen visco-elastische eigenschappen. Door duwen/drukken van de monsters tussen glasplaatjes kan een planaire oriëntatie van de kolommen worden bewerkstelligd. Indien vervolgens een gelijkstroom electrisch veld over de glasplaatjes wordt aangelegd, heroriënteren de kolommen zich in een homeotrope oriëntatie. Dit schakelen van de kolomoriëntatie is afhankelijk van de temperatuur en de grootte van de aangelegde spanning.
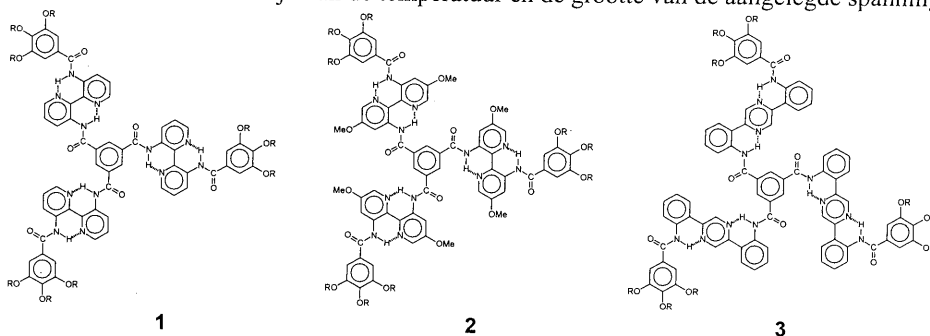
Het aggregatiegedrag van verbindingen **1–3** in verdunde oplossingen (~10^{-5} mol/l) is beschreven in Hoofdstuk 6. Uit UV spectroscopie blijkt dat wanneer verbindingen **1–3** worden opgelost in alkanen, ze een sterke neiging vertonen om in kolommen te aggregeren. Verbindingen **2** en **3** aggregeren ook sterk in meer polaire oplosmiddelen zoals chloroform en *o*-dichloorbenzeen. Met behulp van CD metingen is duidelijk geworden dat de kolommen van verbinding **1** in hexaan chiraliteit vertonen. Een enantiomeer van dergelijke kolommen kan worden bevoordeeld door de inbouw van chirale zijketens of door oplossen in een chiraal oplosmiddel. Bovendien blijkt het "Sergeants-and-Soldiers" principe toepasbaar in dit systeem. Een theoretische behandeling van de experimentele resultaten laat zien dat de persistentielengte in de aggregaten overeenkomt met maximaal 80 moleculen en dat de associatieconstante tussen de moleculen 10^8 l/mol bedraagt.

Per toeval werden zeshoekige kristallen verkregen van N,N',N"-tris(3-pyridyl)trimesamide, een modelverbinding voor de eerder vermelde schijfjesvormige C_3-symmetrische derivaten. De unieke P_{-3} symmetrische kristalstructuur van dit amide waarin poriën met een diameter van ongeveer 8.3 Å aanwezig zijn wordt besproken in Hoofdstuk 7. Deze poriën zijn het resultaat van een superpositie van een oneindige hexagonale bi-laagstructuur. Deze is ontstaan dank zij intermoleculaire N–H---N waterstofbrugvorming tussen telkens zes 3-aminopyridyl eenheden en de "template" activiteit van methanol. De open kanaalstructuur laat niet-destructieve uitwisseling van CH_3OH voor CD_3OD toe, zodat met recht van een poreuze vaste stof gesproken mag worden.

Curriculum Vitae

Anja Palmans werd op 26 juni 1969 geboren te Maaseik, België. In 1981 startte zij met de middelbare school op de "Vrije Humaniora Voor Meisjes" te Maaseik waar zij in 1987 het diploma "Wiskunde-Wetenschappen" behaalde. Aansluitend begon zij met de studie Scheikundige Technologie aan de Technische Universiteit te Eindhoven. Deze studie werd in december 1992 afgerond met een onderzoek naar de toepassingsmogelijkheden van "solid phase" technieken voor de synthese van dendrimeren in de Vakgroep Organische Chemie onder leiding van prof.dr. E.W. Meijer. Vervolgens werd in januari 1993 een AIO-2 opleiding gestart in dezelfde vakgroep. Deze opleiding werd voortgezet in een promotie-onderzoek onder begeleiding van dr. J.A.J.M. Vekemans en prof.dr. E.W. Meijer. De belangrijkste resultaten van het onderzoek staan beschreven in dit proefschrift.

Dankwoord

Vermits het schrijven van een dankwoord geen sinecure is, wil ik beginnen met iedereen te bedanken die mij de afgelopen 4 jaar heeft terzijde gestaan binnen en buiten het lab.

Bert Meijer wil ik graag bedanken voor zijn vertrouwen in mij, zijn regelmatige prikkelingen om mij tot betere prestaties te brengen en de volledige vrijheid die ik heb gekregen in het uitvoeren van het onderzoek. Jef Vekemans wil ik bedanken voor het altijd een minuutje tijd te hebben, voor zijn steun in raad en daad en voor de samenwerking als "Belgisch team" op een Nederlands lab. Jef, niet alleen op wetenschappelijk gebied, maar ook op menselijk gebied heb ik veel van u kunnen leren.

De resultaten beschreven in dit proefschrift zijn niet alleen mijn verdienste maar ook die van een aantal researchstagiaires/afstudeerders. Edwin Ijpeij heeft de eerste aanzet tot dit onderzoek gedaan en wil ik daar bij deze voor bedanken. Researchstagiaires Mariëlle Wouters, Daan v.d. Kerkhof, Dorrit Melsen en Rao V.K. wil ik bedanken voor hun bijdragen aan het initiële onderzoek. Peter Breure —die in zijn eentje het hele onderzoek heeft voortgezet tijdens mijn verblijf in het zuidelijk halfrond—, Dorrit Melsen —die er als allereerste in slaagde de veel besproken "ster" te maken—, Jacco de Kraker —die ondanks weerbarstige chemie nooit de moed liet zakken— en Luc Brunsveld —die zich volledig zelfstandig de ion-geleiding meester maakte en daar nu mee verder gaat— maakten allemaal deel uit van de "sterren" ploeg (om mogelijke verwarring te voorkomen: in dit geval slaat "ster" op de vorm van de moleculen en niet op "sterren" uit een zeker voetbalteam) en wil ik bedanken voor hun enthousiasme en de prettige samenwerking.

Verder wil ik de vaste staf bedanken voor het kritisch volgen van het onderzoek. In het bijzonder Joost van Dongen voor alle hulp en ondervragingen in het scheidingslab (ik zit nog steeds op de cursus wegen en verdunnen te wachten), Hans Damen voor het zorgen voor chemicaliën/glaswerk en alle hulp bij het omgaan met steeksleutels en andere gebruiksonvriendelijke technische attributen en Henk Eding voor het uitvoeren van de element analyses (soms lag het echt aan het apparaat, Henk). Jolanda Spiering wil ik bedanken voor het snel en efficiënt bijmaken van enkele verbindingen toen de tijd echt begon te dringen.

Voor de meer fysische/theoretische kanten van het onderzoek kon ik altijd terecht bij Rifat Hikmet en Edsko Havinga, waarvoor mijn dank. Rifat, *mersi* voor alle hulp bij de "switch" experimenten, het ter beschikking stellen van de DSC en het kritische "fysicus" perspectief op het onderzoek. Hartmut Fischer was gelukkig bereid de broodnodige cursus "vloeibare kristallen" te geven en ben ik zeer erkentelijk voor alle hulp bij de X-ray diffractie metingen, het kritisch doorlezen van manuscripten en de prettige samenwerking (maar ik had soms ook gelijk). Peter Buynsters, Huub Geurts, Heleen Amatdjais-Groenen en Peter van Galen, allen van de Universiteit van Nijmegen, wil ik graag bedanken voor de hulp bij de TEM metingen, elementanalyses (toen ons apparaat uit de running was wegens ouderdom) en FAB-MS metingen. Anick van de Craats en John Warman van het IRI te Delft, wil ik bij deze bedanken voor de PR-TRCM metingen die zij hebben uitgevoerd.

STELLINGEN

behorend bij het proefschrift

Supramolecular structures based on the intramolecular H-bonding in the 3,3'-di(acylamino)-2,2'-bipyridine unit

van

Anja R.A. Palmans

1. De zogenaamde voorspelbaarheid van "self-assembly" processen blijkt soms meer een gevolg van toeval te zijn.

   Melendez, R.E.; Krishnamohan Sharma, C.V.; Zaworotko, M.J.; Bauer, C.; Rogers, R.D. *Angew. Chem. Int. Ed. Engl.* **1996**, *35*, 2213.

2. Woorden als "helical-chiral" in de titel wekken een bepaalde verwachting op en zijn derhalve misleidend wanneer niet met enantiomeer-zuivere verbindingen wordt gewerkt.

   Praefcke, K.; Eckert, A.; Blunk, D. *Liq. Cryst.* **1997**, *22*, 113.

3. Het in omgang zijn van verschillende eenheden om chiroptische data in uit te drukken, is op zijn minst verwarrend, maar bij nader inzien ook optisch bedrog.

   Green, M.M.; Khatri, C.; Peterson, N.C. *J. Am. Chem. Soc.* **1993**, *115*, 4941. Bonazzi, S.; DeMorais, M.M.; Gottarelli, G.; Mariani, P.; Spada, G.P. *Angew. Chem. Int. Ed. Engl.* **1993**, *32*, 248. Hanabusa, K.; Yamada, M.; Kimura, M.; Shirai, H. *Angew. Chem. Int. Ed. Engl.* **1996**, *108*, 2086. Kimikuza, N.; Fujikawa, S.; Kuwahara, H.; Kunitake, T.; Marsh, A.; Lehn, J.-M.; Kimikuza, N. *J. Chem. Soc., Chem. Commun.* **1995**, 2103. Mascal, M.; Wood, I.G.; Bigley, M.J.; Batsanov, A.S.; Walsgrove, T.; Slawin, A.M.Z.; Williams, D.J.; Drake, A.F.; Siligardi, G. *J. Chem. Soc., Perkin Trans. 1* **1996**, 2427.

4. Het gebruik van pretentieuze begrippen als "Dendrimer Periodic Table", "Dendrimer Chemistry Set" en "Dendritic Mutants" kan het gebrek aan creativiteit van de bijhorende chemie niet verhullen.

   Dvornic, P.R.; Tomalia, D.A. *Macromol. Symp.* **1995**, *98*, 403. Tomalia, D.A. *Adv. Mater.* **1994**, *6*, 529.

5. Chiraliteit is handig.

   Hoofdstuk 6 van dit proefschrift. Bouman, M.M.; Meijer, E.W. *Adv. Mater.* **1995**, *7*, 385. Green, M.M.; Peterson, N.C.; Sato, T.; Teramoto, A.; Cook, R.; Lifson, S. *Science* **1995**, *268*, 1860. Janssen, H.M.; Peeters, E.; van Zundert, M.F.; van Genderen, M.H.P.; Meijer, E.W. *Angew. Chem.* **1997**, *36*, 122. Langeveld-Voss, B.M.W.; Peeters, E.; Janssen, R.A.J.; Meijer, E.W. *Synthetic Metals* **1997**, *84*, 611.

6. Het is opmerkelijk dat het tweemaal voorkomen van een stabiel pentavalent koolstof atoom geen verdere uitleg behoeft.

   Raja, K.S.; Ramakrishnan, S.; Raghunathan, V.A. *Chem. Mater.* **1997**, *9*, 1630.

7. Het beleid van de minister van Landbouw Van Aartsen aangaande de varkenspest kan worden afgedaan als pure "Schweinerei".

8. Het verhogen van de accijnzen op autobrandstoffen heeft tot gevolg dat meer mensen extra kilometers rijden aangezien de lagere prijzen in de omringende landen dit alsmaar aantrekkelijker/lonender maakt.

9. De hoeveelheid opgenomen vakantiedagen tijdens een promotieperiode hoeft niet persé omgekeerd evenredig te zijn met de behaalde resultaten.

10. Het instellen van kennisinstandhoudingsplaatsen en werkgelegenheidsprojecten is een creatieve manier om de omvang van de werkeloosheid onder academici te verdoezelen.